A non-conventional model to assess the production potential of the Waipawa Formation – a possible hydrocarbon source rock in the East Coast Basin

A thesis presented in partial fulfilment of the requirements for the degree of

Doctor of Philosophy in Earth Science at Massey University, Palmerston North, New Zealand

MASSEY UNIVERSITY
TE KUNENGA KI PŪREHUROA
UNIVERSITY OF NEW ZEALAND

Sadaf

2013

Abstract

Since the early part of the 20th century, many countries have attempted to diversify their energy resources through exploiting their unconventional hydrocarbon reserves. These include oil shales, native bitumen, oil sands and tar sands. Oil shale, in particular, has received significant interest over recent decades due to the potentially huge reserves stored within this type of resource. Traditional assessment of oil shale deposits is dependent on the analytical technique Source Rock Analysis (SRA), but there are recognised limitations to this technique.

The hypothesis of the current study was that a novel and non-conventional analytical tool would be better suited to assess the hydrocarbon potential of oil shales than conventional SRA. The overall objective of the study was to define a scientifically comprehensive production potential model for non-conventional source rocks using a suite of physical (XRD, organic petrography), thermal (LOI, LECO, TGA) and chemical analytical techniques (FTIR and GC-MS of the solvent-extracted bitumen phase). These techniques were used to characterise international reference shales from the USA (Green River Formation, GRF), Pakistan (Salt Range oil shale, Mir Kalam Kala and Speena Banda oil shale) and China Qianjiang Formation), and shales from New Zealand (Waipawa Formation and Orepuki oil shale). Analysis of each rock by SRA allowed for ranking of the petroleum potential, with the GRF, Orepuki oil shale, and two of four locations from the Waipawa Formation, being inferred as good potential source rocks.

Physical characterisation of the rocks showed that the content of illite in an oil shale is inversely proportional to the hydrocarbon content of the rock. The absence of illite can therefore be used as an index of production potential, and allowed ranking of the petroleum potential of the rocks which was in good agreement with SRA. Organic petrography linked production potential to the presence of macerals in polished sections prepared from selected rocks of the study and provided strong evidence for the environment of deposition of these samples.

Thermal analysis showed that the abundance of organic matter and total organic carbon (TOC) are directly proportional to the oil production potential of an oil shale provided the oil shale is not post mature. Samples with good SRA-defined production potential had LOI and TOC values in excess of 5% and 2.5% respectively, and a weight loss due to decomposition of kerogen (W_B) of 7%. There was a clear distinction between the good and

poor production potential source rocks, with the Pakistan samples showing low values in each of these parameters. The TOC of the Chinese oil shale provided fan ambiguous interpretation, but further investigation defined this rock as post-mature.

Chemical analysis showed that the relative aliphaticity and aromaticity of the bitumen phase extracted by dichloromethane was higher for the highly SRA-ranked shales. No aromatic bands were identified in the low to non-producing oil shales. A direct relationship between the relative content of the constituent chemical compounds of bitumen (alkanes, cycloalkanes, aromatics and heteroatom compounds) and production potential was also observed, and the GC-MS data provided information on the likely quality of oil that might be extracted from an oil shale. The trend in relative aliphaticity and aromaticity of the rocks was consistent under both FTIR and GC-MS analysis.

To formulate the non-conventional production potential model, cut-off values were selected using the SRA-defined production rankings. Good production potential is inferred through LOI >5%, TOC >2.5% and W_B >7%. The presence or absence of illite in the clay fraction, and the presence of both aliphatic and aromatic bands (FTIR) and the four constituent chemicals in the bitumen extract (GC-MS), were defined as qualitative cut-off values. Organic petrography is not integrated into the model at the current time, but provided strong data on the origin of deposition of a shale rock. These cut-off values were integrated into a model that defines a sequence of analytical steps. The analytical techniques become progressively more complex as the potential of a sample becomes more certain. A sample is defined as having good production potential if it meets all criteria.

The non-conventional production potential model was then used to interpret the analytical results obtained through analysis of the Orepuki oil shale and Waipawa Formation shale rocks. The Orepuki oil shale was found to be an oil shale, rich in organic matter with excellent production potential. The Waipawa Formation was similarly found to be an oil shale, with good petroleum potential for two of the four outcrop locations analysed.

The conclusions from the non-conventional production potential model were consistent with those inferred by SRA. But the model yields superior understanding regarding the production potential of the Orepuki oil shale and Waipawa Formation. The low illite content, origin of deposition of these formations, degree of richness of the constituent organic content, and the inferred quality of oil which may be derived from its bitumen, are key information that cannot be obtained from SRA.

Acknowledgements

Undertaking this PhD has been a truly life-changing experience for me, which would not have been possible without the support and guidance of many people. I am deeply grateful to all of them and wish to render my sincerest thanks to them.

I would like to thank my supervisor Dr Christopher Anderson for his scholarly support, encouragement, guidance and patience throughout this project. Without his continuous help and valuable guidance, this PhD would not have been possible.

Thanks to my supervisor Julie Palmer, for her continuous guidance and support throughout my doctoral studies.

I am immensely grateful to the Higher Education Commission (HEC), Pakistan, for granting me a full-time doctoral scholarship which made it possible for me to pursue and complete my doctoral studies at Massey University.

I would like to thank Richard Sykes from GNS for sharing his ideas through discussions with me, sending me publications and reports and helping me with Source Rock Analysis and identifying different macerals under a microscope using polished grain mounts. I greatly appreciate help of Todd Ventura with discussion of GC-MS data.

I am indeed thankful to Associate Professor Bob Stewart for running all the XRD samples. I greatly appreciate his help by critically reading some parts of the manuscript and rendering invaluable advice and guidance from time to time throughout my PhD.

I would like to acknowledge the help and support of Graham Freeman, Senior Technician, Chemistry Department, Massey University. I am indebted to him for his useful discussion and helping me with the FTIR analysis and Soxhlet Extractions. I am immensely grateful to John Sykes from School of Engineering and Advanced Technology, Massey University, for the GC-MS analysis.

I greatly appreciate the assistance I received through my research from the staff of the Soil and Earth Science section, Institute of Agriculture and Environment, especially Professor Mike Hedley, Lance Currie, Peter Bishop, Clel Wallace, Ian Furkert, Glenys Wallace, Ross Wallace, Anja Mobis, Mike Bretherton and Liza Haarhoff.

This thesis is dedicated to my abbu and ammi for their love, endless

support and encouragement.

Table of Contents

List of Tables

List of Figures

Chapter 1 – Literature review and research objectives

1.1 Introduction

Fossil fuels are important to each of the economies of the world (Asif & Muneer, 2007; Murphy, 2012; Seljom & Rosenberg, 2011). Increasing oil and natural gas prices as well as technological advances in fossil fuel extraction have led to the widespread use of the term "non-conventional oil and gas resource" (Lindstrom, 2012; McKellar *et al.*, 2009; Patterson, 2012). According to the International Energy Agency (IEA), conventional oil resources contain a mixture of hydrocarbons that exist in liquid phase under normal surface conditions. In contrast, non-conventional resources are defined as those containing oil or gas that cannot be recovered through pumping in their natural state from an ordinary production well without heating or dilution of the hydrocarbon. Fossil fuels from non-conventional deposits can therefore not be produced, transported or refined using conventional methods (International Energy Agency, 2011).

Non-conventional oil and gas resources include oil shales, native bitumen, oil sands, tar sands and extra heavy oil (Chengzao *et al.*, 2012), and due to an insatiable demand for energy, the development of non-conventional resources has been placed at the forefront of many countries' strategic energy planning (Maloney & Yoxtheimer, 2012; Rajnauth, 2012). According to Rajnauth (2012) the demand for oil and natural gas will continue to increase for the foreseeable future and we must now rely on non-conventional resources to fill the gap between demand and supply. Rajnauth's commentary looks at the implications for the future and the technologies required to develop non-conventional resources. One non-conventional resource that has received attention in recent years is oil shale due to the relatively large scale of oil and gas reserves stored within this type of resource (Kleinberg *et al.*, 2007; World Energy Council, 2007). According to an estimate by Johnson *et al.* (2010) the total global resource of recoverable shale oil is approximately 2.8-3 trillion barrels. This exceeds the world's proven conventional oil

reserves which are estimated to be 1.342 trillion barrels (Owen *et al.*, 2010). About 72% of recoverable shale oil is present in the USA near the common borders of Wyoming, Utah and Colorado (Mittal, 2012).

1.2 Oil shale and shale oil

"Oil shale is a fine-grained sedimentary rock containing sufficient organic matter from which hydrocarbon (either oil and/or gas) can be extracted by distillation" (Mittal, 2012; Watson *et al.*, 1985; World Energy Council, 2007). Tyson (1987) defined oil shales as "dark-coloured, fine-grained mud rocks having the sedimentological, palaeoecological and geochemical characteristics associated with deposition under oxygen-deficient or oxygen free bottom waters" (Tyson, 1987). In a dictionary by the American Geological Institute (1962) the term oil shale is defined as "shale containing such a proportion of hydrocarbons as to be capable of yielding mineral oil on slow distillation". Jamal (2006) defined oil shale as "sedimentary rock where solid organic content is insoluble in organic solvents, but forms liquid oil-like hydrocarbons when exposed to destructive distillations, i.e. to temperatures up to 500-600 ºC, with a minimum oil yield of around 5%". According to Speight (2006) an oil shale is a special class of bituminous rock; defined as "argillaceous, laminated sediments from which shale oil is recoverable only when heated to sufficient temperature causing thermal decomposition of the organic material (kerogen) in the shale" (Speight, 2006).

Literature definitions for oil shales are therefore varied, and reflect the different opinions of researchers in the field. In the context of this research, oil shales are defined as fine grained sedimentary rocks, containing organic matter that releases shale oil under distillation.

Shale oil is not a naturally occurring product, but is formed by the pyrolysis (chemical decomposition by the action of heat) of kerogen in the oil shale. Crude shale oil, sometimes referred to as "retort oil", is the liquid oil product obtained from the retort after pyrolysis (Speight, 2006). Synthetic crude oil is the upgraded oil product resulting from the hydrogenation of crude shale oil (Watson *et al.*, 1985). Oil shale reserves have

been found in over 30 countries (Aunela-Tapola *et al.*, 1998). Estimates of recoverable shale oil around the world in different countries are shown in Table 1.1.

Table 1.1. Estimated recoverable shale oil in the world (Enefit, 2011)

Countries	Percentage of the world's recoverable shale
USA	72.7
Canada	12.4
Eastern Europe	11.7
China	3.5
Western Europe	1.4
South America	0.2
Africa	0.8
Australia and New Zealand	0.1
Other Asia	0.1

According to Lomborg (2001) in his article "Running on empty?" oil shale can fulfil the world's longer term needs for oil; and if shale oil is sold at $40 per barrel (a very economical price which is less than one third of the current price of crude oil) the available resources of oil shale could supply oil to the world at the consumption rate of the time for the next 250 years. According to Heinberg (2003) the total shale oil reserves are enough to fulfil energy needs for 5,000 years. According to Gosden (2012), Saudi Arabia, the world's biggest crude exporter from conventional deposits, risks having no available oil for export by 2030. Therefore, longer term growth in oil production must necessarily come from new supply sources like oil shale, oil sands, deep offshore and Arctic resources (National Petroleum Council, 2011). A Goldman Sachs report (Durham, 2012) and the Chron newspaper (Fowler & Chronicle, 2012), estimated that the United States, currently the No. 3 oil producer behind Saudi Arabia and Russia, was well positioned to take the world's top spot as the largest oil producer by 2017 by exploiting its non-conventional oil resources. Other areas in the world with notable oil shale deposits that have been targeted for exploration include Brazil, Israel,

Jordan, Australia, China, Estonia, France, South Africa, Spain, Sweden and Scotland (Gordon, 2012).

1.3 History of oil shales

The use of oil shale can be traced back to ancient times. Shale rock mined from the Kimmeridge deposit (England) was used by the Iron Age British tribesmen and Romans in the making of armlets (West, 2009), presumably due to the pliable nature of the rock which was a function of its recognised high organic matter content. The use of shale oil was recorded in Switzerland and Austria as early as the 1300s (Alderson, 2008). In 1596, the personal physician of Duke Frederick of Württemburg noted that a mineral oil distilled from oil shale could be used in healing (Moody, 2007). By the 17th century, British Patent Number 330 was issued in 1694 to Martin Eale, who "found a way to extract and make great quantities of pitch, tar and oil out of a sort of rock" (Cane, 1967). At the same time the oil produced from the distillation of oil shale was used to light the streets of Modena, Italy (Moody, 2007).

The modern industrial mining of oil shale began in 1838 in Autun, France, when an oil shale deposit at this location began to be exploited commercially. In Scotland the oil shale industry began in 1859 in Broxburn, West Lothian. Canada produced some shale oil (from 1859 to 1861) from oil shale of the Ordovician Whitby Formation near Collingwood, Ontario (Barker *et al.*, 1983). The Canadian and U.S. shale oil industries closed by 1861 because they could not compete with crude oil production from conventional reserves discovered in Pennsylvania (World Energy Council, 2007).

As shown in Figure 1.1, oil shale extraction gradually increased from the late 1890's because of increased demand and the production of automobiles and trucks, and due to the shortage of gasoline for transportation needs. An important event in the history of shale demand was the switch to oil shale firing at the Tallinn Power Plant in 1924 in Estonia. The electrical capacity of this power plant was 23 MW. After 1924 many oil shale power plants were built in northern Estonia (Ots, 2007). According to Aunela-Tapola *et al.* (1998), more than 90% of Estonia's electricity in the late 1990s was produced from domestic oil shale.

By the 1930's oil shale extraction increased markedly and by the late 1930's the annual mining of oil shale rock from Russia, China, Brazil, Scotland, Estonia and Germany was over 5 million metric tonnes (Figure 1.1). Production fell in 1940's due to World War II (Figure 1.1).
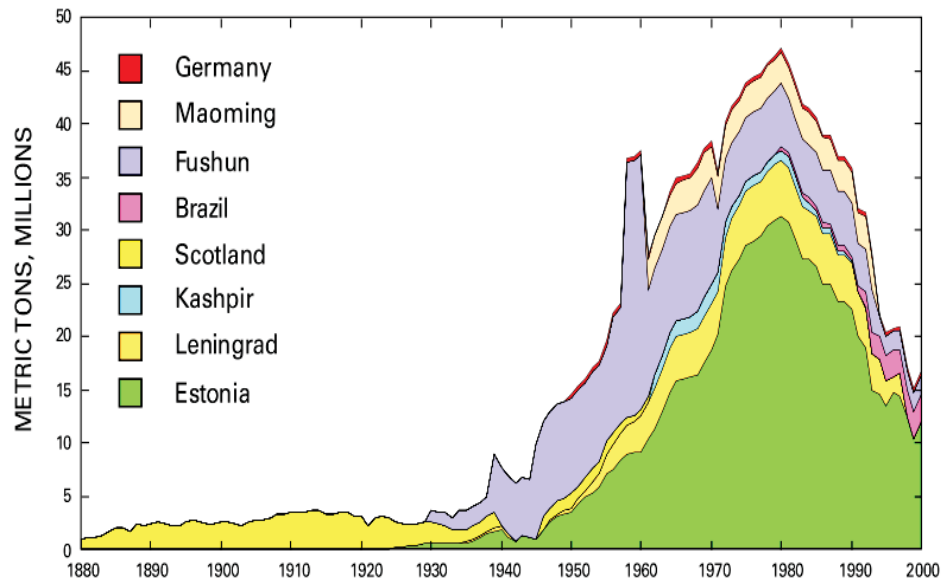
Figure 1.1. *Extraction of oil shale from 1880 to 2000 after (World Energy Council, 2007)*

Around the middle of the 20th century, shale oil became uneconomical in many countries due to cheaper supplies of petroleum crude oil that began to appear from the Middle East. However, oil shale production continued to increase in Estonia, Russia and China. As a result of the oil crisis in 1973, oil shale production again increased. The peak production period was 1979-1981, when in excess of 46 million tonnes of oil shale was mined in the major oil shale production countries (Estonia, Russia, China, Germany, Brazil and Scotland) with two thirds of this amount being mined in Estonia (Figure 1.1). The average shale oil production over this period was 100 L/tonne (Arro *et al.*, 2003; World Energy Council, 2007).

After 1981 there was again a decrease in oil shale extraction due to falling oil prices, the realisation that methods to recover oil from the shale rock (retorting) were expensive,

the common low yield of oil from the shale rock, and due to the termination of development incentives in place in many countries up until this time (Kleinberg *et al.*, 2007). As a result, oil shale could again not compete economically with conventional petroleum as an energy source.

Current commercial extraction of oil shale occurs in China, Brazil and Estonia (Qing *et al.*, 2011; Speight, 2012). The amount of shale oil produced by these countries currently is between 5 and 10 thousand barrels per day (Christian, Pers. comm., 2013). There are some pilot production sites in the United States to produce shale oil from the Green River Formation (RD&D pilot projects at the oil shale basin like Enefit's Utah Project, American Shale Oil and Shell ICP) (National Oil Shale Association, 2013) and projects under study in Jordan, Israel and Morocco (Christian, Pers. comm., 2013; International Energy Agency, 2011).

1.4 Petrogenesis of oil shale

A wide range in physical and chemical properties are associated with oil shales from different areas around the world (McKee & Goodwin, 1923; Yen & Chilingar, 1976). Hence only a much generalized concept of the genesis of oil shale can be presented here due to the variable character of constituent rock types. Oil shales result from the contemporaneous deposition of fine-grained mineral debris and organic material (Yen & Chilingar, 1976). The conditions required for the formation of oil shales include: abundant organic productivity, the early development of anaerobic conditions, and a lack of destructive organisms (Dyni, 2006). Continued sedimentation, perhaps coupled with subsidence, provides the overburden pressure that is necessary for compaction and diagenesis of organically-rich strata. Owing to chemical reactions that occur during diagenesis, even in a relatively low temperature environment ($\approx 150^{\circ}$C), there is a loss of volatile components from the organic fraction. Chemical activity ultimately produces a sedimentary rock having a high content of refractory organic material (Yen & Chilingar, 1976). As oil shales were originally deposited as sediment in an environment of either marine or fresh tranquil water such as isolated marine basins, lakes or deltaic

swamps, it is not surprising that oil shales have a wide range in organic and mineral composition (Yen & Chilingar, 1976).

1.5 Composition of oil shale

Oil shales are normally a heterogeneous mixture of inorganic and organic materials (Sert *et al.*, 2009). The inorganic fraction generally consists of silicates (quartz + feldspar + clay minerals), carbonates (calcite, dolomite) and pyrite (Sert *et al.*, 2009). The organic fraction is mainly composed of the remains of algae, spores, pollens, plant cuticle and corky fragments of herbaceous and woody plants, and the cellular remains of lacustrine, marine, and terrestrial plants (Dyni, 2006). These organic materials are mainly composed of carbon, hydrogen, oxygen, nitrogen, and sulphur. Some organic matter in the oil shale retains its original biological structure and thus the genus or species of the parent material can be identified (Dyni, 2006). While in others, the structure is destroyed and it is thus amorphous (described by the term bituminite). The origin of this amorphous material is not well known, but it is likely a mixture of degraded algal or bacterial remains (Dyni, 2006). The organic matter in oil shales is divided into two fractions: kerogen and bitumen.

1.5.1 Kerogen and bitumen

Kerogen is often defined as the potential source of oil and gas in an oil shale (Speight, 2006). It is a complex solid mixture of large organic molecules and its composition can vary from sample to sample. Because of its complex nature, it is hard to define the molecules' structure. Yen (1976) proposed a chemical model for the structure of kerogen as $C_{220}H_{330}O_{18}N_2S_4$ (Molecular weight of 3,414). Khraisha (2000) represented the kerogen structure as $C_{200}H_{300}O_{11}N_5S$.

The kerogen macromolecule has not gone through the "oil window" i.e., it is not mature enough or at the correct high temperature and pressure conditions to generate liquid oil (Alderson, 2008; North, 1985). The name literally means "producer of wax" (Weitkamp

& Gutberlet, 1970). Kerogen is a light-brown mixture of solids having no appearance of oil (Robinson & Cumins, 1959) and is mainly composed of carbon, hydrogen and oxygen with traces of nitrogen and sulphur (World Energy Council, 2007). It has a high hydrogen-to-carbon ratio as compared to coal and heavy oil and is therefore considered superior to them as a source of liquid fuel (Alderson, 2008).

When oil shale is heated to a sufficiently high temperature in a retort, the kerogen is thermally decomposed (cracked) to produce lower molecular weight products that are liberated in the form of vapours, mist and liquid droplets of shale oil and light hydrocarbon gases such as methane, ethane, ethene, propane and propene, as well as other products such as H_2, N_2, CO_2, CO, NH_3, gaseous H_2O and H_2S. A carbon residue typically remains on the retorted shale (Watson *et al.*, 1985). The quantity of oil that can be extracted from oil shale by heating (distillation) ranges from 4% to more than 50% of the weight of the rock. This is equivalent to between 42 and 568 litres of oil/ tonne of rock (Tucker, 1991).

The composition and structure of kerogen depends on the origin of the organic matter from which it is evolved and also on the degree of its evolution. Kerogen has been classified into three main types based on the contents of carbon (C), hydrogen (H) and oxygen (O) (Figure 1.2) (Tissot & Welte, 1978c).

Kerogen Type-I (algal) Type-I kerogen has a high H/C and low O/C ratio (H/C is typically 1.25 or higher and the O/C is less than 0.10). It mainly consists of lipid material, particularly aliphatic chains which come from algae and also from the severe biodegradation of other organic compounds. Many oil shales contain this type of kerogen. Type-I kerogen is prone to form liquid (oil) (North, 1985; Tucker, 1991).

Kerogen Type-II: (marine) has relatively high H/C and low O/C ratios (H/C is typically 1.3-1.7 and O/C is 0.18 or less). This type of kerogen is common in many marine organic-rich types of sediments which are deposited in reducing environments. The organic matter is mainly derived from phytoplankton, zooplankton and microorganisms (bacteria) (North, 1985; Tucker, 1991).

Kerogen Type-III: (humic – terrestrial) has low H/C and high O/C ratios (H/C ratio is usually <1.0 and O/C ratio is 0.03-0.3) and is largely derived from terrestrial plant matter. Type-III kerogen is prone to form gas and does not generate oil (Tucker, 1991).
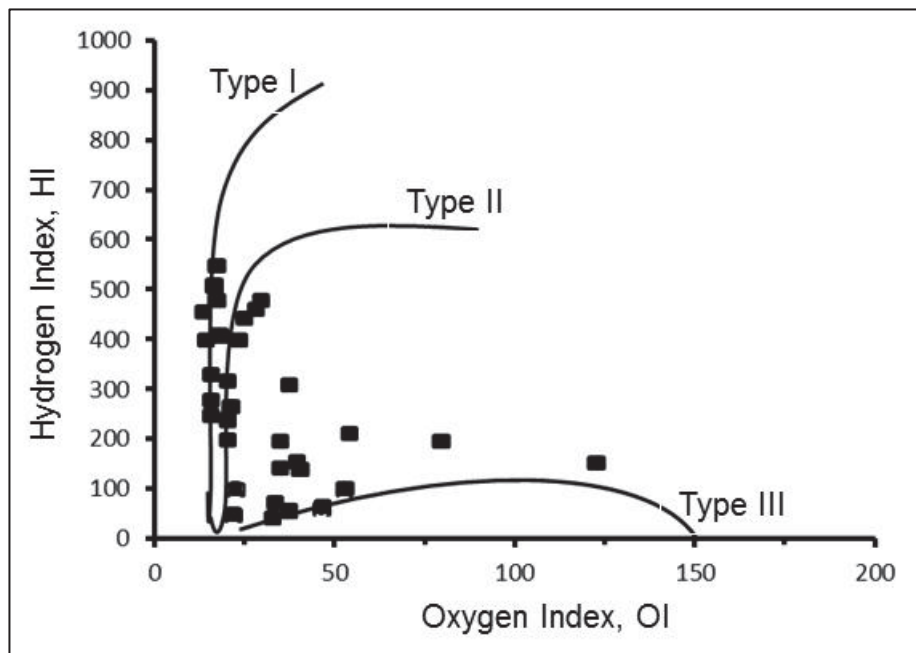
Figure 1.2. *Van-Krevelen diagram showing where kerogen types I, II and III occur in an Hydrogen Index versus Oxygen Index bivariate plot (SRA data). Redrawn from Leckie et al. (1992) who studied the Waipawa Formation.*

Bitumen on the other hand is that part of the organic material containing free hydrocarbons, asphaltenes and resins generated through thermal maturation and diagenesis during burial (Vanderbroucke *et al.*, 1976). When kerogen reaches the onset of thermal maturity, small molecules consisting of hydrocarbons and heterocompounds are broken off the kerogen matrix. These small compounds are much more mobile than the kerogen molecules and are the direct precursors of oil and gas. Tissot and Welte (1978c) named these molecules bitumen. The compounds identified in the bitumen contain paraffins, cycloalkanes, aromatics and heteroatoms with nitrogen, sulphur and oxygen atoms (Wolfson *et al.*, 2011).

Bitumen is an intermediate product between kerogen and oil/gas. With depth of burial and age (thermal maturity) kerogen in sediments is slowly converted first into bitumen and then to oil and gas through secondary decomposition of bitumen. Maturity of source rocks can be inferred through assessment of the bitumen to total organic carbon content (TOC) ratio of a hydrocarbon bearing rock (Bernard *et al.*, 2012; Peters & Cassa, 1994).

Bitumen, unlike kerogen, can be extracted from rocks using different solvents such as dichloromethane (DCM), benzene, carbon disulphide, pyridine and chloroform (Blanco *et al.*, 1992). Such a procedure is very useful during lab-based assessment of the production potential of a potential source rock. But according to Vanderbroucke *et al.* (1976), extraction is never complete and extraction of the bitumen not only depends on the polarity of solvent but also on analytical procedures such as sample grinding, temperature, agitation of the extraction, and the duration of extraction.

1.6 Types of oil shale

Three different types of oil shales are known − *terrestrial, lacustrine and marine*, due to different distinctive organic matter assemblages found within a shale (Hutton, 1987).

1)   ***Terrestrial oil shales*** – These oil shales are formed in small lakes, lagoons and bogs. These contain organic matter with dominant liptinite (vitrinite and inertinite) derived from terrestrial plants (angiosperms and gymnosperms) (Hutton, 1987).

2)   ***Lacustrine oil shales*** – These oil shales are formed in large lakes and their organic matter is dominated by liptinite (principally alginite) derived from lacustrine (freshwater, brackish or saline) algae. Two types of lacustrine oil shales are known *torbanite* and *lamosite*. In *torbanite*, alginite is dominated by *telalginite* derived from *Botryoccoccus*–related algae. In *lamosite*, alginite is dominated by *lamalginite* derived from *Pediastrum*–related algae (Hutton, 1987).

3)   ***Marine oil shales*** – These form in a marine environment, typically shallow seas, and contain liptinite derived from marine organisms. Three types are known

marinate, *tasmanite* and *kuckersite*- depending on the type of precursor algae they contain (Hutton, 1987).

1.7 Assessment of oil shale deposits

1.7.1 Oil shale exploration

The techniques used for oil shale exploration should start with a comprehensive geological evaluation of the potential resource (Bell, 1990; Brown, 1990; O'brien & Blaine, 2009; Rogner, 1997). Good base maps are required for detailed geological or engineering work. Topographic maps are ideal for recording and presenting geologic information and for engineering, planning and design. Aerial photography (where available) should be utilised early in the initial phase of exploration and more detailed resource specific maps can be compiled as exploration progresses (Brown, 1990). The next stage of exploration is drilling and a detailed drilling plan should be prepared by a geologist experienced in sedimentary and structural geology before any drilling is carried out. A drilling programme will help to delineate the size of the resource (Pollastro & Scholle, 1984). The initial exploration boreholes may be spaced many kilometres apart, but will decrease to between 1 and 2 km as definitive drilling to accurately delineate the potential of the resource becomes concentrated on a specific mine area (Brown, 1990). Core and drill cutting samples can be collected for laboratory analysis during this phase of analysis (Brown, 1990). Geophysical borehole logs are used to characterise the geophysical parameters of the resource and as means to correlate results between wells. Different rock characteristics or reservoir parameters can be determined using the well logs. These may include permeability, porosity, resistivity, thickness of strata (Serra, 1984; Tixier & Alger, 1970).

1.7.2 Estimating the production potential of non-conventional oil shale deposits

Samples collected from drill holes and from surface exposures are analysed using a range of techniques to evaluate the oil production potential of oil shale deposits (Peters & Cassa, 1994; Sen, 2011). In most cases these are the same analytical techniques that are applied to the evaluation of conventional hydrocarbon deposits and include Hydrous Pyrolysis, Fischer assay and Rock-Eval Pyrolysis. For example, several European (Francu *et al.*, 2007) and New Zealand source rocks (Sykes, 1996) have been assessed for their production potential using the conventional Fischer and Rock-Eval tests.

Hydrous Pyrolysis – is an approach used to generate pyrolysates similar to natural petroleum. This method involves heating about 200 g of source rock sample with approximately 400 mL of deionized water in a 1 L batch reactor to 360°C at a rate of about 6°C/min and holding for 72 hours. This results in expulsion of petroleum-like oil, which accumulates on the surface of water in the reactor. Other combinations of time and temperature can be used depending on the nature and goals of the particular experiment (Jin *et al.*, 2012; Lewan, 1997; Lewan *et al.*, 1985; Lewan *et al.*, 1979).

Fischer Assay – involves the heating of approximately 100 g of sample, crushed and sieved through 2.38 mm mesh, in a small aluminium retort to 500°C at a rate of 12 °C/min. The heating is then held at 500°C for 40 minutes. The distilled vapours of oil, gas and water are passed through a condenser cooled with ice water into a graduated centrifuge tube. The oil and water are separated through centrifugation (A. Al-Harahsheh *et al.*, 2009; Allix *et al.*, 2010; Dyni, 2003).

Rock-Eval Pyrolysis – otherwise known as Source Rock Analysis (SRA), is the most commonly employed technique used to characterise sedimentary organic matter. This method consists of pyrolysing about 100 mg of ground whole rock samples isothermally at 300°C for 3-4 min. During this time the free hydrocarbons are volatilised and quantitatively detected by a flame ionisation detector (FID). These free hydrocarbons are labelled S1. The CO_2 liberated up to 400°C is detected by an infra-red (IR) cell and is labelled as S3. The next step is programmed pyrolysis at 25°C/min to 650°C. During

this second step organic hydrocarbons are generated from the decomposition of kerogen in the rock. The hydrocarbons are detected by the FID detector, labelled as S2 and when interpreted provide data that can be considered to estimate the generation potential of the rock (Akande *et al.*, 2012; Oyal *et al.*, 2010; Peters, 1986; Weatherford Laboratories Operators Manual, 2010). Both heating steps are performed in an inert helium atmosphere.

In SRA the thermal maturity of a source rock is calculated from a value Tmax. This is a standardised parameter and is defined by the temperature when the S2 peak reaches its maximum. The type of kerogen present in the oil shale can be inferred from its position in the van-Krevelen diagram by plotting its normalised hydrogen content (HI = S2 x 100/TOC[1]) versus its normalised oxygen content (OI = S3 x 100/TOC) (Figure 1.2) (Tissot & Welte, 1978c).

Table 1.2 summarises these conventional techniques that have been used to assess the oil production potential of all source rocks (including oil shales), and briefly outlines the information that can be obtained from each.

Table 1.2. Conventional exploration tools used for assessment of oil potential of source rocks.

Conventional exploration tools	Geochemical parameters	Information
Hydrous Pyrolysis	--	Product oil yield
Fischer Assay	--	Weight percentage of shale oil Water content Quantity of retorted shale
Rock-Eval Pyrolysis/Source Rock Analysis (SRA)	TOC, S1, S2, HI, OI, Tmax	Organic richness Free oil content (bitumen) Remaining hydrocarbon potential (kerogen) Type of organic matter Maturity

---

[1] TOC: Total organic carbon

1.7.2.1 Limitations to conventional production potential assessment techniques

The data obtained through application of the techniques described in Table 1.2 provide an initial assessment of the hydrocarbon potential of a rock. Interpretation of these data is required to confirm the generation potential and to understand the physical and geochemical characteristics of the rock. For example, in the assessment of oil shale deposits the identification of kerogen types is very important because of the strong effect of kerogen on yield, chemistry of the resulting oil, and on the conversion temperature of kerogen into oil (Tissot & Vandenbrouck, 1983). To illustrate with a specific example, *torbanite* (see section 1.6, types of oil shales) is generally regarded to give a high oil yield. The resulting oil has a relatively high aliphatic content and is suitable for cracking to produce crude oil (Sykes, 1996). The kerogen type is not directly quantified by the conventional techniques described in Table 1.2. Ratios like HI and OI from SRA data can help in the interpretation of kerogen types, but such SRA-derived information can be misleading, especially in the scenario where a shale contains mixed kerogen types (Tissot & Vandenbrouck, 1983).

Peters (1986) was perhaps the first commentator to publicly describe the many drawbacks of SRA for the assessment of some fossil fuel resources. Peters described that for immature samples, SRA pyrograms show poorly separated S1 and S2 peaks due to low S1 and S2 responses, and hence can give unexpected values for S1 and PI, which is defined here as Production Index [PI = S1/(S1+S2)], a parameter that is used to estimate thermal maturity (Behar *et al.*, 2001).

The problems of SRA also extend to the assessment of carbon content. High total organic carbon (TOC) does not necessarily correlate with a high S2 because of the types of organic matter in the sample. For example, thermally post mature carbon, or graphite, which will read as 100% TOC, will show no pyrolysis response in the SRA. Such an anomaly in TOC against S2 can only be resolved through microscopy of macerals (defined as recognisable constituents of kerogen that can be differentiated as to type of organic matter by their morphology), and vitrinite reflectance. Table 1.3 illustrates an example from Peters (1986), where two different oil shales collected from the same well but at different depths (from 594 m and 602 m), were assessed by SRA. From the SRA

results it was found that both oil shales had very similar TOC values but their S1 and S2 values were different. A big difference in the HI values of the two samples was also observed, suggesting the presence of different types of organic matter, or more specifically, kerogen. But, as has been highlighted in the current discussion, the identification of kerogen type using SRA can be misleading. Kerogen identification is very important because different types of kerogen (Section 1.5.1) have different origins and thus have different potentials to generate oil and gas. The technique that can be used to identify the types of organic macerals present in kerogen, and therefore to confirm the validity of SRA analysis, is organic petrography.

Table 1.3. TOC and Rock-Eval pyrolysis results for selected oil shale core samples from a well in Montana, after Peters (1986).

Depth (m)	TOC (wt%)	S1	S2	HI (mg HC/g C_{org})	OI (mg CO_2/g C_{org})
		(mg HC/g rock)			
594	3.54	1.77	23.81	673	34
602	3.56	0.28	2.96	83	34

Source Rock Analysis provides direct information on the maturity of an analysed sample inferred from the Tmax values. The Tmax value increases with higher maturity, however it is affected by the type of organic matter present and the inorganic mineral matrix (Hollis & Manzano-Kareah, 2005). The maturity results inferred from Tmax can be misleading, especially where the rock contains Type III kerogen having low S2 response (because they are gas prone) and also in samples with low hydrocarbon yield (Behar *et al.*, 1997). Therefore correlation with other maturity indicators is desirable. Vitrinite reflectance is the most commonly used organic maturation indicator and is usually used to cross-check the maturity suggested from SRA (Oudin & Vandenbrouck, 1993). Vitrinite reflectance is a quick, non-destructive and accurate method to determine maturity as compared to SRA (Dutton, 1980; Tissot & Welte, 1978d).

Identification of the non-carbon minerals present in a potential source rock is also not possible using the conventional SRA assessment technique. Such knowledge is very

important due to the effect of silicate minerals on kerogen decomposition during retorting and hence on the production of oil from a shale or other conventional deposit. Regtop *et al.* (1985) found that clay minerals catalyse the decomposition of various hydrocarbons. Hetenyi (1995) reported a catalytic effect of both calcite and montmorillonite on the decomposition of kerogen. Borrego *et al.* (2000) also found that montmorillonite has some catalytic effect on the initiation of the thermal cracking of kerogen. Al-Harahsheh *et al.* (2011) studying the effect of demineralization on Jordanian oil shales found that the temperature at which maximum devolatalization occurs is lower for oil shales by about 10-12 % compared to oil kerogen. These results suggest that the shift in temperature is due to the presence of non-carbon mineral matter in the oil shales, and that this catalyses the cracking reactions. This may subsequently cause the reactions to occur at lower temperatures.

The decomposition of an oil shale as a function of temperature is similarly not determined during SRA. Source Rock Analysis provides quantitative data on hydrocarbon yields S1 and S2 but does not show the overall weight loss behaviour when the oil shale is heated in an inert atmosphere. Data on thermal decomposition can only be generated through thermal gravimetric analysis (TGA) of a source rock. Source Rock Analysis also does not provide any information on the chemical structure of kerogen or bitumen present in an oil shale. In order to generate data describing the chemical structure of bitumen and kerogen, detailed chemical analyses on extracts of each of these organic materials is required.

In summary, it can be said that research related to oil shale deposits reported in the literature or in industry publications has assessed potential oil shale source rocks according to conventional analytical techniques. These are the same techniques that are used to assess conventional petroleum/gas targets. However, there may be limitations to the understanding that can be gained through the use of such techniques.

1.7.3 Production of oil from oil shale

The production of oil from oil shales presents additional technological challenges over those for oil production from conventional resources. Hydrocarbon products extracted from oil shales are not readily usable and require further upgrading and refining (Nakicenovic *et al.*, 1998; Rogner, 1997).

The commercial process of extracting oil from oil shale is done by retorting which is a heating process in which the oil shale is heated to between 500-600°C. At this temperature the oil shale decomposes and is converted into shale oil along with the release of some gases such as light hydrocarbons, H_2S, NH_3, CO and CO_2 (Khraisha, 2000). The process of retorting was first developed in 1850 by James Young of Ireland (Yen & Chilingar, 1976).

There are two oil shale retorting processes, aboveground (*ex-situ*) and underground (*in-situ*) retorting (Andrews, 2006). In aboveground retorting, oil shale is mined either by open-pit or underground mining methods and then brought to the surface, crushed and retorted or pyrolysed in a fixed retorting plant at a temperature of approximately 500-600°C. Retorting is driven by contacting the shale with a hot solid heat carrier material, such as hot spent shale, ceramic balls, sand or a gaseous heat carrier material, such as light hydrocarbon gases (Carr, 1962; Watson *et al.*, 1985). The final waste product is removed from the retort and is either recycled as a heat carrier material or discarded (Watson *et al.*, 1985). While in i*n-situ* retorting, shale oil is recovered from an oil shale without removing the oil shale from its natural location. This method minimises mining costs (Carr, 1962) and can be used where the oil shale is too deep for mining. The shale is fractured using explosives and heated underground by heaters placed in vertical holes drilled through the entire thickness of a section of oil shale to release oil and gases. Hot gases are then passed through the shale by way of a system of drilled vertical holes to liberate shale oil from the oil shale layer (Qian & Wang, 2006).

In the 1970's, due to the world oil crisis, many oil companies developed retorting technologies. An underground retort was constructed by Occidental Petroleum Co., USA, which was operated in Colorado in 1972. Another *in-situ* retort was operated in

Utah by Geokinetics Inc. in 1981 (Qian & Wang, 2006). After 1990, many projects were closed due to the decrease in oil prices plus technical difficulties and costs associated with these retorting technologies. In March 2011, the United States Bureau of Land Management called into question proposals in the U.S. for commercial operations to produce hydrocarbons from oil shale, stating that "there are no economically viable ways yet known to extract and process oil shale for commercial purposes" (Nedd, 2011). There are no commercial-scale oil shale *in situ* operations anywhere in the world at this time. However, field-scale research, development and demonstration projects are currently operating in western Colorado and eastern Utah (Robertson *et al.*, 2012).

Hydraulic fracturing (also known as fracking) is another technique used to recover hydrocarbon products from oil shales. Fracking is an extraction technique in which fluid (a mixture of water, sand and chemicals) is injected at very high pressure into a shale deposit to create fracture systems (Myers, 2012; PADEP, 2011). Sometimes the fractures are created by injecting gases like nitrogen or propane along with acids into a reservoir. The acid is used to clear pores within the reservoir by removing carbonates resulting in improved flow of fluids through fractures in the shale (Poole, 2012). According to International Energy Agency (IEA) (2011), horizontal drilling and fracturing of oil shales in Texas, Alaska, California, North Dakota and Oklahoma accounted for 56% of US oil production in 2011. Japan Petroleum Exploration Co. succeeded in extracting shale oil from the Ayukawa oil and gas field by pumping HCl into a shale rock layer (The Japan Times Online, 2012). In New Zealand hydraulic fracturing has been used as an exploration technique in the Taranaki Basin and more activity is expected in the near future (Ministry of Economic Development, 2012).

1.8 Non-conventional hydrocarbon deposits

1.8.1 Green River Formation

The two Green River Formation samples in this study, from Anvil Points Mine (APM) near Rifle, Colorado, were supplied by the USGS. These samples were collected from the Mahogany Zone of the Parachute Creek Member of the Green River Formation in Piceance Basin, Colorado. The Green River Formation is a sedimentary unit of Eocene age that occurs extensively throughout Colorado, Utah and Wyoming in the United States of America and is the greatest known potential oil resource in the world (Donnell, 1961; Hartman-Stroup, 1987). The Green River Formation was deposited in two main basins: the Uinta-Piceance Basin[2] and the Greater Green River Basin[3]. These basins are separated from each other by the east-west-trending, anticlinal Uinta uplift (Figure 1.3) (Roehler, 1992). The Piceance Basin formed together with Uinta Basin in eastern Utah and west Colorado and the Greater Green River Basin in the south-western Wyoming, north-eastern Utah and north-western Colorado in a warm-temperate to sub-tropical climate (Smith *et al.*, 2008; Tanavsuu-Milkeviciene & Sarg, 2012). These basins are separated from each another by chains of anticline basement-cored uplifts and were active from Cretaceous through Eocene (Figure 1.3) (Smith *et al.*, 2008). The Piceance Basin in the western Colorado is a structural and sedimentary basin which is bounded by Uinta uplift in the northwest, by an axial basin anticline in the north, in the east by the White River uplift, in the south by Gunnison uplift and in the southwest by the Upcompahgre uplift (Figure 1.3) (Tanavsuu-Milkeviciene & Sarg, 2012).

---

[2] Uinta Basin and Piceance Basin together form Uinta-Piceance Basin (Figure 1.3).

[3] Green River Basin and Washakie Basin together form Greater Green River Basin (Figure 1.3).
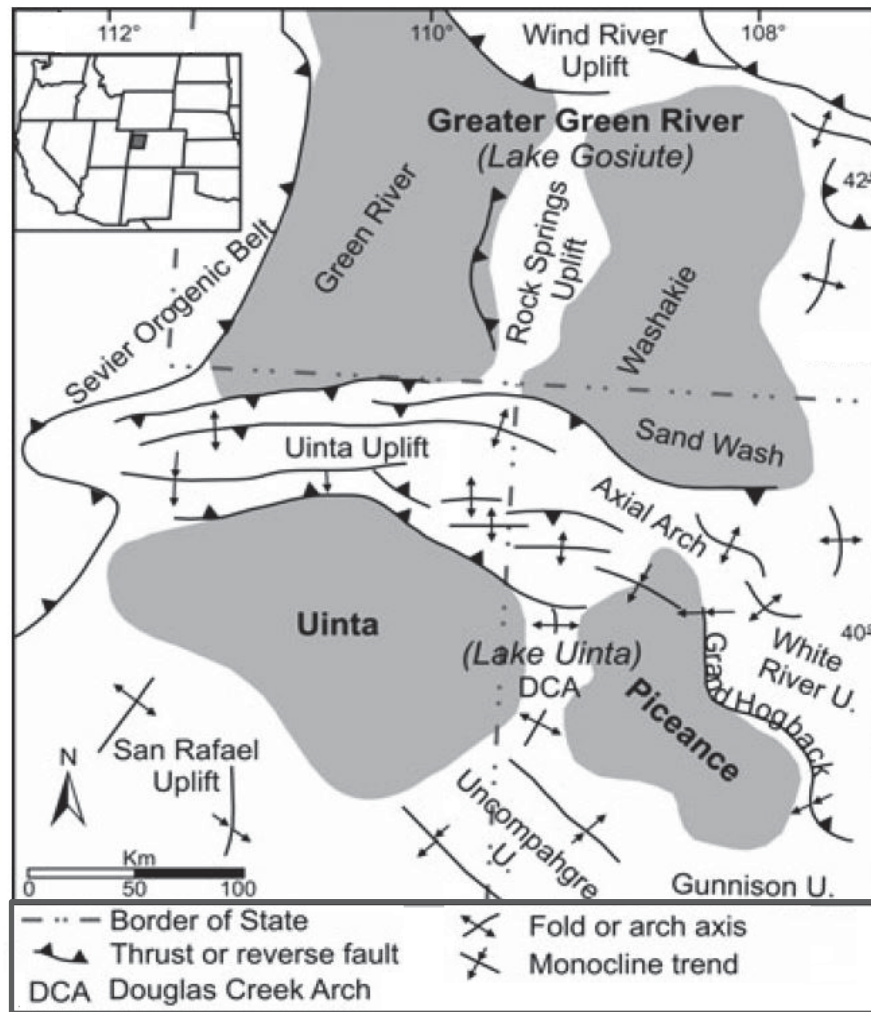
Figure 1.3. Eocene Basins of the western USA (adapted from (Tanavsuu-Milkeviciene & Sarg, 2012)). Green River Basin and Washakie Basin form a larger Greater Green River Basin.

The Green River Formation is composed of ancient lake deposits which occupied the Uinta Basin of Utah, Piceance Basin of Colorado and the Green River Basin of Wyoming; an area of about 65,000 km^2 (Dyni, 2006; Tuttle, 1973). During the early Eocene, fresh water lakes were established in both the Uinta and Piceance Basins. These lakes expanded during the early to middle Eocene across the Douglas Creek Arch[4] forming one large lake. Lake Uinta remained as a single large unbroken lake across both

---

[4] A faulted anticline that separates the Uinta Basin of northeastern Utah from the Piceance Basin of northwestern Colorado

basins and the Douglas Creek Arch throughout most of its history. Lake Uinta became increasingly saline with the passage of time and thus saline minerals were deposited in parts of Green River, Piceance and Uinta Basins (Brownfield *et al.*, 2010; Johnson *et al.*, 2010). These deposits include beds of trona ($Na_2CO_3 \cdot NaHCO_3 \cdot 2H_2O$), nahcolite ($NaHCO_3$) and eitelite; non bedded aggregates, nodules and crystals of nahcolite; microscopic crystals of dawsonite ($NaAlCO_3 (OH)_2$) in oil shale; veinlets and crystals of shortite ($Na_2Ca_2(CO_3)_3$.). These occurrences include deposits of bedded trona in the Green River Basin in southwest Wyoming, deposits of nahcolite and dawsonite commingled with high-grade oil shale in the Piceance Creek Basin in northwest Colorado, and bedded sodium carbonate salts near the town of Duchesne in the Uinta Basin, northeast Utah (Johnson *et al.*, 2010; Self *et al.*, 2010).

The Green River Formation consists of predominantly dark shale and marlstone. Sandstone, siltstone and limestone are other lithologic components present in parts of the formation. The formation as a whole is characterised by regular thin bedding. In the south-western part of Colorado (Piceance Basin), the formation is divided into four lithologic units named as Douglas Creek, Garden Gulch, Parachute Creek and Evacuation Creek Members. The formation in general represents a continuous depositional unit and the contacts between the several members are generally conformable and gradational (Bradley, 1931; Donnell, 1961). The Garden Gulch Member is a clay-rich oil shale and was deposited in the early stages of the lake's history, while the other three members were deposited later in the lake's history which are carbonate-rich zones of the Green River Formation (Self *et al.*, 2010; Tuttle, 1973).

The Parachute Creek Member is about 550 meters thick (Cashion, 1967) and consists of the richest oil shale beds (Bradley, 1931). Samples of the Green River Formation used in the current study are from this member of the formation. This member is divided into a series of rich oil shale zones separated by lean zones as shown in Figure 1.4. It is bounded at the top by a zone of lean oil shale called 'A groove' (Figure 1.4). Of these zones, the upper Mahogany Zone which occurs below the 'A groove' is made up of a group of oil-rich laminated oil shale beds (Figure 1.4) (Berg, 2008; Donnell, 1961; Duncan *et al.*, 1974; Tuttle, 1973). This upper oil shale zone is present throughout the Piceance Basin and is the richest and most important oil shale in the Green River

sequence. This zone has a maximum subsurface thickness of about 190 meters (Duncan *et al.,* 1974).

Figure 1.4. *Stratigraphy of the Green River Formation from the Anvil Points Mine (APM) near Rifle, Colorado (adapted from Berg, 2008). Samples from the southeast Piceance Basin have been analysed in this study.*

Bradley (1931) and Johnson (2012) considered the Parachute Creek Member to be "the oil shale facies of the Green River Formation". They stated that the Parachute Creek Member contains most of the oil-rich beds and very large proportion of low-grade oil shale as well. Burnham *et al.* (1996), Birdwell *et al.*(2011), Lewan & Roy (2011), and Cho *et al.* (2013) from their SRA studies of the Green River Formation from the Mahogany Zone found very high HI and low OI values (Table 1.4).

Table 1.4. Source Rock Analysis (SRA) results of Mahogany Zone oil shale from Green River Formation (--: not identified).

Sample	TOC (wt%)	S1	S2	HI (mg HC/g C_{org})	OI (mg CO$_2$/g C_{org})	Tmax (°C)	References
		(mg HC/g rock)					
Mahogany Zone	--	--	--	--	--	433	(Braun *et al.*, 1991)
Mahogany Zone	10.8	--	91.8	850	--	443	(Burnham *et al.*, 1996)
Mahogany Zone	18.6	4	174.7	944	10.2	443	(Birdwell *et al.*, 2011)
Mahogany Zone	15.8	3.7	134.3	848	34.2		(Lewan & Roy, 2011)
Mahogany Zone	--	--	--	1014	14		(Cho *et al.*, 2013)
Mahogany Zone	11.28	6.45	117.3	1040	18.9	439	(Cumming *et al.*, 2012)
	22.78	11.7	237.1	1041	8.4	443	
	22.59	9.55	248.1	1099	9.3	445	
	25.82	11.9	272.5	1055	7.0	436	
	14.47	7.5	149.1	1031	14.1	437	
	9.69	6.6	95.36	985	25.6	434	
	9.39	6.8	96.77	1031	21.4	434	
	10.30	6.3	108.9	1058	21.4	439	
	11.35	5.7	119.9	1057	14.8	441	
	18.15	14	265.6	944	6.4	436	
	21.14	10	223.9	1060	9.5	432	

The TOC data when plotted against S2 data in Table 1.4, all the Mahogany Zone oil shale samples can be seen representing exceptional potential of the oil shale to generate oil (Figure 1.5) (Peters & Cassa, 1994). The very high HI and low OI values illustrate the lacustrine origin of the oil shale with oil-prone Type I kerogen present in the oil shale (Lewan & Roy, 2011). The Tmax values of the Mahogany Zone oil shale samples range between 432 and 445°C suggesting the oil shale is immature to early-mature (Peters & Cassa, 1994).
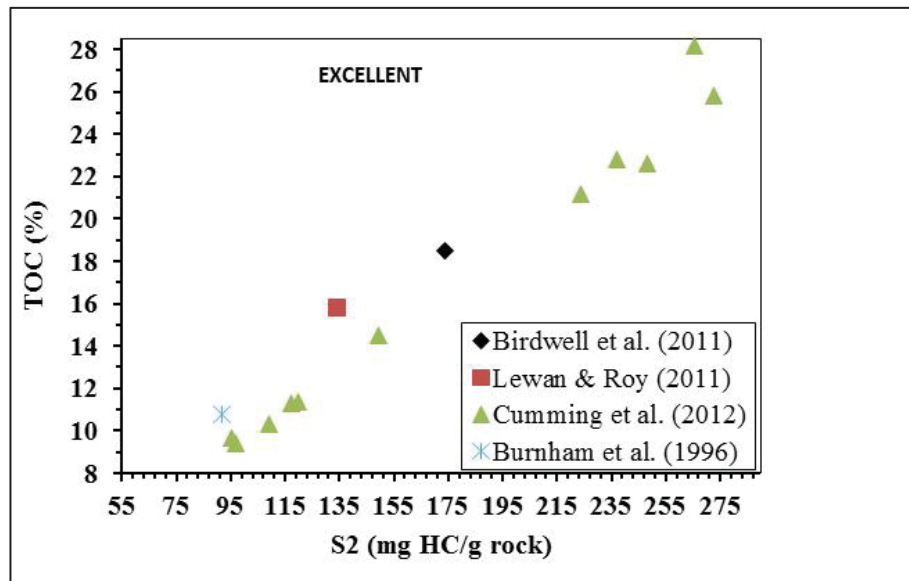
Figure 1.5. *Plot of TOC vs S2 for the Mahogany Zone oil shale samples collected from the Mahogany Zone in the Piceance Basin, Colorado. The exact location can be found from the references mentioned. All the oil shale samples lie in the excellent petroleum potential field.*

The U.S. Geological Survey (Johnson *et al.*, 2009) estimated a total of 1.525 trillion barrels of oil in place in different oil shale zones in the Eocene Green River Formation present in the Piceance Basin, western Colorado. This assessment was made by calculating oil yields using the Fischer Assay method. According to Donnell (1961) about 7000 million barrels of oil is contained in the Green River Formation in the Mahogany Zone yielding around 170 litres/tonne of shale oil.

1.8.2 Non-conventional hydrocarbon deposits in Pakistan

Many oil shale deposits are known in Pakistan, but their development has not occurred, due to very poor knowledge of their extent and characteristics (Jamil & Sheikh, 2012). However, Raza *et al.*(1993) have suggested that some deposits in the Kohat Basin (Figure 1.6) of northern Pakistan are good quality source rocks. A number of source rocks in this basin have been discussed by Raza *et al.*(1993). The Kohat Basin is

approximately 350 km west of the capital city Islamabad and contains sediments from Eocene to Recent in age that are complexly folded and faulted (Jamil & Sheikh, 2012). The general stratigraphy of the basin after Mirza *et al.* (2005) is shown in Figure 1.7.

Figure 1.6. *Map of Pakistan showing the Kohat Basin. After Ahmad et al. (2012).*

The Lower-Eocene sequence of the Kohat Basin has been divided into two parts based on its structural and depositional systems (Figure 1.7). The northern part of the basin represents marine shallow shelf environments of deposition (Panoba Shale and Shekhan Formation); whereas, the southern part of the basin represents marine to restricted

lagoonal environments during the Eocene period (Bahadur Khel Salt and Jatta Gypsum) (Mirza *et al.*, 2005).

AGE			NORTHERN KOHAT		SOUTHERN KOHAT	
MIOCENE			MURREE FORMATION		KAMLIAL FORMATION	
			FATEH JANG MEMBER			
OLIGOCENE						
EOCENE	UPPER	PRIABONIAN				
	MIDDLE	LUTETIAN	KOHAT FORMATION	Habib Rahi Limstone Member	KOHAT FORMATION	Habib Rahi Limstone Member
				Sadkal Member		Kaladhand Member
				Kaladhand Member		
	LOWER	YPRESIAN	KULDANA FORMATION (MAMI KHEL CLAY)		MAMI KHEL CLAY	
			SHEKHAN FORMATION		JATTA GYPSUM	
			PANOBA SHALE		BAHADUR KHEL SALT	
PALEOCENE	UPPER	THANETIAN	PATALA FORMATION		PATALA FORMATION	
			LOCKHART LIMESTONE		LOCKHART LIMESTONE	
	LOWER	DANIAN	HANGU FORMATION		HANGU FORMATION	

Figure 1.7. *Stratigraphy of the Paleocene-Miocene succession of the Kohat Basin, Northern Pakistan, after (Mirza et al., 2005) .*

1.8.2.1 Jatta Gypsum Formation

The Pakistani shale samples from Mir Kalam Kala and Speena Banda villages (supplied by the Centre of Excellence, University of Peshawar) were collected from the gypsiferous Jatta Gypsum Formation in Kohat Basin. The Jatta Gypsum Formation is

exposed only in few localities in the southern part of Kohat Basin (Khan & Zaman, 2003; Raza *et al.*, 1993). It conformably overlies the Bhadur Khel Salt, Panoba Shale and Shekhan Formation and conformably underlies the Kuldana Formation and Mami Khel Clay in different areas of the Kohat Basin (Shah, 2009) (Figure 1.7). A section at Jatta Gypsum Quarry (Lat. 33° 18' N: Long. 71° 17' E), in the Kohat area, has been designated as type section (Meissner *et al.*, 1974; Shah, 2009). Thickness of this formation ranges from 25 to 40 m (Shah, 2009). The Jatta Gypsum Formation is predominantly composed of greenish-white to grey gypsum and is massive to bedded and hard. It is also interbedded with shale, chalky-dolomite, clay-rich carbonate and sandstone at places (Ahmad, 2003; Meissner *et al.*, 1974). Gypsum of this formation interbeds with gypsiferous shale and bentonitic clay (Khan & Zaman, 2003).

The oil shales in the Kohat-Karak region occur 27-30 m below the top of the Jatta Gypsum Formation (Raza *et al.*, 1993). Six oil shale outcrops have been located in the area at Malgin, Banda Daud Shah, Dharangi, Banda Khando, Karak and Jatta Salt Quarry known as Malgin oil shale, Banda Daud Shah oil shale, Dharangi oil shale, Banda Khando oil shale, Karak oil shale and Jatta Salt Quarry oil shale (Raza *et al.*, 1993). These oil shale occurrences are rarely exposed in the area due to complex structural deformation of the area (Shah, 2009). These oil shale deposits occur as thin sheets embedded between the gypsum beds. However, sometimes the shale horizons are very thin or absent and a sharp and distinct contact of oil shale with the gypsum beds can be observed (Raza *et al.*, 1993). Due to the limited exposures and structural complications, it has not been possible to ascertain from the surface studies whether the deposition of oil shale is laterally continuous in the entire Kohat-Karak area or whether these are isolated lenticular accumulations (Raza *et al.*, 1993). The oil shale horizon occurring in the lower part of Jatta Gypsum Formation at the type section Jatta Salt Quarry is 3-4 m thick. It is light grey, loose, friable due to weathering effect and has a TOC of 3.1-7% (Raza *et al.*, 1993).

The TOC distribution of the different oil shales from different localities in the Jatta Gypsum Formation (Raza *et al.* 1993) is shown in Figure 1.8.
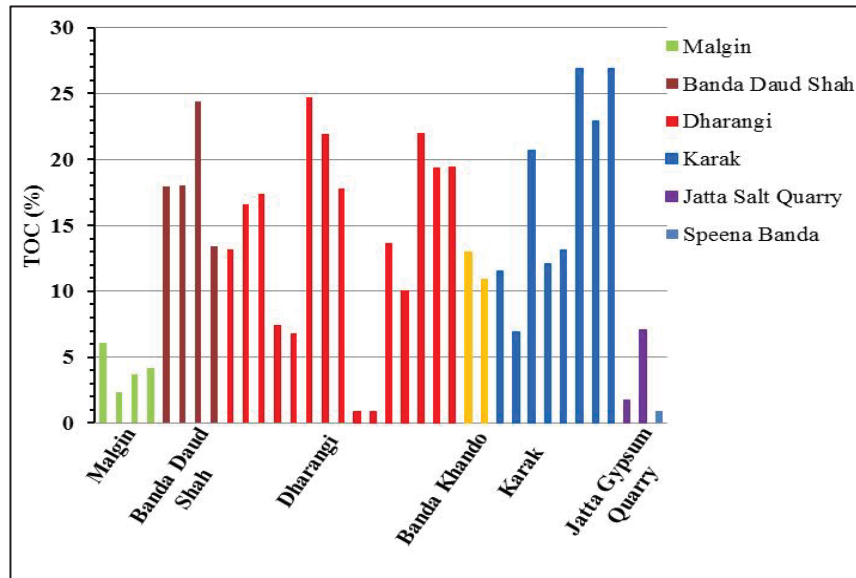
Figure 1.8. *Total organic carbon (TOC) content of outcrop oil shale samples from different localities in Kohat Basin (Pakistan), after Raza et al. (1993) and Fazeelat & Yousaf (2204).*

SRA results of outcrop oil shale samples from Dharangi in the Kohat Basin were published by Fazeelat & Yousaf (2004). They found a huge variation in the quality and quantity of organic matter in the shales (Figure 1.9 and Table 1.5). It can be concluded from Table 1.5 and Figure 1.9 that the Jatta Gypsum oil shale contains a variable amount of organic matter which is consistent with the TOC results of Raza *et al.* (1993).

Table 1.5. TOC and Rock-Eval pyrolysis results for oil shale samples from Dharangi (Kohat Basin, Pakistan), after Fazeelat & Yousaf (2004).

Samples	TOC (wt%)	S1	S2	HI	OI	Tmax
		(mg HC/g rock)		(mg HC/g C_{org})	(mg CO_2/g C_{org})	(°C)
A	0.85	0.5	1.4	160	21	435
A	0.85	0.5	1.3	154	27	435
B	13.6	9.4	21.0	154	0	438
B	10	8.1	21.0	210	1	438
C	22.1	28.4	124.3	564	2	436
C	19.3	25.3	122.0	631	2	437
C	19.4	24.5	123.7	639	3	438
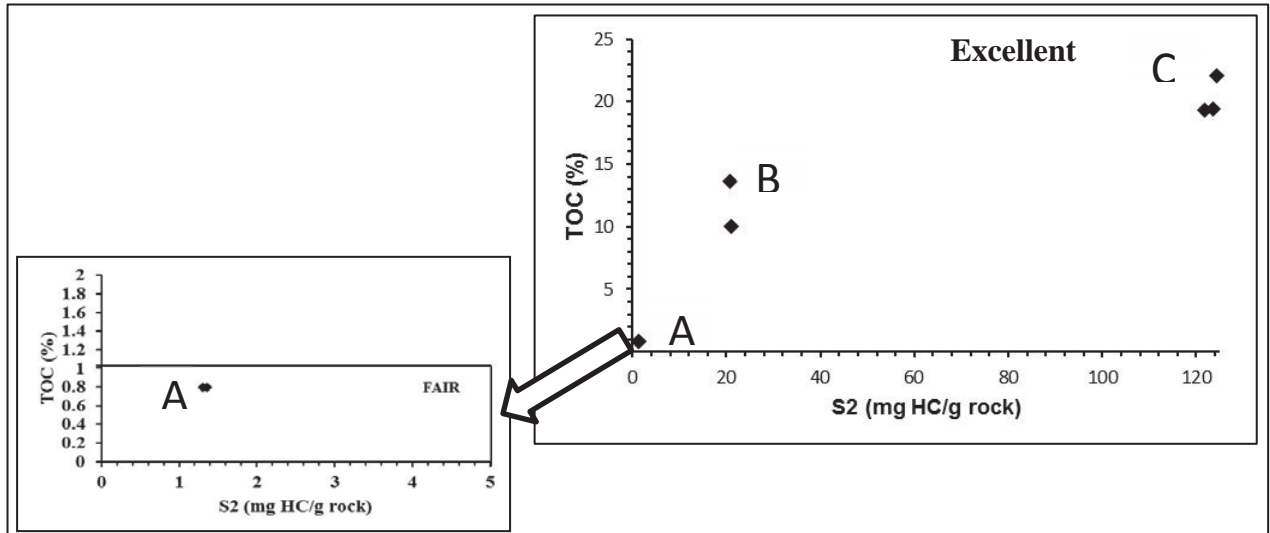
Figure 1.9. Plot of TOC vs S2 (SRA) for oil shale samples collected from three different outcrops at Dharangi in the Kohat Basin, after Fazeelat & Yousaf (2004). The plot to the left is the magnified plot of samples A showing "Fair" potential of the rock. Samples B and C show the excellent potential of the rocks.

1.8.2.2 Mir Kalam Kala and Speena Banda oil shales

Oil shales from Mir Kalam Kala and Speena Banda are analysed in this study. Mir Kalam Kala and Speena Banda villages are located near Karak area in the Kohat Basin, northern Pakistan. These oil shales are interbedded with the Jatta Gypsum Formation in the Kohat Basin (Raza *et al.*, 1993) and were collected from along the Indus Highway, west of Islamabad. There is no literature available specific to the rocks from Mir Kalam Kala and Speena Banda that have been analysed in this study. Raza *et al.* (1993) visited Speena Banda and they only mention that some impregnated rocks are present in the area. No other details of the area and rock sequences are available on these particular areas of Speena Banda and Mir Kalam Kala, therefore work in this thesis will be the first attempt to characterise these oil shales.

1.8.2.3　Salt Range oil shale

The Salt Range of Punjab, Pakistan, covers an area of 10,529 km^2 and is comprised of rocks ranging in age from Precambrian to Recent (Afzal *et al.*, 1999). The Salt Range Formation with salt marl, salt seams and dolomite forms the basement for the Precambrian sequence of the Salt Range (Shah, 2009). This Salt Range Formation is exposed along the southern flank of Salt Range, from Jehlum in the east to Kalabagh in the west (Figure 1.10) (Korte *et al.*, 2008; Shah, 2009).

The base of the Salt Range Formation is only known form Karampur well; where the formation overlies the metamorphic rocks, presumably of Precambrian age (Shah, 2009). The contact with the overlying Khewra Sandstone is generally normal and conformable (Shah, 2009). The age of the Salt Range Formation, its paleontological record and its contact with the overlying rocks has been a controversial topic. Details of this controversy are beyond the scope of this study. The Because of the absence of diagnostic fauna, the exact age within the Precambrian sequence is not known (Asif *et al.*, 2011; Shah, 2009). The overlying Khewra Sandstone is probably of Late-Precambrian to Early Cambrian in age, as observed by Gee (1945). The Salt Range Formation is therefore, assigned a Precambrian age (Shah, 2009).

The Salt Range Formation is composed of gypsiferous marl with thick seams of salt, beds of gypsum, dolomite, clay and oil shale (Shah, 2009). Minor amounts of potassium and magnesium sulphates have been found in association with the shale beds (Shah, 2009). The thickness of the formation varies from 50 m to more than 1000 m in its thickest part (Wandrey *et al.*, 2004) The thickness of the formation in its type section at Khewra Gorge is about 1000m (Shah, 2009).
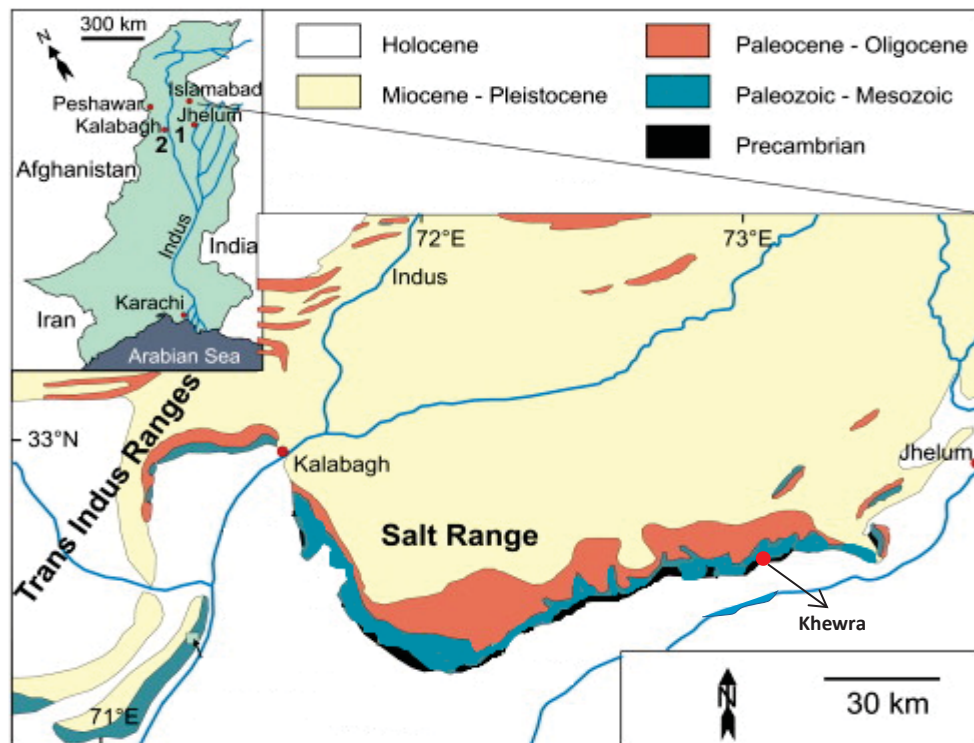
Figure 1.10. Distribution of the Salt Range between Jhelum and Kalabagh, Potwar Basin (Pakistan.), after Korte et al. (2008). Samples analysed in this study came from the Khewra Gorge area.

The Salt Range oil shale (stratigraphically placed within the Salt Range Formation) crops out at Khewra Gorge about 120 km south of Islamabad (Asif *et al.*, 2011) which has been designated as its type section (Shah, 2009). The contact of the Salt Range Formation with the overlying Khewra sandstone is generally conformable (Shah, 2009) (Figure 1.11). The Salt Range oil shale varies in thickness from 3 to 5 m at the type locality (Williams & Ahmad, 1999; Williams & Ahmad, 2000). According to Ahmad and Alam (2007) the Precambrian oil shales of the Salt Range Formation occur in two layers; one is of high grade and one of low grade shale. The high grade oil shale in the upper part of Salt Range Formation is associated with gypsum and extrusive volcanic rocks while the low grade layers of oil shale in the middle part of the formation alternate with sandstone, siltstone and dolomite (Ahmad & Alam, 2007).
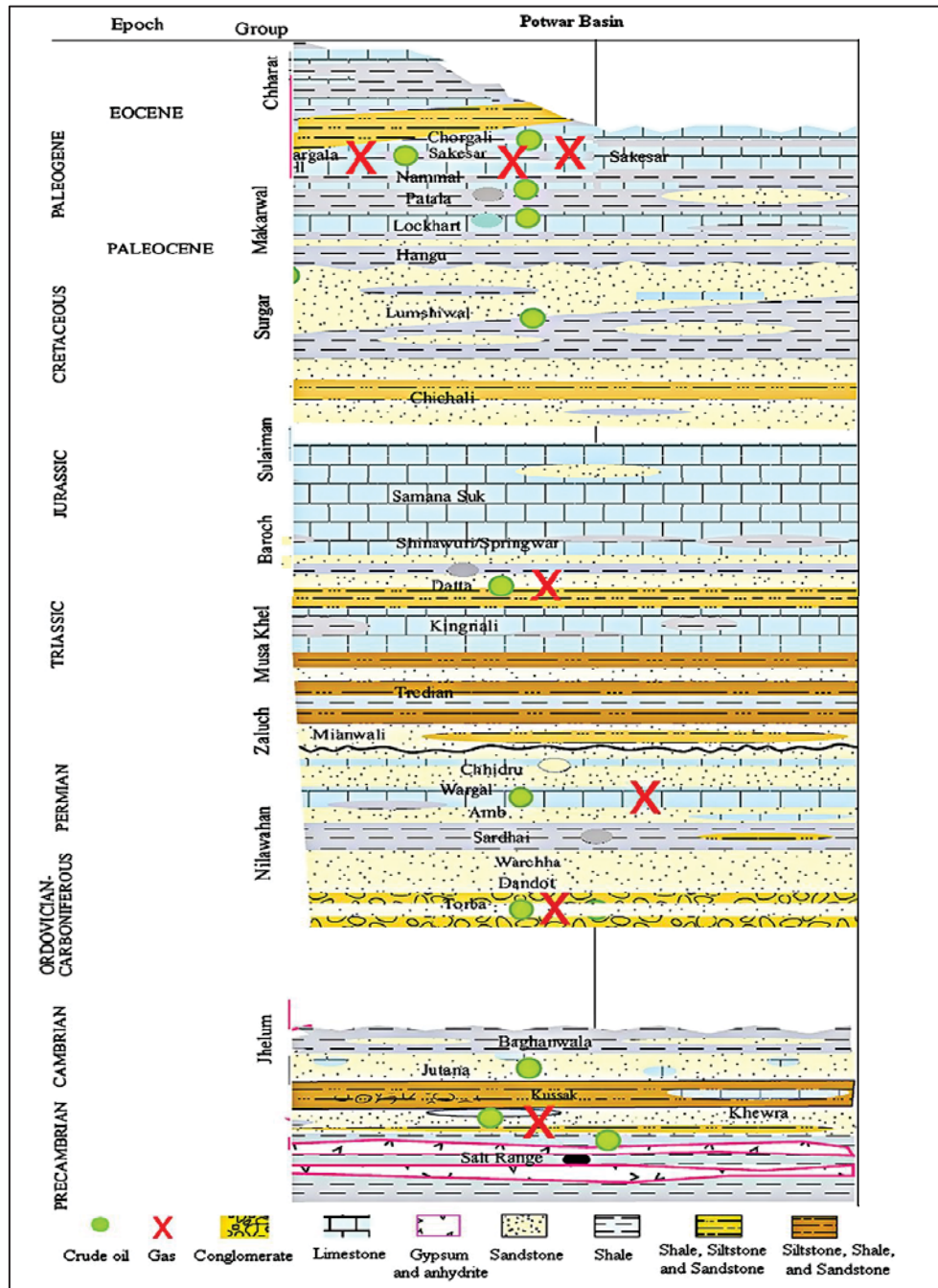
Figure 1.11. *Stratigraphy of the Kohat-Potwar region (Pakistan.),   after Asif et al. (2011) .*

According to Ahmad and Alam (2007), the oil shale horizons developed within the formation have good source rock potential containing high percentage of organic matter. The good quality oil shale is present in the top most part of the formation in the eastern Salt Range and it has TOC values of about 30 wt% (Ahmad & Alam, 2007). This oil

shale is associated with gypsum and extrusive volcanic rocks in the eastern Salt Range (Ahmad & Alam, 2007; Shah, 2009). Oil shale also occurs in the western Salt Range in the middle part of the formation, but here the TOC values are lower, between 6 to 8 wt%. This low quality oil shale alternates with sandstone, siltstone, dolomite and gypsum (Ahmad & Alam, 2007; Shah, 2009). Most oil shale samples from the Salt Range Formation are organically rich. A huge variability in the Salt Range oil shale samples has been observed by Ahmad and Alam (2007). The organic content (% TOC) distribution of 28 samples from the eastern Salt Range collected from five different locations is shown in Figure 1.12. The TOC ranges from 1.6-36% in the Khewra Gorge samples, 0.2-33.7% in Makrach Nala, 31% in Nawabi Kas, 15-25% in Sohal Nala and 0.58-41.7% in Nila Wahan samples (Figure 1.12) (Ahmad & Alam, 2007).
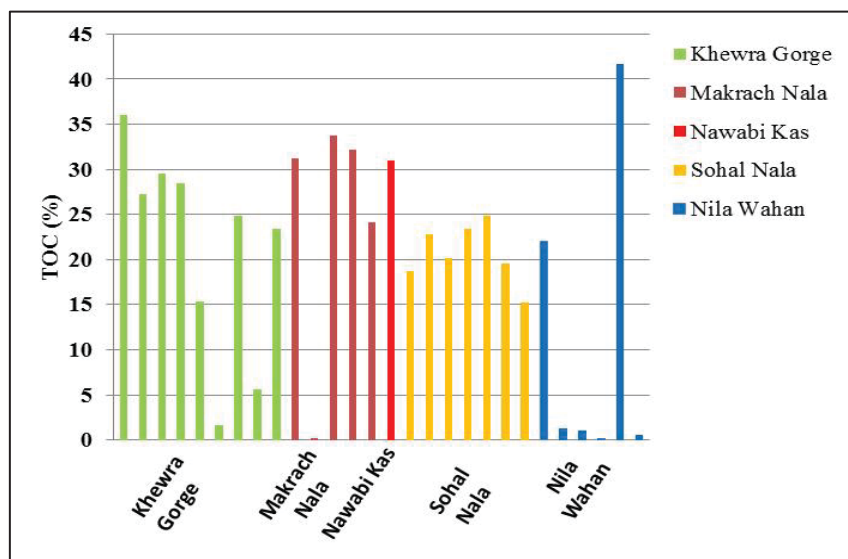
Figure 1.12. *Range of organic richness (% TOC) of outcrop samples of the eastern Salt Range from the Salt Range Formation, after Ahmad and Alam (2007).*

Hence the organic content of the oil shale is very variable suggesting the presence of dispersed organic matter and heterogeneity of the Formation.

1.8.3 Qianjiang Formation (Jianghan Basin), China

Three samples from China have been analysed in this study. These samples were collected from the Qianjiang Formation in Jianghan Basin which is located in the southern part of Hubei Province, China, and covers an area of 28,000 km^2 near the Changjiang River (Philp & Zhaoan, 1987) (Figure 1.13). The Jianghan Basin is a Cretaceous-Tertiary fault-bounded salt bearing basin that developed during the Yanshanian structural movement (Peng *et al.*, 2013). The generalised stratigraphy of the Jianghan Basin is shown in Figure 1.14 It is a Mesozoic to Cenozoic basin containing up to 10,000 m thick sequence of Cretaceous-Lower Tertiary sediments (Peng *et al.*, 2013).

a: Jiayin Basin
b: Sanjiang Basin
c: Songliao Basin
d: South Yellow Sea Basin
e: Erlian Basin
f: Bohai Gulf Basin
g: Zhujiangkou Basin
j: Jianghan Basin
x: Jungaar Basin
y: Tarim Basin
z: Qiadam Basin
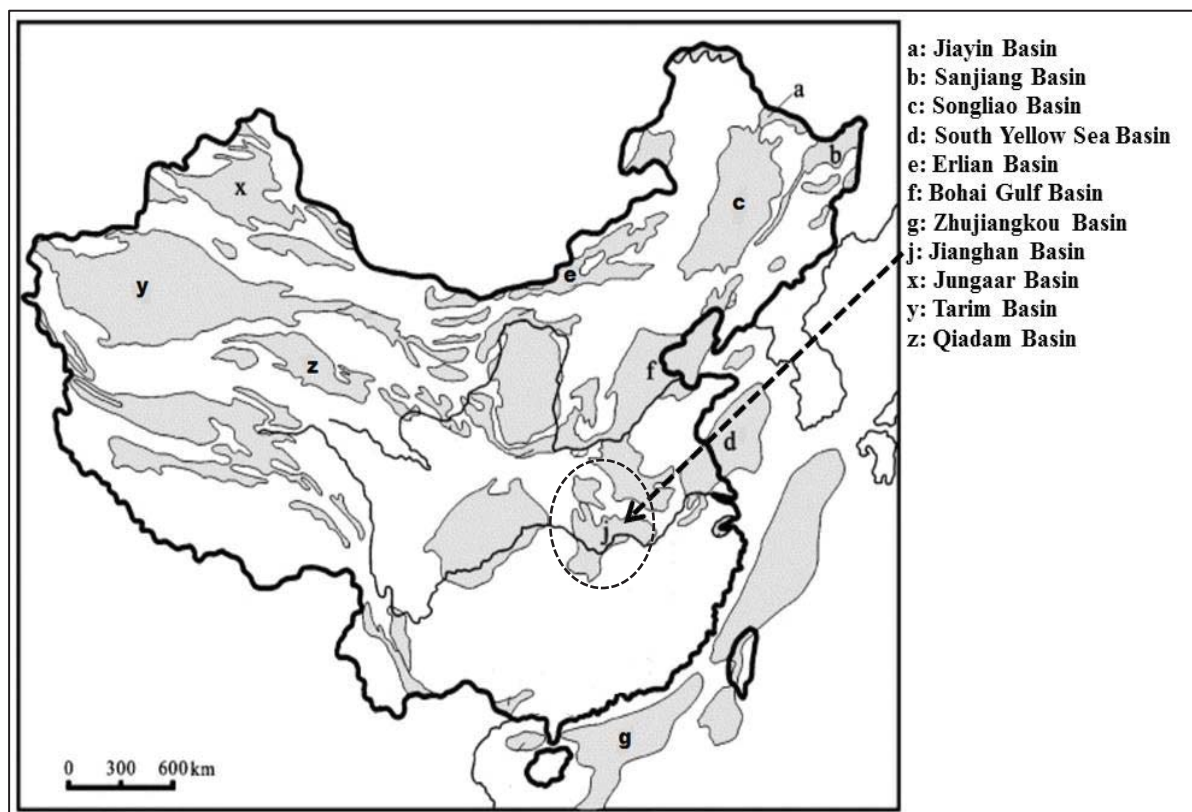
Figure 1.13. Major Cenozoic sedimentary basins in China, after Sun and Wang (2005)

Hydrocarbon-bearing strata are present throughout the basin which is divided into three formations (Jinghezhen Formation, Qianjiang Formation and Xingouju Formation) that contain various proportions of oil shale, mudstone, siltstone and halite (Peng *et al.*, 2013; Zheng *et al.*, 2011). Out of these three formations, the Xingouju Formation and the Qianjiang Formation are the two main oil-bearing formations (Peng *et al.*, 2013).

The Qianjiang Formation is Eocene-early Oligocene in age, covering an area of about 2500 km^2 in the middle of the Jianghan Basin (Grice *et al.*, 1998; JianPing *et al.*, 2009; Youheng, 2010). It was deposited in a saline lake (Gang, 2007). This formation is about 3000 m thick and is dominated with hundreds of halite beds with various thicknesses, ranging from few centimetres to 2 m (Zheng *et al.*, 2011).

System	Formation	Layer	Formation lithology	Depth (m)
Quaternary	Pingyuan		grey mudstone, siltstone, sandstone and sand-conglomerate	50-150
Neogene	Guanghuasi		grey mudstone, sandstone and sand-conglomerate	300-900
Paleogene	Jinghezhen		grey mudstone, siltstone, and shale	150-1000
	Qianjiang		grey mudstone, halite, siltstone, and shale	750-4600
	Jingsha		Brown, purple-red mudstone, siltstone and basalt	600-1870
	Xingouju	Upside layer	Red sandstone, mudstone	200-300
		Gypsum layer	Grey mudstone, Gypsum	5-20
		I Oil layer	Red and grey mudstone interbedded with sandstone	100-150
		II Oil layer	Grey mudstone interbedded with marlstone and sandstone	150-300
		Argillaceous layer	Grey mudstone interbedded with argillaceous minerals	20-40
		III Oil layer	Grey mudstone interbedded with marlstone and sandstone	100-150
	Shashi	Upside layer	Red and grey interbedded mudstone, argillaceous	200-400

Figure 1.14. Generalised stratigraphy of the Jianghan Basin, after Peng et al. (2013).

SRA results of the Qianjiang Formation were published by Grice *et al.* (1998) and Peters *et al.* (1996) (Table 1.6). They found that the Eocene Qianjiang Formation from

the Sha 13 well contains 2.4–6.6% TOC representing a very good to excellent source rock potential (Figure 1.15). The Qianjiang Formation from the Sha well is thermally immature (Tmax = <435°C) containing dominantly Type I organic matter which is prone to generate oil and lacustrine in origin (HI >600 mg HC/g TOC) (Table 1.6) based on SRA results and interpretive guidelines by Peter and Cassa (1996). The two Qianjiang Formation rock samples from the Ling 80 well at different depths contain 0.3 and 1.3% TOC representing poor and a good source rock potential respectively (Figure 1.15). The organic matter at depth of 1808 m in the Ling well is oil-prone Type II organic matter (HI = 501 mg HC/g TOC) which is early-mature (Table 1.6). However the organic matter at depth 1833 m is Type IV with no petroleum generation potential and is immature (Tmax = 417°C) (Table 1.6) following the interpretive guidelines by Peter and Cassa (1996). It can also be observed from Table 1.6 and Figure 1.15, that the Qianjiang Formation in the Sha well has a variable content of organic matter (TOC= 3.9-6.6 wt%) and the content of organics increases with increasing depth suggesting inhomogeneity of the formation at different depths.

Table 1.6. TOC and Rock-Eval pyrolysis results of Qianjiang Formation core samples from Sha and Ling wells in Jianghan Basin (China), after Peters *et al.* (1996) and Grice *et al.* (1998).

Well	Depth (m)	TOC (wt%)	S1	S2	HI (mg HC/g	OI (mg CO_2/g	Tmax (°C)
			(mg HC/g rock)				
Sha	1322	6.6	1.6	52.5	794	43	421
Ling	1808	1.3	0.6	6.4	501	101	436
Ling	1833	0.3	0.0	0.1	45	336	417
Sha	1198	3.9	1.0	27.6	712	55	424
Sha	1322	5	1.5	41.7	838	44	426
Sha	1409	2.4	0.5	17.2	724	75	430
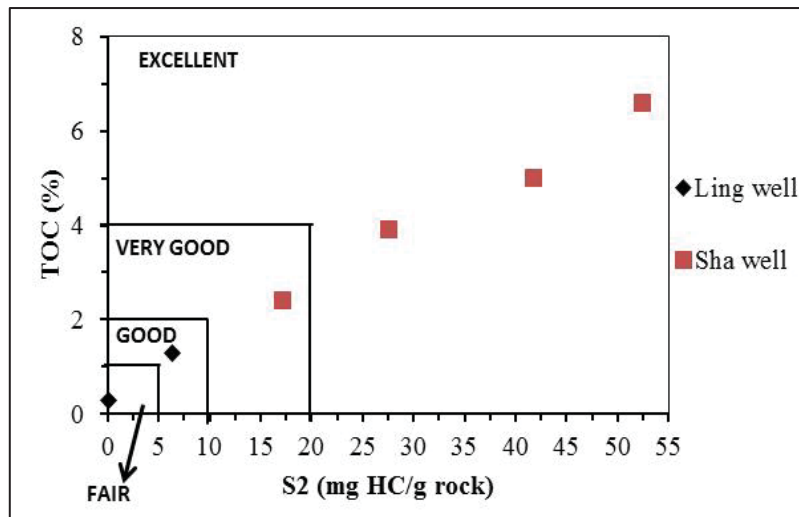
Figure 1.15. *Plot of TOC vs S2 (SRA) for oil shale samples collected from Ling and Sha wells from the Qianjiang Formation, Jianghan Basin, (China), after Peters et al. (1996) and Grice et al. (1998).*

1.8.4 Non-conventional hydrocarbon deposits in New Zealand

Oil shales have been known in New Zealand since 1866, when "bituminous shale" was reported from near Mangonui (Northland) and Kaikorai Valley (Dunedin) (Hector, 1866). Since then, many rocks described as "oil shales" or "bituminous shales" have been described and analysed. However, the only oil shale to have been commercially exploited in New Zealand was the Orepuki oil shale, for short time between 1899 and 1903 (Willett & Wellman, 1940).

New Zealand contains a number of sedimentary basins (Figure 1.16). Within these a number of formations are recognised as being oil shales. These are the Koranga, Waitahaia, Karekare, Glenburn, Whangai and Waipawa Formations (East Coast Basin) and the Tartan Formation in the Great South Basin and adjacent Canterbury Basin (Rogers *et al.*, 1994).

The Waipawa Formation samples in the current study have been collected from four different outcrops in the ECB: the Waipawa type locality, Lower Angora Road quarry, Upper Angora Road and Old Hill Rd (Porangahau) (Appendix B, image B4, B5 and B6).

The Orepuki oil shale samples have been collected from an outcrop which is situated on the eastern side of Te Wae Wae Bay, the south coast of the South Island (Appendix B, image B2).

Figure 1.16. *Sedimentary basins in the New Zealand region after Mrigadat (2008).*
Scale: 1 cm = 200 km

East Coast Basin

The East Coast Basin (ECB) lies on an active plate margin boundary, where the Pacific Plate is being subducted under the Indo-Australian Plate. This subduction began in the early Miocene (Field *et al.*, 1998). Parts of the margin are well exposed onshore. In the pre-Miocene history of New Zealand there was a mid-Cretaceous subduction system to the northwest of Northland and East Cape (Field *et al.*, 1998), and a Gondwana break-up rifting phase that commenced in the Late Cretaceous when the New Zealand

continent of Zealandia separated from Antarctica and Australia (Uruski *et al.*, 2003). Following the separation of New Zealand from Gondwana, the East Coast Basin formed firstly from subsidence on a passive margin that later developed into a subduction margin in the Miocene (Sutherland & King, 2008; Uruski *et al.*, 2003). The region has a long and varied history of tectonism with extensional, compressional and wrench structures all present (Field *et al.*, 1998).

The ECB is a sedimentary basin containing Cretaceous to Recent sedimentary rocks. It is bounded by the axial mountain ranges of the North Island and extends offshore across the continental shelf and slope to the Kermedec-Hikurangi subduction margin (Davies *et al.*, 1998). It was recognised as a petroleum province from as early as 1865 (Rogers *et al.*, 1994).

More than 300 oil and gas seeps occur throughout the ECB (Ministry of Economic Development, 2009). During the 20th century about 50 wells were drilled onshore and three offshore. Nearly all of these wells had shows of oil/gas but there were no commercial discoveries (Uruski, 2010). Sub-commercial discoveries were made near Wairoa in northern Hawkes Bay (Davies *et al.*, 2000). The Whangai and Waipawa formations are considered to be the main source rocks (Field *et al.*, 1997; Uruski *et al.*, 2006).

The ECB is thought to contain a 10,000 m thick sequence of sediments and covers an area of about 70,000 km^2 with approximately half of this area onshore (Rogers *et al.*, 1994). The source(s) of the oil and gas for the ECB are unknown, although potential source rocks exist throughout the Cretaceous-Paleocene sequence (Moore, 1987). Davies *et al.* (2000) proposed likely source rocks of the oil and gas could be the Waipawa, Whangai and older Cretaceous formations.

1.8.4.1 The Waipawa Formation: a potential New Zealand source rock

1.8.4.1.1 Distribution of the Waipawa Formation

The Waipawa Formation has been proposed as one of the potential source rocks in the ECB (Moore, 1987). It has a wide onshore distribution across the eastern North Island, in two main areas: (1) between Te Hoe River and East Cape (northern region), and (2) in southern Hawkes Bay – Wairarapa (southern region) (Figure 1.17). The type section locality for the Waipawa Formation is near the township of Waipawa in the southern Hawkes Bay [Waipawa (V22/155340), Tikokino Road]. The Waipawa Formation is 30 m thick at the type locality (Lee *et al.*, 2011) but it has not been encountered onshore in central Hawkes Bay as no wells have been drilled in this area (Ministry of Economic Development, 2009). The offshore distribution of this formation is unknown as no offshore well has been drilled deep enough to establish its presence or absence (Moore, 1989; Schiøler *et al.*, 2010). The outcrops of the Waipawa Formation within the East Coast Basin have been discussed by Moore (1988) and (1989) and are shown on Figure 1.17.
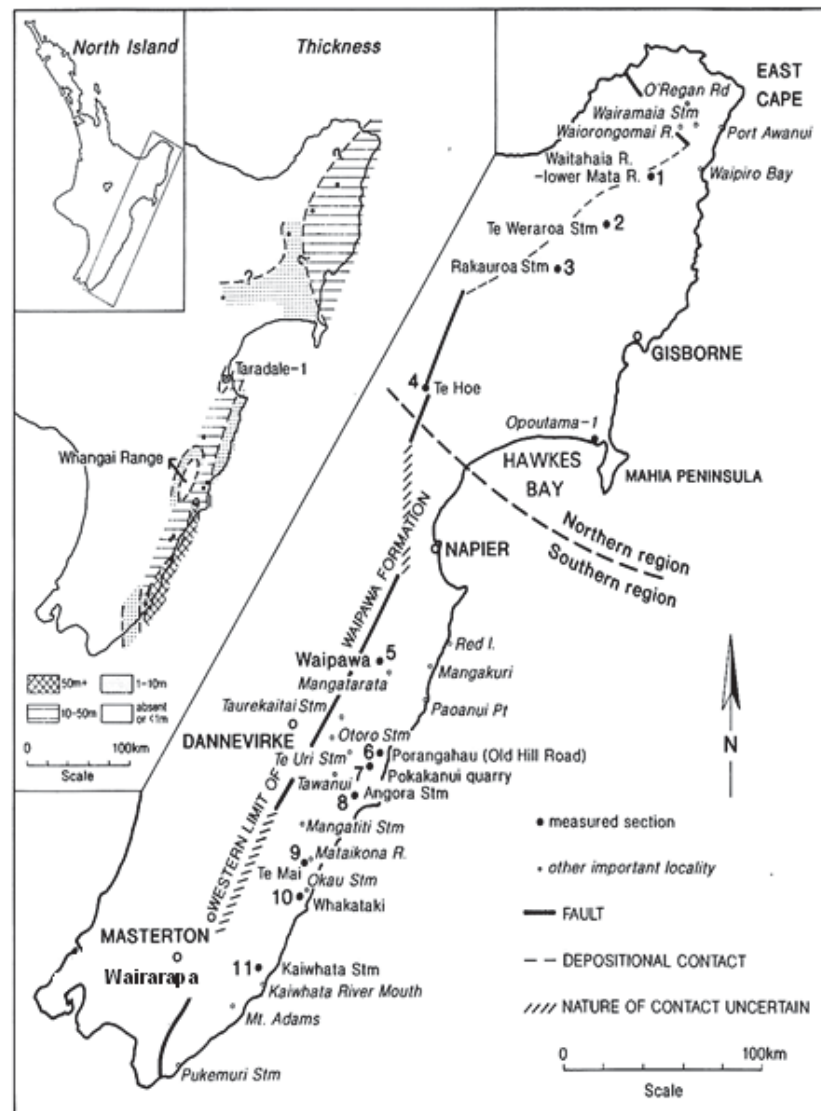
Figure 1.17. *Locations and thickness map of measured sections and other important localities for the Waipawa Formation in eastern North Island, (after Moore 1988). The 11 numbers record the sections of the Waipawa Formation studied by Moore (1988).*

1.8.4.1.2 Classification of the Waipawa Formation

The Waipawa Formation lies stratigraphically between the Whangai and Wanstead Formations (Figure 1.18) and was first recognized by Finlay (1939) who named it as the Waipawa Black Shale in 1940. However it was not adequately described until 1957 (Hornibrook & Harrington, 1957) and only formally defined in 1959 (Hornibrook, 1959). Throughout the 1960's and early 1970's the terms 'Chocolate Shale' and 'Black

Shale' were used for the Waipawa Formation (Moore, 1988). These informal names resulted from the dark chocolatey brown colour of the unit at its type locality.

Age Ma	Epoch	Series	Formation	Max thickness (m)
0	Paleocene	Hawera Wanganui		2800
	Pliocene			
10	Miocene	Taranaki	Waitere	3000
		Southland	Narrows	800
20		Pareora	Whakamaru	500
30	Oligocene	Landon	Weber	1500
40	Eocene	Arnold	███████████	
50		Dannevirke	Wanstead	400
60	Paleocene		Waipawa	50
			Whangai	600
70	Late-Cretaceous	Mata	Tahora	500
80			███████████	
90		Raukumara	Karekare	3000
100	Early-Cretaceous	Clarence		
110			Te Wera	250
		Taitai	███████████	
120				
130			Urewera	

Figure 1.18. Stratigraphy of the northern East Coast Basin (Rogers et al., 1994).

1.8.4.1.3 General description

The Waipawa Formation is described as a poorly bedded, hard to moderately soft, dark brown-grey to brownish black, bioturbated, non-calcareous micaceous siltstone of Teurian (mid to Late Paleocene) age (Killops *et al.*, 2000; Moore, 1986, 1988, 1989; Rogers *et al.*, 1994). In places the Waipawa Formation is sulphurous (1-3%) and locally

includes glauconitic sandstone beds and calcareous siltstone (Killops *et al.*, 2000; Rogers *et al.*, 1994). At weathered outcrop exposures the Waipawa Formation has a yellow coating of jarosite[5] and has an oily smell (Lee & Begg, 2002; Lee *et al.*, 2011). At some localities terrestrial plant debris with a low diversity of macro- and micro-fauna are also noted (Rogers *et al.*, 1994). Faunal evidence, supported by redox potential data, shows that it was deposited in a shallow marine, largely anoxic environment (Killops *et al.*, 2000; Moore, 1988). According to Leckie *et al.* (1992) the Waipawa Formation has well preserved terrestrial plant debris and palynomorphs which supports Moore's (1988) suggestion of deposition in an anoxic environment. However, more recent study on its correlative unit "the Tartan Formation" in the Great South Basin suggests deposition in a marginal marine, hyposaline and near-shore environment under bottom conditions that ranged from anoxic to oxic (Schiøler *et al.*, 2010). In the East Coast region, its thickness is commonly less than 20 m but its thickness in parts of Wairarapa and southern Hawke's Bay is up to 50-60 m. It is absent over the Whangai Range (Figure 1.17) (Hollis & Manzano-Kareah, 2005).

1.8.4.1.4 Stratigraphic relationship

The Waipawa Formation conformably overlies the Whangai Formation and its contact with the Whangai Formation is typically gradational over centimetres to metres (Figure 1.19a) (Field *et al.*, 1997; Moore, 1989). Its contact with the overlying Wanstead Formation is sharp and conformable (Moore, 1988, 1989). The Waipawa Formation overlies different facies of Whangai Formation at different places within the basin and interfingers with the Whangai beds in the eastern and central parts of the basin (Figure 1.19b). There is a facies change from the Te Uri Member (Whangai Formation) to the Waipawa Formation in places and thus the upper Te Uri Member is a lateral equivalent of the Waipawa Formation (Figure 1.19b). The Upper Calcareous Member of the Whangai Formation changes laterally into the Porangahau Member farther east (Moore, 1988). The upper contact of the Waipawa Formation with the Wanstead Formation is rarely exposed (Moore, 1989).

---

[5] Jarosite is a sulphate mineral which is formed by the oxidation of iron sulphides. It is a hydrous sulphate of potassium and iron with a chemical formula of $KFe_3(OH)_6(SO_4)_2$.
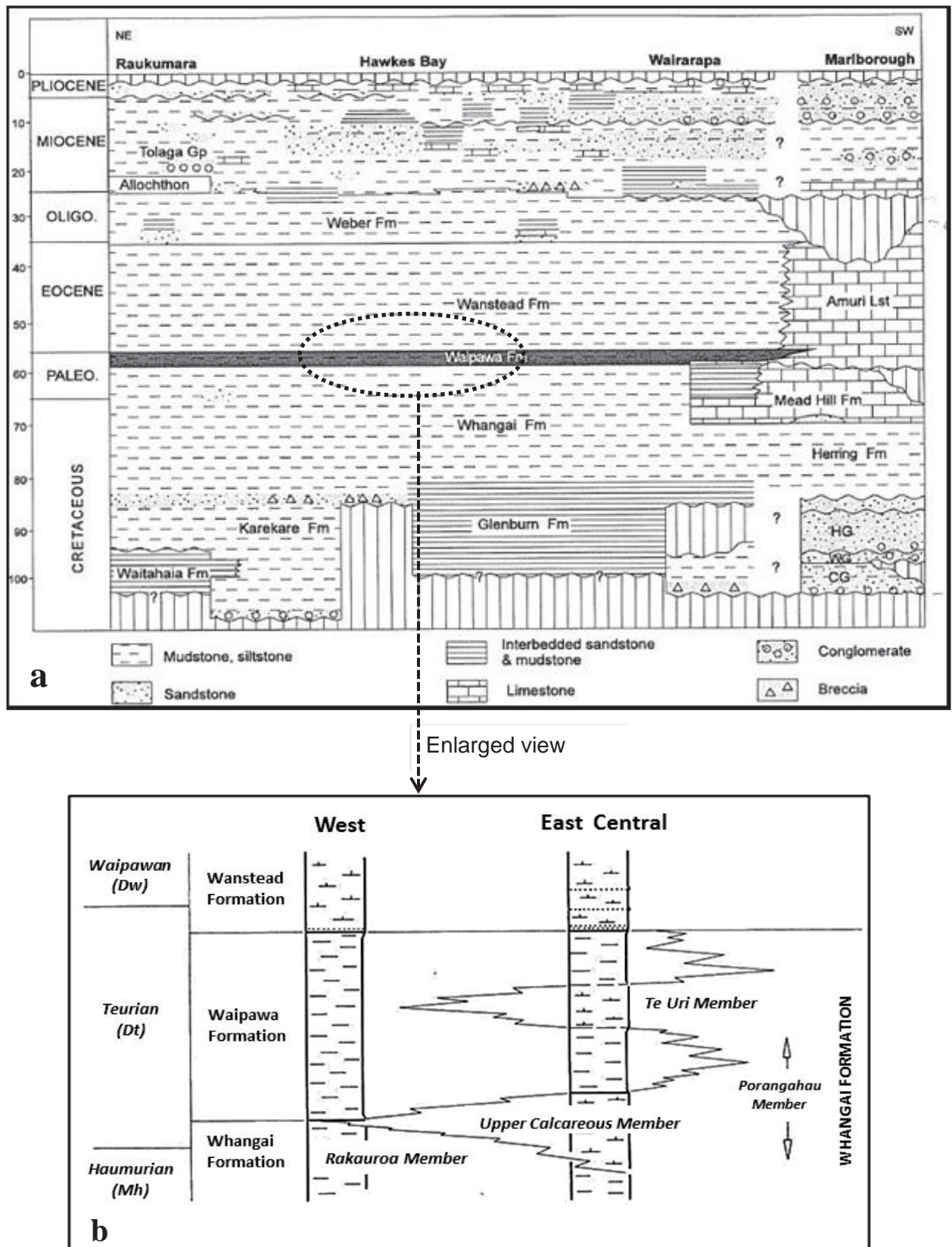
Figure 1.19: (a) - Overview of the stratigraphy of the East Coast region (from Field et al. (1997), (b) - Stratigraphic relationship of the Waipawa Formation and different members of the Whangai Formation (from Moore, 1988).

1.8.4.1.5 Type and Reference Sections

Kingma (1971) designated the type section [6] for the Waipawa Formation to be at Waipawa between NZMS1 N141/002847 (at the base of the exposed section) to NZMS 1 N141/008849 (at the top of the section) in southern Hawkes Bay. About 30 m of the Formation is exposed at the type locality. Other important sections are at the Te Hoe River, Te Weraroa Stream, Porangahau, Kaiwhata Stream, Angora Stream, Te Mai Stream and Rakauroa Stream (Figure 1.17) (Moore, 1988).

1.8.4.1.6 Age of the Waipawa Formation

The Waipawa Formation has been designated Teurian in age (Kingma, 1971). But it is difficult to more closely constrain the age and duration of the Waipawa Formation deposition due to the absence of reliable information on changes in depositional rates throughout the Teurian stage (Killops *et al.*, 2000). The best accepted age range (based upon paleontology) is between 59.1 and 55.5 Ma (Moore, 1988; Turnbull *et al.*, 1993). This places the shale within the Paleocene Epoch and Dannevirke Series (Figure 1.18). During the Paleocene the oceanic circulation was very low due to warm climate and low pole-to-equator temperature gradients (Fischer & Arthur, 1977). In this type of environment, the deposition of organic rich sediments, like the Waipawa Formation, is favoured (Kennett, 1982; Neef, 1992).

1.8.4.1.7 Petroleum potential of the Waipawa Formation

The most likely source rock for oil expulsion in the deeper parts of the East Coast Basin is regarded as the Waipawa Formation (Gibbons, 1980). Analyses of earlier works show it consists dominantly of Type II kerogen with some contribution of Type III kerogen (Davies *et al.*, 1998; Field *et al.*, 1998; Johnston *et al.*, 1991; Rogers *et al.*, 1994). The

---

[6] Exposed from the north bridge head of the old wooden Waipawa bridge for about 700 yards (640 m) along the Tikokino Highway towards Waipawa (Kingma 1971).

Waipawa Formation has TOC values ranging from 2-12% and hydrogen indices (HI) ranging from 50-500 mg HC/g TOC with an average HI of 245 mg HC/g TOC (Hollis & Manzano-Kareah, 2005). These values infer that the Formation has both oil and gas potential (Uruski, 2010). The Waipawa Formation is widespread in outcrop throughout the North Island and extends offshore with an estimated volume of over 500 km^3 (Field *et al.*, 1998).

SRA studies (Field *et al.*, 1997; Hollis & Manzano-Kareah, 2005; Leckie *et al.*, 1992; Moore, 1987) indicate that the Waipawa Formation is a potential source rock for oil generation. Although the Waipawa Formation is immature in outcrop, it is inferred that this shale is deeply buried in some regions within the East Coast Basin where oil generation might be possible (Rogers *et al.*, 1994). Analyses of the carbon molecules in the organic material have identified a number of biomarkers that are suitable for correlation between the three main oil seeps and the type of organic matter the oil is derived from (Johnston *et al.*, 1991; Rogers *et al.*, 1994).

Field *et al.*(1997) and Hollis & Manzano-Kareah (2005) conducted detailed SRA analysis of Waipawa Formation samples collected from 51 different localities in the East Coast Basin and have produced extensive data sets that summarise the recorded SRA parameters. Review and interpretation of the reported SRA data show that the Waipawa Formation is heterogeneous and the organic matter content of samples collected across the formation varies widely. The petroleum potential of the formation, defined by the plot of TOC vs the parameter S2, ranges from poor to excellent (Figure 1.20).
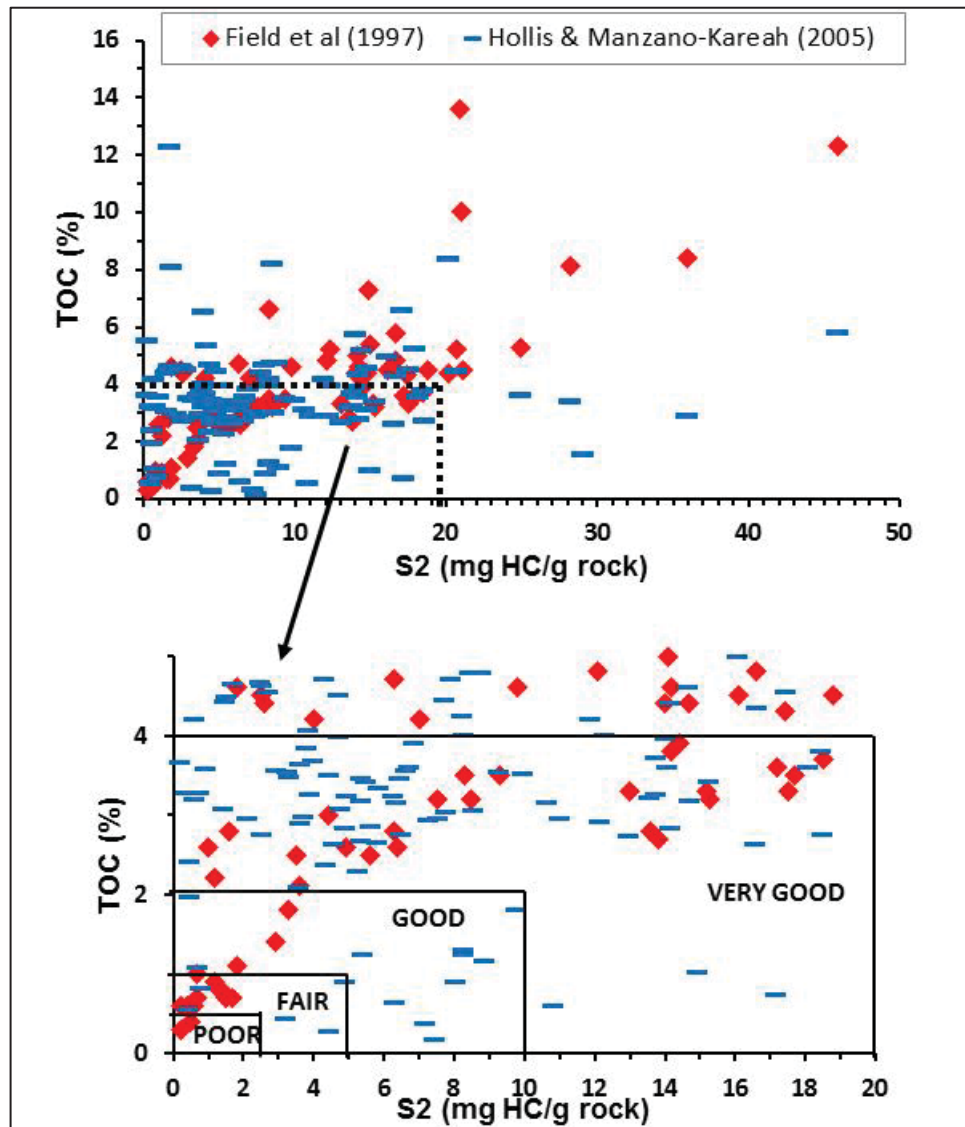
Figure 1.20. Bivariate plot of TOC vs S2 (SRA) for Waipawa Formation samples collected from 51 different localities in the East Coast Basin. After Field et al. (1997) and Hollis & Manzano-Kareah (2005).

To explore variability in the quality of organic matter, Field *et al.* (1997) identified five localities the in the East Coast Basin (Angora Stream, Te Weraroa Stream, Castle Point, Riversdale and Mead Stream) [7] out of the 27 localities analysed. These five localities were identified to represent variability in organic content and petroleum potential

---

[7] The grid references for these locations can be found in Field *et al.* (1997) and Hollis & Manzano-Kareah (2005).

between different outcrops of the Waipawa Formation and also to assess variability (if any) that may occur within an outcrop of the formation. In this study analyses from those five localities by Field *et al.* (1997) and Hollis & Manzano-Kareah (2005) along with Field *et al.* (1997) and Hollis & Manzano-Kareah (2005) analyses from the Waipawa type locality, are selected to compare with the results of this study to show variability in organic content between the outcrops of the Waipawa Formation and variability in organic content within an outcrop (if any). The SRA parameters TOC and S2 reported by Field *et al.* (1997) and Hollis & Manzano-Kareah (2005) for samples from these localities are plotted in Figure 1.21. A wide distribution in TOC and S2 data were observed in samples collected from the same outcrop and also between samples collected from different outcrops. This clearly highlights the variability in the quality and quantity of organic matter between and within outcrops of the Waipawa Formation (Figure 1.21). Both Field *et al*. (1997) and Hollis & Manzano-Kareah (2005) have stated that the formation is not homogeneous throughout the East Coast Basin. Similarly Leckie *et al.* (1992) found considerable variation in TOC (0.59-5.3%), S2 (0.44-24.91 mg HC/g rock) and HI (45-550 mg HC/g rock) for samples collected from across the Waipawa Formation.
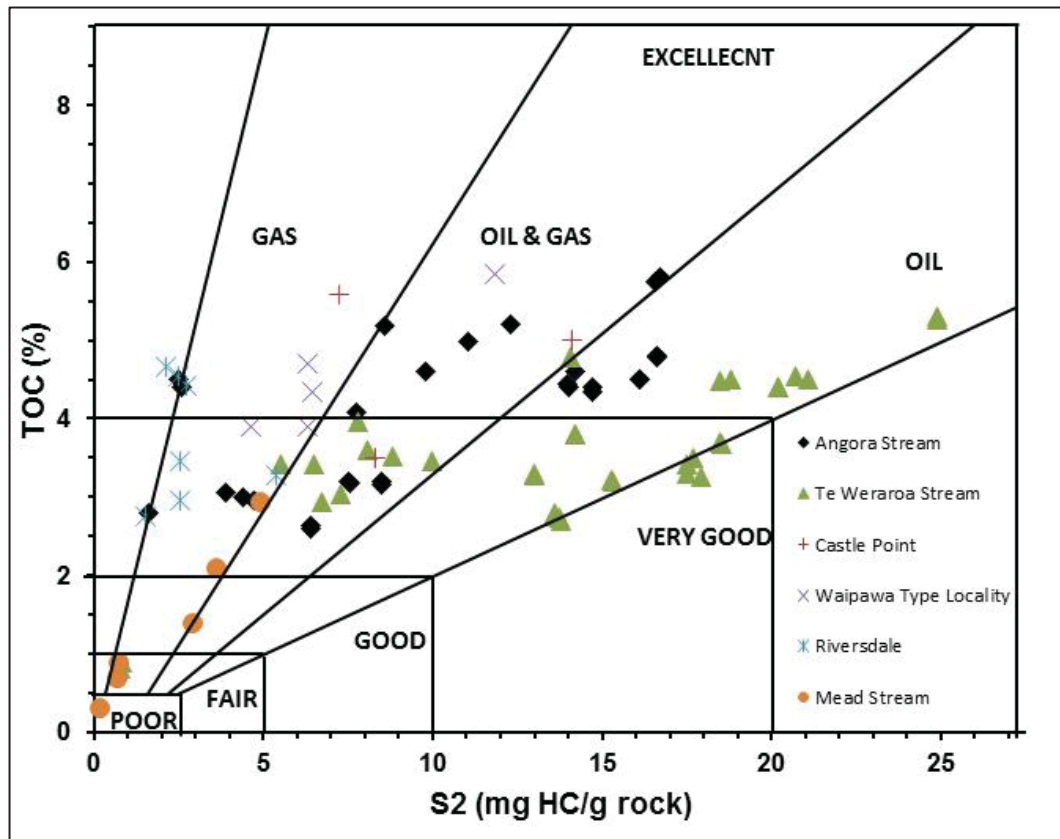
Figure 1.21. *Plot of TOC vs S2 (SRA) for the Waipawa Formation samples from six different localities in the East Coast Basin. After Field et al. (1997) and Hollis & Manzano-Kareah (2005).*

Two petroleum exploration permits, operated by Trans Orient Ltd., PEP 38348 located north of Napier and Hawkes Bay (covering an area of 530,535 acres) and PEP 38349 to the south of Napier (covering an area of 1,633,651 acres) (Figure 1.22), have potential total in-place petroleum grade Waipawa Formation with an estimated richness of 15 litres/tonne (Bertram *et al.*, 2008). Currently TAG Oil is exploring and assessing both the Waipawa and Whangai formations in the ECB (TAG Oil, 2012).
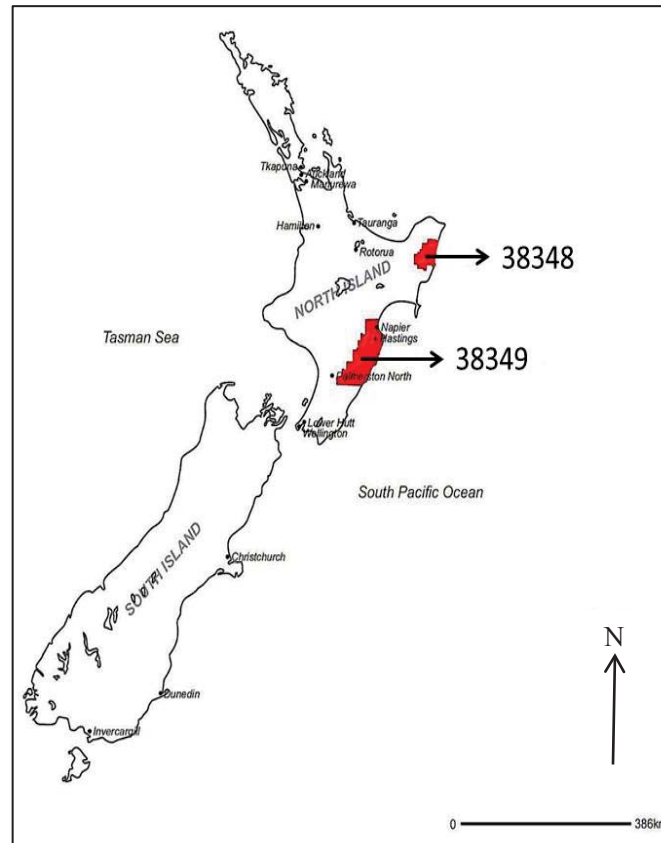
Figure 1.22. *New Zealand map showing the locations of Permits 38348 and 38349. Taken from Bertram et al. (2008)*

1.8.4.2 The Orepuki oil shale: an example of a historically producing New Zealand oil shale

Three Orepuki oil shale samples were collected by Dr Christopher Anderson from outcrop along the eastern margin of the Waiau Basin (Turnbull *et al.*, 1993). The Waiau Basin contains up to 5000 m thick sequence of Cenozoic sediments in the Murihiku area of Southland (Turnbull & Allibone, 2003). It is one of the three basins in Southland that has been of interest to petroleum exploration companies (Turnbull & Allibone, 2003; Turnbull *et al.*, 1993). It is separated from the Winton Basin in the east by the Longwood Ranges and from the Te Anau Basin in the west by the Takitimu Ranges (Figure 1.23) (Cahill, 1995).
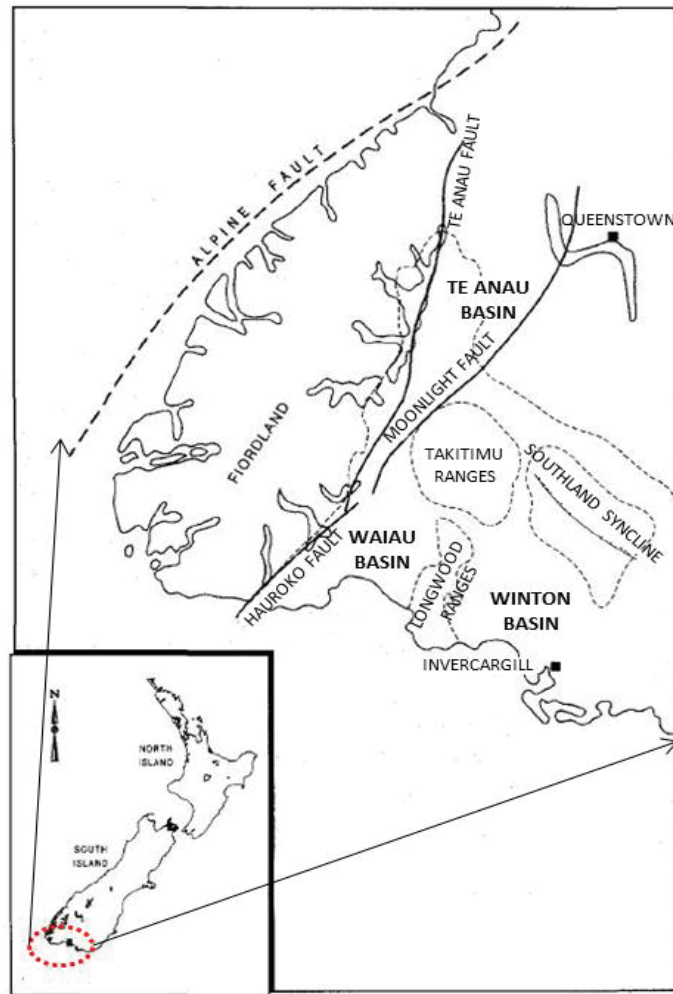
Figure 1.23. *Regional map highlighting the south of the South Island showing three sedimentary basins, after Cahill (1995).*

At depth the Waiau Basin sequence has potential source rocks (Ohai and Nightcaps groups), with potential reservoir rocks and also structural and stratigraphic traps in several locations (Turnbull & Allibone, 2003). The Orepuki deposit, within the Nightcaps group is the only deposit in New Zealand which has been mined and was processed for oil between 1899 and 1903 (Willett & Wellman, 1940). This deposit occurs within the Orepuki coal and oil shale field, situated on the eastern side of Te Wae Wae Bay, which is on the south coast of South Island (Te Ara The Encyclopedia of New Zealand, 2006). This field is adjacent to Orepuki township and 67 km west of Invercargill (Sykes, 1996).

This oil shale was first discovered in 1879 (Te Ara The Encyclopedia of New Zealand, 2006) and its resource is estimated at between 1,770,850 and 6,769,000 tonnes of oil shale (Willett & Wellman, 1940). The geology of the deposit is poorly known because of limited data available from its outcrop and drill holes studies. This deposit is part of Waimeamea Series which is now considered part of Beamont Coal Measures Formation (Sykes, 1996). It overlies a sandstone and varies in thickness from 0.2 m (8 inches) to 1.4 m (4 ft. 6 in) (Figure 1.24) (Willett & Wellman, 1940). The oil shale itself is overlain by a carbonaceous mudstone with thin coal interbeds and is described as dark-brown to black, centimetre bedded shale (Hutson & Smith, 1987; Wood, 1969).
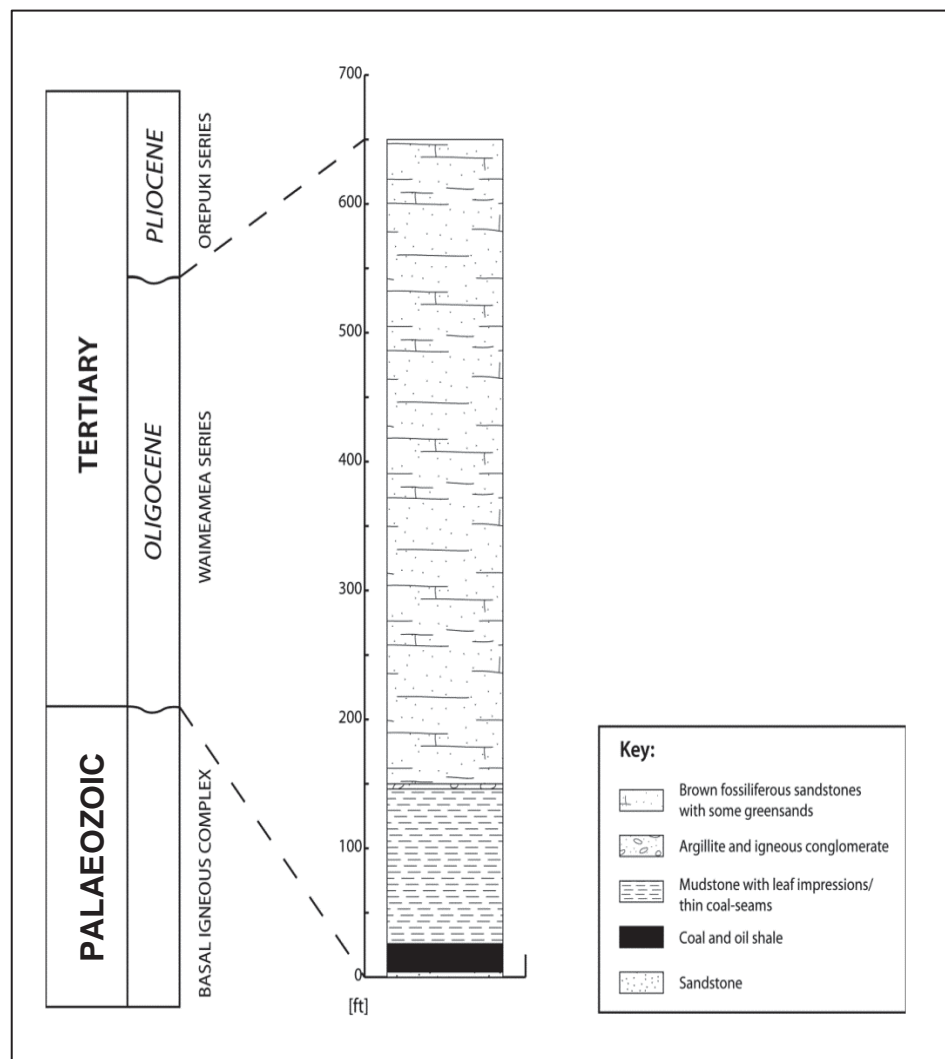
Figure 1.24. *Stratigraphic column showing the different lithologies of the Waimeamea Series, adapted from Willett and Wellman (1940) and Sykes (1996).*

The Orepuki oil shale is Eocene in age (Willett & Wellman, 1940; Wood, 1969). Turnbull *et al*. (1993) and earlier workers (Comstock, 1981; Willett & Wellman, 1940) attributed it to deposition in a terrestrial environment. However Sykes (1996) and a report by GeoSphere Ltd (1999) suggest a pure lacustrine origin of the oil shale based upon the very high S2 (618, 770 mg HC/g rock) and low OI (39, 18 mg CO_2/g TOC) (Table 1.7). They also found very high TOC values for the oil shale suggesting the excellent petroleum potential of the oil shale (Table 1.7). Sykes (1996) working on one Orepuki sample found a TOC value of 38% and GeoSphere Ltd (1999) reported a TOC value of 42%. The very high HI values of this oil shale favour a lacustrine origin (GeoSphere Consulting Ltd, 1999). From the petrographic analysis of the oil shale (Sykes, 1996), it was found that the oil shale contains abundant lacustrine alginite (*lamalginite*). This maceral is responsible for its high oil yield. Due to the abundance of lamalginite, he called it a *lamosite* type oil shale.

Table 1.7. SRA data of Orepuki oil shale available in the literature after Turnbull *et al*. (1993), Sykes (1996) and GeoSphere Ltd (1999).

Sample	S1	S2	TOC	HI	OI	References
	mg HC/ g rock		(wt%)	mg HC/g TOC	mg CO_2/g TOC	
Orepuki oil shale	1.3	58	20	287	73	Turnbull *et al.* (1993)
	12	235	38	618	39	Sykes (1996)
	6	321	42	770	18	GeoSphere Ltd (1999)

A significant variation in the SRA parameters is observed (Turnbull *et al.* (1993); Sykes 1996; and Geosphere Ltd, 1999). This shows variability in the organic content of this oil shale.

Cane (1942) measured an oil yield of 300 litres/tonne of the Orepuki oil shale using the Gray King Assay method (Appendix A), but this was calculated for a single 20 g sample and cannot be considered typical of the whole oil shale deposit. This oil shale

was exploited by a London-based New Zealand Coal and Oil Company in 1899-1903 yielding ~145 litres/tonne of shale oil (Willett & Wellman, 1940). Around 14,000 tonnes of oil shale were mined and processed between 1899 and 1903 before closure of the plant (Willett & Wellman, 1940). Studies of the Orepuki oil shale by Willett and Wellman (1940), Cane (1942) and Elphick (1954), have shown that the oil shale contains a variable content of shale oil from 176 litres/tonne to 323 litres/tonne.

The Orepuki deposit has been subjected to very little drilling. Willett and Wellman (1940) have mentioned four holes, which were drilled in 1911 to depths between 55-146 m and these intersected 1.3-1.4 m of shale. In addition 12 bores are shown in Figure 5 of Willett and Wellman's paper (1940). No details of thicknesses and depths of these bores have been given. According to Willett and Wellman (1940) and Willett (1946), because of insufficient information on the thickness and continuity of the oil shale, the quantity of recoverable shale oil is unknown.

1.9 Research objectives

Review of the literature has highlighted that global exploration and production interest in non-conventional oil shale deposits has had intermittent periods of high activity since the turn of the 20th century. Currently, such deposits support a level of interest, primarily due to a decrease in new conventional discoveries and the high prices for oil extracted from conventional deposits. Key to the assessment of oil shales as production targets is analysis of the type, content and quality of their constituent hydrocarbons. Conventional analytical techniques are used by industry to assess these parameters, and the primary technique utilised around the world is Source Rock Analysis. But there are recognised limitations to the accuracy and extent of information that can be generated by SRA of oil shales. Perhaps for these non-conventional deposits, a non-conventional analytical package for assessment is needed.

No research group has proposed an analytical approach to assess the petroleum potential of source rocks using commonly available physical and geochemical techniques that can be found in laboratories around the world. Many physical, chemical and thermal

analyses have been completed to understand the chemistry of kerogen, bitumen and shale oil, and in the characterisation of oil shales (Aboulkas *et al.*, 2012; Ahmad & Alam, 2007; Budinova *et al.*, 2009; Song *et al.*, 2012), but no integrated model has been proposed to assess the source rock potential of such resources.

The overall aim of the research conducted for this thesis was therefore to generate a novel 'non-conventional analytical model' to assess the production potential of oil shale deposits. The specific purpose of this model was to understand the physical and geochemical characteristics of the Waipawa Formation and the Orepuki oil shale, and to evaluate their oil production potential.

The hypothesis of the current study was that a novel and non-conventional analytical tool would be better suited to the assessment of the production potential of oil shales. The overall objective of the study was therefore to define a scientifically comprehensive production potential model for non-conventional source rocks. In order to achieve this objective a suite of physical, thermal and chemical analytical techniques, specifically XRD, organic petrography, LOI, LECO, TGA, Soxhlet Extraction, FTIR and GC-MS were used to characterise a set of international and New Zealand oil shales. These techniques were chosen because of their ready availability in earth science laboratories around the world.

The aim of the research described in this thesis is not to provide a comprehensive and critical analysis of one technique over another. Furthermore, this work does not attempt to discredit the accuracy of conventional SRA analysis. Instead, the intention of this work is to examine if the sum of knowledge generated through the analysis of oil shale rock samples by a sequence of widely available analytical techniques can provide superior scientific understanding of the hydrocarbon production potential of oil shales. This work is predicated on the idea that SRA analytical facilities are not available in all earth science laboratories around the world. Yet most earth science laboratories will have access to most if not all of the analytical techniques utilised in this study. The work described in this thesis is a first attempt at created a non-conventional hydrocarbon production potential model, and should serve as a starting point for the work of research groups in the future who which to explore the hypothesis of this study further.

The detailed objectives of the research are:

1. To collect and describe key sections of the Waipawa Formation

Key sections of the Waipawa Formation were identified from published studies. Outcrops at each location were visited and described, and samples were collected from each location for analytical study.

2. To collect oil shale samples from other parts of world for comparison to the Waipawa Formation

Oil shale samples from both producing and non-producing formations were sought from locations around the world. Samples that ranged from well-studied oil shales to poorly studied examples were obtained to compare the production potential of the Waipawa Formation to other world examples. Two reference samples, sand and argillite were also used to provide a no-production potential baseline to the oil shales.

3. To characterise the physical properties of the samples using *XRD and Organic Petrography*

A detailed understanding of the physical properties of each of the samples of the study was obtained through XRD analysis to describe the constituent clay minerals and find the relative abundance of clay minerals present. Visual inspection of polished grain mounts was also conducted to assess the different types of kerogen in each sample.

4. To characterize the samples using thermal techniques *LOI, LECO and TGA*

Thermal techniques were used to quantify the abundance of organic matter in each sample when the shales were heated under different conditions. The rapid and inexpensive techniques LOI and LECO were first performed to estimate the organic matter content followed by a programmed thermal gravimetric analysis (TGA) where the rocks were heated according to a defined heating sequence.

5. To characterise the bitumen fraction of the samples using chemical techniques
FTIR and GC-MS

The bitumen content in each sample was extracted into a solvent and then characterised using the two chemical techniques Fourier Transform Infrared Spectroscopy (FTIR) and Gas Chromatography-Mass Spectrometry (GC-MS).

6. To define a scientifically comprehensive non-conventional production potential model based on the suite of analytical techniques employed

The data obtained through the physical, thermal and chemical analysis of the worldwide oil shales in this thesis were used to define a new model to assess production potential based on the use of non-conventional analytical techniques. In the context of this work a model is defined as a framework of information that provides support for decision making (Henley & Berger, 1993). This new model was designed to provide superior scientific information relative to conventional SRA. This production potential model was designed such that it could be run at research institutions around the world, rather than at specialised petroleum studies laboratories (i.e. facilities that offer SRA). The conclusions obtained through use of this new production assessment model were compared to and validated against those generated by SRA of the same samples (contracted to a commercial lab).

7. To use this non-conventional production assessment model to define the hydrocarbon production potential of the Waipawa and Orepuki oil shales

The final objective of the research described in this thesis was to use the newly defined and validated production potential model to define the future potential for hydrocarbon extraction from the Waipawa Formation and from the historically productive Orepuki oil shale.

1.10 Thesis overview

The research described in this thesis is predicated on the hypothesis that conventional Source Rock Analysis is not optimal for the assessment of the production potential of non-conventional hydrocarbon deposits such as oil shales. A review of oil shales, the current standards for production of shale oil from identified resource, the limitations of conventional analysis of oil shales, and the occurrence of potential oil shale resource in New Zealand has been presented in this chapter (Chapter 1). This review has provided a framework for the justification that a set of thermal, physical and chemical analyses may generate superior information on an exploration target than conventional Source Rock Analyser (SRA) analysis (Figure 1.25).

Chapter 2 describes the methodology and materials used in the study. The lithologies of each of the rocks analysed in this research are described, along with information about their ages and environments of deposition. Samples of the Mir Kalam Kala, Speena Banda and Salt Range oil shale from Pakistan, Qianjiang Formation samples from China and samples from the Green River Formation in the USA were used in this study. Two baseline samples, sand and argillite, with no oil production potential, were also used. These oil shale samples from Pakistan, China and the USA, together with the no-production potential rocks, were used to generate the non-conventional production potential model of the thesis. Samples from the Waipawa Formation and the Orepuki oil shale from New Zealand were then analysed and their production potential assessed using the new model. The preparation of samples for physical, thermal and chemical analysis and the analytical techniques employed are described in Chapter 2.
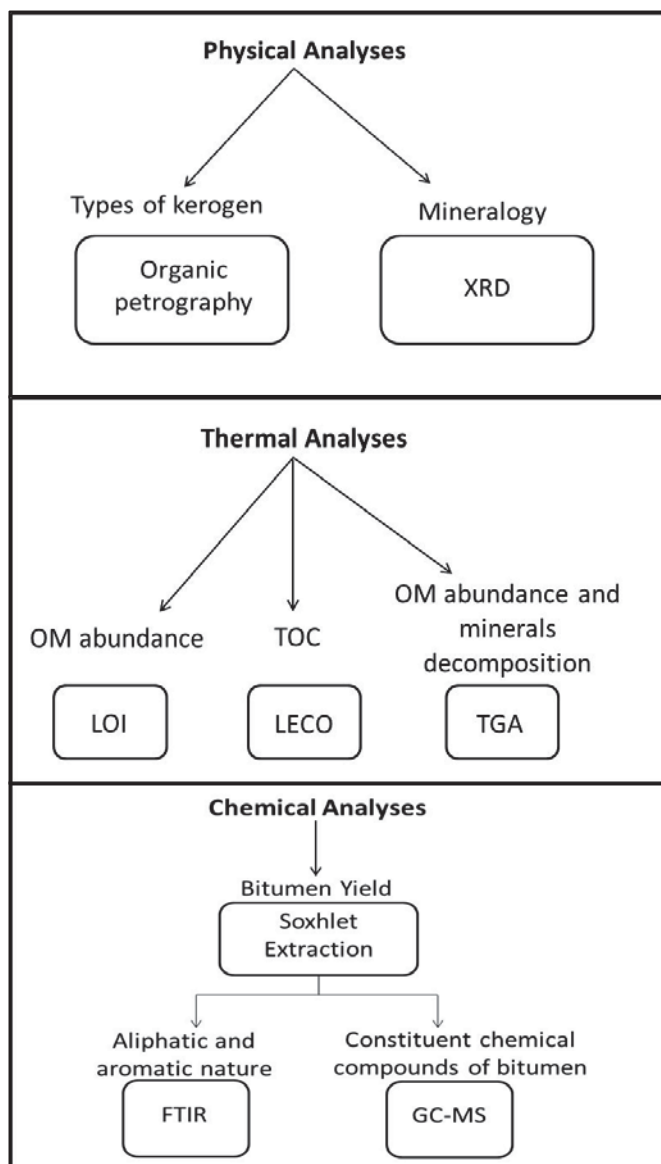
Figure 1.25. *The thermal, physical and chemical analytical techniques used in this thesis to identify the petroleum potential of source rocks and to propose a novel and non-conventional model to assess the production potential of oil shale resources.*

In Chapter 3 the results from conventional Source Rock Analysis of each sample, as conducted by GNS Science in Wellington, New Zealand are presented and discussed. These results provide a conventional assessment of each rock.

The results from physical analyses of all samples are presented and described in Chapter 4. Minerals present in each sample were identified using X-ray diffraction and the

relative abundance of each clay mineral present was established in clay concentrated fraction of each rock. Kerogen present in each rock was visually assessed through microscopy of polished grain mounts (organic petrography).

The results of the thermal analysis of all samples are presented in Chapter 5. Direct thermal analysis (Loss on Ignition and LECO) provides information on the total carbon and total organic carbon content of the samples, while thermogravimetric analysis (TGA) allows for comparative identification of the temperature windows for weight loss in each sample.

Chapter 6 presents the results of the chemical analyses of each sample, and describes the chemical functional groups in the extracted bitumen phase of each rock. Fourier Transform Infrared Spectrometer (FTIR) was used to quantify and compare the aliphaticity and aromaticity of each bitumen extract. Calculation of the bitumen yield of each sample to total organic carbon ratio allowed for an estimation of the maturity of the rocks. Gas Chromatography-Mass Spectrometry of the bitumen extracts (GC-MS) identified the different hydrocarbons in each extract and thus allowed for the determination of the relative proportions of aliphatics, aromatics, cycloalkanes, and heteroatom compounds in each rock. Selected index compounds chosen from the list of identified hydrocarbons are used to discuss the paleoenvironment and maturity of the rocks.

In Chapter 7 the physical, thermal and chemical analytical results of Chapters 4-6 are combined to derive the novel non-conventional production potential model that represents the final output of this thesis. The validity of the conclusions of this non-conventional model was confirmed by the results of conventional SRA. The physical, thermal and chemical results obtained through analysis of the Waipawa Formation and Orepuki oil shale were then applied to the non-conventional model, and final conclusions made on the source rock potential of these two oil shales. The derived production potential model is finally proposed as an initial framework for the future assessment of non-conventional source rocks, based on the superiority of the scientific data and availability of the component analytical techniques relative to conventional SRA.

Chapter 2 − Materials and methods

2.1.   Introduction

This chapter explains the materials used and the methodologies/techniques applied to achieve the objectives of the current study as stated in Chapter 1. A range of oil shale samples were sourced from Pakistan, China and the USA. These reference samples represent both production potential and poor potential oil shales. Samples were also collected from the Waipawa Formation and from the Orepuki oil shale.

The purpose for obtaining samples from this range of locations was to allow for comparison of the New Zealand shale examples to other international shale deposits, and to provide data for development of a new production assessment model based on more readily available analytical techniques.

2.2.   Oil shale and reference samples for the current study

Samples of the Waipawa Formation were collected from four different outcrops within the East Coast Basin as shown on sample location map Figure 2.1. The weathered surfaces at each outcrop were first removed with a hammer and spade to expose the freshest available material for analysis. Approximately 1 kg of this material was broken from the outcrops and bagged in labelled press-seal plastic bags. Fresh samples of the formation were collected from three different points within each outcrop. For example samples from the Waipawa type locality outcrop were labelled as WFT1, WFT2 and WFT3 (Table 2.1). Samples of the Orepuki oil shale were collected from an exposure in Southland by Dr. Chris Anderson (Institute of Agriculture and Environment, Massey University). However as weathering can affect the resultant data such as composition of the organic matter and changes in mineralogy (Clayton & King, 1987), every effort was made to get as much fresh sample as possible by removing the exposed weathered surface. Samples were thus selected carefully to get reliable results.
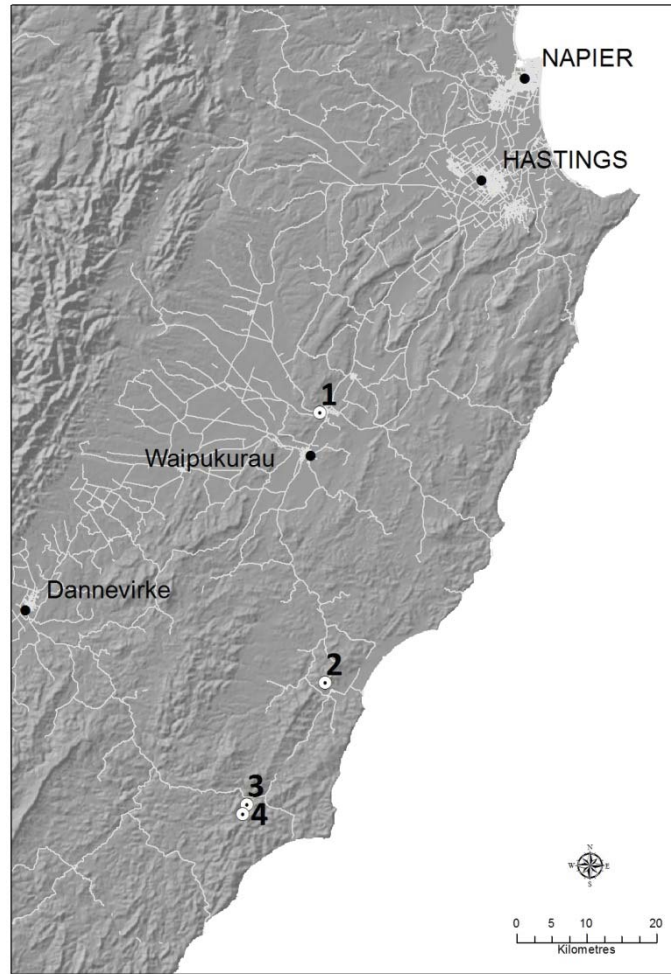
Figure 2.1. *Sampling locations for the Waipawa Formation.* **1**: *Waipawa type locality,* **2**: *Old Hill Road (Porangahau),* **3**: *Lower Angora Road quarry locality and* **4**: *Upper Angora Road locality.*

Samples of the Green River Formation, Colorado, were supplied by the USGS and the Pakistani oil shale samples by the Centre of Excellence, Department of Geology, University of Peshawar, Pakistan. Samples of the Qianjiang Formation (from Jianghan Basin) were provided by the Institute of Geochemistry of the Chinese Academy of Sciences in Guiyang China. Acid-washed quartz sand was taken from the IAE laboratory, Massey University, and argillite was collected from the Linton quarry near Palmerston North. Coding used to identify each sample in the current research is defined in Table 2.1.

Table 2.1. Identification codes for samples of the current study including their localities and grid references (where available).

Samples	Keys/symbols	Location	Easting	Northing	Coordinate System
Sand	Sand	IAE Laboratory, Massey University[8]	--	--	--
Argillite	Argillite	Linton quarry near Palmerston North	2730000	6082500	New Zealand Map Grid (NZMG)
Waipawa Formation	WFT1, WFT2, WFT3	Waipawa type locality	2815500	6134000	
	WFAQ11, WFAQ12, WFAQ13	Lower Angora Road quarry	2805050	6078000	
	WFAQ21, WFAQ22, WFAQ23	Upper Angora Road	2804500	6076600	
	WFOH31,WFOH32, WFOH33	Old Hill Road, Porangahau	2816250	6095400	
Orepuki oil shale	OOS1, OOS2, OOS3	East of Waiau River mouth, Orepuki	2104138	5422770	
Samples	**Keys/symbols**	**Location**	**Latitude**	**Longitude**	**Coordinate System**
Green River Formation (dark brown)	CBl	Anvil Points Mine, Colorado	39.5346N	107.9544W	World Geodetic System (WGS 1984)
Green River Formation (light brown)	CBr				
Qianjiang Formation	QF1, QF2, QF3	Jianghan Basin	--	--	--
Mir Kalam Kala shale	MKK1, MKK2	Mir Kalam Kala, Pakistan	33.3105N	71.3135E	World Geodetic System (WGS 1984)
Speena Banda shale	SB	Speena Banda, Pakistan	33.2177N	71.2508E	
Salt Range oil shale	SR1, SR2, SR3	Salt Range, Pakistan	--	--	

---

[8] Location for the sand is unknown

2.2.1 Sand and argillite

Acid-washed quartz sand sourced from Sigma chemicals, and argillite, collected from Linton quarry, near Palmerston North, were used as reference samples. They have no production potential and were analysed to provide a non-source rock base-line for comparison to the shale samples of the study.

2.2.2 Green River Formation

The Green River Formation samples for current study were obtained from the Parachute Creek Member of the Piceance Basin which is composed mainly of marlstone, oil shale, siltstone, sandstone and tuff (Cashion, 1967).

The two Green River Formation samples analysed in this research were collected by the USGS from outcrops at the Anvil Points Mine (APM) near Rifle, Colorado (Figure 2.2) (Appendix B, Image B1). The two samples differ in their physical appearance. One rock (defined as CB1) is very dark brown in colour (10YR 2/2) (Munsell Soil Colour Charts, 1954), indurated and very finely laminated, while the other type (CBr) contains alternating light brownish grey (10YR 6/2) to dark greyish brown (10YR 4/2) 5-15 mm thick alternating bands. Due to the difference in physical appearance these two rocks were treated as two different samples and therefore given separate identity codes.
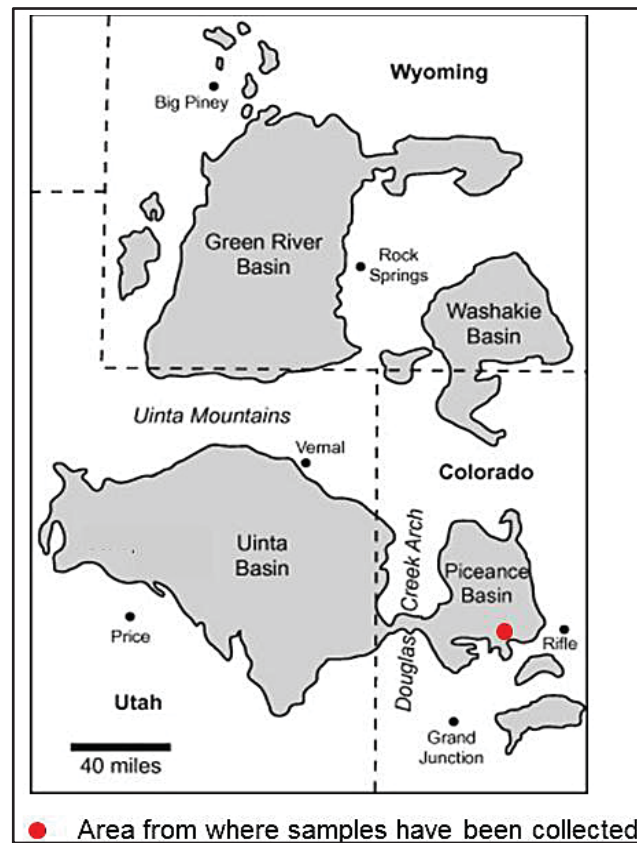
Figure 2.2. *Green River Formation sample location from the Anvil Points Mine (APM) near Rifle, Colorado, from Self et al. (2010)*

2.2.3 Orepuki oil shale

Samples of Orepuki oil shale were collected by Dr. Christopher Anderson from a coastal outcrop at the mouth of Falls Creek (Figure 2.3) (Appendix B, image B2). Samples were collected from three different points within the same outcrop in three different bags labelled as OOS1, OOS2 and OOS3. This oil shale is dark grey (7.5YR 4/2), inhomogeneous, friable in nature and very thinly laminated.
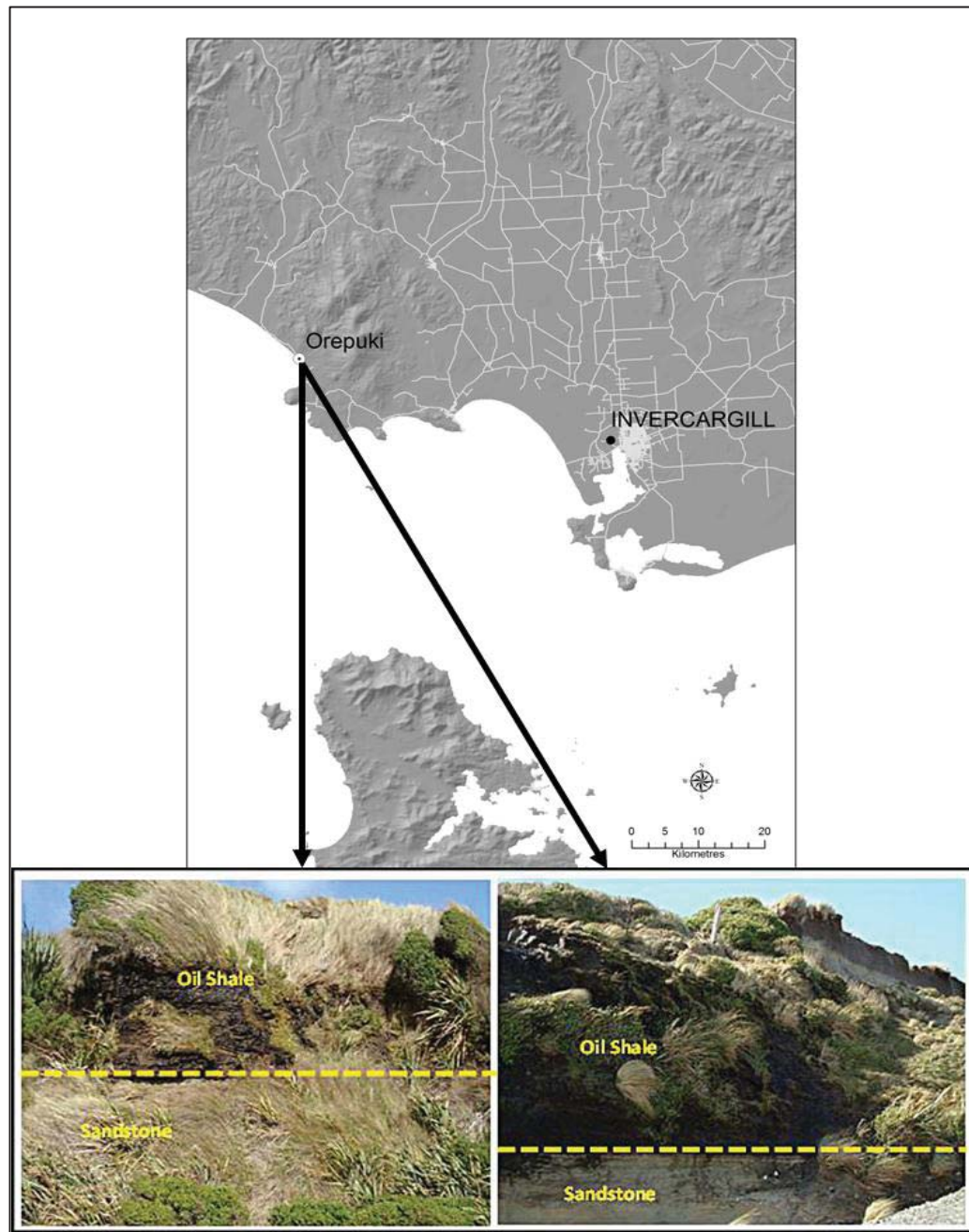
Figure 2.3.*Orepuki oil shale from the mouth of Falls Creek, Southland*

2.2.4 Qianjiang Formation

The Qianjiang Formation samples investigated in the current study were provided by the Institute of Geochemistry of the Chinese Academy of Sciences in Guiyang, China. Samples arrived at Massey University in three bags so they were treated as three

different samples with identification codes QF1, QF2 and QF3. The oil shale in each of the three bags could be described as a claystone and all were similar in colour, being black (2.5YR 4/2), lithified, homogeneous and thinly laminated (0.5-1mm thick). However, the shale in bag 2 (QF2) was notably friable. The weathered surface of all the rocks was pale red (2.5YR 6/2).

2.2.5 Mir Kalam Kala oil shale, Pakistan

Samples of oil shale from Mir Kalam Kala were supplied by the Centre of Excellence, University of Peshawar (Pakistan), collected from an outcrop along the Indus Highway in the Kohat area (Appendix B, image B3). These samples were received in two different bags and were therefore treated as two separate samples coded as MKK1 and MKK2. The samples are grey (10YR 6/1) in colour and lithified. Gypsum crystals are visible to the naked eye and under the binocular microscope.

2.2.6 Speena Banda oil shale, Pakistan

The Speena Banda oil shale sample was supplied by the Centre of Excellence, Department of Geology (University of Peshawar), collected from an outcrop along the Indus Highway in the Kohat area (Appendix B, image B3). This sample was received in one bag and was therefore treated as one sample coded as SB. The sample is greyish brown (10YR 5/2) in colour and lithified. Gypsum crystals are visible.

2.2.7 Salt Range oil shale, Pakistan

Samples from the Salt Range Formation were supplied by the Centre of Excellence (University of Peshawar), collected from Khewra Gorge area (Figure 1.10). The samples were received in three different bags and were treated as three different samples coded as SR1, SR2 and SR3. All three samples are dark grey (5YR 4/1) in colour and lithified.

2.2.8 Waipawa Formation

The samples of the Waipawa Formation in the current study were collected from four different outcrops (Figure 2.1) (Appendix B, images B4 and B5) located at:

- Waipawa type locality (V22/155340) – Tikokino Road (Figure 2.4)
- Lower Angora Road quarry (U24/051780) – Angora Road (Figure 2.5)
- Upper Angora Road (U24/045766) – Angora Road (Figure 2.5), and
- Porangahau (V24/163954) – Old Hill Road (Figure 2.6)

The samples of Waipawa Formation from the type locality are very dark brownish grey (10YR 4/1), well indurated siltstone with pale yellow (2.5Y 8/4) jarosite coating on the weathered surface and in between fractures (Figure 2.4). Samples from the Lower Angora Road, from a quarry-face outcrop, are dark grey (10YR 4/1) with pale yellow (2.5Y 8/4) coating on the weathered surface and in between the laminae which was identified as jarosite by Lee and Begg (2002) and Lee *et al*. (2011) (Figure 2.5). Samples from the Upper Angora Road, were collected from a roadside outcrop which is about 1.5 km apart from the Lower Angora Road locality (Appendix B, image B5). These samples are very dark grey (10YR 3/1). These have irregular fractures. Jarosite with a pale yellow colour (2.5Y 7/6) can be seen on the weathered surface and in between fractures (Figure 2.5). Samples of the Waipawa Formation from the road side Old Hill Road outcrop at Porangahau are also very dark grey (10YR 3/1). These have irregular fractures. Jarosite with a pale yellow colour (2.5Y 8/6) can be seen precipitated out at the weathered surface and in between the fractures (Figure 2.6). All these outcrops are deeply weathered and for that reason they appear quite variable on first sight. When digged below the surface it was found that the rocks were not as variable as they first seem. Samples were collected from three different parts of each outcrop and labelled as shown in Table 2.1. For example samples collected from three different points in the Waipawa type locality outcrop were labelled as WFT1, WFT2 and WFT3 (Table 2.1). In the same way samples from three different points were collected from Lower Angora Road quarry, Upper Angora Road and Old Hill Road outcrops.

Figure 2.4. *Waipawa Formation at the Waipawa type locality – jarosite can be clearly seen crystallised out at the weathered surface and in between fractures.*

Figure 2.5. Waipawa Formation at the Lower Angora Road quarry/Upper Angora Road. In the right hand photo jarosite can be seen precipitated on the weathered surface and within fractures.

Figure 2.6. Waipawa Formation at the Old Hill Road site, Porangahau. In the right hand photo jarosite can be seen precipitated on the weathered surface and within fractures.

2.3 Primary sample preparation for thermal, physical and chemical analysis

Samples from each sampling location were received in the laboratory in a different state, depending on where the sample had come from, and how it had been collected. Therefore, different stages of primary sample preparation were required to ensure all samples were clean and dried appropriately for analysis.

The Orepuki, Qianjiang Formation samples and samples of Waipawa Formation from Lower Angora Road quarry, Upper Angora Road and Porangahau were removed from the sealed plastic bags and spread out into trays to dry. Two to three days were required to air dry these samples. The Colorado oil shale samples (CBl, CBr) and samples of the Waipawa Formation (WFT1, WFT2 and WFT3) from the Waipawa type locality and argillite were first washed to remove any dirt and then air dried overnight. The Pakistani oil shale from Salt Range (SR1, SR2, and SR3) and Mir Kalam Kala (MKK1, MKK2) were received in a dry, powdered form with some hard pieces. There was no need to wash or air dry them. Samples from Speena Banda (SB), Pakistan, came as hard rocks, so they too were washed and air dried. The sand taken from the Soil and Earth Sciences laboratory, was already clean, so there was no need for additional preparation.

2.3.1 Grinding

Once all the samples were air dry, they were crushed to smaller pieces in a metal mortar and pestle. The crushed pieces were then ground to fine powder in a ring grinder for 20 seconds. The samples were then subjected to further treatment where necessary according to the requirements of each physical, thermal and chemical characterisation technique being undertaken.

2.3.2 Concentration of minerals

In order to obtain the best results from certain techniques it is necessary to concentrate certain minerals by removing other material that might compromise the results. For LECO analysis, removal of carbonates was performed so that the content of total organic carbon could be quantified without a carbon contribution from the carbonate fraction. XRD was used for mineral identification so it was necessary to isolate the mineral phase of each sample through the removal of organic carbon. For XRD analysis, carbonates, organic matter and iron were also removed prior to analysis in order to better resolve the clay mineral peaks in each sample. Specifically, for XRD, care was taken to remove overlapping carbonate mineral peaks. The isolation methods employed are described more fully in the following sections.

2.3.2.1   Removal of carbonates

Sample treatment to remove carbonates largely followed the techniques of Whitton and Churchman (1987). To remove carbonates approximately 20 g of the ground rock was randomly taken from the bulk sample (using a spatula) and was placed in a centrifuge tube with 100 mL of water. Five mL of 1M HCl was added and stirred until frothing ceased. The samples were then centrifuged for 10 mins at 1500 rpm to sediment the samples. The supernatant liquid was then poured off and the samples were washed by adding RO (reverse osmosis) water to the tubes. After shaking well, the suspension was again centrifuged and the water was then removed through decantation. The same process was repeated 10 times in order to remove all chlorides present due to the addition and action of HCl. The samples were then oven dried at 50°C before analysis.

2.3.2.2 Removal of organic carbon

Sample treatment to remove organic matter largely followed the techniques of Whitton and Churchman (1987) and Kunze and Dixon (1986). To remove organic matter, approximately 20 g of the ground rock was randomly taken from the bulk sample (using

a spatula) and was placed in a 600 mL beaker. Distilled water (20 mL) and 6% hydrogen peroxide (H_2O_2) (50 mL) was then added initially. The suspension was stirred with a Teflon rod until frothing subsided. The samples were then heated gradually, stirring occasionally. The samples were not allowed to become dry so small aliquots of water was added when required. This process was repeated, and the strength of added H_2O_2 was increased in steps up to 30%, until no more reaction occurred with further addition. The samples were then transferred to centrifuge tubes when the frothing finished. The tubes were centrifuged for 15 min at 1500 rpm and the supernatant liquids discarded. The samples were oven dried at 50°C before further analysis.

2.3.2.3 Removal of iron and aluminium oxides and oxyhydroxides

Once organic material was removed (see section 2.3.2.2), samples were then taken and 30 mL of 0.26 M citrate reagent and 5 mL of 1M sodium bicarbonate were added. After stirring well, the tubes were placed in a boiling water bath for 10 mins. When the solutions were hot, they were stirred again. Approximately 1 g of powdered sodium dithionite was then added to each tube and stirred. Cold water was used to damp down excessive frothing as required. Tubes were left in the water bath for 15 mins with periodic stirring. The tubes were then removed from the bath, stirred well and centrifuged for 20 mins at 2000 rpm and the clear or in some cases coloured solution was discarded. Some solutions, such as those from Qianjiang Formation, were cloudy. These were flocculated by adding 2-3 mL of 0.5M NaCl solution, stirred and centrifuged again. The clear solution was then discarded (Kunze, 1965; Whitton & Churchman, 1987).

2.3.3 Separation of clay free from carbonates, organic carbon and iron and aluminium oxides

Distilled water was added to samples obtained from section 2.3.2.3. The suspension was then transferred to beakers and ultrasonic vibration was used to disperse the clay sized

material. The beakers were then filled with water up to the 10 cm mark. After four hours the suspension from the top 5 cm was collected. This was defined as the clay (<2 micron) fraction (Jackson, 1956).

2.4 Major analytical techniques used to characterise rocks of the study

A suite of physical, thermal and chemical analytical techniques:- XRD, LOI, LECO, TGA, FTIR and GC-MS were used to characterise the physical and geochemical characteristics of the different source rocks collected for the study. These techniques were chosen because of their availability at Massey University. Organic petrography had to be undertaken at GNS in Lower Hutt. The principles behind each technique are described in the following section.

2.4.1 Analytical techniques used for physical analyses

2.4.1.1 X-ray Diffraction (XRD)

X-ray crystallography is used to determine the atomic and molecular structure of the crystalline phases of minerals by analysis of the diffraction patterns produced when X-rays pass through the sample (Toby, 2005). XRD can be used to characterise heterogeneous solid mixtures and to determine if different crystalline components, or minerals are present (Toby, 2005).

XRD utilises a focussed X-ray beam approximately 20 mm wide that is directed at varying angles onto a sample. The focussed X-ray beam is partly transmitted and partly diffracted by the molecular layers in the sample. The angle of diffraction is dependent on the lattice spacing of the atoms or molecules (d-spacing): a simple equation (Bragg's law: $n\lambda = 2d\sin\theta$) calculates the d-spacings of the crystal (measured as 2-theta) from the angles of the incident and diffracted beams. The diffraction spectrum is recorded by a

detector as peaks on a chart (a diffractogram or XRD trace) of diffraction angle versus intensity (Tucker, 1988).

The X-ray machine used in this study was a GBC EMMA X-ray Diffractometer with copper CoK_α radiation operated at 35 kV voltage and approximately 30 mA current in the Soil and Earth Sciences Laboratory of the Institute of Agriculture and Environment, Massey University. This X-ray machine was used for qualitative purpose and therefore no analytical standards were used. The machine was, however, calibrated according to manufacturer instructions.

Powdered whole-rock samples were mounted in aluminium sample holders and run through the X-ray machine and the diffraction patterns recorded. Slides were also made for samples subjected to the primary preparation steps for clay separation as discussed in sections 2.3.2 and 2.3.3 (samples from which carbonates, organic carbon and iron and aluminium oxides have been removed). To assist in the identification of the clay minerals different secondary pre-treatments (Table 2.2) were applied. These were necessary because different clays expand or collapse in response to different treatments. All samples were scanned between 3° and 60° 2θ on the X-ray machine. Minerals were identified using the mineral powder diffraction data book (JCPDS, 1980).

Four secondary pre-treatment methods were used (K-saturation, Mg-saturation, heating and glyceration) on each clay fraction separated from each sample to aid the identification of clay minerals present. Table 2.2 shows the diagnostic d-spacings of several common clay minerals and how these d-spacings change in response to the pre-treatments used.

Table 2.2. Selected diagnostic d-spacings (Å) of common soil minerals at specified conditions of cation saturation, glycerol solvation and heat treatment. Taken from Eslinger and Pevear (1926) and Harris and White (2008).

Mineral	Diagnostic d-spacings (Å)			
	K, 25°C	Mg	K, 550°C (3 hours)	Mg+glycerol
Kaolinite	7.2	7.2	No peak	7.2
Illite	10	10	10	10
Montmorillonite	10-14	14-15	10	15-18
Vermiculites	10-12	14	10	14
Chlorites	14, 7	14, 7	14, 7	14, 7

Kaolinite is not affected by the Mg^{2+}−glycerol treatment but collapses when heated to 550°C for 3 hours. The 2:1 clay mineral, illite, has a non-expandable lattice after Mg^{2+}−glycerol treatment and a lattice spacing that is not affected by heat treatment. The peak at 14.0Å due to 2:1:1 mineral chlorite only slightly widens with potassium saturation but is not affected by any other treatment (Ghazi & Mountney, 2011; Harris & White, 2008; Reeves *et al.*, 2006; Velde & Barre, 2010; Whitton & Churchman, 1987). According to Hussain *et al.* (1985) and Afzal *et al.* (1999), heat treatment causes an increase in the reflection at 14.0Å due to chlorite, with a slight shift from 14.0Å to 13.6Å giving the reason that this shift might be due to partial dehydration, but does not expand with glyceration. However, montmorillonite has an expandable lattice after glyceration and collapses when heated. Vermiculite also expands with glyceration and collapses on heating (Avery & Bullock, 1977; Whitton & Churchman, 1987).

Each of these pre-treatments was carried out according to the method of Whitton and Churchman (1987) and is described as follows:

Potassium saturation

Approximately 10 mL of the clay suspension (from section 2.3.3) were poured into a tube and 3 drops of 1M HCl and 3-5 mL of 1M KCl solutions were added. The tubes were stirred well with a Teflon rod and allowed to settle overnight. The next day the clear supernatant liquid was extracted with a pipette and a further 10 mL of KCl

solution was added and allowed to stand overnight. The clear supernatant was extracted and the tubes were filled with distilled water, shaken gently and allowed to stand overnight. The supernatant liquid was extracted again. This was repeated until the clays began to disperse (Whitton & Churchman, 1987). Then 1 mL of clay suspension of the clay fraction for each sample was sedimented onto aluminium discs for clay mineral analysis. The clay suspension was added drop by drop with a pipette to the disc which was then kept overnight to dry. These discs were then run through the XRD.

Magnesium saturation

About 10 mL of clay suspension were taken in a tube and 10 mL of 1M $MgCl_2$ solution together with 2-3 mL of 1M HCl were added. This mixture was stirred well with a Teflon rod and allowed to stand overnight. The clear supernatant liquid was extracted with a pipette the next morning and the tubes were refilled with distilled water, shaken gently and allowed to stand overnight. The next morning the supernatant was extracted. This was repeated until the clay began to disperse. Then 1 mL of clay suspension of the clay fraction for each sample was sedimented onto aluminium discs for clay mineral analysis. The clay suspension was added drop by drop with a pipette to the disc which were then kept overnight to dry. These discs were then run through the XRD.

Heating

The K^+-saturated discs were heated to 550°C in a muffle furnace for 3 hours, cooled and another diffractogram was obtained (Whitton & Churchman, 1987).

Glyceration

The Mg^{2+}-saturated slides were sprayed with a 10% glycerol and water solution using an aerosol spray bottle. Each slide was allowed to dry for 3-4 hours and another diffractogram was again obtained (Whitton & Churchman, 1987).

2.4.1.2 Organic petrography

Organic petrography is widely used to characterise organic matter of source rocks. The technique is used to identify the organic constituents (macerals) present in sedimentary rocks of all ages (Alpern, 1980), and is conducted on a polished section. The identification of macerals in a source rock is useful for source rock diagnosis, as macerals are mainly related to biological units and allow reconstruction of the environment of deposition of the source rock (Bertrand *et al.*, 1993; Schiøler *et al.*, 2010).

To investigate the macerals, polished grain mounts of four samples were examined by Richard Sykes at GNS Science (Lower Hutt) using a Leica DMRXA2 petrological microscope fitted with a Leica DC500 digital camera. The mounts were scanned at 500 and 625x magnification under both white light and blue light (fluorescence mode). No quantitative macerals analyses were undertaken.

2.4.2   Analytical techniques used for thermal analyses

2.4.2.1 Loss on ignition (LOI)

Loss on ignition (LOI) is a very widely used, rapid, inexpensive and accurate method to estimate the total carbon content of sediments. The weight loss can be determined by taking the weight of an oven-dried sample before and after ignition.

To perform LOI, a powdered randomly gathered sub-sample (15g) of each analytical sample was first oven dried at 105°C for two hours. Ten grams of each sample were then weighed into a borosilicate beaker, placed in a muffle furnace, and heated to 550°C for five hours. Each sample was re-weighed upon cooling to a manageable temperature. The loss in weight is a measure of the carbon lost due to the combustion or decomposition of organic matter and carbonates (Dean, 1974).

2.4.2.2 LECO

The LECO system provides a rapid, simple, accurate and precise method for the determination of total carbon in sediments. All samples in the current study were analysed for total carbon (TC) using a LECO FP-2000 analyser operated by Landcare Research, Palmerston North. Fine powdered samples were analysed for TC. Total Organic Carbon was quantified through measuring the TC content of acid washed samples (section 2.3.2.1) from which carbonates had been removed[9].

During the LECO technique, sediment is combusted in an oxygen atmosphere at 1050°C. Any carbon present in the sample is converted to CO_2 which flows through a non-dispersive infrared (NDIR) detection cell where the mass of CO_2 is determined and the results are expressed as percentage carbon based on the dry weight of the sample (Churcher & Dickhout, 1987; Etheridge *et al.*, 1998; Nelson & Sommers, 1996). The TOC present is subtracted from the TC to derive the total inorganic carbon.

---

[9] Assuming that carbonate carbon + organic carbon = total carbon

2.4.2.3 Thermogravimetric analysis (TGA)

Material may lose/gain weight due to volatilization/oxidation of species such as H_2O, CO_2 and SO_3 during heating or cooling. TGA is a laboratory technique used for material characterisation in which the mass of a substance is monitored as a function of temperature or time as the sample is subjected to a controlled temperature program in a controlled atmosphere.

TGA involves isothermal and non-isothermal analyses. In an isothermal analysis the rate of reaction is determined at a constant temperature whereas in non-isothermal analysis, time and temperature are coupled via a constant heating rate. In the current study non-isothermal TGA was performed as it is generally preferred over the isothermal method for the following reasons (Williams & Ahmad, 2000).

- It permits a rapid scan of a temperature range of interest
- It eliminates the errors introduced by the thermal induction period
- It more closely simulates conditions expected in retorting processes
- It also permits a rapid and complete scan of the entire temperature range of interest in a single run

The TGA of all rock samples in the current study was undertaken using a TG analyser (SDT Q600, TA Instruments) operated by the Institute of Agriculture and Environment, Massey University. Rocks were analysed in powdered form (10-15 mg) and were heated to about 1200°C using nitrogen as a purge gas with a flow rate of 20 mL/min. The heating rate was kept constant at 5°C per minute. No extraction was expected from sand and argillite but these samples were still extracted as analytical reference controls.

2.4.3 Analytical techniques used for chemical analyses

2.4.3.1 Soxhlet extraction

Organic geochemical studies of source rocks usually require solvent extraction techniques like soxhlet extraction and ultrasonic extractions to separate bitumen for further chemical analyses. Routine analytical techniques to study the organic fraction include Fourier Transform Infrared spectroscopy (FTIR), Gas Chromatography (GC) and Gas Chromatography-Mass Spectrometry (GC-MS) (Blanco *et al.*, 1992). Oil shale bitumen can be analysed by GC-MS or GC to deduce its environment of deposition and maturity (Hwang *et al.*, 1998; Ruble *et al.*, 1994). In the current study, the bitumen phase of organic matter was isolated in preference to kerogen. The rationale for this choice was as follows:

- Bitumen can be extracted with organic solvents (kerogen cannot be).
- The bitumen yield of a shale after soxhlet extraction is not contaminated and can therefore be reliably analysed by FTIR in order to determine the relative aliphaticity and aromaticity of the extract. It can also be analysed through GC-MS in order to identify the different types of hydrocarbons present.
- Bitumen was extracted to suggest the environment of deposition and maturity of the different samples. Spectroscopic and chromatographic techniques can be used to draw these conclusions.

Powdered sample (approximately 20 g) was accurately weighed into a thimble and covered with cotton. The thimble was then put in a soxhlet apparatus, which was fitted into a flask with 250 mL of dichloromethane (DCM) and some boiling chips. A condenser (running water as a coolant) was connected to the soxhlet apparatus. The flask with DCM was gently heated in the beginning using a hot plate to avoid bumping of the DCM and temperature was increased slowly to about 200°C. Extraction was performed by refluxing the solvent for 48 hours (Akinlua *et al.*, 2012; Blanco *et al.*, 1992). The solvent became clear after 5-8 hours, depending on the sample. The DCM dissolved in the extract was then evaporated in a rotary evaporator until about 4-5 mL of the extract dissolved in DCM was left.

2.4.3.2 Fourier transform infrared spectroscopy (FTIR)

Infrared spectroscopy provides qualitative information on organic and inorganic functional groups, including aliphatic and aromatic carbon and hydrogen. The IR spectroscope is used to identify compounds or to investigate the molecular structure of a sample (Derenne *et al.*, 2000; Kayacan & Do Gan, 2008; Solomon & Miknis, 1980). When infrared radiation is passed through organic molecules, absorption peaks can be observed. The molecules of the sample absorb IR wavelengths by either stretching or bending molecular motions. Different functional groups and different elemental bonds absorb different wavelengths, resulting in an absorption band (Sperling, 2006). This results in a spectrum that can be analysed with the help of tables which correlate frequencies with functional groups. Mid IR (MIR) provides a spectrum of compounds in the range 4000 to 400 cm^{-1} (Pavia *et al.*, 2009).

At the outset of the FTIR study, the raw, powdered oil shale samples, sand and argillite were analysed using an FTIR. But the spectra were not good. To improve the quality of the spectra a second analysis was made using the potassium bromide (KBr) pressed disc technique (Rouxhet *et al.*, 1980). KBr pellets were prepared by uniformly mixing approximately 5 mg fine powdered sample and 80 mg KBr before the mixtures were ground in a mortar and pestle. The mixture was transferred to a die and a manual press was used to form a pellet. The KBr pellet was oven dried under vacuum for 18 hours at 200°C. These KBr pellets were then placed directly into the FTIR using a holder for spectral analysis.

The results from the KBr disc technique were good but there was a wide OH peak in the region 3300-3500 cm^{-1}. Although the pellets were oven dried, there was no assurance that the OH peak was not adsorbed moisture from air rather than due to a sample constituent (KBr is known to absorb water from the air very quickly). Therefore, to avoid any peaks with an origin due to absorbed moisture, and furthermore due to the potential for overlapping peaks with inorganic carbonates, a final methodology of running FTIR on solvent extracts of each rock sample was adopted.

The extracts dissolved in the solvent DCM were added to discs made of NaCl drop by drop with evaporation of the DCM at the same time using a hair dryer until a visible film formed on each disc. The discs were then placed in a holder and analysed using the FTIR. There was a clear improvement in results as the preparation technique evolved from powdered rock samples to thin film extracts. The FTIR peaks of the extract thin films were clear, sharp and reliable.

The samples were analysed on a Nicolet 5700 FT-IR spectrometer at the Institute of Fundamental Sciences, Massey University. Operating conditions were between 4000 and 400 cm^{-1} wavenumbers with a resolution of 4 cm^{-1} and each FTIR transmittance spectrum was based on an average of 32 scans.

2.4.3.3 Gas Chromatography ─ Mass Spectrometry (GC-MS)

Gas Chromatography ─ Mass Spectrometry (GC-MS) is generally used to identify and quantify volatile and semi-volatile organic compounds in complex mixtures. This technique can also determine the molecular weight of unidentified compounds in complex mixtures. This analytic technique has many applications and can be used for the determination of pollutants in drinking and waste water, for the determination of drugs in urine and blood, and for quality control analysis of industrial products (Azevedo *et al.*, 2000; Polettini *et al.*, 1998; Stein, 1999).

GC-MS of the soxhlet extracts was performed on all oil shales, sand and argillite with a SHIMADZU GC-MS QP2010S GC-MS instrument operated by John Sykes from the School of Engineering and Advanced Technology, Massey University, using a 30 m x 0.25 mm internal diameter Thermo Scientific TG-5MS -5MS column (0.25 μm film). The injector temperature was 250°C. The oven temperature was maintained at 50°C for 2 min, and then slowly increased to 250°C at a rate of 10°C min^{-1} with the final temperature being held for 20 minutes. The GC–MS interface consisted of a heated transfer line kept at 280°C. The mass spectrometer was operated with ionization energy of 70 eV and a mass range of 40–400 every second.

2.5 Conventional source rock analysis (SRA)

Source Rock Analysis (SRA) is the method most widely used by petroleum companies to assess the generative potential of organic rich rocks. The method is rapid and requires only a small amount of sample. The SRA instrument was first developed by the Institute Francais du Petrole (IFP) in 1977 (Espitalie *et al.*, 1977).

Analysis for the current study was performed at GNS Science, New Zealand, using an SRA TPH/TOC Weatherford Laboratories instrument for powdered rock samples. Approximately 60–100 mg of powdered rock was accurately weighed into an SRA crucible and placed in the SRA-Agilent auto sampler. The auto sampler transfers the crucible from the auto sampler tray to the SRA pedestal which is raised, placing the sample into a 300°C oven. The sample is heated isothermally at 300°C for 3 mins. During this time the free hydrocarbons are volatilised and quantitatively detected by a FID detector. The free CO_2 liberated up to 400°C is detected by an IR cell.

The temperature is then increased from 300°C to 650°C at a rate of 25°C/min using Helium as a carrier gas. During this step the organic hydrocarbons are generated from the pyrolytic degradation of the kerogen in the rock which is roughly similar to the generative potential of the rock. The hydrocarbons are detected by the FID.

The free hydrocarbons volatilised in the first 3 mins are labelled as S1, and reported as milligrams (mg) of S1 per gram of rock. The free CO_2 detected is labelled as S3 and reported as milligrams (mg) of S3 per gram of rock. The hydrocarbons detected from 300°C to 650°C are labelled as S2, and reported as milligrams (mg) of S2 per gram of rock.

At the end of the pyrolysis the oven is cooled to 580°C and the carrier lines are purged for 5 mins. The temperature of the oven is kept at 580°C while the sample is purged with oxygen to oxidize remaining organic carbon (Weatherford Laboratories Operators Manual, 2010). The TOC value is composed of three fractions: the convertible fraction, which represents the hydrocarbons already generated (S1), the potential to generate hydrocarbons (S2) and the residual carbon (S4) which comes from the oxidation cycle.

The SRA pyrogram does not give the S4 value, but rather it uses it internally to calculate TOC using the equation: $TOC = [k(S1 + S2) + S4]/10$, where $k = 0.83$ (an average carbon content of hydrocarbons by atomic weight (Weatherford Laboratories Operators Manual, 2010).

2.6 Quality control procedures used throughout the study

The analytical work conducted for this thesis involved both quantitative and qualitative determinations. All techniques used in this research were used to provide absolute results, and therefore no standardisation of each instrument was performed prior to each analytical determination. The techniques that require analytical standards for quantitative determination, GC-MS and XRD, were deliberately run without standardisation. Each machine was, however, calibrated according to manufacturer instructions.

In any research such as that conducted for this thesis, a high degree of confidence that sample results are representative of the rock type being analysed, is essential. Each analytical determination required only a small sample size for analysis. Therefore, to ensure sample homogeneity and confidence in the applicability of the results to source-rock geology, bulk samples were collected in the field, or received at Massey University. These samples were subsequently ground for 20 seconds to obtain a uniform homogeneous sample for analysis. There is always a risk during grinding that organic matter can be volatilised as a consequence of heating the sample. However, the risk of organic matter loss was considered to be minimal during the 20 second grinding period.

The number of samples analysed for each formation varied. For the Salt Range oil shale, Orepuki oil shale and the Qianjiang Formation, three samples from each formation (collected from three different points within an outcrop) were analysed (ID code in Table 2.1). For the Waipawa Formation, samples were collected from four localities (outcrops). At each outcrop three samples were collected from three different points and analysed (Table 2.1). For the Green River Formation and Mir Kalam Kala oil shale only two samples (ID codes in Table 2.1) collected from two different points in an outcrop

were analysed. However for the Speena Banda oil shale (ID code in Table 2.1) only one sample was analysed.

The number of analyses performed on each sample varied as a function of each analytical technique and is summarised in Table 2.3. Where the number of replicate analyses was greater than one, the mean and standard deviation of the mean are reported in this thesis. Triplicate LECO combustion analyses were performed on each sample described in Table 2.1 (Appendix C) (n=3). For TGA analysis, each sample was subjected to six replicate scans (Appendix C) (n=6). For FTIR analysis each sample was subjected to 32 spectral scans collected at 4 cm^{-1} resolution. An average scan was subsequently calculated and presented by the machine. Therefore, a composite of 32 scans represents a single analysis. To check the possibility for intra sample variability that might occur through replicate machine scans, a further 11 scans were made of each sample (n=12). In no case was variability observed, and therefore one of the 12 scans was randomly chosen as the final sample output. A single analysis was made of each sample by both XRD and GC-MS (n=1).

Table 2.3. Summary of analytical replications performed on each sample defined in Table 2.1.

Analytical technique	Number of replicate analyses (n)
LOI	1
LECO	3
TGA	6
Organic petrography	Note 1
XRD	1
FTIR	12
GC-MS	1

Note 1: only one sample for four of the rocks of this study was assessed by organic petrography

Chapter 3 – Source Rock Analysis

3.1 Introduction

Source Rock Analysis (SRA), also known as Rock-Eval pyrolysis, is a quick and inexpensive conventional technique that is widely used in the field of petroleum exploration to assess different types of source rocks, their petroleum potential, maturity and to characterize their degree of evolution (oil zone/gas zone), type of kerogen and depositional environment. This conventional geochemical technique has been used to define the petroleum potential of the oil shales of the current study according to industry standard methods in order to provide a conventional benchmark against which a non-conventional production potential assessment could be made.

3.2   Source Rock Analysis (SRA)

3.2.1 Results

The results from SRA analysis of the rocks of this study are shown in Table 3.1 and define the type and quantity of organic matter, thermal maturity and source rock generative potential (SP) of the samples according to values for the parameters TOC[10], S1, S2, HI, OI and PI (discussed below).

---

[10] TOC in this chapter refers to SRA (TOC)

Table 3.1. Source Rock Analysis results.

Samples	Load size	S1	S2	SP = (S1+S2)	Tpeak	Tmax	S3	*TOC	HI	OI	PI
	mg	mg HC/g rock		mg HC/g rock	°C		mg CO$_2$/g rock	Wt%	mg HC/g TOC	mg CO$_2$/g TOC	[S1/(S1+S2)]
Sand	96.3	<0.1	0.2	0.3	--	--	--	<0.1	--	--	--
Argillite	69.1	0.1	0.4	0.5	516	--	0	0.9	47	0	9
WFT1	50.5	0.5	12.9	13.4	444	405	1.8	6.1	214	30	0.04
WFAQ11	70.5	0.2	8.8	9.0	446	407	0.9	4.4	200	21	0.02
WFAQ21	69.5	0.1	2.8	2.9	455	416	1.6	2.7	103	59	0.04
WFOH31	68.0	0.1	3.4	3.5	449	410	0.7	2.7	129	27	0.04
OOS1	30.8	4.9	31.8	36.7	459	428	8.8	13.2	241	67	0.13
CBl	31.2	4.8	147.7	152.5	480	441	2	18.2	811	11	0.03
CBr	50.1	4	61.2	65.2	478	439	1.2	9.1	675	13	0.06
QF1	20.9	0.4	1	1.4	309	--	1.5	13.8	7	11	0.27
QF2	20.4	0.3	0.9	1.2	655	--	0.1	12	8	1	0.25
QF3	19.4	0.2	1	1.2	513	--	5.2	17.5	6	30	0.16
MKK1	70.7	0.1	1	1.1	477	--	1.2	2.6	33	44	0.11
MKK2	68.9	0.1	1.2	1.3	460	--	2.4	2.2	47	109	0.10
SB	97	0.1	1.2	1.3	479	--	0	0.9	242	2	0.09
SR1	71.3	0.1	0.2	0.3	466	--	0	0.5	45	0	0.19
SR2	71.5	0.1	0.2	0.3	411	--	0	0.5	46	0	0.19
SR3	70.3	0.1	0.2	0.3	362	--	0	0.3	60	0	0.20

Tmax = Tpeak – 39°C, Tmax is the maximum S2 peak (the temperature at which maximum rate of generation of hydrocarbons occur). However, Tmax for the current study is actually 39°C less than the actual maximum of the S2 peak (Tpeak), and this is due to the difference in temperature within the chamber of the instrument between the thermocouples and sample holder (Jarvie, 1991).

*TOC is calculated from the equation: $TOC = [k(S1 + S2) + S4]/10$, where k=0.83. The parameters S1 and S2 are defined by the SRA but the parameter S4 is not defined specifically by the SRA.

3.2.1.1 Amount and type of organic matter

3.2.1.1.1   TOC

The quantity of organic matter in a hydrocarbon-bearing sample is best described by the total organic carbon value (TOC) and the amount of TOC that is converted to hydrocarbons and other compounds when pyrolised. The TOC includes both the kerogen and bitumen fractions. However, TOC is not a clear indicator of source rock generative potential. For example, graphite is 100% carbon which will be part of TOC, but it will not generate petroleum (Peters & Cassa, 1994). The range of values for TOC for inadequate to adequate organic matter richness is shown in Table 3.2.

Table 3.2. Geochemical parameters describing the generative potential of immature to marginally mature source rock from Peters and Cassa (1994).

Petroleum Potential	TOC (wt %)	S1	S2
		mg HC/g rock	
Poor	<0.5	<0.5	0-2.5
Fair	0.5-1	0.5-1	2.5-5
Good	1-2	1-2	5-10
Very Good	2-4	2-4	10-20
Excellent	>4	>4	>20

The total organic carbon (TOC) value of argillite (0.9 wt%, Table 3.1) reflects the poor generation potential of this control rock. The Salt Range oil shale samples (SR1, SR2, and SR3) have very low TOC values of (0.3-0.5 wt%) indicating that these rocks have inadequate organic richness for petroleum generation. Although most of the Salt Range samples studied previously by Ahmad and Alam (2007) are organically rich (Figure 3.1), large variability can be observed in the TOC distribution in samples from a single outcrop and in samples from different outcrops. The TOC values of the Salt Range samples in this study are very low but are within the range of TOC distribution

calculated by Ahmad and Alam (2007) (Figure 3.1). The TOC values of the Salt Range samples in the current study are however very different to the TOC values from Khewra Gorge measured by Ahmad and Alam (2007) (Figure 3.1).
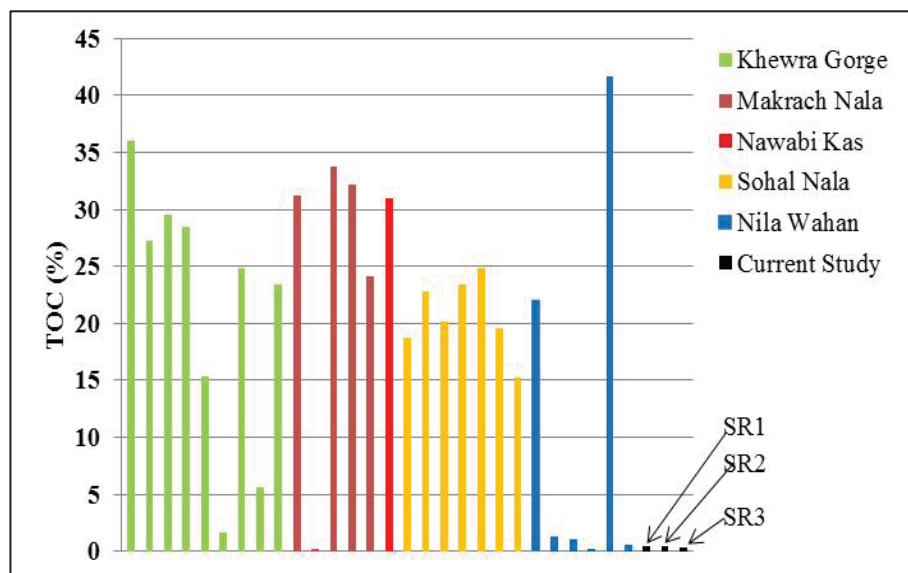
Figure 3.1. *Ranges of organic richness (% TOC) of outcrop samples from the Salt Range Formation, after Ahmad and Alam (2007). Values for the three Salt Range samples (SR1, SR2 and SR3) have been generated in this study.*

The sample from Speena Banda (SB) has a TOC value of 0.9 wt% and has therefore a fair petroleum potential (Table 3.2). The Mir Kalam Kala oil shale samples (MKK1, MKK2) have TOC values of 2.2 and 2.6 wt% suggesting that these rocks have very good petroleum potential (Table 3.2). There is no literature report of SRA parameters for oil shale samples collected from the Jatta Gypsum Formation from the Speena Banda and Mir Kalam Kala localities. However, when the TOC values of the rocks of the current study are compared with the TOC of different oil shales (from the Jatta Gypsum Formation) from nearby localities as measured by Raza *et al.* (1993) and Fazeelat & Yousaf (2004) (Figure 3.2), the samples of the current study fall towards the lower range of TOC values for samples collected from the Kohat Basin (Figure 3.2).

Figure 3.2. *Total organic carbon (TOC) content of outcrop oil shale samples from different localities in the Kohat Basin (Pakistan), after Raza et al. (1993) and Fazeelat and Yousaf (2004). The Speena Banda and Mir Kalam Kala samples have been analysed in this study.*

The Qianjiang Formation samples have very high TOC values of 12-17.5 wt% (Table 3.1) suggesting a very high organic matter content and excellent petroleum potential. Results from the current study are in contrast to those of Peters *et al.* (1996) who found relatively very low TOC values of 0.3-6.6 wt% for the Qianjiang Formation (see Table 1.2 in Chapter 1 where TOC values of core samples at different depths calculated by Peters *et al.* (1996) are tabulated).

The Orepuki oil shale sampled during the current research has a high TOC value of 13.2 wt% as shown in Table 3.1, suggesting that the rock is highly organic-rich with excellent potential. However, this value is low in the context of SRA-determined TOC values reported by Turnbull *et al*. (1993), Sykes (1996) and GeoSphere Ltd (1999) which were 20, 38 and 42 wt% respectively (Table 1.7, Chapter 1). This apparent spread of data indicates that the organic matter content within the Orepuki oil shale is heterogeneous and may be a function of sampling location.

The TOC content of the Green River Formation samples (CBl, CBr) from the Mahogany Zone (APM) recorded in the current study are 18.2 and 9.1 wt% respectively. These values are in the range of TOC values (9-26 wt%) measured by other authors (Birdwell *et al.*, 2011; Cumming *et al.*, 2012; Lewan & Roy, 2011) (Figure 3.3). The high TOC content of the Green River Formation from the Mahogany Zone, although variable as shown in Figure 3.3 (Birdwell *et al.*, 2011; Cumming *et al.*, 2012; Lewan & Roy, 2011), signifies the exceptionally high petroleum potential of the oil shale.
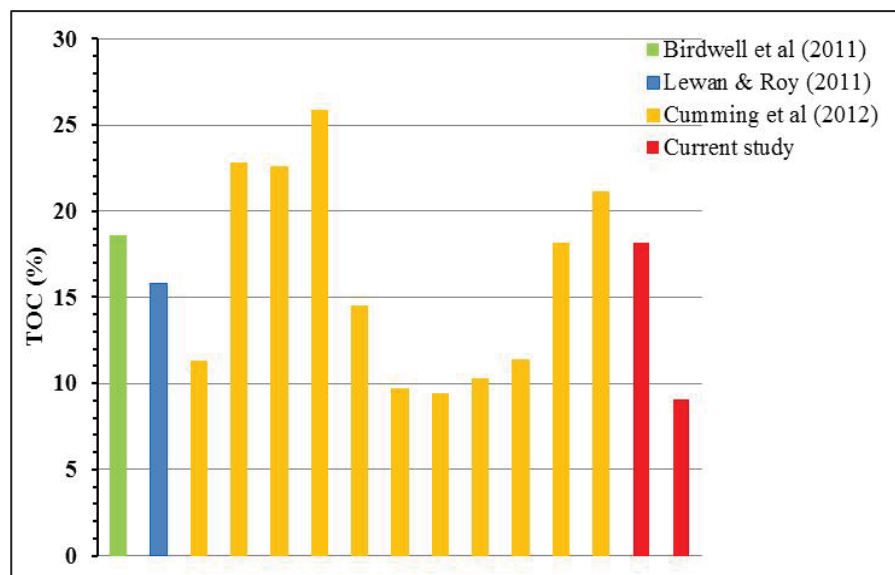
Figure 3.3. *Ranges of organic richness (% TOC) of the Mahogany Zone samples of the Green River Formation, after Birdwell et al. (2011), Lewan & Roy (2011), Cumming et al. (2012). The CBl and CBr samples of the Mahogany oil shale have been analysed in the current study.*

The Waipawa Formation samples (WFT1, WFAQ11, WFAQ21, and WFOH31) have TOC values between 2.7-6.1 wt% (Table 3.1) suggesting that this formation has very good to excellent petroleum potential (Table 3.2). Literature shows that there is a wide range of reported TOC values for samples collected from different outcrops of the Waipawa Formation throughout the East Coast Basin. Comprehensive studies of this formation are described by Field *et al.*(1997) (TOC range = 0.3-12.3 wt%, mean = 3.7 wt% and standard deviation = 2.1 wt%) and Leckie *et al.* (1992) (TOC

range = 0.6-5.3 wt%, mean = 3.1 wt%, standard deviation is unknown as the raw data has not been given in the paper) and Hollis & Manzano-Kareah (2005) (TOC range = 0-12.3 wt%, mean = 3.3 wt% and standard deviation = 1.8 wt%). These datasets are based on extensive research to quantify the resource potential of the Waipawa Formation.

TOC values obtained in the current study generated through analysis of samples collected from the four different outcrops lie with the range of TOC values measured by the previous authors (Field *et al.*, 1997; Hollis & Manzano-Kareah, 2005; Leckie *et al.*, 1992). However, extensive variability in TOC values between the four different outcrops is also observed in this study (2.7-6.3 wt%) (Table 3.1). This variability agrees with the findings of Hollis & Manzano-Kareah (2005), Field *et al.*(1997) and Leckie *et al.* (1992) and suggests that the Waipawa Formation has a variable content of organic matter within an outcrop and also between the different outcrops.

3.2.1.1.2   S1 and S2

The parameter S1 (mg of HC/g rock) defines the amount of free hydrocarbons that can be volatilised from a rock without kerogen decomposition. S2 on the other hand measures the hydrocarbon yield from the cracking of kerogen (mg HC/g rock) and heavy hydrocarbons. S2 therefore represents the existing potential of a rock to generate petroleum. S2 is a more realistic measure of source rock potential than TOC because TOC might include inert carbon which is incapable of petroleum generation. The S1 and S2 signal strength is in millivolts (mV) in Figures (3.4-3.7). In addition to the sample properties, the signal strength is also a function of how much sample has been run (i.e. load size).

Based on the interpretive guidelines by Peters and Cassa (1994) for immature to marginally mature source rocks, S1 and S2 can be used to describe the generative potential of source rocks (Table 3.2). The S1 and S2 FID signals for the different rocks and the reference samples (sand and argillite) are summarised in Figures 3.4-3.7 and the data are tabulated in Table 3.1.

The S1 and S2 values for argillite are 0.1 and 0.4 (mg HC/g rock) respectively, showing the poor or zero petroleum potential of this control rock. Source of this low hydrocarbon content in argillite is unknown but it is likely to represent contamination of the sample with organic material from nearby rocks as argillite should have no petroleum potential. All the Pakistani and Qianjiang Formation samples have very low S1 and S2 values (Table 3.1, Figures 3.4 and 3.5) lying in the range of poor petroleum potential source rocks   (Table 3.2). The S1 values of the Qianjiang Formation samples lie in the range of S1 values found by Peters *et al.* (1996) and Grice *et al.* (1998) (Table 1.2, Chapter 1) but the S2 values of these samples in the current study are very low compared to the S2 values previously measured for the Qianjiang Formation (Table 1.2, Chapter 1).

The S1 and S2 values of the Orepuki oil shale sample are 4.9 and 31.8 (mg HC/g rock) respectively (Table 3.1). These values define this oil shale as having excellent petroleum potential (Table 3.2). But these S1 and S2 values of the Orepuki oil shale are very low relative to the S1 and S2 values obtained by Turnbull *et al*. (1993) (S1= 1.3, S2= 58 mg HC/g rock), Sykes (1996) (S1= 12, S2= 235) and GeoSphere Ltd (1999) (S1= 6, S2= 321 mg HC/g rock) (Table 1.7)[11].

The Green River Formation samples have S2 values even higher than the Orepuki oil shale sample (Table 3.1, Figure 3.6), defining the formation as a very high potential source rock. The S1 and S2 values of CBl are in the range of values measured by Birdwell *et al.* (2011) (4 and 175 mg HC/g TOC respectively), Lewan & Roy (2011) (3.7, 134 mg HC/g TOC respectively) and Cumming *et al.* (2012) (5.7-14 and 95.4-272 mg HC/g TOC respectively). The S2 value of CBr is lower than the S2 values previously reported, but still signifies the excellent petroleum potential of the source rock. The S1 value for CBl is 4.8 mg HC/g TOC and for CBr is 4 mg HC/g TOC, yet the S1 peak in the CBl plot appears smaller the the S1 peak for CBr (Figure 3.6). The reason for this anomaly is that, in addition to the sample properties, the signal strength for both S1 and S2 is also a function of how much sample has been run (i.e. load size). Therefore when 50.1 mg was run for CBr and only 31.2 mg was run for CBl, this has influenced the conversion of signal strength to S1.

---

[11] S1 and S2 measured by Turnbull *et al.* (1993), Sykes (1996) and GeoSphere Ltd (1999) are given in Chapter 1 (Table 1.7).

Different load sizes in SRA have been used for the various samples in the study because of their wide variability in TOC (Table 3.1). Samples CBl and CBr have quite high TOCs and to run "standard" load sizes of 100 mg would have exceeded the linearity range of the IR cells (that measures S4). So, in the case of high TOC samples, such as coals and some oil shales, a smaller load size <u>must</u> be used (Sykes, Pers. comm., 2013; Sykes & Snowdon, 2002). CBl has a TOC of 18.2%, and CBr 9.1%, therefore less load size was used for CBl.

The S1 and S2 values of the Waipawa Formation samples from the Waipawa type locality and Lower Angora Road quarry are higher than the samples from Upper Angora Road and Porangahau (Table 3.1, Figure 3.7). Although the S1 and S2 values of Waipawa Formation are very low relative to those of the Orepuki and Green River Formation (Table 3.1), they still define the formation as having fair to very good petroleum potential according to the interpretive guidelines of Peters and Cassa (1994) (Table 3.2). According to their guidelines, the Waipawa Formation samples from the Waipawa type locality (S2 = 12.9 mg HC/g rock) and Lower Angora Road quarry (S2 = 8.8 mg HC/g rock) are very good and good petroleum potential source rocks respectively (Table 3.2), while samples from Upper Angora Road (S2 = 2.8 mg HC/g rock) and Old Hill Road, Porangahau (S2 = 3.4 mg HC/g rock) are fair petroleum potential source rocks (Table 3.2). The S1 and S2 values of the Waipawa Formation samples vary from outcrop to outcrop. Among the Waipawa Formation samples, the Waipawa Formation sample from the Waipawa type locality (WFT1) has the highest S1 and S2 values. These values of S1 and S2 are within the ranges calculated previously by Hollis & Manzano-Kareah (2005), Field *et al.* (1997) and Leckie *et al.* (1992) (Table 3.3).

Table 3.3. Ranges, means and standard deviations of S1 and S2 of previous data from the Waipawa Formation from Hollis & Manzano (2005), Field *et al.* (1997) and Leckie *et al.* (1992).

References	S1 (mg HC/g rock)	S2 (mg HC/g rock)
	Δ **range**	Δ **range**
	• **mean**	• **mean**
	─ **standard deviation**	─ **standard deviation**
Hollis & Manzano-Kareah (2005)	Δ 0-3	Δ 0-46
	• 0.5	• 7.4
	─ 0.6	─ 7.2
Field *et al.* (1997)	Δ 0-2.8	Δ 0.2-45.9
	• 0.4	• 11
	─ 0.6	─ 8.9
Leckie *et al.* (1992)	Δ 0.02-2.7	Δ 0.4-24.9
	• 0.8	• 9.4
	─ --	─ --
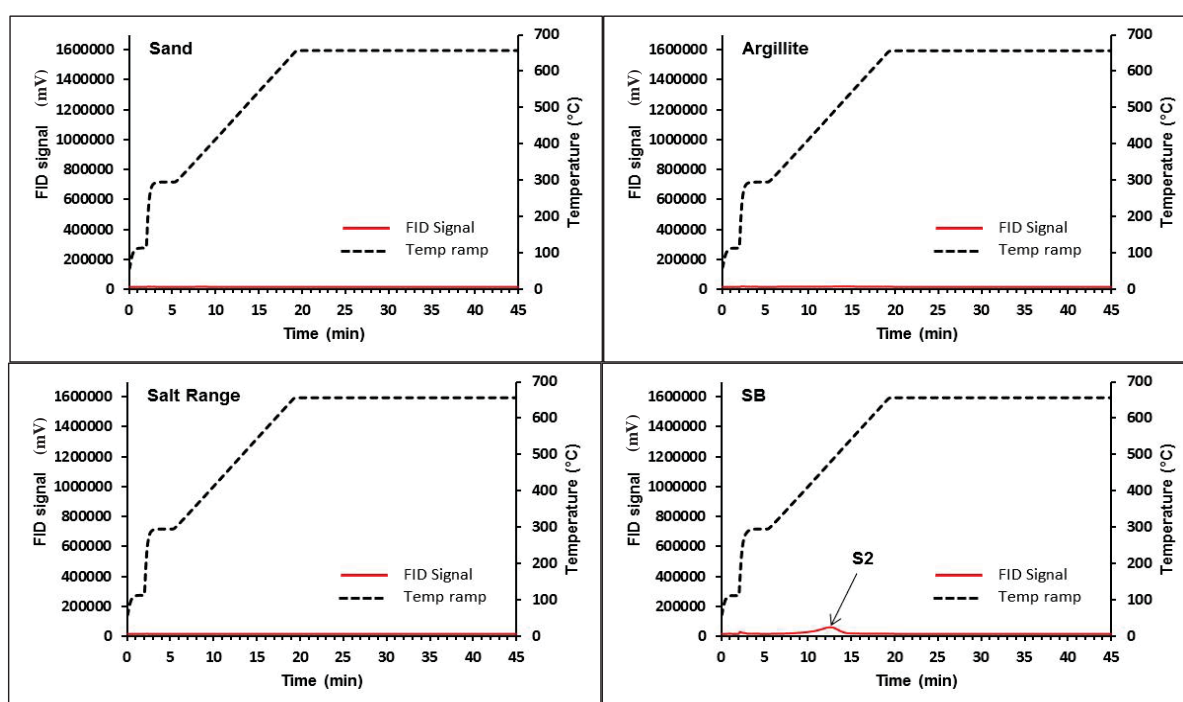
Figure 3.4. *Source Rock Analysis of the sand, argillite, Salt Range samples and Speena Banda (SB) oil shale samples as a function of time and temperature.*
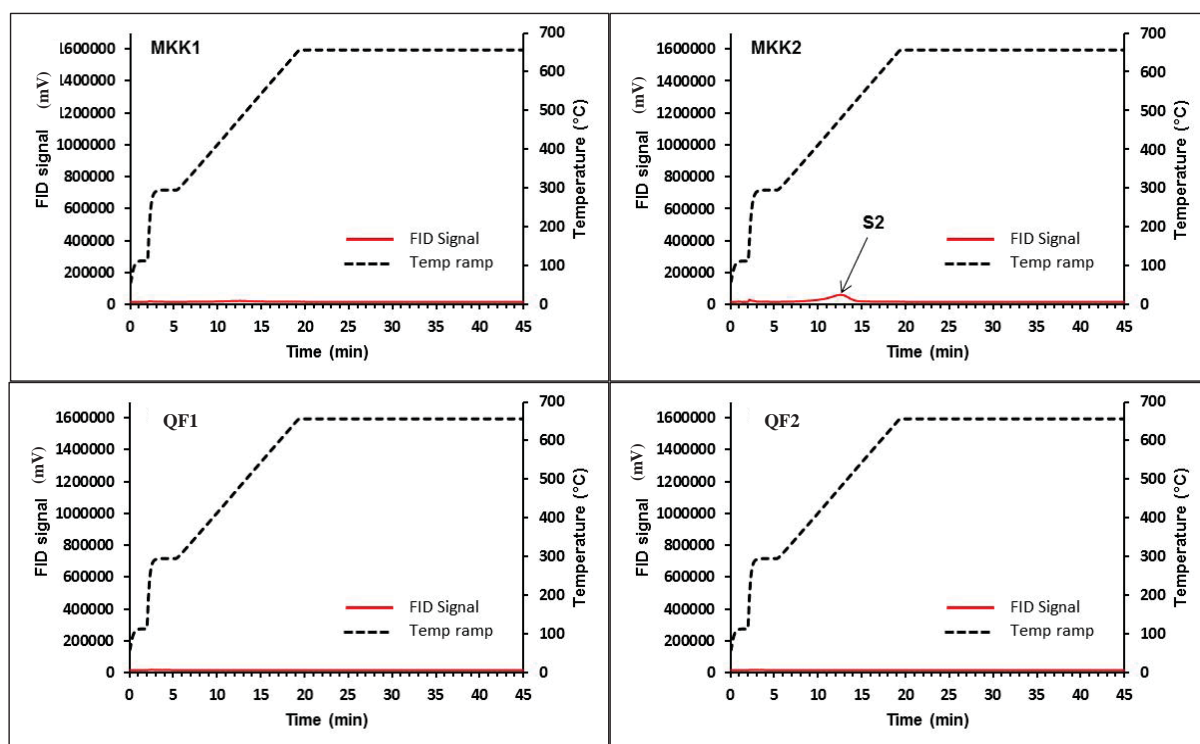
Figure 3.5. *Source Rock Analyses of the Mir Kalam Kala and Qianjiang Formation as a function of time and temperature.*
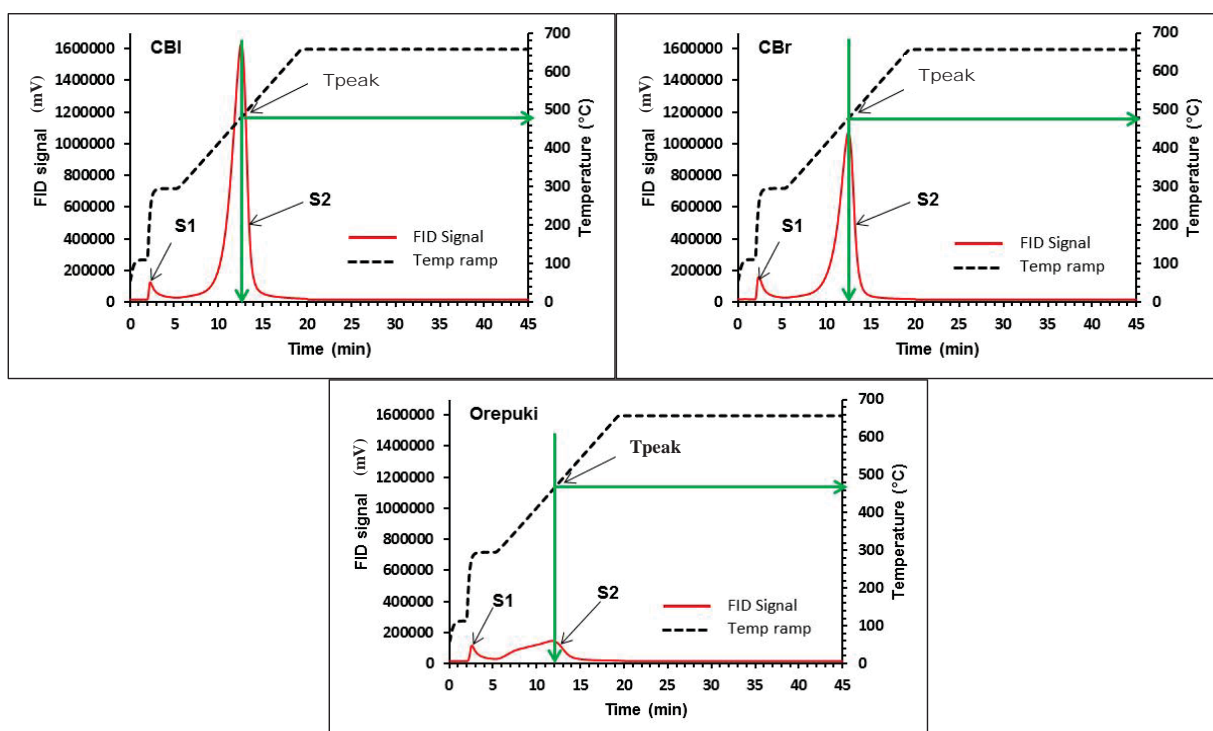
Figure 3.6. *Source Rock Analyses of the Green River Formation and Orepuki oil shale as a function of time and temperature.*
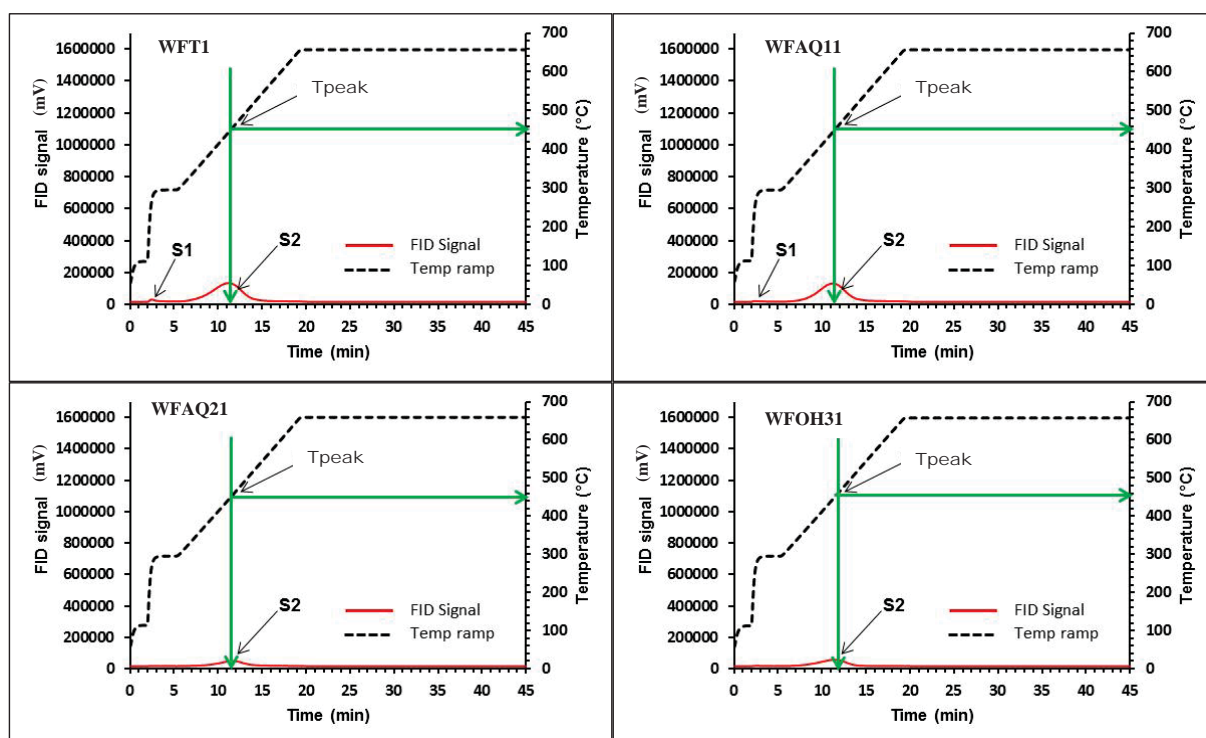
Figure 3.7. Source Rock Analyses of samples of the Waipawa Formation from four different outcrops within the East Coast Basin as a function of time and temperature.

3.2.1.1.3   Total organic carbon (TOC) vs S2

The TOC content of a rock provides a general indication about its hydrocarbon potential. For example the greater the TOC content of a rock the greater the petroleum potential is likely to be (Field *et al.*, 1997). A more accurate assessment of source rock potential however is obtained from SRA (Espitalie *et al.*, 1977). A guide to generative potential of source rocks based on TOC and S2 (from SRA) data is given in Table 3.2.

Limited SRA data for the Dharangi oil shale is available in international literature. Fazeelat & Yousaf (2004) published data for the Dharangi oil shale collected from three different outcrops in the Kohat Basin (Figure 3.8). The bivariate plot of TOC vs S2 of the Dharangi oil shale shows that its potential varies from fair to excellent for the different outcrops (Figure 3.8). When SRA data (TOC and S2) of the Mir Kalam Kala samples and Speena Banda samples of the current study are compared with the available published data, the Speena Banda and Mir Kalama Kala samples show fair and very good petroleum potentials respectively.
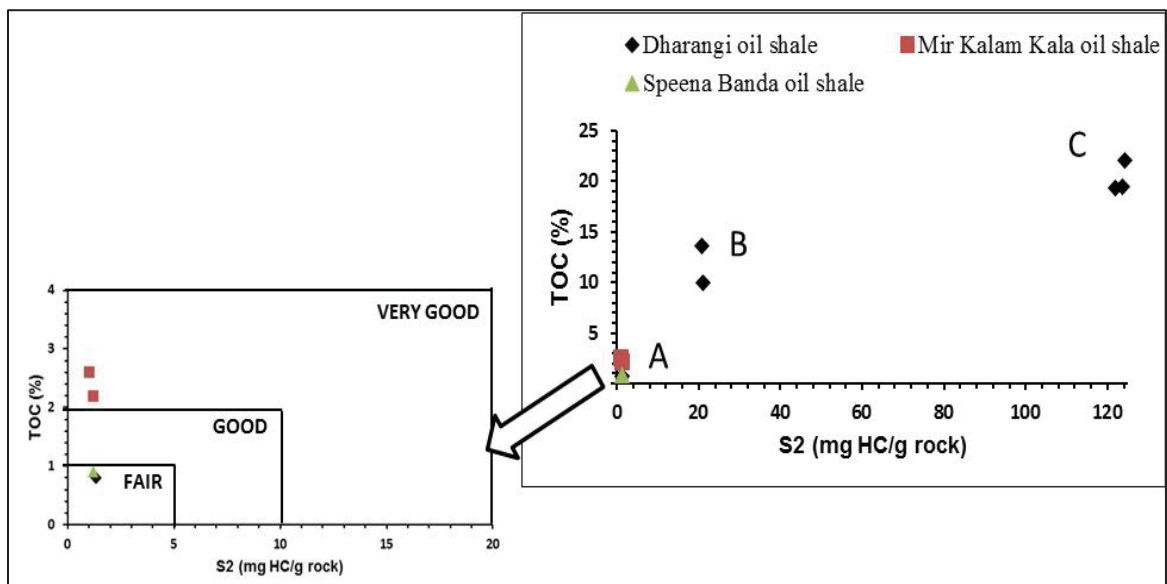
Figure 3.8. *Bivariate plot of TOC versus S2 for the Dharangi oil shale based on published data (after Fazeelat & Yousaf (2004)). SRA parameters for the Mir Kalam Kala and Speena Banda samples analysed in the current study are overlain on this plot for comparison.*

Peters *et al.* (1996) and Grice *et al.* (1998) have reported TOC and S2 data for the Qianjiang Formation. In Figure 3.9, the data from the current study are plotting in the context of published data. Previous data has suggested that the Qianjiang Formation is mainly very good to excellent potential source rock. However, Figure 3.9 shows that the data from the current study differ to that reported in literature. Data from the current study shows that the formation has a very high content of organic matter (high TOC) but has no potential for petroleum generation (very low S2) in the rock. SRA data alone does not infer a reason for this apparent anomaly.
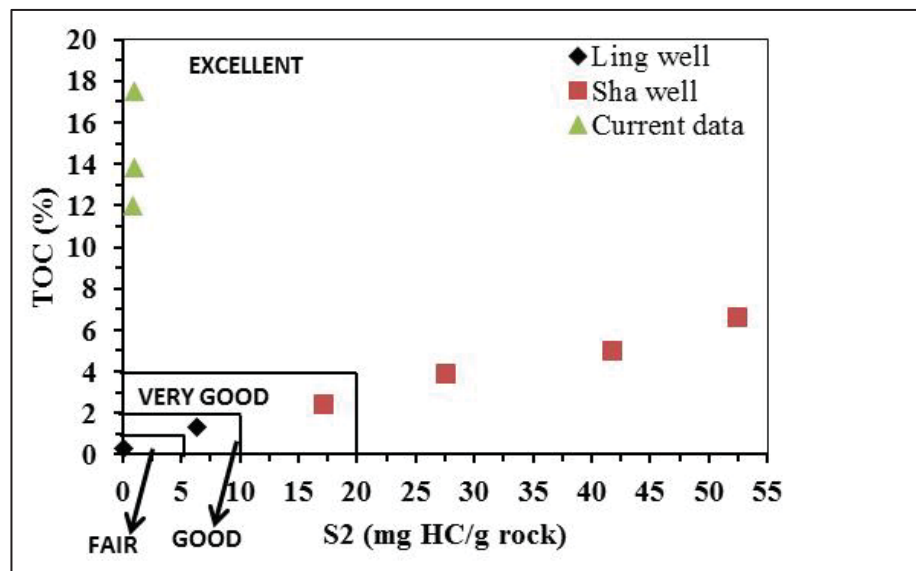
Figure 3.9. Bivariate plot of TOC versus S2 for the Qianjiang Formation based on published data (after Peters et al. (1996) and Grice et al. (1998)). SRA parameters for the Qianjiang Formation samples analysed in the current study are overlain on this plot for comparison.

Burnham *et al.*(1996), Birdwell *et al.* (2011), Cumming *et al.* (2012) and Cho *et al.* (2013) have reported TOC and S2 data of the Green River Formation samples (from the Mahogany Zone) from the Anvil Points Mine (APM), Colorado. In Figure 3.10, the data from the current study are plotting in the context of published data. All these data including current data (Figure 3.10) suggest the formation to be an excellent source rock.
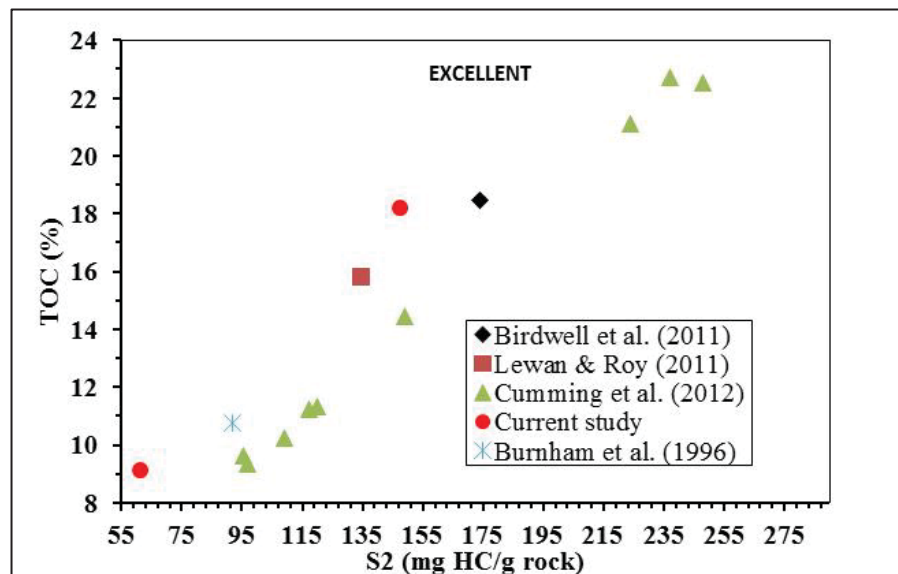
Figure 3.10. *Bivariate plot of TOC versus S2 for the Green River Formation from the Mahogany Zone based on published data (after Birdwell et al. (2011), Cho et al. (2013) and Cumming et al. (2012)). SRA parameters for the Green River Formation samples from Mahogany Zone collected from Anvil Points Mine (APM) analysed in the current study are overlain on this plot for comparison.*

Field *et al.*(1997) and Hollis & Manzano-Kareah (2005) present extensive data sets for the parameters TOC and S2 for samples of the Waipawa Formation collected from 51 different locations. When the TOC values of these samples are plotted against S2 the data points are widely spread (Figure 3.11). Plotting TOC and S2 values of the four outcrops from the current study within this widely distributed data does not allow for any meaningful contextual placement of the SRA of the current study with literature data. Therefore five different locations within the ECB were selected as chosen by Field *et al.*(1997). The TOC and S2 data for outcrops from these locations as reported by Field *et al.*(1997) and Hollis & Manzano-Kareah (2005) were extracted along with the Waipawa type locality and plotted against each other (Figure 3.11). The TOC and S2 data for the four different outcrops in the current study are then added to this bivariate plot. This apparent wide TOC distribution suggests variability in the organic content of the formation between the outcrops and within the outcrops as well (Figure 3.11). The source rock potential of the Waipawa Formation generally varies from good to very good. Samples of the Waipawa Formation collected as part of the current study fall

within the range of published data for the ECB and highlight variability in organic content and petroleum potential.
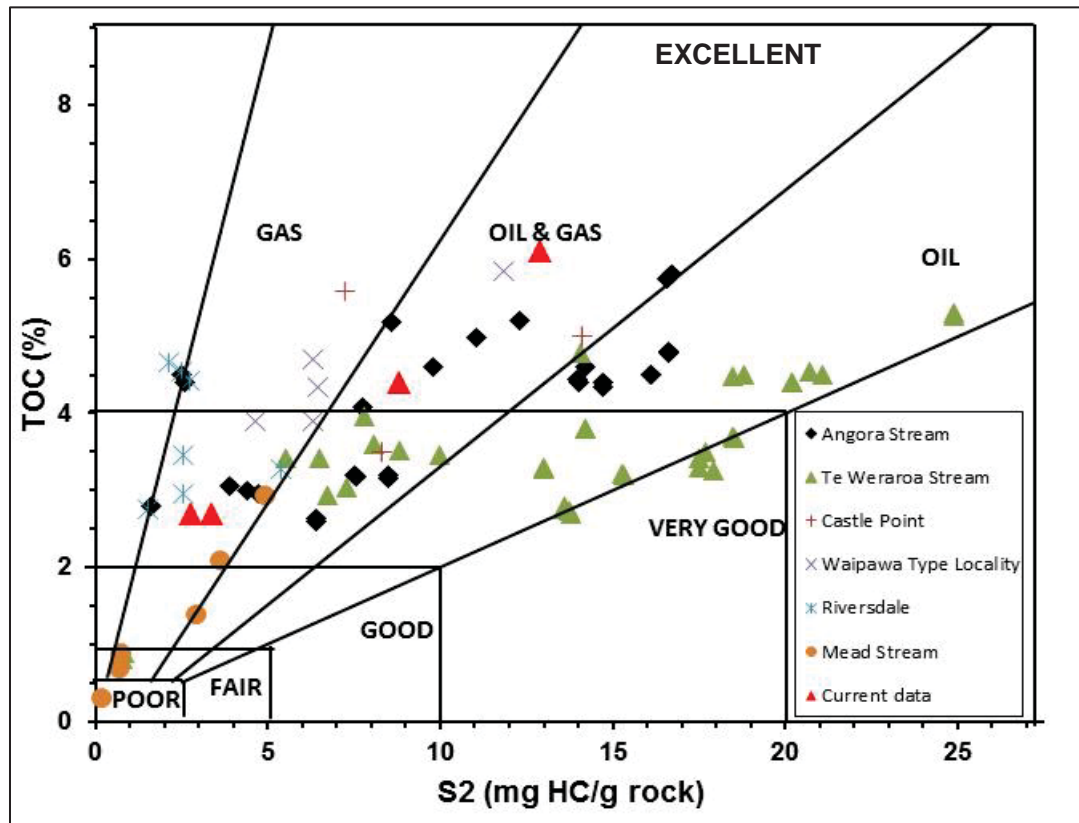
Figure 3.11. *Bivariate plot of TOC versus S2 of the Waipawa Formation collected from six different outcrops in the East Coast Basin (drawn from Field et al.(1997) and Hollis & Manzano-Kareah (2005)). Current SRA data measured in this study has been also added to the plot to see consistency between the previous data and current data.*

3.2.1.1.4 Hydrogen index (HI) vs oxygen Index (OI)

The Hydrogen Index (HI) is the normalised hydrogen content ($HI = S2 \times {100}/{TOC}$) and the Oxygen Index (OI) is the normalised Oxygen content ($OI = S3 \times {100}/{TOC}$) of a rock sample (Dahl *et al.*, 2004; Jarvie, 1991). The bivariate plot of HI vs OI was defined in Figure 1.2 as a van- Krevelen diagram, and when used in the context of SRA

data (Figure 3.12), delineates fields which define the type of kerogen present within a sample. The position of kerogen on this plot is independent of the amount of organic matter present and is strongly related to the elemental composition of kerogen (Tissot & Welte, 1978c). Type I kerogens are lacustrine and very oil prone (Table 3.4). Type II kerogens are marine and oil prone (Table 3.4). Type III are terrestrial or coaly and gas prone while Type IV kerogens are inert (Table 3.4).

Table 3.4 Geochemical parameters describing kerogen type and the character of expelled products. After Peters and Cassa (1994).

Expelled product at peak maturity	HI (mg HC/g TOC)	S2/S3	Kerogen Type
None	<50	<1	IV
Gas	50-200	1-5	III
Mixed oil & gas	200-300	5-10	II/III
Oil	300-600	10-15	II
Oil	>600	>15	I

The HI values for the Salt Range oil shale (SR1, SR2 and SR3) samples are very low and range from 45 to 60 mg HC/g TOC, similar to the argillite (Figure 3.12). These values plot on the Y-axis of the van-Krevelen diagram near the bottom of Figure 3.12. The very low S2 values of these samples (Table 3.1) indicate the virtual absence of kerogen.
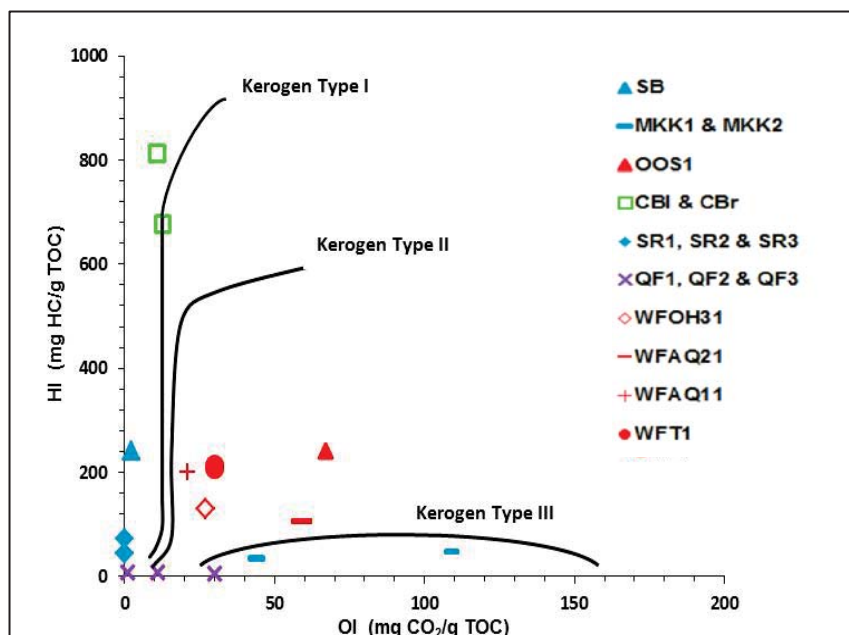
Figure 3.12. *Bivariate plot of Hydrogen Index (HI) versus Oxygen Index (OI) for the source rock samples of the current study (van-Krevelen diagram) from Tissot and Welte (1978c)*

The HI value of the SB sample is 242 mg HC/g TOC, suggesting that the rock has organic matter of Type II/III that will generate both oil and gas (Table 3.4). But this value is not a reflection of production potential according to the classification of Peters and Cassa (1994) but rather a TOC value less than 1. When the small S2 yield is normalised to a very low TOC value, a very high HI value is obtained, which probably has a large uncertainty because of the poor precision of SRA at very low TOC. Thus at very low TOC values, HI, OI, Tmax and other parameters are unreliable. Based on the position of the SB shale in the HI vs OI diagram (Figure 3.12) it is difficult to identify with clarity the type of organic matter present.

The HI values of the Mir Kalam Kala samples are very low (33 and 47 mg HC/g TOC respectively), and the organic matter is therefore classified as Type III Kerogen (Figure 3.12) suggesting that the organic matter is gas prone. According to Tissot and Welte (1978c), Type III kerogen is comprised of a good proportion of polyaromatic nuclei, heteroatomic ketone and carboxylic acid groups, but no esters. Aliphatic groups are present in only small amounts. This type of kerogen originates from higher plant waxes,

methyl groups and other short chain organic molecules and suggests that the organic material source in the Mir Kalam Kala samples is of terrestrial origin. This type of kerogen has only a limited potential for oil generation but may produce gas if buried to sufficient depths and attains sufficient temperature. This type of kerogen is less responsive to pyrolysis.

The Qianjiang Formation samples have very low HI values (Table 3.1), and thus plot near the bottom of Figure 3.12. Although the TOC values are very high, due to almost no pyrolysis response, the organic matter is considered to be post mature (Table 3.4). The HI values of the Qianjiang Formation are not consistent with the HI values (500, 700, 790 and 850 mg HC/g TOC) determined by Grice *et al.* (1998) for this formation. However Peters *et al.* (1996) found HI values of 45, 501 and 794 mg HC/g rock for Qianjiang Formation samples collected from three different wells in the Jianghan Basin. The difference in the HI data for the Qianjiang Formation samples with the HI data in the literature suggest that these samples analysed in the current study might not be representative of the formation. But variability even within literature data suggests that the formation has variable content of organic matter.

The HI values of the Green River Formation samples are exceptionally high (811 and 675 mg HC/g TOC respectively), and the organic matter is classified as Type I kerogen (Figure 3.12, Table 3.4) suggesting that the organic matter is highly oil prone. Tissot and Welte (1978a) reported that Type I kerogen has a high initial H/C and low initial O/C ratio and contains a large amount of aliphatic chains. The small amount of oxygen is mainly due to ester bonds. When this type of kerogen is subjected to pyrolysis at 550-600°C, it has a very high potential to produce large amounts of volatile and/or extractable hydrocarbons compared to other types of kerogen. In other words Type I kerogen is capable of producing high yields of oil. But this type of kerogen is not very common and occurs mostly in lacustrine environments. Tissot and Welte (1978c) and Jin *et al.* (2012) working on the Green River Formation from the Anvil Point Mines (APM), near Rifle, Colorado found that the organic matter was Type I and proposed a source from a lacustrine depositional environment. Burnham *et al.* (1996) found an HI value of 850 mg HC/g TOC for the Green River Formation from APM. Birdwell *et al.* (2011) and Cho *et al.* (2013) found comparatively high HI values of 944 and 1014 mg HC/g TOC respectively (Table 1.4). However they found low OI values of 6.4-34 mg

CO_2/g TOC (Table 1.4) and hence suggested that the formation was purely lacustrine in origin.

The HI values of the Waipawa Formation samples from the Waipawa type locality and from the Lower Angora Road quarry (WFAQ11) are 214 and 200 mg HC/g TOC respectively, suggesting a mixed gas and oil potential for this formation at these localities (Table 3.4). The HI values of the Waipawa Formation samples from Upper Angora Road (WFAQ21) and Porangahau, Old Hill Road (WFOH31) are low compared with the HI values of the Waipawa Formation from the type section and Lower Angora Road quarry (WFAQ11) and are 103 and 129 mg HC/g TOC respectively. These values suggest that the potential of these respective outcrops is for gas production (Table 3.4). The position of Waipawa samples between the Type II and Type III pathways in the HI vs OI diagram (Figure 3.12), classifies the organic matter of the Waipawa Formation as Type II-III kerogen, suggesting that the organic matter in the samples will generate both oil and gas (Table 3.3). This is consistent with a mixed terrestrial and marine organic matter source as previously reported by Leckie *et al*. (1992), Killops *et al*. (1997), Killops *et al*. (2000), Field *et al*. (1997) and Hollis *et al*. (2006).

The HI and OI values of the Orepuki oil shale are 241 mg HC/g TOC and 67 mg CO_2/g TOC respectively, suggesting that this rock is a potential source rock for oil and gas (Table 3.3). These values are not consistent with the HI (287 mg HC/g TOC) and OI (72 mg HC/g TOC) obtained by Turnbull *et al*. (1993). The intermediate position of the Orepuki oil shale between Type II and Type III pathways on the van-Krevelen diagram (Figure 3.12) suggests a mix of organic matter types. The HI values of the Orepuki oil shale reported by Turnbull *et al.* (1993), Sykes (1996) and GeoSphere Ltd (1999) are 287, 618 and 770 mg HC/g TOC respectively. Owing to these very high HI values, these authors suggested a lacustrine depositional environment for the Orepuki oil shale. As no literature is available on the type of organic matter in the Orepuki oil shale, it is unclear whether the organic matter is TypeII/III or Type I/III.

Although both the Orepuki oil shale and the Waipawa Formation have an intermediate position in the Van-krevelan diagram (Figure 3.12), the significant difference in the S1, S2, HI, OI data between the two deposits (Table 3.1) suggests a difference in origin or diagenetic history.

3.2.1.1.5   Hydrogen index (HI) vs T$_{max}$

To further define the type of organic matter in the SB oil shale, HI values were plotted against Tmax as a way to overcome the difficulty of differentiating mixed types of kerogen on the van-Krevelen plot (Figure 3.13). Figure 3.13 clearly shows that SB lies in the mixed Type II/III zone making it capable of generating oil and gas.
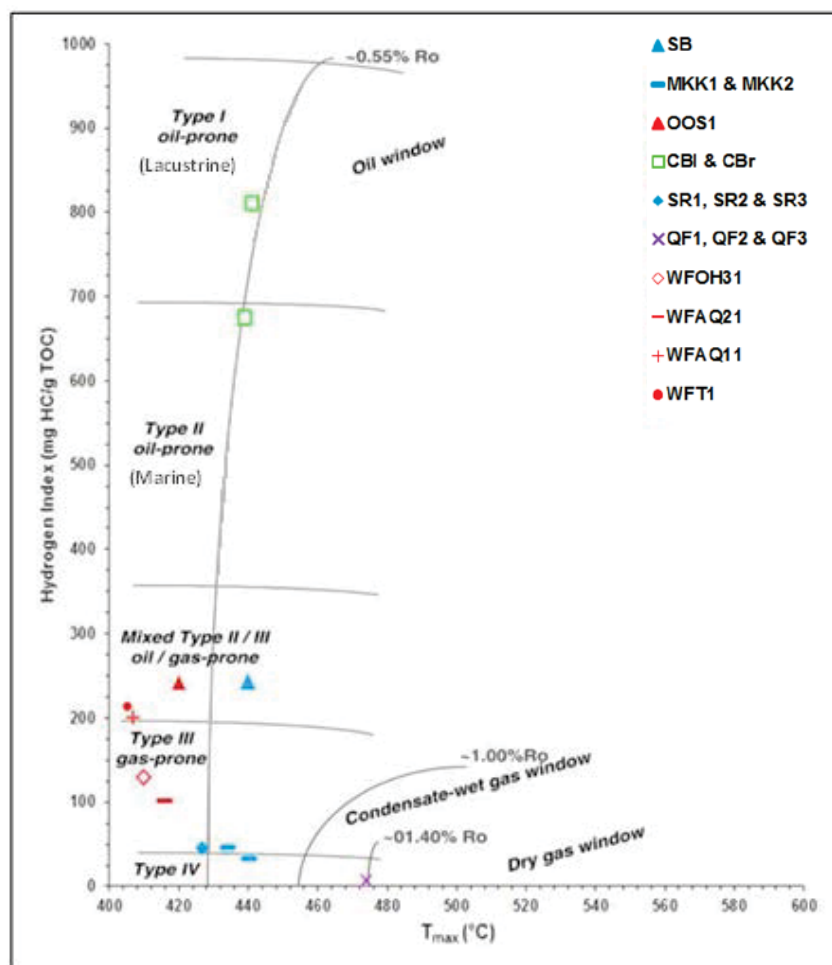
Figure 3.13. *Cross plot of Hydrogen Index (HI) versus Tmax from Dahl et al. (2004)*

A further subdivision can be seen in the Waipawa Formation samples. WFT1 and WFAQ11 also lie in the Type II/III (oil/gas-prone) region, whereas samples WFAQ21 and WFOH31 lie in the Type III (gas-prone) zone. This means that there is a range of

facies within the Waipawa Formation, some with mixed gas and oil potential and some only with gas potential. According to Leckie *et al*. (1992), Killops *et al.* (1997) and Killops *et al*. (2000), the Waipawa Formation is a source rock with Type II/III kerogen with mixed terrestrial and marine organic matter input, and having mixed oil and gas potential.

Samples QF1, QF2, SR2 and SR3 lie outside the range of the HI vs Tmax plot (Figure 3.13) and so could not be classified by this means.

The kerogens and organic matter in sediments are generally regarded as heterogeneous. Therefore the concept of differentiating the different types of kerogens based only the parameters from SRA is debatable (Dahl *et al.*, 2004). According to Hutton *et al.* (1994) there are several factors involved which can tend to change the position of data points in the van-Krevelen diagram:

i)   Types of precursor organisms
ii)   Environment of deposition
iii)   Maturation
iv)   Weathering
v)   Composition of organic matter

Dahl *et al*. (2004), Espitalie *et al*. (1985) and Peters (1986) have all shown that the mineral matrix can reduce the S2 pyrolysis yield, resulting in the reduction of hydrogen index and thus lowering the apparent source quality. According to Dahl *et al.* (2004), the best way to assess the type of kerogen, is to do SRA in combination with organic petrography, and combined pyrolysis and gas-chromatography.

3.2.1.2 Thermal maturity

The parameters Production Index (PI) (where $PI = S1/(S1 + S2)$) and Tmax, are used to estimate thermal maturity (Akande *et al.*, 2012; Akinlua *et al.*, 2011; Behar *et al.*, 2001). Tmax is a standardised parameter and is calculated when the S2 peak reaches its maximum. However, Tmax for the current study is actually 39°C less than the actual maximum of the S2 peak (Tpeak); this is due to the difference in temperature within the chamber of the instrument between the thermocouples and the sample holder (Jarvie, 1991; Sykes, Pers. comm., 2012). Production Index increases with maturity as thermally labile components in the kerogen (S2) are converted into free hydrocarbons (S1). Tmax is also used to estimate thermal maturity and it corresponds to the rock-eval pyrolysis oven temperature at which maximum S2 generation occurs (Peters & Cassa, 1994). Reported Tmax ranges for different levels of maturity are summarised in Table 3.5, but these are broad and only approximate guidelines. Estimating maturity on the basis of Tmax should be done with care as Tmax maturity ranges are different for different kerogen types. Similarly Akinlua *et al.* (2011) described limitations as to the reliability of PI for samples with low S1 and S2 parameters. Therefore, in the current study, for samples with very low S1 (0-0.5 mg HC/g rock) and S2 (0-2.5 mg HC/g rock) (sand, argillite, Salt Range oil shale, Mir Kalam Kala oil shale, Speena Banda and Qianjiang Formation samples), the use of PI as a thermal maturity indicator might not be useful.

Table 3.5 Geochemical parameters describing the level of thermal maturation. After Espitalie *et al*. (1985) and Peters and Cassa (1994).

Stage of thermal maturity for oil	Production Index, PI [S1/(S1+S2)]	Tmax (°C)
Immature	<0.1	<435
Mature		
Early	0.1-0.15	435-445
Peak	0.25-0.40	445-450
Late	>0.40	450-470
Post mature	--	>470

The Tmax of sand, argillite and the Pakistani and Qianjiang Formation samples cannot be observed in Figures 3.4 and 3.5 as the FID signals are not significant due to zero or minimal pyrolysis response; the values are reported in Table 3.1. Similarly the Tmax results of Qianjiang Formation samples cannot be determined due to zero or minimal pryrolysis response. This is inconsistent with the Tmax determined by Grice *et al.* (1998) and Peters *et al.*(1996). They determined Tmax values of 421, 426, 430 and 436°C for the Qianjiang Formation suggesting it to be an immature source rock. The cracking of kerogen for CBl and CBr occurs between 9 and 15 minutes as shown in Figure 3.6 with maximum devolatalisation occurring at 12.5 minutes, giving Tpeak of 480°C and 478°C respectively, and hence Tmax (which is 39°C less than Tpeak) values of 441°C and 439°C respectively. Similarly a Tmax value of 428°C and 405-416°C can be observed for the Orepuki and Waipawa Formation samples (Figure 3.6 and 3.7).

Due to the very low S2 values (<2.5 mg HC/g rock), quantified for samples from Salt Range, Mir Kalam Kala, Speena Banda and Qianjiang Formation, the Tmax values may be unreliable. The Green River Formation (CBr, CBl) with Tmax values of 439°C and 441°C respectively, qualify as early-mature source rocks. Burnham *et al.* (1996), working on the Green River Formation from APM, also found it to be an early-mature source rock with a Tmax value of 443°C (Table 1.4 and 3.5). However Braun *et al.* (1991) found the Tmax value of the Mahogany Zone oil shale to be 433°C (an immature oil shale) (Table 1.4 and 3.5) . However, the PI values of CBl and CBr are 0.03 and 0.06 which are not consistent with the maturity suggested by their Tmax values. According to Clayton and King (1987), weathering affects the quality and amount of organic matter in source rock outcrops and hence the inconsistency in PI and Tmax values may be due to weathering.

The Orepuki oil shale has a Tmax of 428°C, suggesting an immature source rock below the oil window (Table 3.5). However in the report by GeoSphere Ltd (1999) a Tmax of 437°C has been obtained for the Orepuki oil shale. However, the PI value of the Orepuki oil shale is 0.13 (Table 3.1) which is not consistent with the maturity suggested by its Tmax value. The Waipawa Formation samples have PI values ranging from 0.02-0.04, indicating that these too have not reached the oil window. Tmax values between 400-416°C for the Waipawa Formation support the immature source rock interpretation.

3.2.1.3 Source rock generative potential (SP)

The Source Rock generative potential $[SP = S1 + S2]$ is defined as the sum of S1 and S2. The Pakistani and Qianjiang Formation samples have very low S1+S2 values, in the range 0.3-1.4 mg HC/g rock (Table 3.1), and are comparable to the results for the sand and argillite control samples. In contrast, the Green River Formation and Orepuki oil shale samples have very high SP values shown in Table 3.1, reflecting hydrocarbon rich source rocks with excellent generative potential (Table 3.2). This is supported by the TOC and HI values.

The Waipawa Formation samples WFT1 and WFAQ11 with mixed gas and oil potential have SP values of 13.4 and 9 mg HC/g rock (Table 3.1). This suggests that these are moderately rich source rocks with good generation potential. However, the SP values of the WFAQ21 and WFOH31 samples are 2.9 and 3.5 mg HC/g rock (Table 3.1), suggesting only fair generation potential (Table 3.2). Thus a range of generation potentials is observed for the Waipawa Formation from different outcrops confirming the suggestion of different facies existing within the Waipawa Formation and that these have different production potential in the East Coast Basin.

3.3 Conclusion

SRA has allowed the conventional production potential of all the rocks to be quantified, although there are stated limitations to this quantification (Chapter 1). According to the SRA results, oil shale samples from Pakistan and Qianjiang Formation samples have no production potential. Green River Formation and Orepuki oil shale have excellent potential for petroleum generation. The Waipawa Formation samples from different outcrops show a range of potential for petroleum generation. Therefore, it is considered a heterogeneous formation containing facies with different production potentials.

The TOC values of the Pakistani Salt Range oil shale samples are low in the context of published TOC data for these samples from Khewra Gorge. The TOC values of the Qianjiang Formation samples are in contrast with the published data. The TOC values

of the Green River Formation from Mahogany Zone are also very similar to those
determined in the literature. The TOC values of the Waipawa Formation from the
different outcrops in the study also lie in the range of TOC values determined by Hollis
& Manzano-Kareah (2005), Field *et al.* (1997) and Leckie *et al*. (1992). The Qianjiang
Formation has poor petroleum potential from the SRA studies of the samples collected
in this study. This is in contrast with the very good to excellent petroleum potential for
the Qianjiang Formation defined from the analyses from previous studies (Figure 1.15).
From the TOC vs S2 plot of the Green River Formation from the previous data
including the current data, the formation is suggested to be an excellent source rock. A
distribution of data is observed in the excellent generation potential range and CBr lies
outside the range of data points from the previous data to some extent, but looking into
the distribution of data it is not of any concern. The difference between the literature
reported SRA data (S1 and S2) and SRA data in the current study for the Orepuki oil
shale suggests a variable content of hydrocarbons in the oil shale. However all data
suggest the excellent production potential of the oil shale. From the range of TOC and
S2 data for the Waipawa Formation from the previous literature, the Waipawa
Formation has a range of potentials from poor to excellent. This variability in petroleum
potentials exists between different outcrops and also within an outcrop. The petroleum
potential of the Waipawa Formation in current study from four different outcrops varies
from very good to excellent.

The different oil shales are ranked from low to high according to their source rock
generative potential (SP) from the SRA values of S1 and S2 (Table 3.6) with the Salt
Range oil shale having very low to no production potential and the Green River
Formation having the highest potential for petroleum generation.

Table 3.6. Ranking of rocks of the current study based on their source rock generative potential from SRA.

Samples	SP
	mg HC/g rock
Sand	--
SR1	0.3
SR2	0.3
SR3	0.3
Argillite	0.5
MKK1	1.1
QF3	1.2
QF2	1.2
SB	1.3
MKK2	1.3
QF1	1.4
WFAQ21	2.9
WFOH31	3.5
WFAQ11	9
WFT1	13.4
OOS1	36.7
CBr	66
CBl	151.7

The measurement of source rock generative potential (SP) and maturity are intimately linked. S2 (and S1) always depend on the exact maturity of the sample. The S1 is low for immature source rocks, and increases with maturity and then decreases when the source rock becomes post mature (Stein, 2007; Sykes & Johansen, 2007). However S2 is different and depends on source rock type. For marine and lacustrine source rocks, S2 is constant and then from the onset of generation or oil expulsion, it decreases (Sykes, Pers. comm., 2013; Sykes & Johansen, 2007).

Chapter 4−Physical analyses

4.1 Introduction

Oil shale is a complex mixture of organic and inorganic components (Dyni, 2006). The inorganic fraction generally consists of silicates (quartz, feldspar and clay minerals), carbonates (calcite, dolomite) and pyrite, while organic matter is heterogeneously and finely dispersed within this inorganic matrix (Kok, 2001). The organic fraction is comprised of kerogen and bitumen. Bitumen is soluble in organic solvents, while kerogen, which constitutes the major part of the organic fraction, is insoluble in organic solvents and is mainly composed of carbon, hydrogen and oxygen with minor amounts of nitrogen and sulphur (Sert *et al.*, 2009). While the inorganic fraction of an oil shale is generally crystalline, organic matter within an oil shale is amorphous. The origin of this amorphous material is not well known, but it is likely to reflect the environment of deposition and be a mixture of degraded algal or bacterial remains (Dyni, 2006).

A range of physical analytical techniques can be used to physically characterise the inorganic and organic fractions of oil shale. Weaver (1960) conducted a mineralogical investigation of more than 2,000 oil shale samples from most of the major shale-containing basins of the USA and suggested a possible statistical relationship between montmorillonite and shale oil content. Al-Harasheh *et al*. (2009; 2011) investigated the mineral composition of a Jordanian oil shale and subsequently studied the effect of demineralisation on oil yield. He found that with demineralisation the oil yield increased. Ingram *et al*. (1983) related the composition of a shale oil to the petrology of the parent organic matter and the mineralogy of the inorganic matrix. He found a direct relation between organic matter content and shale oil potential while there was an inverse relation between mineral matter content and shale oil potential. Tao *et al.* (2012), through quantifying the total maceral content of different oil shales, suggested that the content of total macerals can be used as an index along with other supportive techniques to classify oil shales into groups with different oil generation potentials.

In this chapter, X-ray diffraction (XRD) will be used to investigate the crystalline mineral components in the oil shales under investigation. The mineralogy of the index shales, in particular the clay mineralogy, is compared to their SRA-defined production potential, in an attempt to determine a relationship to production potential based on the presence or absence of the clay minerals. The amorphous organic matter fraction of the oil shales is investigated using qualitative organic petrography to determine the origin of different kerogens. Based on the relative abundance of total macerals the oil generation potential is qualitatively inferred, as is an index of the environment of deposition.

4.2 X-ray diffraction (XRD)

X-ray diffraction is an essential tool for the analysis of crystalline clay minerals in a variety of matrices (Bhargava *et al.*, 2005). XRD plays a major role in identifying the mineral components of fine grained rocks, including oil shale. In the current study, XRD is used qualitatively to identify the relative abundances of the clay minerals present in the samples under investigation. XRD analysis of all unprocessed whole rock powdered samples was undertaken. In addition the clay-size fraction was separated from the whole rock samples to concentrate the clay-size minerals fraction to assist identification of the clays present. The clay mineral concentrate was necessary as the XRD spectra of the bulk oil shale samples were dominated by quartz, feldspar and calcite and these minerals mask the presence of the accessory clay minerals illite, montmorillonite, kaolinite, chlorite and mixed layered clays such as illite-montmorillonite, illite-vermiculite. Clay-size quartz has been reported from shales by D'Ath (2002), so it is likely that fine grained silicates will also be present in the clay-size concentrate. The organic matter was also removed from the samples before analysis to provide better XRD resolution of the clay minerals present. The purpose of the clay mineralogy was to investigate whether there is a relationship between the oil generative potential of the oil shale and its clay mineralogy.

4.2.1 Results and discussion

The relative abundance of clay minerals as determined from XRD analysis of sand, argillite and the different oil shales from Pakistan, China, Colorado, Orepuki and the Waipawa Formation are summarised in Table 4.1. All analyses are qualitative and relative abundances are reported as dominant (d), common (c) and present (p) according to the relative intensity of the counts of the spectra. The determination of dominant, common and present are explained below.

The XRD spectra of the powdered whole rock and untreated samples are dominated by quartz and feldspar. These silicate minerals mask the presence of the accessory clay minerals. In order to see the clay minerals more clearly on the XRD spectra, the clay-size fraction was isolated and concentrated (section 2.3.2) for each rock sample in this study. There is no clay fraction in sand but it was still treated and analysed using exactly the same procedures as the other rocks in the study (section 2.3.2). The XRD spectra of the samples where clays minerals have been concentrated and treated show the clay mineral peaks more clearly making them easier to identify. Although the XRD spectra used in this study are qualitative, because of the unavailability of appropriate clay mineral standards, an attempt is made to establish the relative abundance of each clay mineral present in the concentrated clay fraction of each rock. The method uses the principal that the heights of the peaks (from background to maximum values as represented by the number of counts on the y-axis) in the K-saturated scans for each mineral are proportional to the amount of each constituent mineral present in the sample (Whitton & Churchman, 1987). A mineral is considered to be dominant (d) if the number of counts recorded on the Y-axis for its major peak is greater than about 500 (Figure 4.1). If the number of counts, calculated from the difference between the maximum and background of a main peak of a mineral is between about 150 and 500, it is considered common (c). Similarly a mineral for which the number of counts is less than 150, is considered present (p).

Table 4.1. Mineralogy of clay-size fraction concentrate of sand, argillite and oil shale samples of the current study from XRD analysis (d: dominant, c: common, p: present, --: not identified) [12].

Locations	Samples	Quartz	Kaolinite	Illite	Chlorite	Montmori-llonite	Vermicu-lite	Analcime
	Sand	d	--	--	--	--	--	--
	Argillite	d	c	d	p	--	--	--
Salt Range	**SR1**	d	c	d	p	--	--	--
	SR2	d	c	d	p	--	--	--
	SR3	d	c	d	p	--	--	--
Mir Kalam Kala	**MKK1**	d	p	d	--	--	--	--
	MKK2	d	p	c	--	c	--	--
Speena Banda	**SB**	d	--	c	--	--	--	--
Jianghan Basin	**QF1**	d	--	p	--	--	--	--
	QF2	d	--	p	--	--	--	--
	QF3	d	--	p	--	--	--	--
Colorado (APM)	**CBl**	d	p	c	p	--	--	c
	CBr	d	p	c	p	--	--	c
Orepuki	**OOS1**	c	c	--	--	--	p	--
	OOS2	c	c	--	--	--	p	--
	OOS3	c	c	--	--	--	p	--
Waipawa	**WFT1**	d	d	c	--	c	--	--
	WFT2	d	d	c	--	c	--	--
	WFT3	d	d	c	--	c	--	--
Angora quarry	**WFAQ11**	d	c	p	--	p	--	--
	WFAQ12	d	d	p	--	p	--	--
	WFAQ13	d	d	p	--	p	--	--
	WFAQ21	d	c	c	--	c	--	--
	WFAQ22	d	c	c	--	c	--	--
	WFAQ23	d	c	c	--	c	--	--
Porangahau	**WFOH31**	d	p	c	--	c	--	--
	WFOH32	d	p	c	--	c	--	--
	WFOH33	d	p	p	--	c	--	--

---

[12] In this study a mineral is said to dominant (d) if the number of counts between the maximum and background of the main peak of the mineral in the K-saturated XRD spectrum is >500. The mineral is said to be common (c) if the number of counts is 150-500. Similarly if the number of counts for the main peak of a mineral is <150, then it is considered present (p).

4.2.1.1 Mineralogy of the sand and the argillite

The XRD spectra of sand and argillite are shown in Figures 4.1. The spectra of powdered sand (untreated) and the four different pre-treated sand samples with K-saturation, Mg-saturation, heating and glyceration (section 2.4.1.1), are the same as shown in Figure 4.1. This confirms that the sand is a monomineralic quartz sand.

The clay-size fraction of the argillite consists of quartz, kaolinite, illite and chlorite. Whereas the XRD spectrum of the bulk-untreated powdered argillite in the K-saturated scan is dominated by quartz. The dominating presence of quartz masks the presence of the accessory clay minerals illite, kaolinite, and chlorite. The XRD spectra of the clay fraction of the argillite after the various pre-treatments shows that illite is dominant (d) because the number of counts recorded for the main illite peak at 10.00Å (between maximum and background (base of peak) of the peak in the K-saturated scan) is greater than 500 (Figure 4.1). Similarly the number of counts recorded for main kaolinite peak at 7.00Å is about 250 and hence it is considered common (c). Counts for chlorite between maximum and background of the main peak (14.00Å) number less than 100 and is thus considered present (p). It is noteworthy that quartz is present in the clay-mineral fraction. This quartz is likely fine clay sized quartz present in the argillite (Potter *et al.*, 2005) but could also include additional clay-size quartz that was generated during the sample preparation, i.e. by grinding.
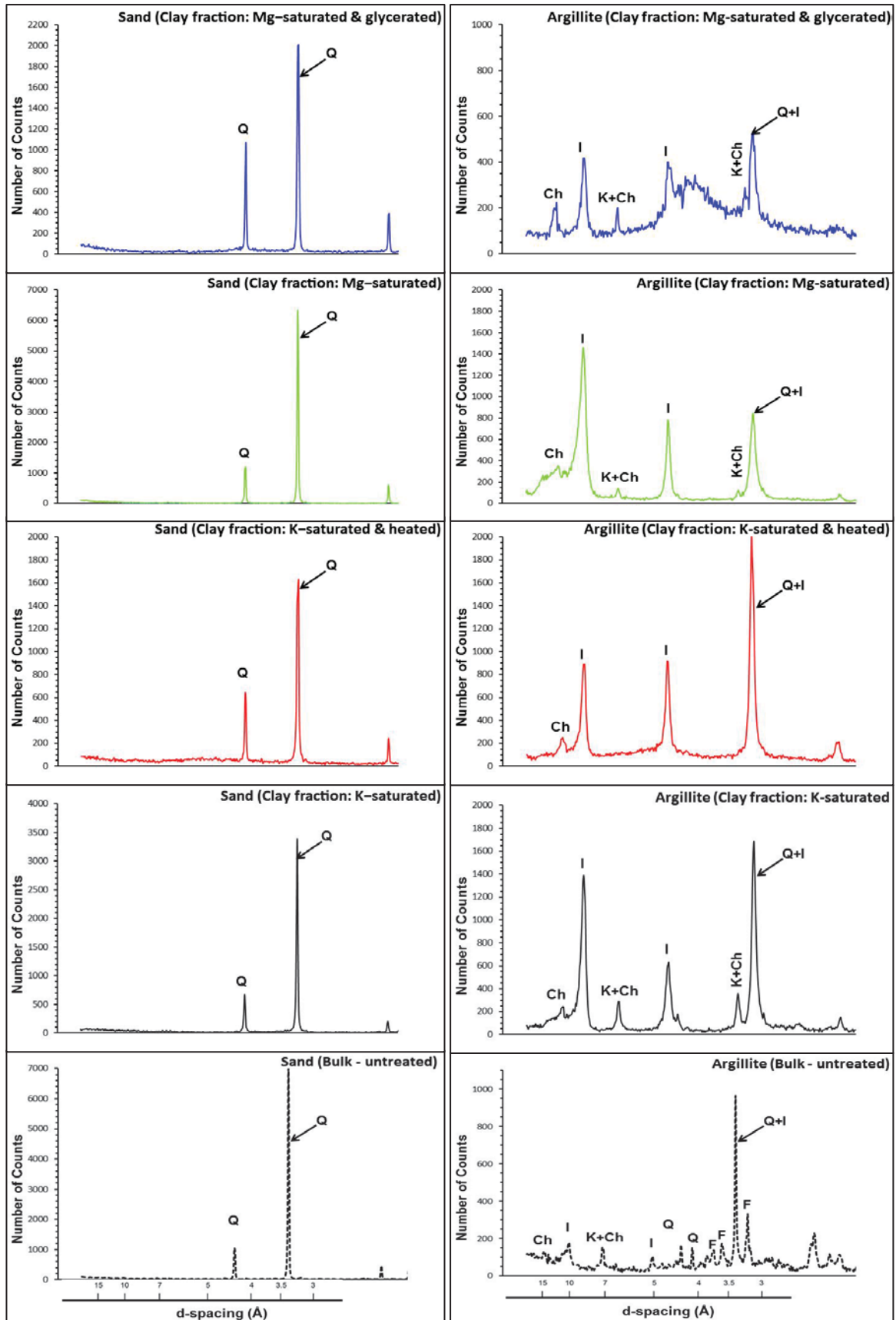
Figure 4.1. *XRD spectra of sand and argillite show that the sand is composed of only **Quartz** (**Q**) = 4.26Å, 3.35Å, 2.46Å, while argillite is composed of **Quartz** (**Q**), **Feldspar** (**F**) = 6.39Å, 4.03Å, 3.86Å, 3.77Å, 3.67Å, 3.19Å, 2.46Å, 2.97Å, **Illite** (**I**) = 10.00Å, 5.00Å, 3.33Å, **Kaolinite** (**K**) = 7.10Å and 3.50Å and **Chlorite** (**Ch**) = 14.00Å, 7.07Å, 4.72Å, 3.50Å.*

4.2.1.2 Mineralogy of the Green River Formation, Qianjiang Formation, Orepuki and Pakistani oil shale samples

The clay mineral fraction of the Colorado black rock (CBl) and brown rock (CBr) both contain kaolinite, illite and chlorite togather with quartz. Their relative abundances are shown in Table 4.1. Illite is common (c) in both CBl and CBr, while chlorite and kaolinite are present in minor amounts (p) (Figure 4.2) (Appendix D) [13]. The non-clay minerals present in the whole rock samples are quartz, feldspar (plagioclase) and analcime (Figure 4.2). Small amount of feldspar is also present in the clay separated samples of Green River Formation (CBl, CBr) which is likely fine clay sized feldspar present but could be a product of grinding process as well (Potter *et al.*, 2005).

The mineralogy results for the Green River Formation in the current study differ from the findings of Ingram *et al.* (1983) and Dyni (1981) who also worked on samples from the Mahogany Zone of the Green River Formation Parachute Creek Member (source of the samples for the current study). They reported that the only clay mineral present in the oil shale is illite along with the non-clay minerals analcime, calcite, quartz and feldspar. However, the current results are more consistent with the mineralogy results of Laird & Scharff (1983), who studied the decomposition of minerals in the Green River Formation. They determined that the minerals identified in the oil shale are illite, chlorite and analcime. Johnson (2012) has also mentioned the presence of illite in the oil shale from Anvil Points Mine.

---

[13] All XRD plots of bulk-untreated and pre-treated samples are plotted separately in Appendix D in order to see each plot clearly.
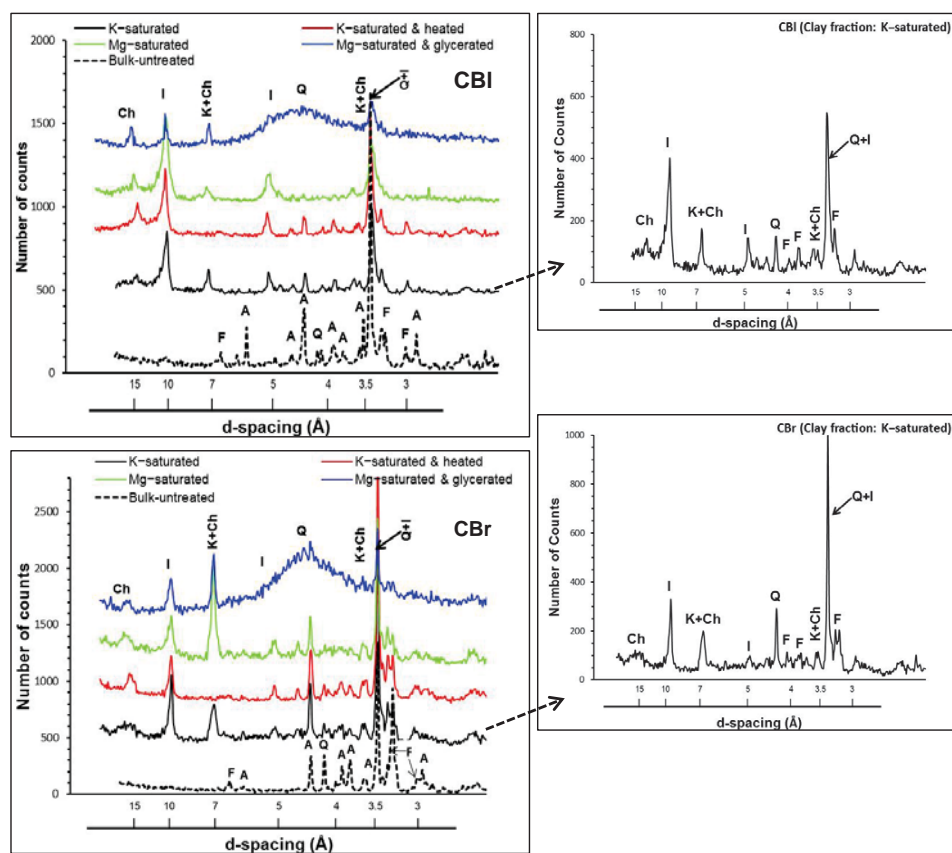
Figure 4.2. XRD spectra of the Green River Formation (CBl,CBr) shows it contains

Quartz (Q) = 4.26Å, 3.35Å, 2.46Å, 2.28Å

Feldspar (F) = 6.39Å, 4.03Å, 3.86Å, 3.77Å, 3.67Å, 3.19Å, 2.46Å, 2.97Å

Analcime (A) = 5.60Å, 4.85Å, 3.67Å, 3.43Å, 2.93Å

Illite (I) = 10.00Å, 5.00Å, 3.33Å

Kaolinite (K) = 7.10Å, 3.50Å

Chlorite (Ch) = 14.00Å, 7.07Å, 4.72Å, 3.50Å

The XRD spectra of the clay separated Orepuki oil shale samples (OOS1, OOS2, and OOS3) show the presence of quartz, kaolinite and vermiculite (Figure 4.3). Their relative abundances are shown in Table 4.1. Vermiculite is judged from the peak at 12.01Å in the spectrum of K^+−saturated sample which collapses to 10.0Å when heated to 550°C and expands to 14.0Å with Mg^{2+}− glycerol treatment (Figure 4.3). It is present in small amounts (p) while there appears to be more kaolinite present (c) (Figure 4.3, Appendix D). Small amount of feldspar is also present in clay separated fraction (Figure 4.3), which could be a product of grinding.

The XRD spectra of the Qianjiang Formation samples, QF1, QF2 and QF3 are shown in Figure 4.4. Examination of the spectra shows the only clay mineral present in these sample is illite togather with clay-size quartz (Figure 4.4). In QF1, QF2 and QF3 illite appears to be a minor component (p) (Table 4.1, Appendix D).

The XRD spectra of Mir Kalam Kala samples (MKK1, MKK2) are shown in Figure 4.5. Quartz dominates in the bulk-untreated (whole rock) MKK1 sample, while gypsum dominates in the bulk-untreated MKK2 sample (Figure 4.5). The clay minerals present in these samples are kaolinite and illite (Figure 4.5) and their relative abundances are shown in Table 4.1. Montmorillonite is also present in MKK2 togather with illite (Figure 4.5). As shown in Figure 4.5, the Mg−glycerol XRD pattern exhibits a peak near 17Å which has been shifted to a lower d-spacing with K^+−saturation and collapses to 10.0Å at 550°C confirming the presence of montmorillonite in MKK2 (Daoudi *et al.*, 2008; Hussain *et al.*, 1985). The XRD pattern of bulk-untreated Speena Banda (SB) oil shale shows the presence of dominant (d) gypsum. The XRD pattern of treated MKK1 sample shows that illite is dominant (d) (Table 4.1, Figure 4.5, Appendix D), while illite is common (c) in both MKK2 and SB samples as shown Figure 4.6 (Table 4.1, Appendix D).

The XRD spectra of each of the Salt Range oil shale samples (SR1, SR2, and SR3) are all similar (Figure 4.7). The clay minerals present in these samples are kaolinite, illite and chlorite. Illite in these samples is dominant (d), kaolinite is common (c) and chlorite is present (p) (Table 4.1, Appendix D). Feldspar is also present in the untreated samples (Figure 4.7).

Figure 4.3. XRD spectra of the Orepuki oil shale
(**A**: OOS1, **B**: OOS2, **C**: OOS3) shows it contains
Quartz (Q) = 4.26Å, 3.35Å, 2.46Å, 2.28Å
Feldspar (F) = 6.39Å, 4.03Å, 3.86Å, 3.77Å, 3.67Å, 3.19Å, 2.46Å, 2.97Å
Kaolinite (K) = 7.10Å and 3.50Å
Vermiculite (V) = 12.0Å
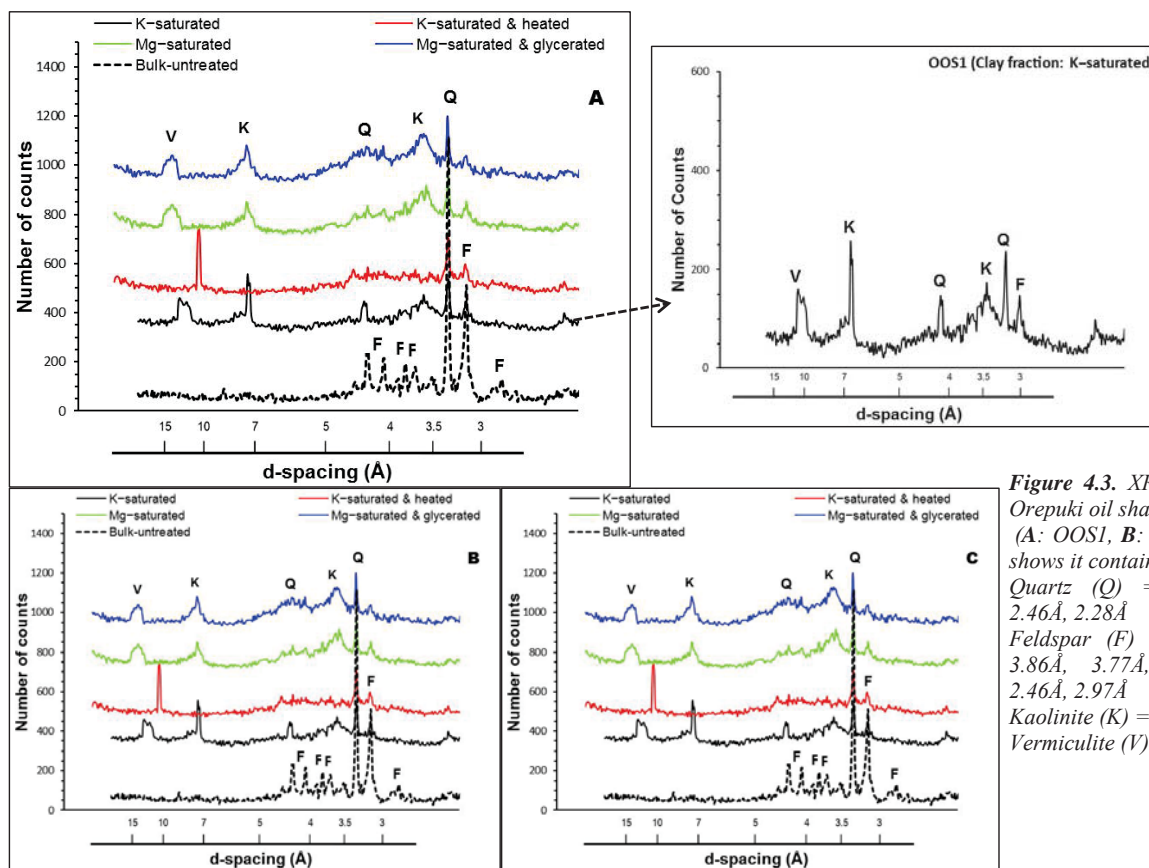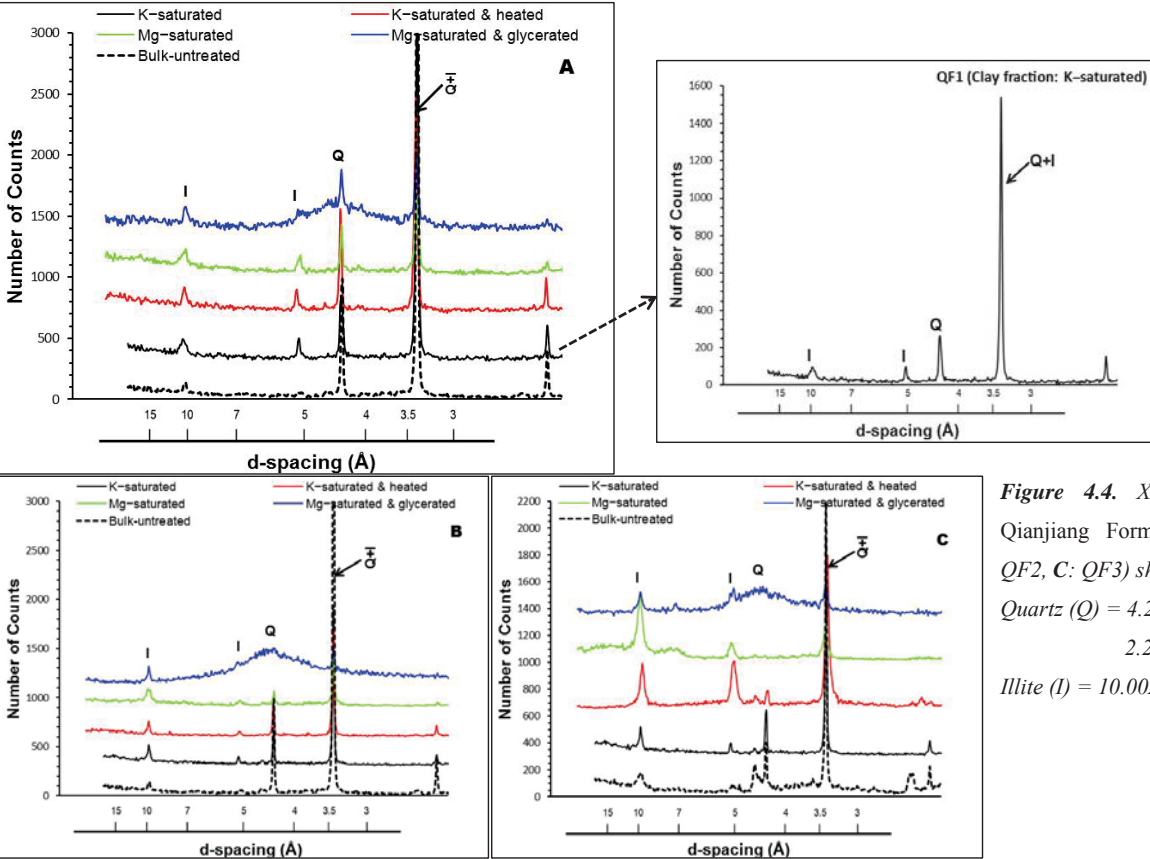
Figure 4.4. XRD spectra of the Qianjiang Formation *(A: QF1, B: QF2, C: QF3) shows the presence of Quartz (Q) = 4.26Å, 3.35Å, 2.46Å, 2.28Å*

Illite (I) = 10.00Å, 5.00Å and 3.33Å
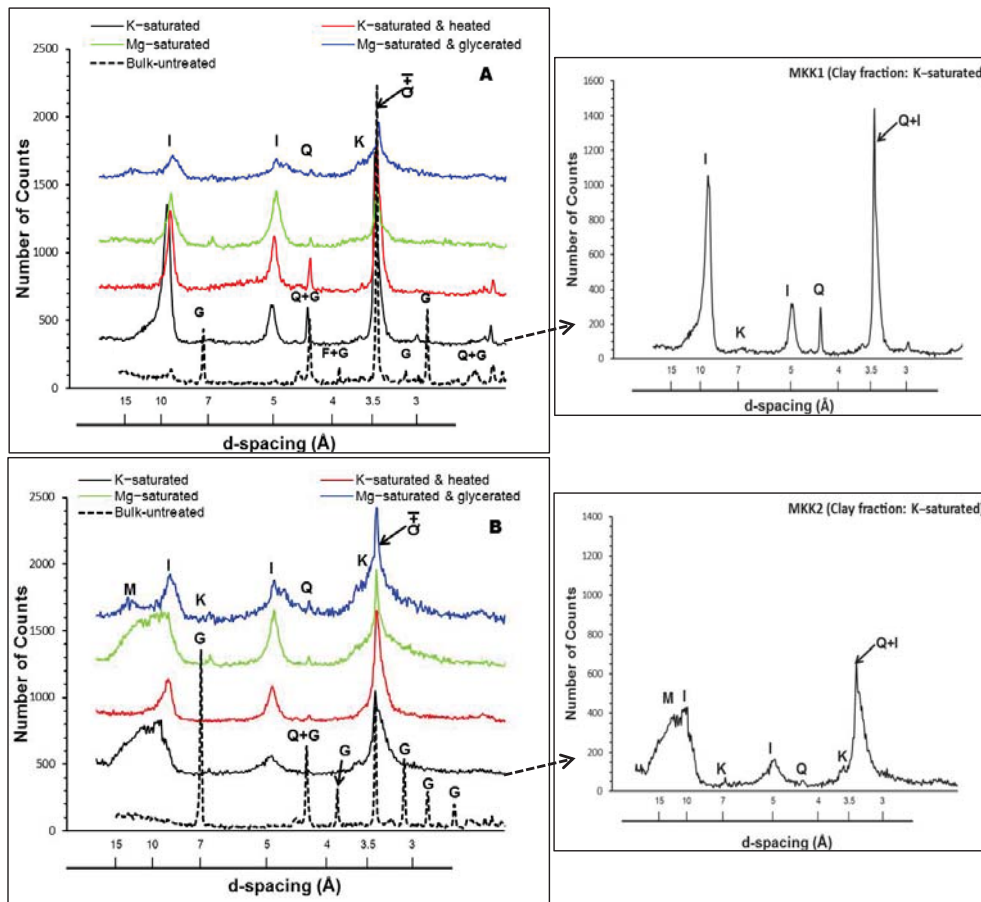
Figure 4.5. XRD pattern of the Mir Kalam Kala oil shale (**A**: MKK1, **B**: MKK2) shows it contains

Quartz (Q) = 4.26Å, 3.35Å, 2.46Å, 2.28Å

Gypsum (G) = 7.56Å, 4.27Å, 3.79Å, 3.06Å, 2.86Å, 2.78Å, 2.68Å, 2.48Å

Illite (I) = 10.00Å, 5.00Å and 3.33Å

Kaolinite (K) = 7.10Å and 3.50Å

Montmorillonite (M) = 15.0Å, 5.01Å, 4.50Å, 3.77Å, 3.50Å
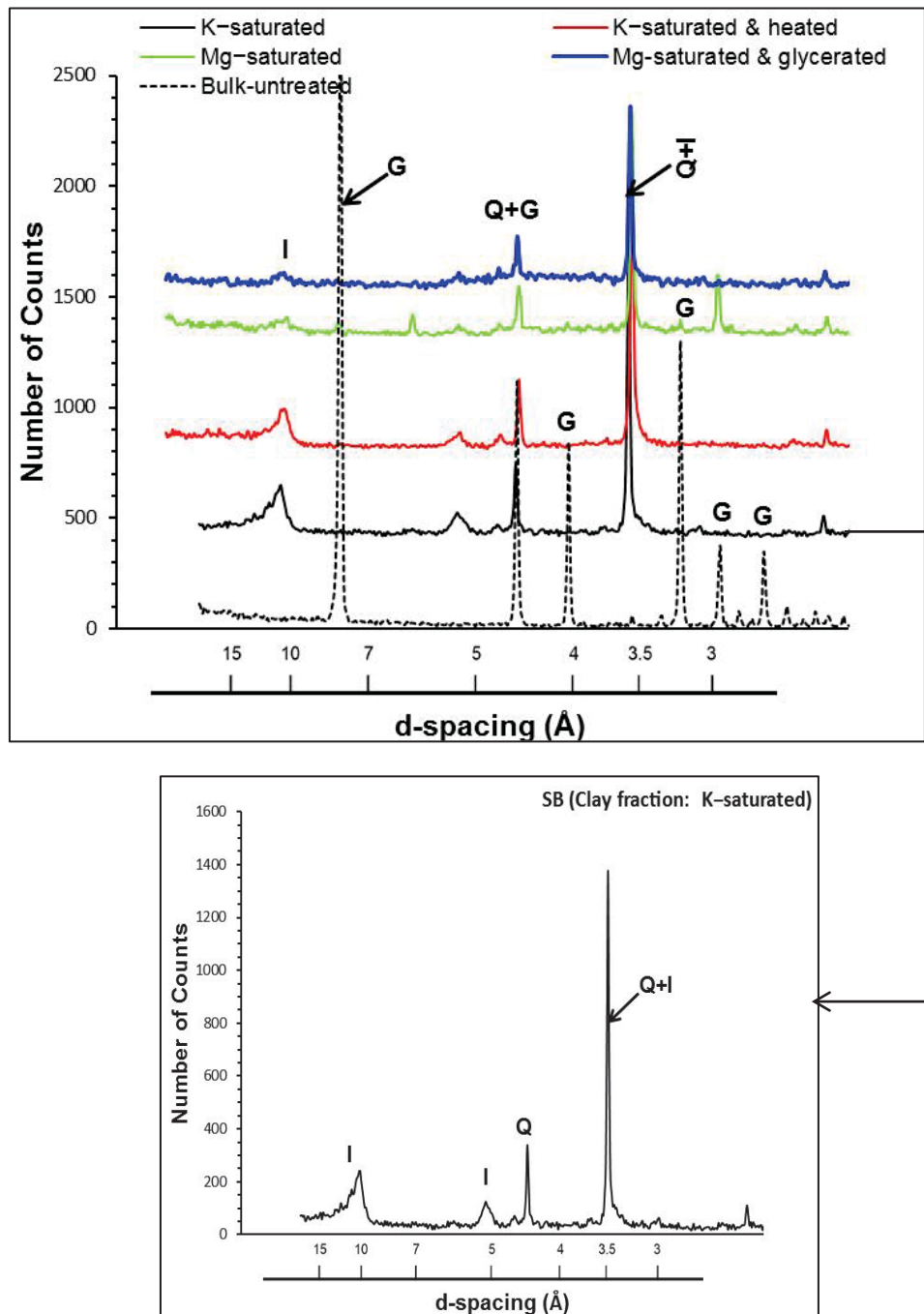
Figure 4.6. *XRD pattern of the Speena Banda oil shale (SB) shows the presence of*

Quartz (Q) = 4.26Å, 3.35Å, 2.46Å, 2.28Å

Gypsum (G) = 7.56Å, 4.27Å, 3.79Å, 3.06Å, 2.86Å, 2.78Å, 2.68Å, 2.48Å

Illite (I) = 10.00Å, 5.00Å and 3.33Å
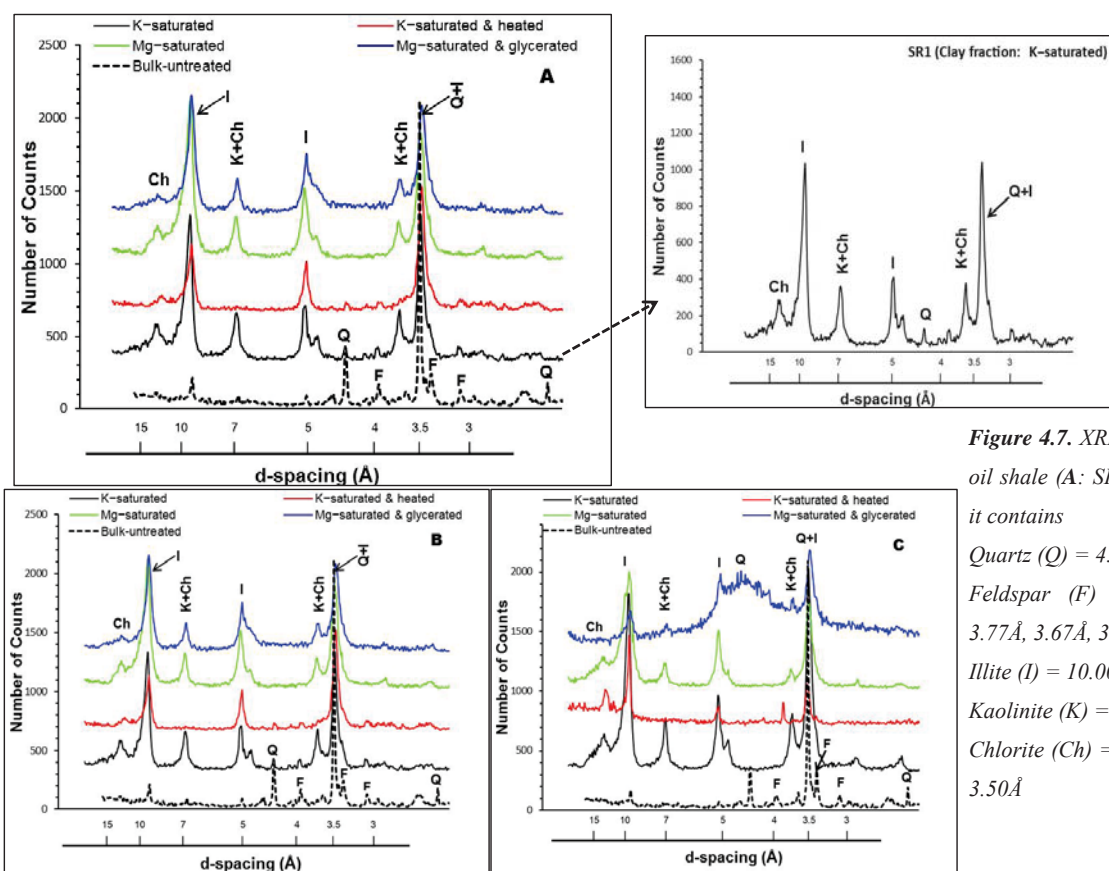
Figure 4.7. XRD pattern of the Salt Range oil shale (**A**: SR1, **B**: SR2, **C**: SR3) shows it contains

Quartz (Q) = 4.26Å, 3.35Å, 2.46Å, 2.28Å

Feldspar (F) = 6.39Å, 4.03Å, 3.86Å, 3.77Å, 3.67Å, 3.19Å, 2.46Å, 2.97Å

Illite (I) = 10.00Å, 5.00Å and 3.33Å

Kaolinite (K) = 7.10Å and 3.50Å

Chlorite (Ch) = 14.00Å, 7.07Å, 4.72Å and 3.50Å

4.2.1.3 Mineralogy of the Waipawa Formation

Samples of the Waipawa Formation collected from each of the four outcrops investigated during the study (Waipawa type locality, Lower Angora Road quarry, Upper Angora Road and Old Hill Road, Porangahau) display similar XRD spectra (Figures 4.8a−4.8d). The clay minerals present are kaolinite, illite and montmorillonite (Table 4.1); quartz is present in all samples. The amounts of the different minerals present vary between the samples from the different outcrops (Table 4.1, Appendix D). Illite is present (p) in samples from Lower Angora Road quarry and Old Hill Road outcrp sample WFOH33, whereas it is common (c) in samples from Waipawa type locality, Upper Angora Road and Old Hill Road outcrop (WFOH31, WFOH32) (Table 4.1).
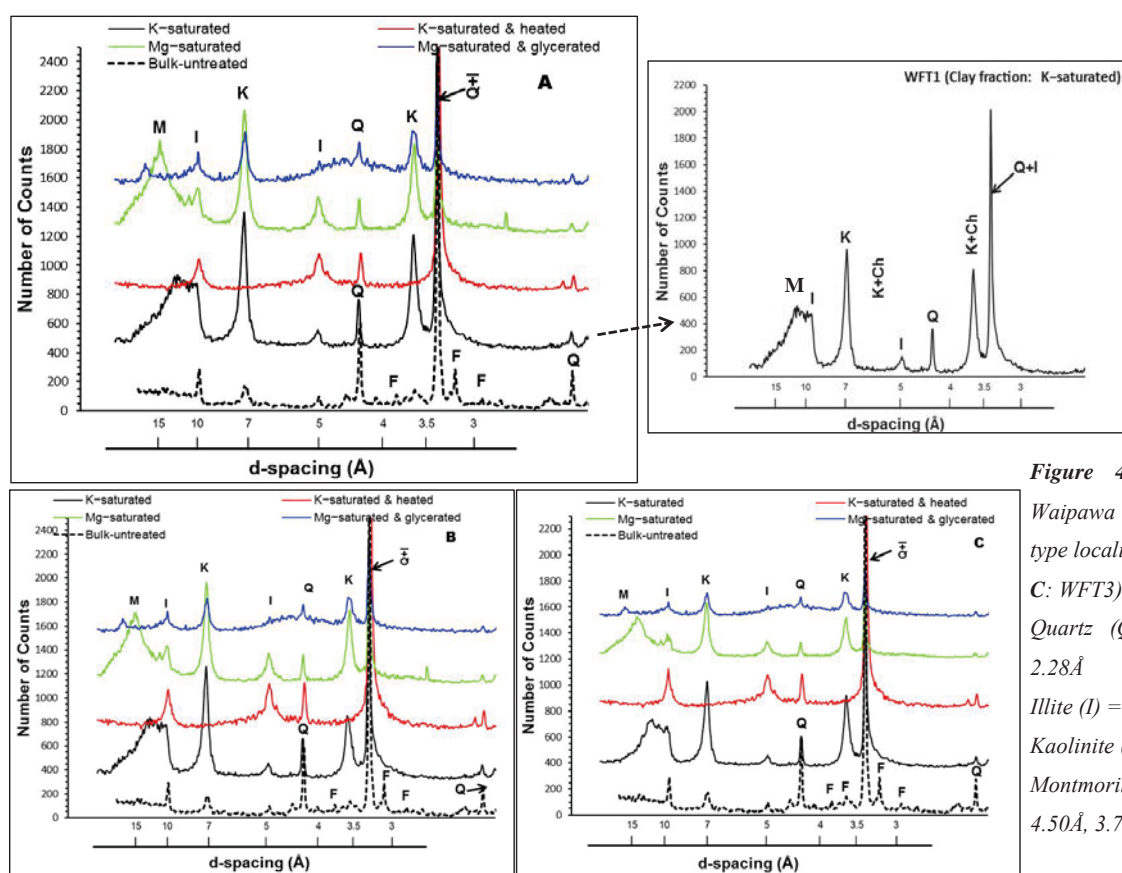
Figure 4.8a. XRD spectra of the Waipawa Formation from Waipawa type locality (*A*: WFT1, *B*: WFT2, *C*: WFT3) shows it contains

Quartz (Q) = 4.26Å, 3.35Å, 2.46Å, 2.28Å

Illite (I) = 10.00Å, 5.00Å and 3.33Å

Kaolinite (K) = 7.10Å and 3.50Å

Montmorillonite (M) = 15.0Å, 5.01Å, 4.50Å, 3.77Å, 3.50Å
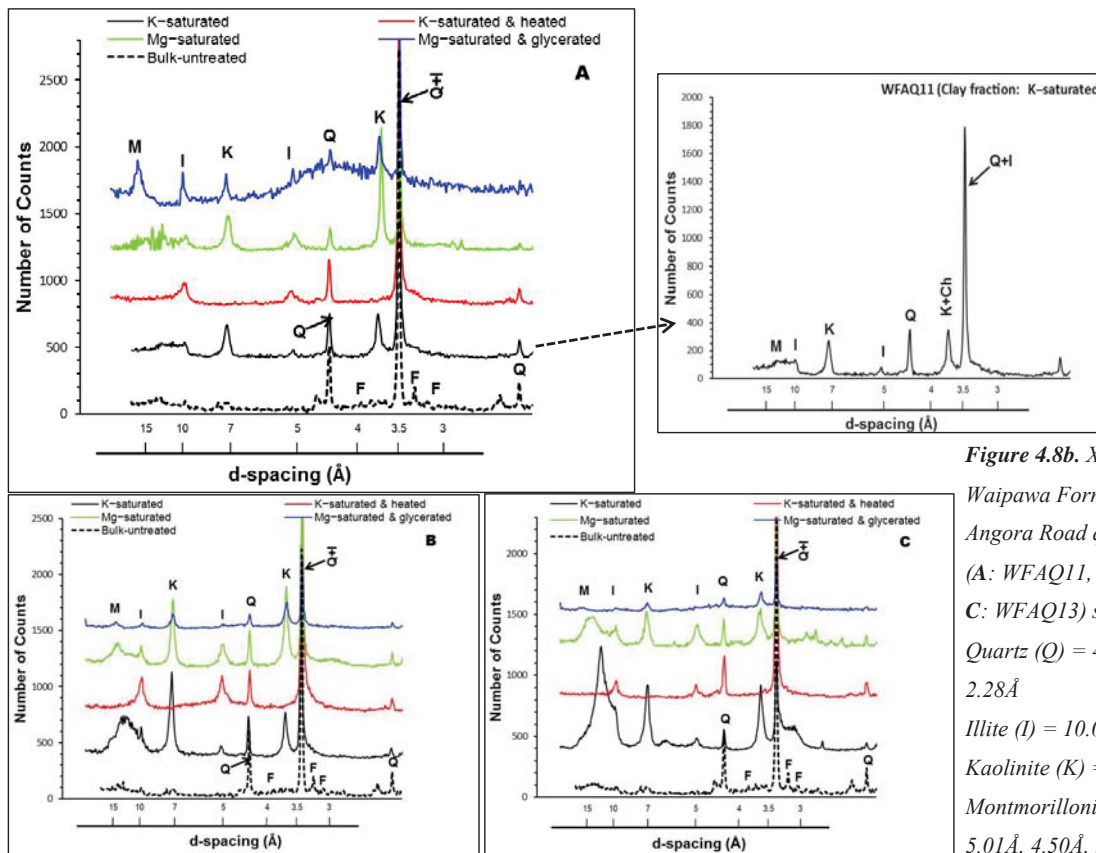
Figure 4.8b. XRD spectra of the Waipawa Formation from Lower Angora Road quarry locality (*A*: WFAQ11, *B*: WFAQ12, *C*: WFAQ13) shows it contains

Quartz (Q) = 4.26Å, 3.35Å, 2.46Å, 2.28Å

Illite (I) = 10.00Å, 5.00Å and 3.33Å

Kaolinite (K) = 7.10Å and 3.50Å

Montmorillonite (M) = 15.0Å, 5.01Å. 4.50Å. 3.77Å. 3.50Å

Figure 4.8c. XRD pattern of the Waipawa Formation from Upper Angora Road locality (A: WFAQ21, B: WFAQ22, C: WFAQ23) shows it ontains Quartz (Q) = 4.26Å, 3.35Å, 2.46Å, 2.28Å Illite (I) = 10.00Å, 5.00Å and 3.33Å Kaolinite (K) = 7.10Å and 3.50Å Montmorillonite (M) = 15.0Å, 5.01Å, 4.50Å, 3.77Å, 3.50
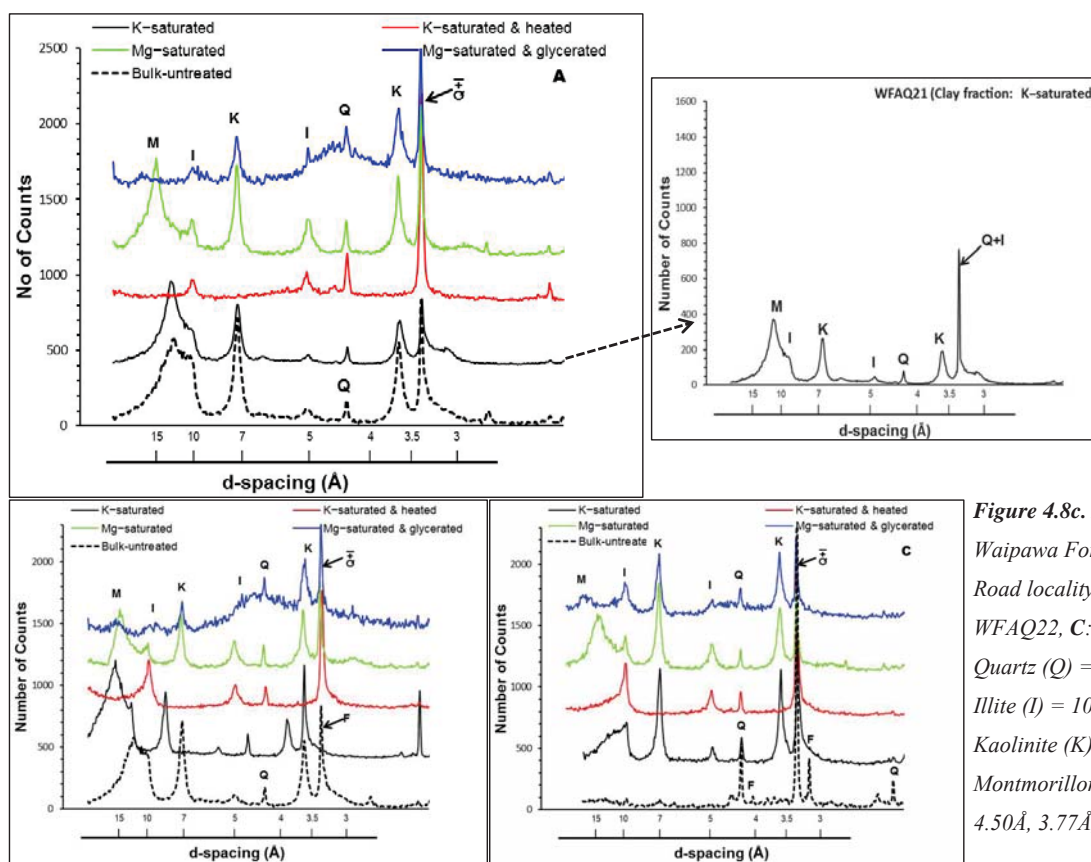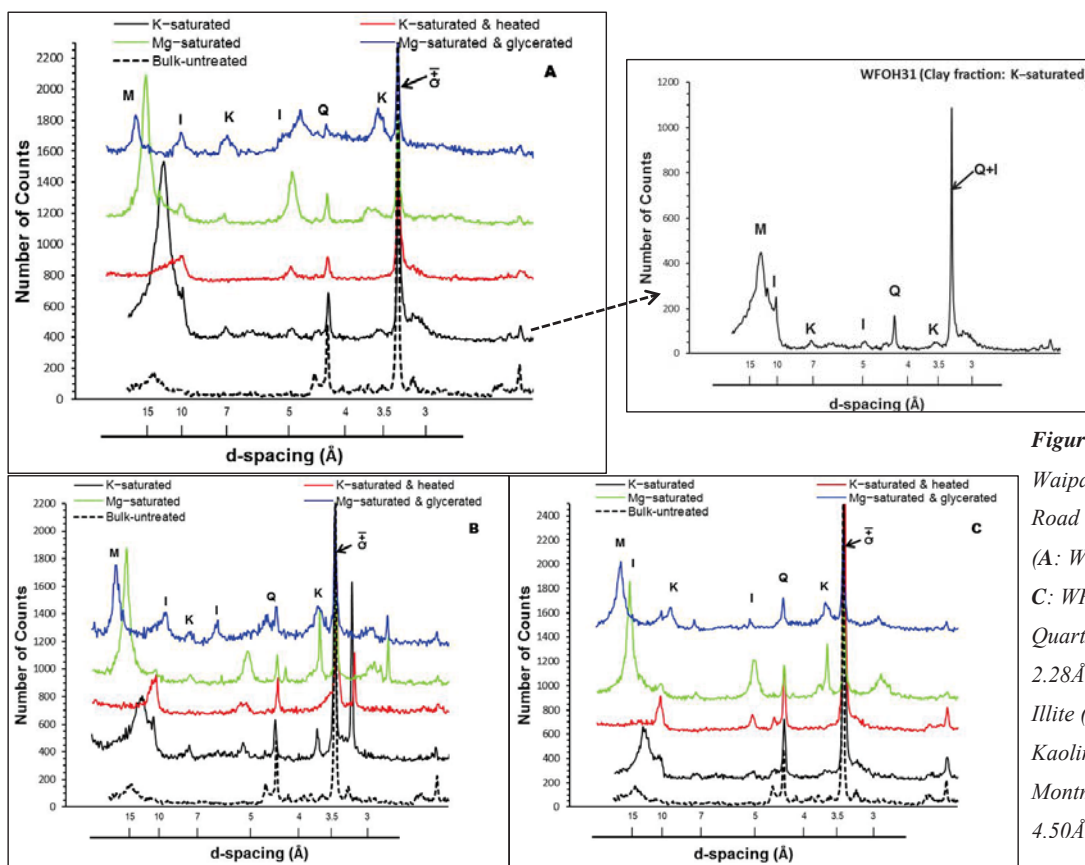
Figure 4.8d. XRD spectra of the Waipawa Formation from the Old Hill Road (Porangahau) outcrop (**A**: WFOH31, **B**: WFOH32, **C**: WFOH33) shows it contains

Quartz (Q) = 4.26Å, 3.35Å, 2.46Å, 2.28Å

Illite (I) = 10.00Å, 5.00Å and 3.33Å

Kaolinite (K) = 7.10Å and 3.50Å

Montmorillonite (M) = 15.0Å, 5.01Å, 4.50Å. 3.77Å. 3.50Å

4.2.2 Discussion

The mineralogy results of the different producing and non-producing oil shales highlight that the non-producing oil shale samples with poor generation potential (SR1, SR2, SR3, MKK1and argillite) contain illite as the dominant clay mineral. The mineralogical composition of samples of the producing Green River Formation contains less illite, and the Orepuki oil shale shows no illite present. Illite is present in all the Waipawa Formation samples but generally in low abundance (common) (Table 4.1).

The conclusion proposed from the mineralogical properties of the reference samples is that the production potential of an oil shale is inversely proportional to the amount of illite present. This is a qualitative relationship that is apparent for the rocks of the current study only, and analysis of additional shales is part of future work that can be conducted to verify the more widespread validity of this conclusion. However, in the context of the current study, the conclusion is valid. This relationship between the shale oil potential of oil shales and the content of illite is consistent with the work of Burnham (2008). This author, working on shale samples from the Green River Formation, found that illitic-rich oil shales produce less oil per unit of organic carbon. However, the magnitude of this effect was not large and the significance of the result is not certain. Weaver (1960), however, working on more than 20,000 samples from different basins in the U.S. found that the amount of montmorillonite is directly proportional to the amount of shale oil.

There is clearly a precedent for a relationship between mineralogy and oil content, but the parameters of this relationship appear to vary between studies. In the current study, where different oil shales from different countries with different origins and environments of deposition were analysed, there is no relationship between the detrital mineral (montmorillonite; which forms during weathering of silicates) and shale oil production potential. No montmorillonite was identified in the international producing or non-producing oil shales analysed except in the Mir Kalam Kala sample (MKK2). Montmorillonite was also identified present (p) or common (c) in the Waipawa Formation.

A trend in illite content, however, is observed. Therefore, the mineralogical index of oil-production potential defined in the current study is a low abundance or absence of illite, rather than a greater abundance or presence of another clay mineral, as has been defined in previous studies. This relationship is interesting because it means a shale with hydrocarbon potential can be screened quickly and inexpensively as yes it has potential or no it doesn't, based on a simple XRD analysis of the clay mineral fraction without undertaking involved analyses and calculations to determine the quantity of illite present. This relationship warrants further verification, through analysis of a larger number of samples, so definite conclusions can be reached.

The progressive transformation of montmorillonite to illite through an intermediate mixed-layered illite/montmorillonite is the most important diagenetic clay reaction in shales (Milliken, 2005; Pevear, 1999; Pollastro, 1993). According to Meunier and Velde (2004) illite/montmorillonite is an important geothermometer in diagenetic studies and approaches to utilize this geothermometer are:

1) Vertical profiles from wells and outcrops (where illite/montmorillonite is studied through several hundred or thousand feet of sedimentary rock)

2) Paleotemperature or thermal maturity mapping on local or regional scale (where illite/montmorillonite of a particular unit or bed is studied using both outcrop and well samples to produce geothermal history map of the unit in the study area) (Pollastro, 1993).

These approaches have not been utilized in the scope of this study.

There is no montmorillonite present in the argillite and Salt Range samples but illite is dominant (d). In Mir Kalam Kala sample, MKK2, both montmorillonite and illite are common (c). In the Green River Formation samples montmorillonite is absent and illite is common (c). In the all Waipawa Formation samples from Waipawa type locality, Upper Angora Road and Old Hill Road (Porangahau) both illite and montmorillonite are common (c) except the Old Hill Road outcrop sample WFOH33 in which illite is present in minor amounts (p). In the Waipawa Formation samples from Lower Angora Road quarry both illite and montmorillonite are present in small amounts (p). This may be due to the fact that during diagenesis montmorillonite is transformed into authigenic illite with geologic time, depth of burial and temperature (Milliken, 2005). Primary factors controlling the montmorillonite to illite transformation are temperature and the

availability of potassium and aluminium ions (Hower *et al.*, 1976; Pearson & Small, 1988; Pytte & Reynolds, 1989).

According to Hower *et al.* (1976), the chemical changes involved in the conversion of montmorillonite to illite are represented by the reaction:

$$montmorillonite + Al^{3+} + K^+ = illite + Si^{4+}$$
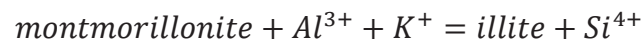
Montmorillonite holds more pore water than the non-expandable clays: kaolinite, illite and chlorite and a greater pressure is required to squeeze that pore water from between the clay particles (Bruce, 1984). Water is necessary to move hydrocarbons from shales to more permeable rocks (Bruce, 1984; Weaver, 1960). For the formation of hydrocarbons an appreciable depth of burial and pressure is required (Tana *et al.*, 2013) and this pressure which is due to burial may cause the water-bearing clays to loose most of their pore water with only shallow burial before the majority of the hydrocarbons form (Weaver, 1960). This may explain that why the well-known Green River Formation and the historically producing Orepuki oil shales, both of which contain no expanded clay, are oil shales. By the time oil was formed not enough water was left to remove the oil from the shale (Weaver, 1960).

4.3   Organic petrography

Organic petrography of oil shales can be used to describe the constituents of the organic matter (Hutton, 1988; Tao *et al.*, 2012). These include the different macerals present and the petrography provides insight of their distribution in the rock thus providing an indication of the hydrocarbon-generating potential of the rock (Tao *et al.*, 2012). The macerals are derived from different precursor organisms and/or plants that lived in many different environments, and are the major source of oil in oil shales (Hutton, 1987). As the precursor organisms of most macerals are known, organic petrography can also provide information on the environment of deposition in which the oil shale deposit accumulated (Hutton, 1987; Hutton, 1988).

The organic petrography investigation in the current study was limited to four samples. The necessary technical and scientific expertise was provided by Richard Sykes, GNS Science, Lower Hutt. This was the only aspect of the non-conventional production potential assessment model not conducted at Massey University. One producing and one, non-producing, overseas oil shale were selected from the list of reference oil shale samples: one sample from the Green River Formation (CBl) and one sample from Mir Kalam Kala (MKK1), as examples of a producing and non-producing oil shale respectively. Two of the New Zealand samples were then selected for comparison to these reference samples: one sample from the Orepuki oil shale (OOS1), and one sample from the Waipawa Formation type locality (WFT1).

4.3.1 Description of maceral assemblages

4.3.1.1 Green River Formation, CBl (Figure 4.10; a, b)

Polished sections of Green River Formation were studied in blue light under oil immersion. The sections showed the presence of abundant, strong, yellow fluorescing lacustrine alginite (Figure 4.9; a,b), and it is this maceral that is responsible for the high oil yield (Hutton, 1987; Hutton, 1988). There are two types of alginite. One is a fine lamellar type called *lamalginite*, derived from *Pediastrum (*Lam; *Pediastrum*) (precusor organism); and the other is an oval to circular type termed *telalginite*, derived from *Botryococcus* (Tel: *Botryococcus*) (precursor organism) (Hutton, 1987). The Green River Formation contains abundant *lamalginite* (Lam) (Figure 4.9; a,b) and is essentially mono-maceralic in terms of primary macerals (that is, it appears to contain no other primary macerals other than *lamalginite*). No *telalginite* was observed and this is consistent with an organic petrography study of the Green River Formation reported by Ingram *et al.* (1983). Furthermore, no vitrinite or inertinite macerals were observed. Common patches of strong, orange fluorescing solid bitumen (SB) are clearly visible in the photomicrographs, and some of these can be seen infilling intergranular voids. This solid bitumen has almost certainly been generated from the thermal maturation of the constituent *lamalginite* (Sykes, Pers. comm., 2012).

The dominance of *lamalginite* suggests a lacustrine origin for the Green River Formation. The high content of algal organic matter present in this rock makes this an oil shale of exceptional quality (more oil prone). Ingram *et al.* (1983) also found the presence of *lamalginite* (described as alginite B) and bitumen in polished sections from the Green River Formation (Mahogany Zone). These authors also studied the Rundle Formation from Australia and determined that the amount of *lamalginte* present in the Green River Formation was almost double the amount present in the Rundle Formation, and that the shale oil yield from the Green River Formation was four times greater than the Rundle Formation. Evidence in the literature suggests that the relative presence of *lamalginite*, as determined through organic petrography, can be used to infer relative information on the potential hydrocarbon yield that an oil shale may have (Hakimi & Abdullah, 2013; Kolonic *et al.*, 2002).

4.3.1.2 Mir Kalam Kala oil shale, MKK1 (Figure 4.10; c, d)

The Mir Kalam Kala oil shale sample contains only very sparse organic matter. The macerals present include small, dispersed fragments of terrestrial *inertodetrinite* (Id) and *vitrodetrinite* (Vd) and marine *liptodetrinite* (Ld) (Figure 4.9; c,d). According to Sykes (Pers. Comm., 2012) the *liptodetrinite* may be derived from the degradation of alginite material, but the sparseness of algal material has rendered this a very low quality oil shale with limited production potential.
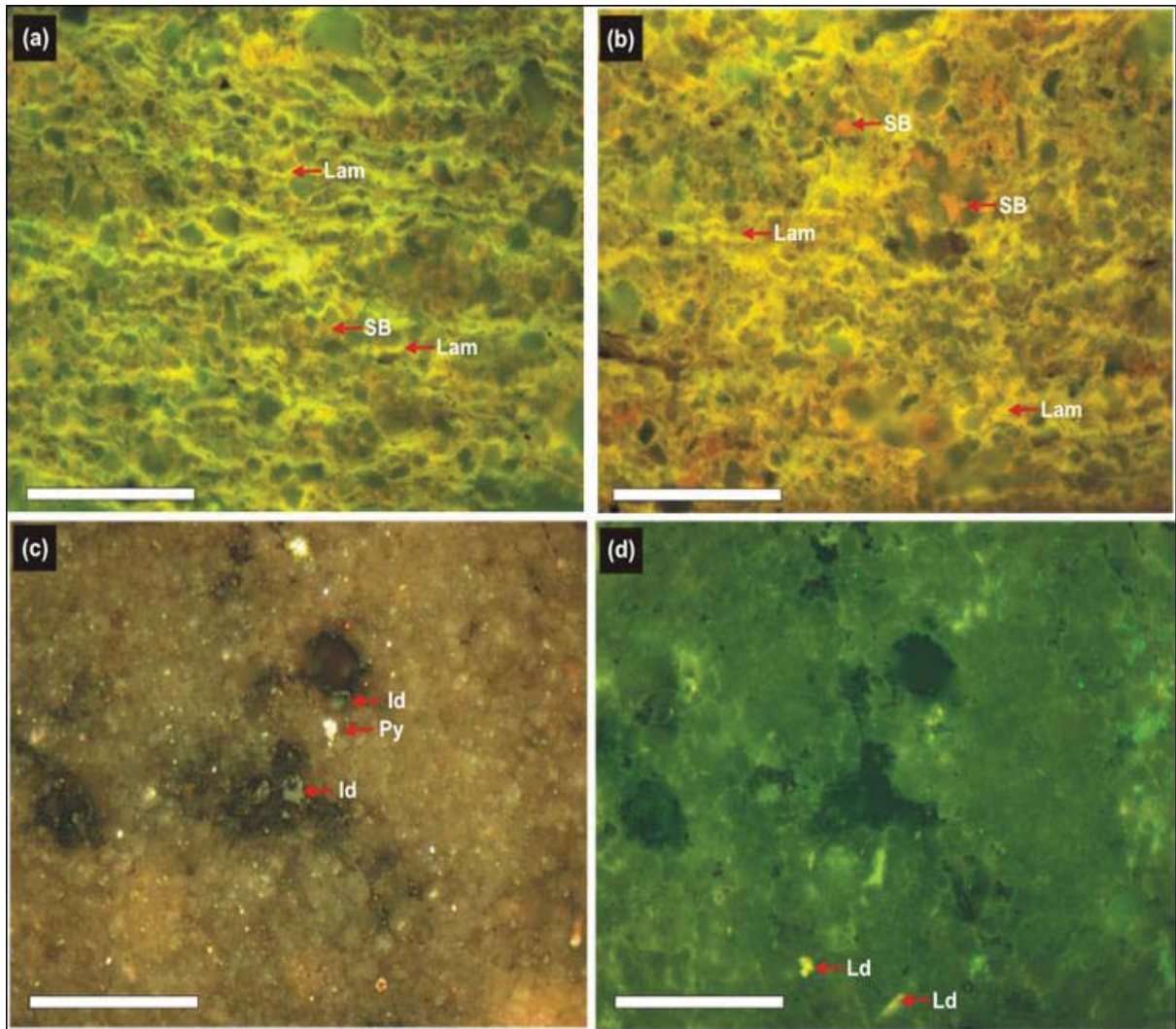
Figure 4.9   *Photomicrographs of the macerals present in the reference samples subjected to organic petrography; (a, b) Sample CBl (Green River Formation) contains an abundance of strong, yellow fluorescing lamalginite (Lam) and patches of strong, orange fluorescing solid bitumen (SB);*

(c, d) Sample MKK1 (Mir Kalam Kala) displays very sparse particles of inertodetrinite (Id) and liptodetrinite (Ld) with minor pyrite (Py).

All photomicrographs were taken under oil immersion, and the scale bars represent 50 µm; (c) was taken in reflected white light, whereas (a), (b), and (d) were taken in reflected blue light (fluorescence mode). (c) and (d) are same field of view. Plate supplied by R. Sykes, GNS Science.

4.3.1.3 Orepuki oil shale, OOS1 (Figure 4.11; a,b)

The photomicrographs of the Orepuki oil shale, taken in blue light under oil immersion, show the presence of moderately abundant organic matter, but the organic matter is dominated by dispersed fragments of terrestrial vitrinite, specifically *vitrodetrinite* (Vd), with lesser amounts of *inertodetrinite*, *liptodetrinite*, and higher-plant cork and wood tissue. There is only sparse *lamalginite* present, and no *telalginite* was observed (Figure 4.10; a,b). These macerals in the Orepuki oil shale are responsible for its low oil yield (Sykes, 1996). Tiny pyrite crystals are common. It appears to be a marginal, poor quality oil shale. Thus the Orepuki oil shale is of freshwater lacustrine origin with some terrestrial input (Sykes, Pers. comm., 2012). This is consistent with the study of Sykes (1996) studying different New Zealand oil shales including the Orepuki oil shale using organic petrography.

4.3.1.4 Waipawa Formation, WFT1 (Figure 4.11; c, d)

The sample of the Waipawa Formation from the type locality contains a moderately sparse organic matter assemblage dominated by dispersed fragments of terrestrial vitrinite, specifically *vitrodetrinite*, lesser *inertodetrinite*, and even less *lamalginite* and *liptodetrinite*. Pyrite is common, including pyrite in a framboidal form (Figure 4.10; c,d). As *lamalginite* is the minor organic maceral present, the definition of Hutton (1987)[14] can be used to describe the Waipawa Formation as a Tasminite type marine oil shale with some terrestrial vitrinite (Figure 4.10; c, d) based on organic petrography of this sample. The Waipawa Formation is a marine unit (Killops *et al.*, 1996), but recent research of samples from equivalent strata in the Great South and East Coast basins has shown that its organic matter consists predominantly of terrestrial-derived vitrinite and inertinite material transported into a marine shelf environment (Schiøler *et al.*, 2010). The low content of algal organic matter makes this sample a poor quality oil shale with relatively low production potential.

---

[14] Types of oil shales discussed in Chapter 1 (section 1.6)
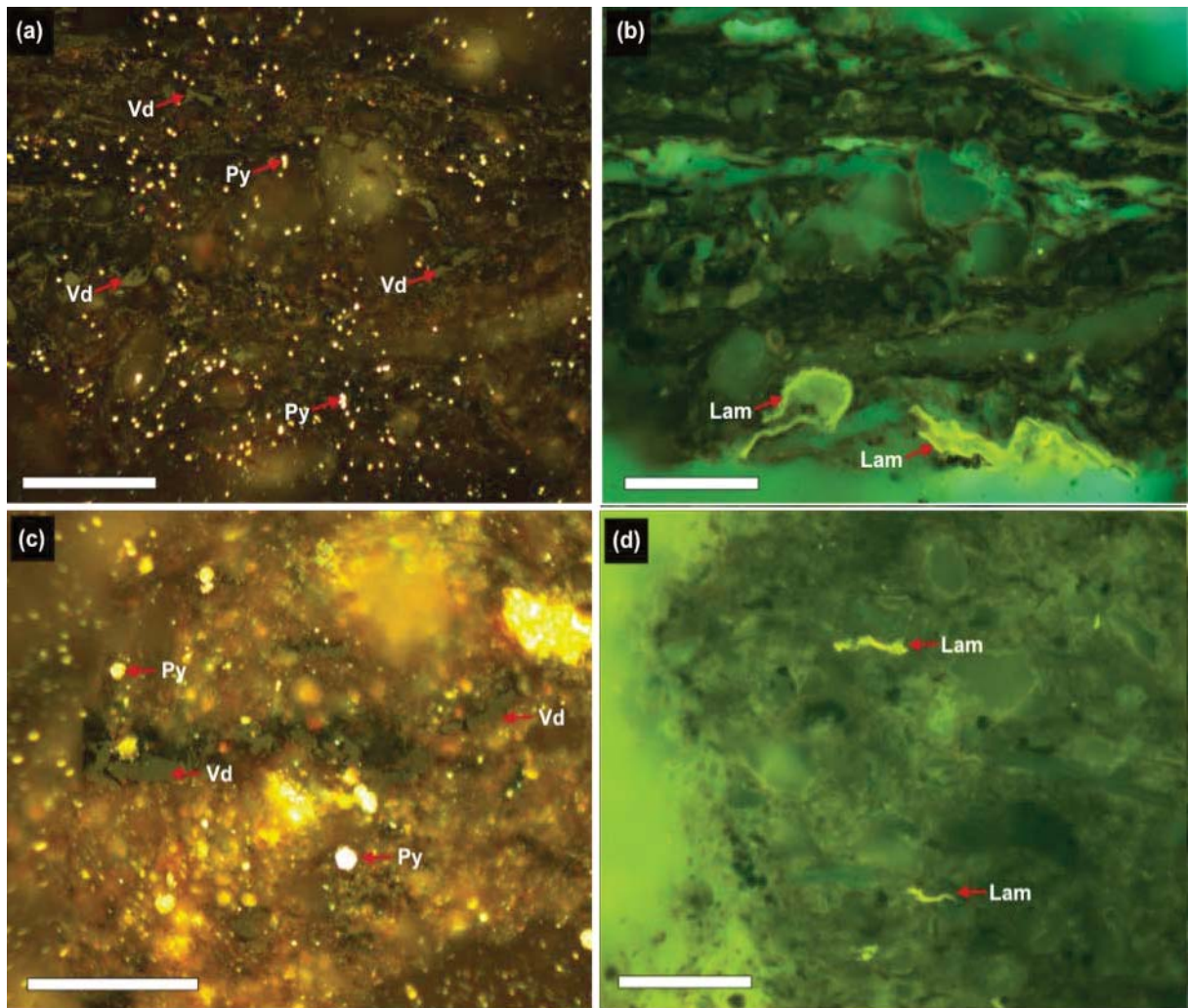
Figure 4.10 *Photomicrographs of the macerals present in the analysed Orepuki oil shale and Waipawa Formation samples; (a, b) Sample OOS1 contains a moderately abundant organic matter assemblage dominated by dispersed fragments of vitrodetrinite (Vd), with relatively minor lamalginite (Lam). Common tiny (<2 μm) dispersed pyrite crystals (Py) are scattered throughout.*

(c–d) Sample of the Waipawa Formation (type locality) exhibiting sparse dispersed fragments of vitrodetrinite (Vd), with only minor lamalginite (Lam). Pyrite (Py) is common.

All photomicrographs were taken under oil immersion and the scale bars represent 50 μm; (a) and (c) were taken in reflected white light, whereas (b), and (d) were taken in reflected blue light (fluorescence mode). (b) and (d) are the same fields of view as (a), and (c), respectively. Plate supplied by R. Sykes, GNS Science.

4.3.2 Discussion

The organic petrography of the four different oil shales shows the presence of abundant macerals in the Green River Formation but a sparse and very low content of macerals in the Mir Kalam Kala shale. There is a strong relationship between maceral content and oil content. The Green River Formation, an example of an oil shale with very good production potential, is rich in alginite and solid bitumen. The Mir Kalam Kala shale in contrast has a very low content of macerals and is a very low quality oil shale. These conclusions match those deduced through consideration of the SRA data. The conclusions drawn through consideration of the organic petrography of the Orepuki oil shale are not, however, consistent with those generated by SRA analysis (Chapter 3). Organic petrography infers that the Orepuki shale has limited production potential due to the presence of sparse lamalginite, whereas SRA infers that this shale has excellent production potential. Poor agreement may be due to the fact that only one sample was subjected to petrographic analysis. In a single sample, only a limited number of grains are studied under the microscope, and these grains may not be representative of the whole sample. According to the organic petrography of the Waipawa Formation from the type locality, this formation may be defined as a low quality oil shale due to the low content of organic macerals present.

Chapter 5 – Thermal Analyses

5.1 Introduction

The dominant phase of organic matter in an oil shale is kerogen (Robinson & Cumins, 1959; Sonibare *et al.*, 2011). Thermal decomposition of the kerogen occurs at temperatures of approximately 550°C and yields volatile materials in the form of oil and gas, and a solid residue of char (Durand, 1988). The oil yield of an oil shale upon pyrolysis depends on the abundance and nature of the constituent kerogen and its thermal evolution (Tissot & Welte, 1978c). Understanding the processes and kinetics of the thermal decomposition of this kerogen and its geochemical characteristics is therefore essential in planning for effective extraction and utilization of shale oil from an oil shale resource (Al-Harahsheh *et al.*, 2011; Thakur & Nuttall Jr, 1987). The specific application of thermal analyses to oil shale studies was comprehensively reviewed by Rajeshwar (1983).

The purpose of the experimental work described in this chapter was to evaluate the organic carbon content of all samples in the study. Loss on Ignition (LOI) and LECO were first performed to get an initial estimate of the abundance of organic matter in the different samples.

Thermogravimetric Analysis (TGA) was then performed to accurately calculate the weight change in each sample as a function of increasing temperature at a constant heating rate. The TGA analysis of oil shales has been used extensively in the past as a means to determine the characteristics of devolatilisation (Hillier *et al.*, 2009; Li & Yue, 2003; Rajeshwar, 1981). Thermogravimetric analysis in the current study was performed to investigate the different weight loss regions as the pyrolysis temperature increased, and to estimate the amount of organic matter being lost in a certain temperature region. TGA also provides information on mineral decomposition. The slope of the TGA curve (expressed as Differential Thermal Analysis or DTA) changes in different regions of weight loss and provides an estimation of the amount of organic

matter present. The thermal decomposition of oil shale in the TGA is a very complex process involving a series of reactions as a sample is heated (Jaber *et al.*, 2005; Kerimov, 2004) and therefore the loss in organic matter decomposition region can be associated with other losses such as loss of mineral matter (Jiang *et al.*, 2007). Therefore TGA should be performed in conjunction with LOI or LECO (TOC) analysis to have a better estimation of organic matter present.

5.2 Loss on ignition (LOI)

The results of LOI are presented in Table 4.1. A large range of total organic matter content was recorded for the samples of this study, from a of 0.1 wt% to a maximum of 30 wt%.

Table 5.1. Total organic matter content of the shales and non-generative reference materials of this study as determined by LOI.

Samples	LOI (wt%)	Samples	LOI (wt%)
Sand	0.1	OOS1	30.0
Argillite	3.1	OOS2	29.0
CBl	25.8	OOS3	30.0
CBr	18.0	WFT1	14.9
QF1	9.5	WFT2	14.0
QF2	12.5	WFT3	15.3
QF3	25.0	WFAQ11	9.0
MKK1	5.4	WFAQ12	8.9
MKK2	8.0	WFAQ13	9.3
SB	8.8	WFAQ21	7.0
SR1	1.0	WFAQ22	5.5
SR2	1.3	WFAQ23	8.6
SR3	1.3	WFOH31	5.6
Graphite	6.3	WFOH32	6.0
		WFOH33	6.0

Loss on ignition quantifies the amount of mass lost through combustion of a sample. In sedimentary rocks this mass is predominantly organic matter, therefore LOI values can be used to estimate the abundance of organic matter in a sample (Veres, 2002).

The data in Table 5.1 defines three groupings of rocks based on LOI. Sand and argillite populate the grouping with the lowest LOIs (less than 5 wt%). The Salt Range samples (SR1, SR2 and SR3) also have LOI values in this grouping. In contrast, the Orepuki oil shale (OOS1, OOS2, and OOS3), Green River Formation (CBl, CBr) and one of the Qianjiang Formation samples (QF3) populate the group with the highest values (18-30 wt%).

All the Waipawa Formation samples from the Waipawa type locality (WFT1, WFT2, WFT3), Lower Angora Road quarry (WFAQ11, WFAQ12 and WFAQ13), and Upper Angora Road (WFAQ21, WFAQ22 and WFAQ23), Old Hill Road in Porangahau (WFAQ31, WFAQ32 and WFAQ33), two of the Qianjiang Formation samples (QF1 and QF2), Mir Kalam Kala oil shale (MKK1, MKK2) and the Speena Banda shale (SB) have LOI values in a medium range (5-15 wt%).

5.3 LECO

LECO is a combustion technique, which has been used in this study for the determination of total carbon (TC) and total organic carbon (TOC). In order to provide specific and accurate data on the total organic matter content of the rocks of this study, inorganic carbon in the rocks was removed prior to LECO analysis by acid washing (Chapter 3). Both the raw rocks and the acid washed samples (Section 2.3.2.1) were analysed and the subsequent results enabled quantification of both of these carbon fractions (Table 5.2).

Table 5.2. Total carbon (TC) and total organic carbon (TOC) of each sample as obtained by LECO[15].

Samples	Raw samples	Acid-washed samples	Total inorganic carbon	Samples	Raw samples	Acid-washed samples	Total inorganic carbon
	T C	TOC	(TC-TOC)		T C	TOC	(wt %)
	(wt %)	(wt %)	(wt %)		(wt %)	(wt %)	
Sand	--	0.06	--	OOS1	15.7	15.6	0.1
Argillite	0.6	0.6	0.0	OOS2	15.8	15.0	0.8
CBl	21.1	18.0	3.1	OOS3	14.7	14.3	0.4
CBr	15.3	12.6	2.7	WFT1	7.2	7.0	0.2
QF1	11.9	11.0	0.9	WFT2	6.4	6.2	0.2
QF2	11.0	10.1	0.9	WFT3	6.7	6.1	0.6
QF3	17.4	17.3	0.1	WFAQ11	4.6	4.4	0.2
MKK1	3.1	2.7	0.4	WFAQ12	4.1	4.0	0.1
MKK2	2.8	2.2	0.6	WFAQ13	4.3	4.3	0.0
SB	1.1	1.0	0.1	WFAQ21	2.8	2.7	0.1
SR1	0.4	0.2	0.2	WFAQ22	2.9	2.7	0.2
SR2	0.4	0.3	0.1	WFAQ23	2.7	2.6	0.1
SR3	0.2	0.2	0.0	WFOH31	2.5	2.5	0.0
Graphite	9.5	9.6	0.1	WFOH32	2.7	2.7	0.0
				WFOH33	2.1	2.1	0.0

The highest TOC values are observed for CBl (18%) and QF3 (17.3%). The TOC values of QF1, QF2 and graphite are similar (Table 5.2). But the Green River Formation sample CBr has a much lower TOC (12.6%) than CBl (18%). A range of TOC values (2-7%) are observed for the Waipawa Formation with the highest TOC for the Waipawa Formation from the Waipawa type locality and the lowest for samples from Upper Angora Road and Old Hill Road, Porangahau. The MKK1 and MKK2 have TOC values of 2.7% and 2.2% respectively, similar to Waipawa Formation samples from the Upper Angora Road (WFAQ21, WFAQ22 and WFAQ23), and Old Hill Road, Porangahau (WFOH33). The Speena Banda rock has a low TOC content of 1% (Table 5.2).

---

[15] All results in Table 5.2 are mean of three experiments with a maximum standard deviation of 0.6.

In agreement with the grouping defined on the basis of their LOI in the previous section, argillite, Speena Banda and Salt Range samples also have the lowest TOC values in the current study (0.2-1.0%). The Qianjiang Formation samples, Orepuki oil shale samples and those from the Green River Formation have the highest TOCs (10-18%) while the Waipawa Formation samples have intermediate TOC values (2-7%). The Waipawa Formation has intermediate values of TOC when compared to the Orepuki, Green River Formation and Qianjiang Formation samples. Similar intermediate values of LOI can be found for the same set of samples.

The higher LOI and TOC values recorded for samples CBl as compared to CBr suggest that these samples may come from different beds/facies of the Green River Formation. According to Robson and Saulnier (1981) the rich Mahogany Zone is bedded and consists of alternating layers of rich and lean oil shale. Thus the different coloured rocks with different TOC may be from different layers within the Mahogany Zone. Similarly the difference in TOC and LOI values for samples collected from different outcrops of the Waipawa Formation, suggest the variable content of organic matter within this formation and thus the heterogeneous nature of the formation.

The LOI value of the Speena Banda sample is higher than the LOI values of Old Hill Road outcrop samples, but its TOC is lower than the Old Hill Road outcrop samples. During LOI weight loss not only occurs due to organic matter decomposition, but also due to dehydration and dehydroxylation of mineral matter (Haddadin & Mizyed, 1974). The XRD studies (Table 4.1), identified gypsum within the SB sample (see Chapter 4, section 4.2.1.2). Gypsum dehydration (0-300°C) is likely contributing to the high LOI value of the SB sample (Bhargava *et al.*, 2005; Deer & Howie, 1966).

The LOI of SB (8.8 wt%) is similar to that of WFAQ12 (8.9 wt%). However the TOC value of SB (1 wt%) is low relative to WFAQ12 (4 wt%). The reason for this discrepancy is therefore the presence of gypsum in the SB sample (as confirmed through XRD analysis) (Chapter 4). Similarly LOI values of the Orepuki samples are higher than that of CBl (Table 5.1, Table 5.2). However the TOC value of CBl (18 wt%) is high relative to the TOC values of the Orepuki samples (Table 5.2). The reason for this discrepancy might be the greater weight loss due to mineral matter in the Orepuki samples contributing to their higher LOIs. Therefore LOI is not a precise estimate of the

abundance of organic matter and it should be performed in conjunction with or be followed by LECO in order to define a more reliable estimate of the organic content or hydrocarbon potential of source rocks.

Figure 5.1a shows a good good correlation ($R^2 = 0.87$) between LOI and TOC. This is suggesting that the two data sets (LOI and TOC) can be used to estimate to the amount of organic matter content or TOC[16]..
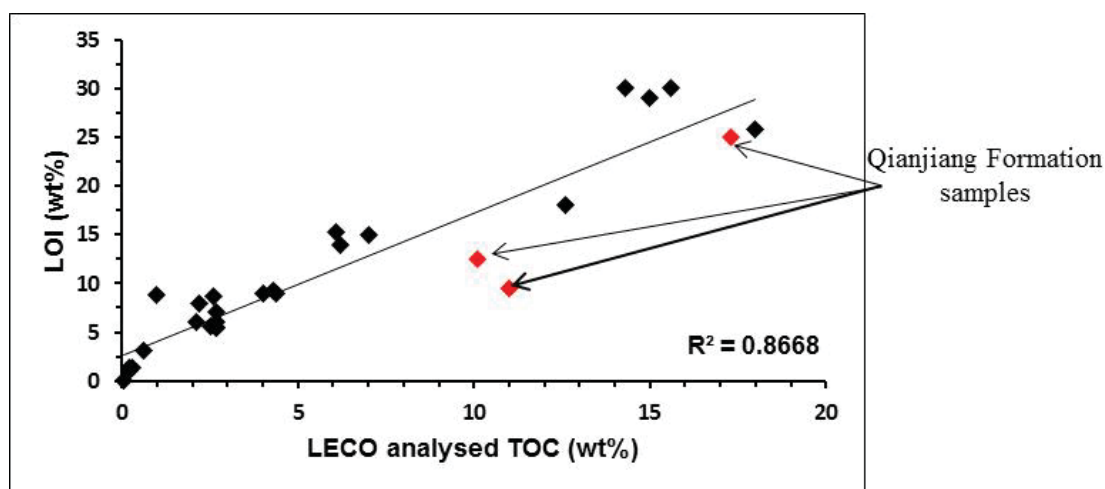
Figure 5.1a. Correlation graph between LOI and LECO-analysed TOC of all samples of this study.

To improve the fit of the correlation in Figure 5.1a, samples from the Qianjiang Formation were removed from the model. The justification for doing so was the fact that these samples are post mature (Chapter 3, section 3.2.1.1.4) and are anomalous to the other data points. Removal of these improves the correlation which increases ($R^2 = 0.93$) (Figure 5.1b). In the bivariate plot (Figure 5.1b) the samples CBl and CBr also appears anomalous. The reason being that LOI is considered a loss of weight mainly due to organic matter but there is contribution of mineral matter weight losses as well (Haddadin & Mizyed, 1974).

---

[16] Both LOI and LECO combustiuon can be used to estimate the amount of organic matter in a sample but LECO combustion is regarded in literature and through this work as being more precise than the LOI. Choice of which to use will depend on the the level of precision required.
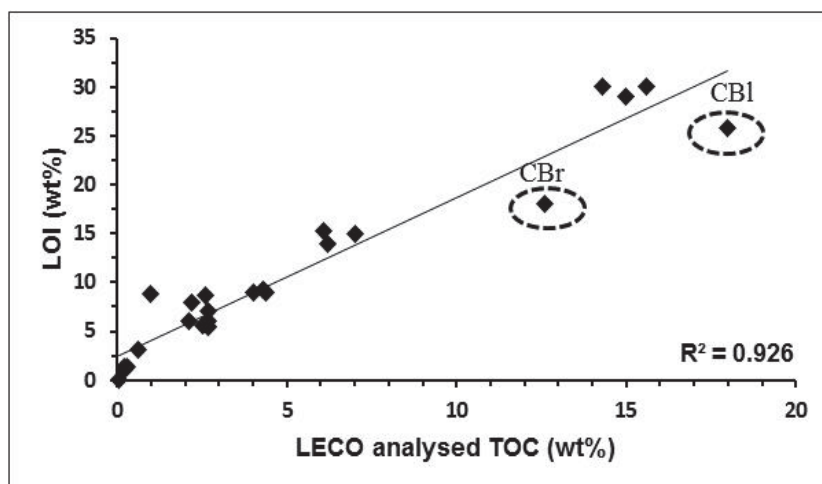
Figure 5.1b. Correlation graph between LOI and LECO-analysed TOC of all samples of this study except the Qianjiang Formation samples.

A strong correlation (R^2 = 0.99) is observed between TC and TOC (Figure 5.2). However, as LOI and TC values for weight loss can incorporate non-organic carbon (i.e., mineral decomposition), TOC is considered a more accurate indicator of organic matter content. TOC is quantified by the same technique as TC (LECO), but carbonate minerals are removed from the samples before analysis.
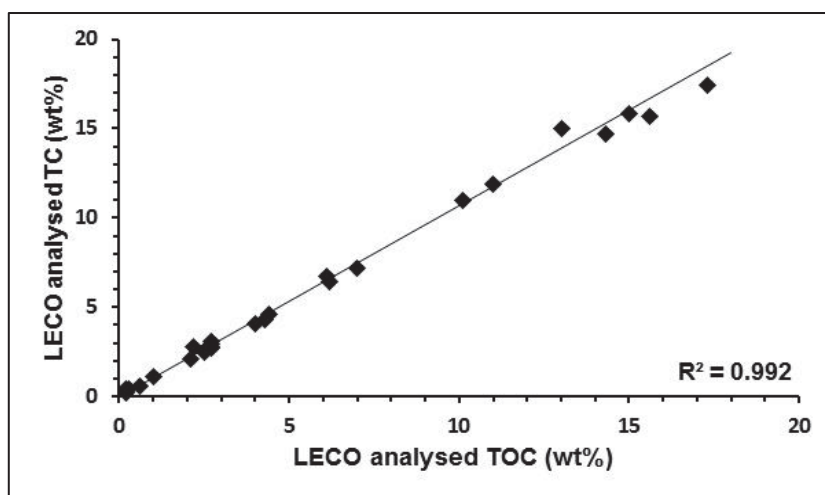
Figure 5.2. Correlation graph between LECO-analysed TC and TOC.

When the LECO analysed TOC data are compared with the SRA derived TOC data, the correlation between the two data sets is very good (R^2 = 0.95) (Figure 5.3). The difference between SRA (TOC) and LECO analysed TOC in some samples such as OOS1, CBr, QF1 and QF2 may be due to the response of each mineral matrix to the experimental conditions of each technique. But the correlation between both TOC results from SRA and LECO analyser is very high (0.95) and without further investigation, it is not possible to say which technique is more accurate.
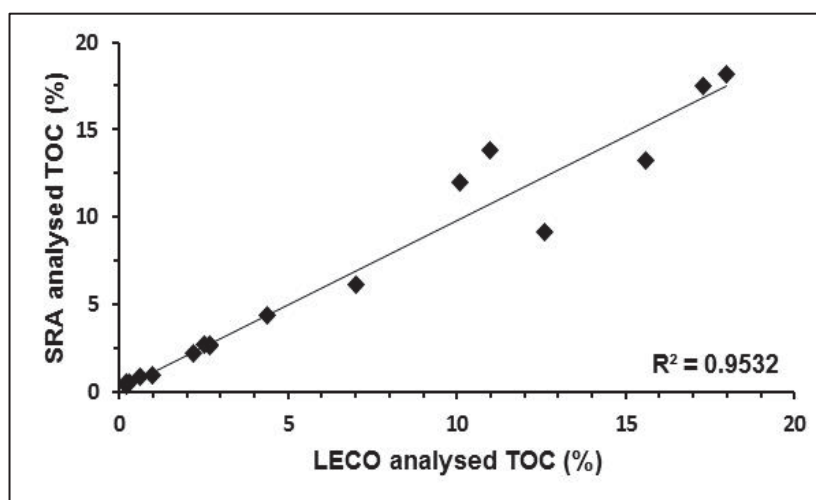
Figure 5.3. *Correlation graph between LECO (TOC) and SRA (TOC).*

5.4 Thermogravimetric analysis, TGA

Thermogravimetric analysis gives a continuous measurement of weight loss/gain as a function of temperature in a controlled atmosphere, and can characterise materials that exhibit weight loss or gain due to decomposition, oxidation or dehydration (Jaber & Probert, 2000). The thermal decomposition of oil shale is a very complex process involving a series of reactions within the sample as it is heated (Jaber *et al.*, 2005; Kerimov, 2004). The different temperature regions that can be attributed to specific phases of weight loss for the samples of the current study vary, to some extent, to those recorded in the literature. For example in the current study, weight loss due to organic matter occurs between 200-650°C Weight loss in this temperature region was attributed

to organic matter by Carmona *et al.* (2013) and Santana *et al.* (2013). However Jaber *et al.* (1999) proposed that organic matter weight loss occurs between 200-550°C. This difference may be due to different operating parameters such as final temperature, heating rate, pyrolysis atmosphere, particle grain size and flow rate (Williams & Ahmad, 1999).

Figure 5.4 presents a generalised TGA profile of weight loss of an oil shale and defines three stages of mass loss over the temperature interval 0-1200°C (Williams & Ahmad, 1998; Williams & Ahmad, 2000). Generally the first region of weight loss (20- 200°C) is attributed to the loss of moisture from clay minerals and mineral decomposition. This weight loss can also be, in part, attributed to the physical changes occurring in the kerogen such as molecular rearrangement and release of gases (Burnham *et al.*, 1983; Haddadin & Mizyed, 1974). This stage is called Phase I in the current study. Clay minerals present in the oil shale samples may continue to release structural water as temperature increases up to about 550°C (Qing *et al.*, 2007; Qing *et al.*, 2005). For example kaolinite will fully lose bound water at approximately 430°C (M. Al-Harahsheh *et al.*, 2009). Tiwari and Deo (2012; 2012) suggested that dehydroxylation of illite occurs between 500-600°C. Therefore, for some minerals, the region of Phase 1 weight loss can extend past the normal range of 0-200°C.
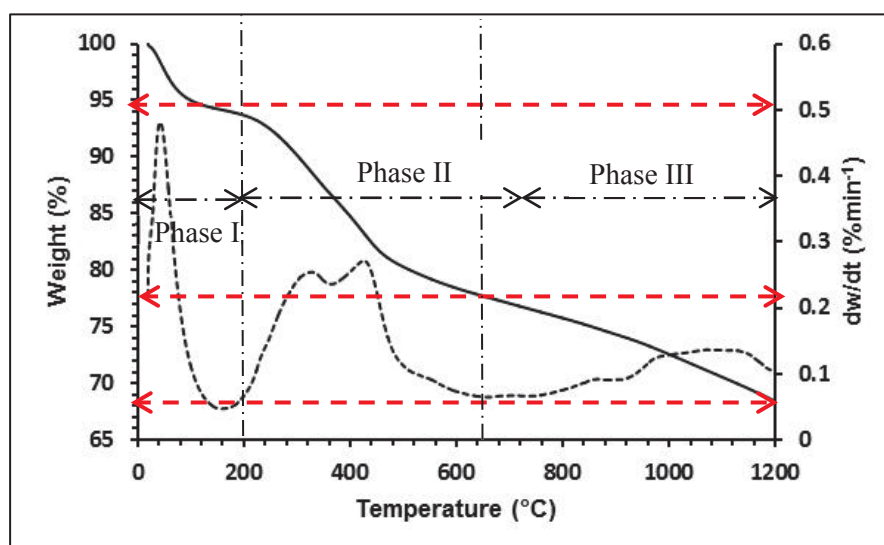
Figure 5.4. *General TGA profile for a shale over the temperature range 0-1200°C. A Peak during phase I is due to water loss. Peaks during phase II are due to*

decomposition of organic matter and weight loss during phase III is due to mineral matter.

The weight loss during the second region (Phase II), between 200 and 650°C is mainly attributed to the decomposition of organic matter (Figure 5.4). This includes the loss of hydrocarbon volatiles and evolution of gases and oil vapours (Jaber & Probert, 1999; Jaber *et al.*, 1999; Williams & Ahmad, 2000). According to Jiang *et al*. (2007) weight loss during Phase II is primarily due to thermal decomposition of organic matter, but could also include mineral weight losses from the matrix that hosts the organic matter. Previous literature on the TGA analysis of oil shales has shown that the thermal decomposition of kerogen can be either a single-step or two-stage process. The appearance of a single peak during Phase II indicates single-step decomposition of kerogen while the appearance of two consecutive peaks shows the two stage decomposition of kerogen (Dogan & Uysal, 1996; Haddadin & Mizyed, 1974; Williams, 1985; Williams & Ahmad, 1998). Allred (1966) defined the thermal decomposition of kerogen in the Colorado oil shale to be a two-stage process which involves the decomposition of kerogen into bitumen in the first step and then decomposition of bitumen into other products (oil, gas and char) in the second step.

The stage between Phase I and Phase II is interpreted as a transition stage where some mass loss occurs due to physical changes occurring in the organic matter. Such changes may include molecular rearrangement associated with the release of gases (Jaber & Probert, 2000). Borrego *et al*. (2000) suggested that this transition stage is likely due to the volatilisation of hydrocarbons trapped in mineral matter or free bitumen.

The third stage of decomposition above 650°C (Phase III) (Figure 5.4) is attributed to the continued pyrolysis of organic material within the oil shale and also to the decomposition of mineral matter (Jaber & Probert, 2000). Weight loss during Phase III could also be attributed to the possibility that CO_2 is present (which has evolved as a result of carbonate decomposition) reacts with the residual char, forming carbon monoxide (Jaber & Probert, 2000; Watanabe *et al.*, 2013). Sonibare *et al*. (2011) and Vassileva & Vassilev (2006) described carbonate decomposition as occurring between 800°C and 900°C.

The TGA weight loss curve can also be interpreted if electronic differentiation is made for the weight signal to give the rate of weight loss (DTG) (Figure 5.4). Differential thermal analysis (DTA) gives the temperature difference between the sample and a reference material during the heating or cooling of a sample. DTA gives a curve (temperature differences against sample temperature) which shows deviations from the zero line if there are any temperature differences. For example, during exothermic and endothermic reactions, the curve slopes upward or downward of the zero line (Kloss, 1974). From the DTA profile the parameter Tmax can be identified which is the temperature at which maximum devolatilisation occurs (Borrego *et al.*, 2000). The TGA parameter Tmax is different to the SRA parameter Tmax because the SRA S2 peak (from which SRA Tmax is derived) is measuring a different analyte to that being measured by TGA.

Previous work on TGA of oil shales

Extensive TGA analysis has appeared in the literature on different oil shales, including the Green River Formation (Hillier & Fletcher, 2011; Li & Yue, 2003; Rajeshwar, 1981), Chinese oil shales (Deng *et al.*, 2011; Li & Yue, 2003; Qing *et al.*, 2007), and Pakistani oil shales (Williams & Ahmad, 1998; Williams & Ahmad, 1999). Analysis has been conducted to determine characteristics of devolatilisation and also to determine kinetic parameters such as activation energy and order of a reaction. A large number of physical and chemical reactions occur during the decomposition of organic material. TGA measures the overall weight loss due to these reactions, providing general information on the overall reaction kinetics rather than individual reactions (Jaber & Probert, 2000; Pankaj Tiwari & Millind Deo, 2012; Williams & Ahmad, 2000).

In the following section the TGA and DTA data for each of the rocks investigated during the study are presented and discussed.

5.4.1 Sand and argillite (reference samples)

The TGA profiles of sand and argillite do not clearly show the three defined stages of weight loss as the pyrolysis temperature is increased from room temperature to 1200°C (Figure 5.5).
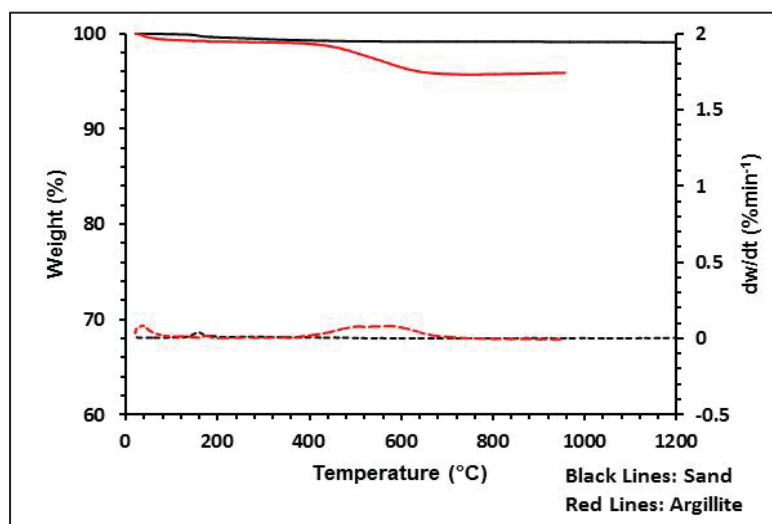
Figure 5.5. *Non-isothermal TGA (solid line) and DTA (dotted line) pyrolysis thermograms of sand and argillite at 5°C min⁻¹.*

A very low weight loss occurs during Phase I in the temperature region 0-200°C for both sand and argillite (0.42 and 0.86 wt% respectively) (Table 5.5). Weight loss of this order of magnitude is too small to be detectable in Figure 5.5. The weight loss during Phase II in the temperature region 200-650°C for sand is approximately zero or extremely low, while argillite shows approximately 3.2 wt% weight loss relative to the initial weight. These values of weight loss during Phase II are similar to the LOI values in Table 5.1. No weight loss during Phase III in the temperature region 650-1200°C can be observed for sand. For argillite, weight loss during this phase III due to mineral matter decomposition is 0.2 wt%.

The DTA of sand (Figure 5.5) shows only a low intensity peak in the water loss region and no peak for weight loss during Phase II. This means that sand contains no organic matter. The DTA of argillite on the other hand shows a low intensity peak during the

Phase II weight loss region. Hence the peak between 400°C and 650°C is attributed to the decomposition of organic matter. The curves during Phase II are virtually flat, and therefore the parameter Tmax cannot be reliably identified for sand and argillite.

Table 5.3. Total weight loss in relation to pyrolysis temperature using TGA. Tmax values marked -- could not be identified due to the virtually flat curves apparent for Phase II [17].

Samples	Weight Loss (wt%)			Total weight Loss (wt%)	Tmax (°C)
	W_A, Phase I (0-200°C)	W_B, Phase II (200-650°C)	W_C, Phase III (650-1200°C)		
Sand	--	--	--	0.9	--
Argillite	0.9	3.2	0.2	4.3	--
OOS1	6.2	14.7	10.0	30.9	440
OOS2	4.8	14.9	7.6	27.3	441
OOS3	6.3	16.0	9.0	31.3	440
CBl	0.4	13.6	21.0	35.0	450
CBr	0.1	8.6	21.7	30.0	446
QF1	0.8	1.0	2.5	4.3	--
QF2	1.6	2.5	7.5	11.5	--
QF3	6.5	7.0	9.5	23	--
MKK1	12.2	5.2	17.5	34.9	--
MKK2	12.7	5.8	16.7	35.1	--
SB	16.0	3.5	10.0	29.5	--
SR1	0.8	2.0	4.0	6.8	--
SR2	0.9	2.2	2.8	5.9	--
SR3	1.0	2.1	1.0	4.1	--
WFT1	4.9	10.5	5.7	21.1	465
WFT2	4.8	10.1	4.6	19.6	460
WFT3	4.8	10.1	4.6	19.5	460
WFAQ11	3.5	7.2	3.9	14.6	470
WFAQ12	4.1	7.2	3.1	14.4	465
WFAQ13	3.5	8.2	2.8	14.5	470
WFAQ21	3.7	6.0	1.5	11.2	455
WFAQ22	4.4	5.7	1.3	11.5	470
WFAQ23	4.7	8.2	1.7	14.6	460
WFOH31	8.2	7.0	0.8	15.9	470
WFOH32	8.5	5.1	2.4	16.0	470
WFOH33	8.8	6.0	0.7	15.5	460
Graphite	1.0	1.4	4.1	6.4	--

---

[17] All results in Table 5.3 are mean of six experiments with a maximum standard deviation of 0.1.

5.4.2 Green River Formation (CBl, CBr), Colorado

The TGA and DTA curves for the Green River Formation samples (CBl & CBr) are shown in Figure 5.6. The behaviour of the curves at various temperatures is similar, but the weight losses are different between the two samples at each of the defined phases of weight loss (Table 5.3).

There is no significant peak detection nor weight loss during Phase I for CBl and CBr (0.1-0.4 wt%) suggesting the absence of moisture in the samples. The weight loss during Phase II for CBl and CBr is approximately 13.6 wt% and 8.6 wt% respectively suggesting that the content of organic matter in CBl is higher than that in CBr. The weight losses during Phase III for CBl and CBr are 21 and 21.7 wt% respectively (Table 5.3). This indicates that the Green River Formation has a high carbonate content. The results for total extractable kerogen (weight loss during Phase II) and carbonate content in the current study are consistent with previous TGA analysis of the Green River Formation from the Mahogany Zone reported by Tiwari and Deo (2012). These authors determined that the weight loss during Phase II and Phase III was about 10-12 wt% and 25-30 wt% respectively.

The DTA profiles shown in Figure 5.6 demonstrate that the analysed samples of the Green River Formation exhibit a one-step thermal decomposition in the temperature region between 200°C and 650°C, representing single-stage thermal evolution of hydrocarbons (Williams & Ahmad, 2000). The Tmax values identified for CBl and CBr are 450°C and 446°C respectively. As the weight loss during Phase III for both CBl and CBr is high, a significant and distinguishable peak appears in this region (Figure 5.6).

The weight losses during Phase II for CBl and CBr are different to the results of the LOI study (Table 5.1). LOI is weight loss of a sample heated to 550°C in the presence of oxygen, while in TGA the sample is heated in an inert atmosphere at a certain heating rate and the weight loss (Phase II) is recorded between 200-650°C. Figure 5.6 describes a major phase of weight loss between 650°C and 720°C, ascribed to thermal decomposition of analcime. According to Likhacheva *et al*. (2004) the major weight loss due to analcime decomposition occurs between 550°C and 700°C. XRD analysis of

the raw samples confirmed the presence of analcime in the analysed shales of the Green River Formation.

Weight loss due to illite also contributes to the Phase II weight loss. The Phase II weight loss defined in the current study is consistent with the findings of Tiwari and Deo (2012) who worked on samples collected from the Mahogany Zone of the Green River Formation. These authors defined weight loss ascribed to kerogen to be about 10-12% of the initial weight in the temperature region 200-650°C. They suggested that weight loss due to the dehydroxylation of illite occurs in the temperature region 500-600°C. They further suggested that OH groups released during dehydroxylation react with organic matter catalysing organic matter decomposition. Tiwari and Deo (2012a) quantified weight loss of approximately 1 wt% over the temperature region 500-600°C. In the current study, weight loss over this temperature range was 2.2 wt% for CBl and 1.4 wt% for CBr (Figure 5.6). The presence of illite in both CBl and CBr was confirmed through the XRD analysis (Chapter 4, section 4.2.1.2). In contrast, Allred (1966) described weight loss from the Green River Formation in the temperature region 480-600°C to be the second step of kerogen decomposition in which bitumen is converted into the final products oil, gas and char. Clearly there is some degree of conjecture as to the exact mechanism for Phase II weight loss in the Green River Formation.
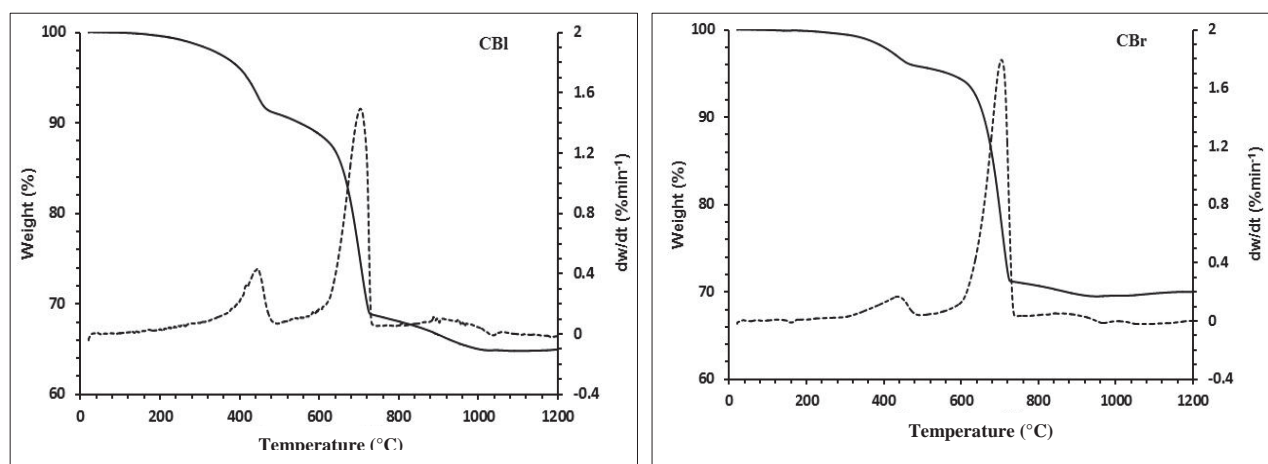
Figure 5.6. *Nonisothermal TGA (solid line) and DTA (dotted line) pyrolysis thermograms of samples of the Green River Formation, at 5°C min^{-1}*

5.4.3 Orepuki oil shale (OOS1, OOS2, OOS3)

TGA and DTA analysis of the Orepuki oil shale samples (OOS1, OOS2, and OOS3) shows similar weight loss behaviour in each sample across the isothermal temperature range (Figure 5.7). The quantified weight losses during Phase I, II and III for the three Orepuki oil shale samples are 4.8-6.3 wt% , 14.7-16 wt% and 7.6-10 wt% respectively.

The differential curves show a significant peak during Phase I (0-200°C) (Figure 5.7) which is attributed to the weight loss due to the moisture content of samples. Two peaks are observed during the second phase of weight loss suggesting a two-step evolution of hydrocarbon volatiles from the oil shale. This two-step decomposition of kerogen has also been observed by other researchers working on different oil shales; for example the Jordanian oil shale (Khraisha, 1998), Moroccan oil shale (Thakur & Nuttall Jr, 1987), Turkish oil shale (Kok & Pamir, 2000) and Pakistani oil shales (Williams & Ahmad, 1999). From the DTA curve of each of the Orepuki oil shale samples, a similar Tmax value of approximately 440°C is defined (Table 5.3).
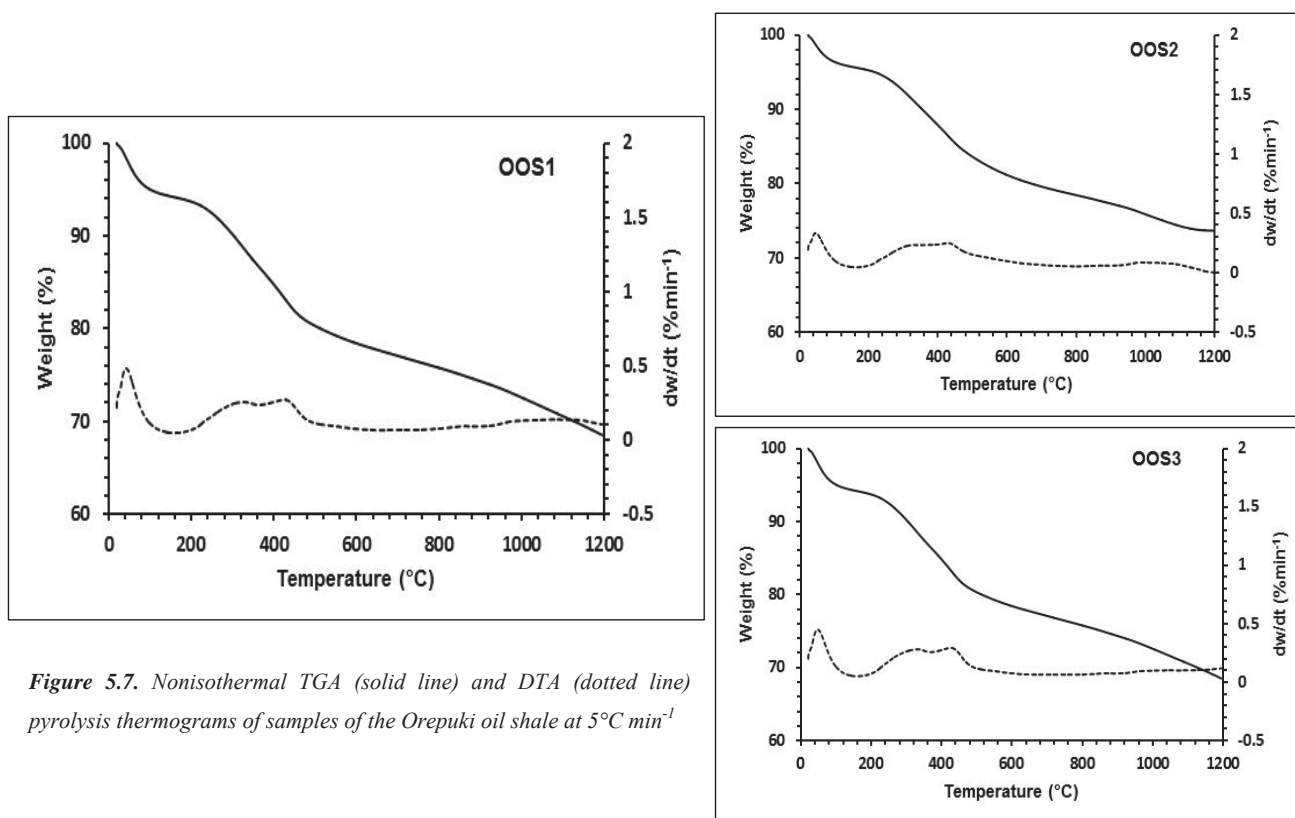
Figure 5.7. Nonisothermal TGA (solid line) and DTA (dotted line) pyrolysis thermograms of samples of the Orepuki oil shale at 5°C min^{-1}

5.4.4 Qianjiang Formation samples (QF1, QF2, QF3)

The TGA and DTA profiles of QF1, QF2 and QF3 are shown in Figure 5.8. Samples QF1 and QF2 show similar profiles, but that of QF3 is very different. The TGA profiles of QF1 and QF2 do not define distinct regions of weight loss as evidenced by a continuous loss of weight with temperature from 25-1200°C. The TGA profile of QF3, however, shows three distinct regions of weight loss.

The quantified weight loss during Phase I for samples QF1 (0.8 wt%) and QF2 (1.6 wt%) is low relative to QF3 (6.5 wt%) (Table 5.3). A similar pattern is apparent for Phase II; that for QF3 (7 wt%) is greater than that for QF1 (1 wt%) and QF2 (2.5 wt%). Samples QF2 and QF3 have a higher carbonate loss (Phase III) relative to QF1.

From the DTA profiles of QF1 and QF2, no Phase II peak is apparent. This is due to the very low weight loss during this phase. Based on the DTA profiles, the conclusion can be reached that both QF1 and QF2 contain no organic matter. However, a low intensity peak during Phase II can be observed for QF3 suggesting the presence of some organic matter. As the curves during Phase II are virtually flat, Tmax values cannot be reliably determined.

The weight loss during Phase III for QF1, QF2 and QF3 samples is 2.5-9.5 wt%. However from LECO combustion analysis, it can be observed that there is very little difference between the TC and TOC values (Table 5.2) suggesting the presence of only small amount of carbonates (any difference between TC and TOC in LECO combustion is attributed to the presence of carbonates). Hence the continuous weight loss in the TGA spectra from 0°C to 1200°C suggests the presence of post mature organic matter or inert carbon. To confirm this theory, a sample of graphite was analysed. The thermal parameters of graphite were LOI 6.3 wt%; TOC 9.6 wt%; and using TGA, total continuous weight loss was 6.4 wt%. Also weight loss behaviour (TGA curve) of graphite is similar to the Qianjiang Formation samples (Figure 5.8). Consideration of the data for graphite confirms that the organic matter present in the Qianjiang Formation samples is post mature, with minimal hydrocarbon content.
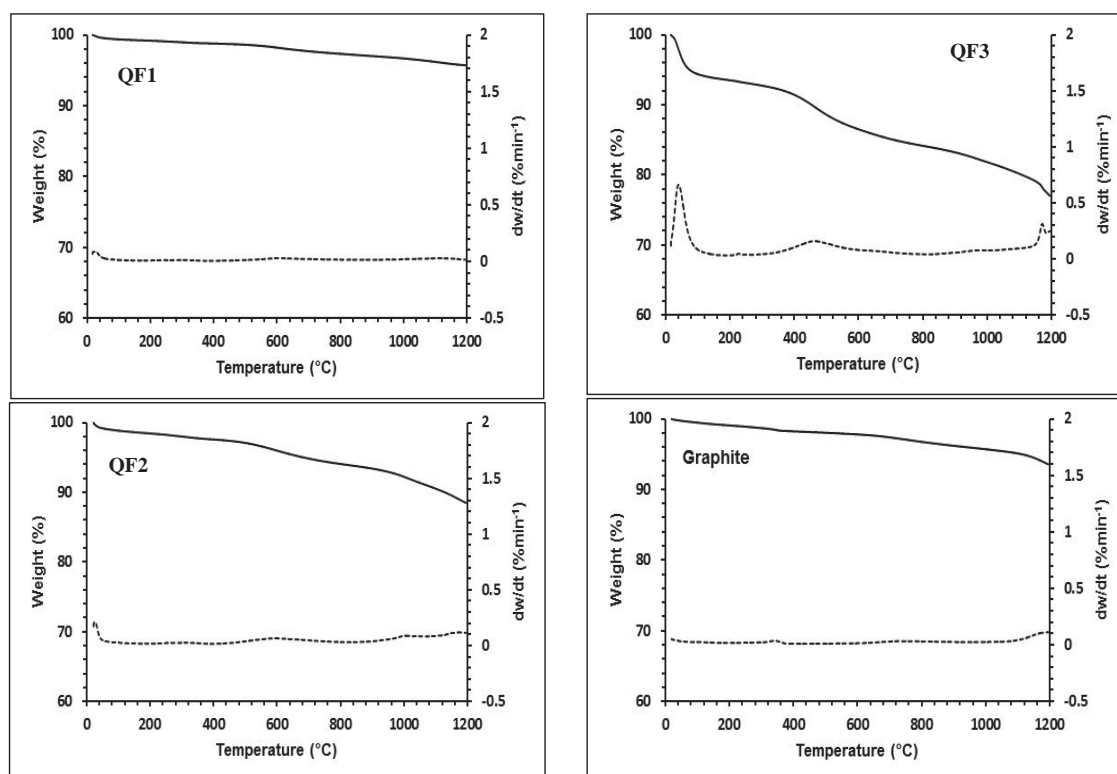
Figure 5.8. *Nonisothermal TGA (solid line) and DTA (dotted line) pyrolysis thermograms of the Qianjiang Formation samples and graphite, at 5°C min^{-1}*

5.4.5 Mir Kalam Kala oil shale (MKK1, MKK2), Pakistan

The TGA curves for MKK1 and MKK2 (Figure 5.9) show three distinct phases of weight loss, that associated with Phase III (17 wt%) being high relative to Phase I (12.5 wt%) and Phase II (5.5 wt%) (Table 5.3). The quantified weight losses during Phase II, due to organic matter decomposition, for both MKK1 and MKK2 are low compared to the respective weight losses during Phase I and Phase III.

The DTA profiles of MKK1 and MKK2 show very low intensity peaks apparent due to organic matter decomposition during Phase II (Figure 5.9). This is due to the very low weight loss due to organic content during this phase. As the curves during Phase II are virtually flat, Tmax values cannot be identified reliably.
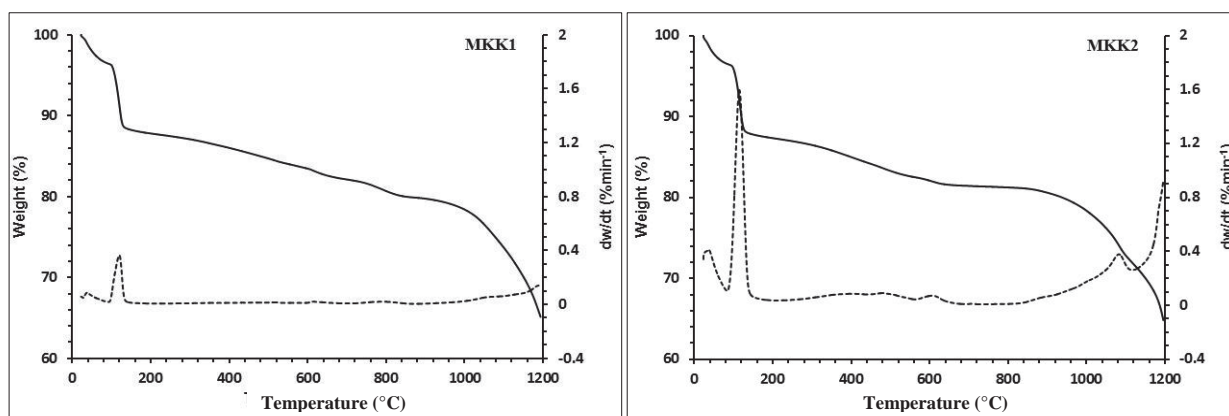
Figure 5.9. *Nonisothermal TGA (solid line) and DTA (dotted line) pyrolysis thermograms of the Mir Kalam Kala oil shale, at 5°C min^{-1}*

5.4.6 Speena Banda oil shale (SB), Pakistan
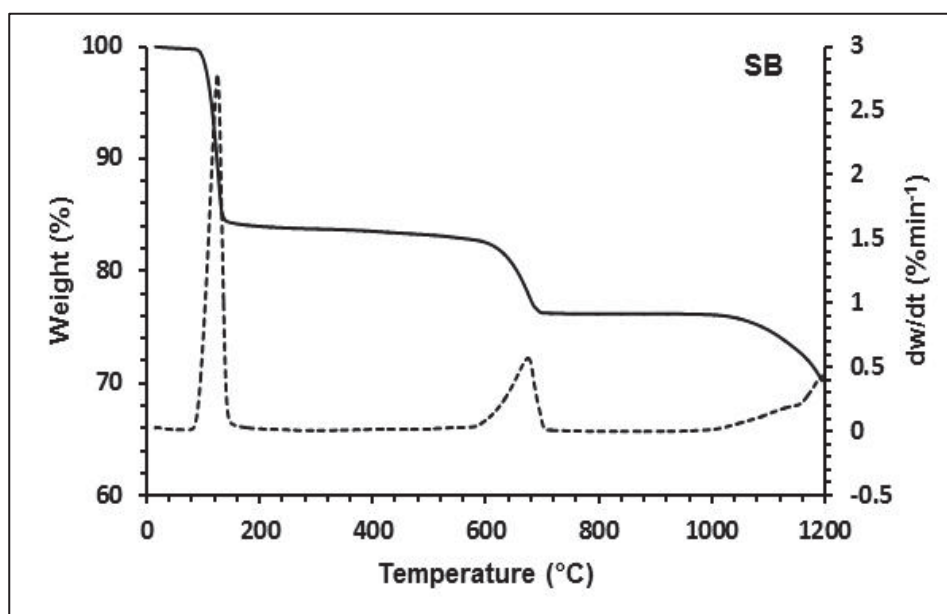
Figure 5.10. *Nonisothermal TGA (solid line) and DTA (dotted line) pyrolysis thermograms of the Speena Banda oil shale, at 5°C min^{-1}*

The TGA and DTA curves for the single sample collected from the Speena Banda sample (SB) shows three distinct phases of weight loss (Figure 5.10), with weight losses during Phase I and Phase III being dominant (16 wt% and 10 wt% respectively). The Phase II weight loss for this samples is relatively low (3.5 wt%) (Table 5.3), a value that is very close to the Phase II weight loss defined for the low-carbon reference rock argillite (3.2 wt%) (Table 5.3). Hence it can be suggested that this is a low potential source rock.

From the DTA profile of the Speena Banda oil shale, no peak is apparent due to organic matter decomposition during Phase II. This is due to the very low weight loss in this Phase. As the curve during Phase II is virtually flat, Tmax values cannot be identified reliably.

5.4.7 Salt Range oil shale (SR1, SR2, SR3), Pakistan

The TGA profiles for each of the Salt Range shale samples do not clearly define distinct phases of weight loss (Figure 5.11). However, DTA analysis of the data quantifies the extent of weight loss for each phase (Table 5.3).

Weight loss during Phase I is 1 wt% across the three samples. Weight loss during Phase II is also consistent across the three samples, at approximately 2 wt% of the initial weight. However, weight loss during Phase III highlights some differences between the samples; 4 wt% for SR1, 2.8 wt% for SR2 and 1 wt% for SR3. The weight loss during Phase II for the Salt Range shale in this study is very low relative to argillite (Table 5.3) suggesting the presence of low organic matter.

From the DTA curves only a single low intensity peak can be observed for SR1 and SR2 in the temperature region 520-620°C suggesting a one-step decomposition of the organic matter. However, a two-stage thermal decomposition associated with a weight loss of approximately 22 wt% over the 200-600°C temperature region was reported by Williams and Ahmad (1998), (1999) and (2000) for the Salt Range oil shale. As the peaks have very low intensity, Tmax values are difficult to reliably quantify.
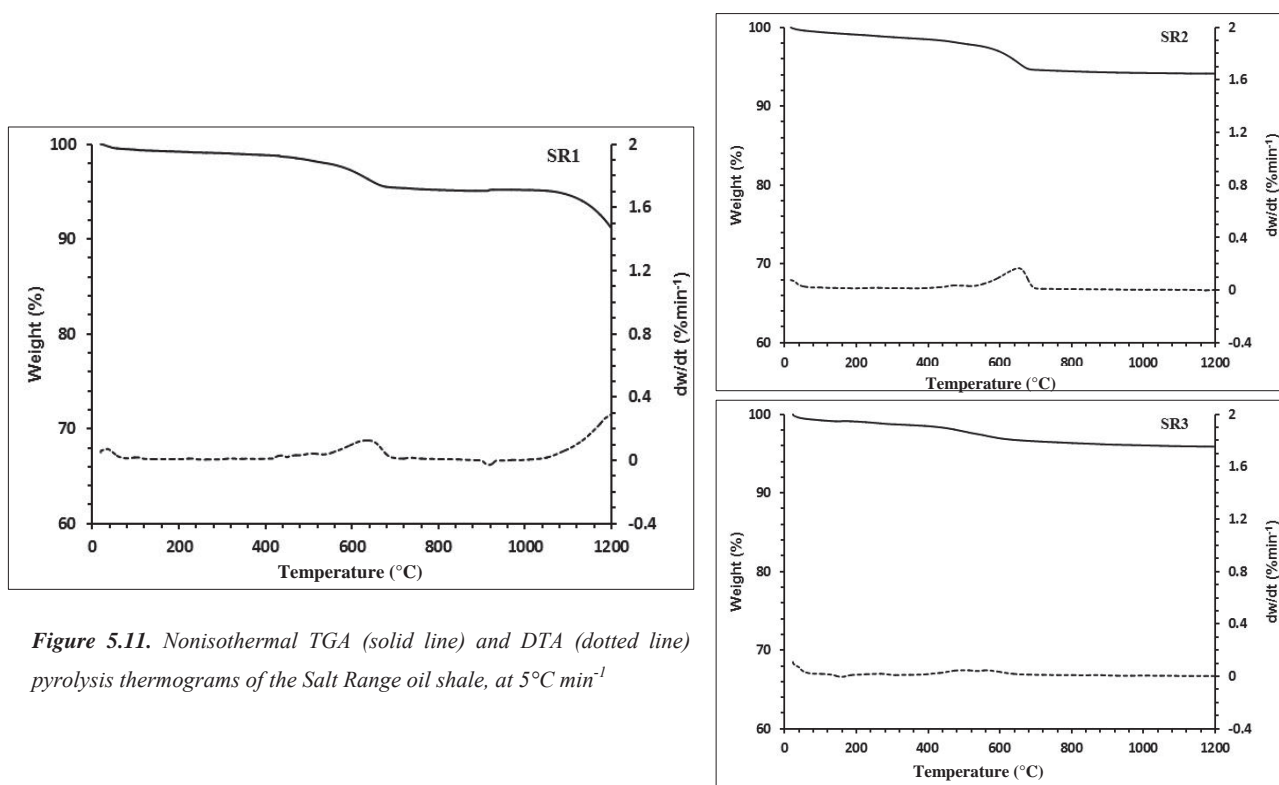
Figure 5.11. *Nonisothermal TGA (solid line) and DTA (dotted line) pyrolysis thermograms of the Salt Range oil shale, at 5°C min^{-1}*

5.4.8 Waipawa Formation

The TGA and DTA curves for the Waipawa Formation samples (Figures 5.12a, 5.12b, 5.12c, 5.12d) from the four different outcrops show three distinct phases of weight loss. The weight loss during Phase I for samples from the Waipawa type locality, Lower Angora Road quarry and Upper Angora Road are similar, but lower than the samples from Porangahau (Old Hill Road) (Table 5.3). The phase II region of weight loss in these samples is the dominant region of weight loss. The recorded weight loss during Phase II varies between the outcrops and also between the samples collected from the same outcrop (Table 5.3). The greatest Phase II weight loss occurs in samples from the Waipawa type locality (10 wt%). In contrast, the lowest value of Phase II weight loss is for the Porangahau, Old Hill Road sample (6 wt%) (Table 5.3). A variation in weight losses during Phase II is observed between samples collected from Lower Angora Road quarry, Upper Angora Road and Old Hill Road, Porangahau (Table 5.3). These variations in weight loss are regarded as being due to natural variability in organic content within the same outcrop. Weight losses attributed to mineral decomposition as quantified during Phase III also show the greatest magnitude for samples collected from the Waipawa type locality, with the lowest values for the Porangahau, Old Hill Road samples.

The DTA profiles of the Waipawa Formation samples (Figures 5.12a, 5.12b, 5.12c, 5.12d), show that with the exception of samples from the Waipawa type locality, the Waipawa Formation generally exhibits two peaks, or a peak with a shoulder, associated with weight loss during Phase I. Weight loss below 100°C from the Waipawa Formation is high relative to the other oil shales analysed in this study, and could be due to a high adsorbed water content of montmorillonite (Frost *et al.*, 2000) which is present in the Waipawa Formation (Chapter 4, section 4.2.1.3). The interlayer water of montmorillonite is lost between 100°C and 250°C (Deer & Howie, 1966). Illite and kaolinite are the common clay minerals in the other rocks of the current study. Weight loss observed between 100°C and 200°C is interpreted by Borrego *et al*. (2000) as likely due to the volatilisation of hydrocarbons trapped in mineral matter. The single peak during Phase II for all the Waipawa Formation samples could be attributed to either a one-step thermal decomposition of kerogen (Williams & Ahmad, 1999), or may be associated with the decomposition of minerals (Borrego *et al.*, 2000). A low intensity peak attributed to Phase III for all Waipawa Formation samples suggests the presence of a very low level of carbonates in the Waipawa samples.
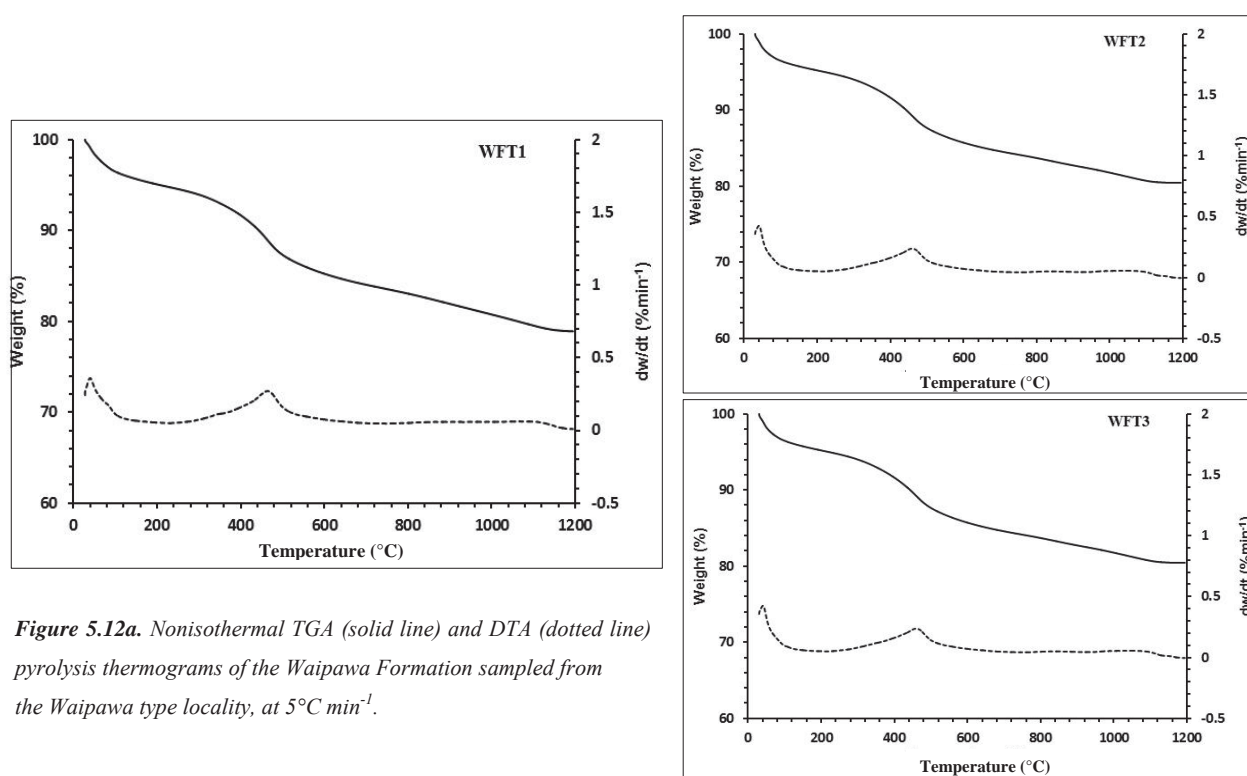
Figure 5.12a. Nonisothermal TGA (solid line) and DTA (dotted line) pyrolysis thermograms of the Waipawa Formation sampled from the Waipawa type locality, at 5°C min^{-1}.
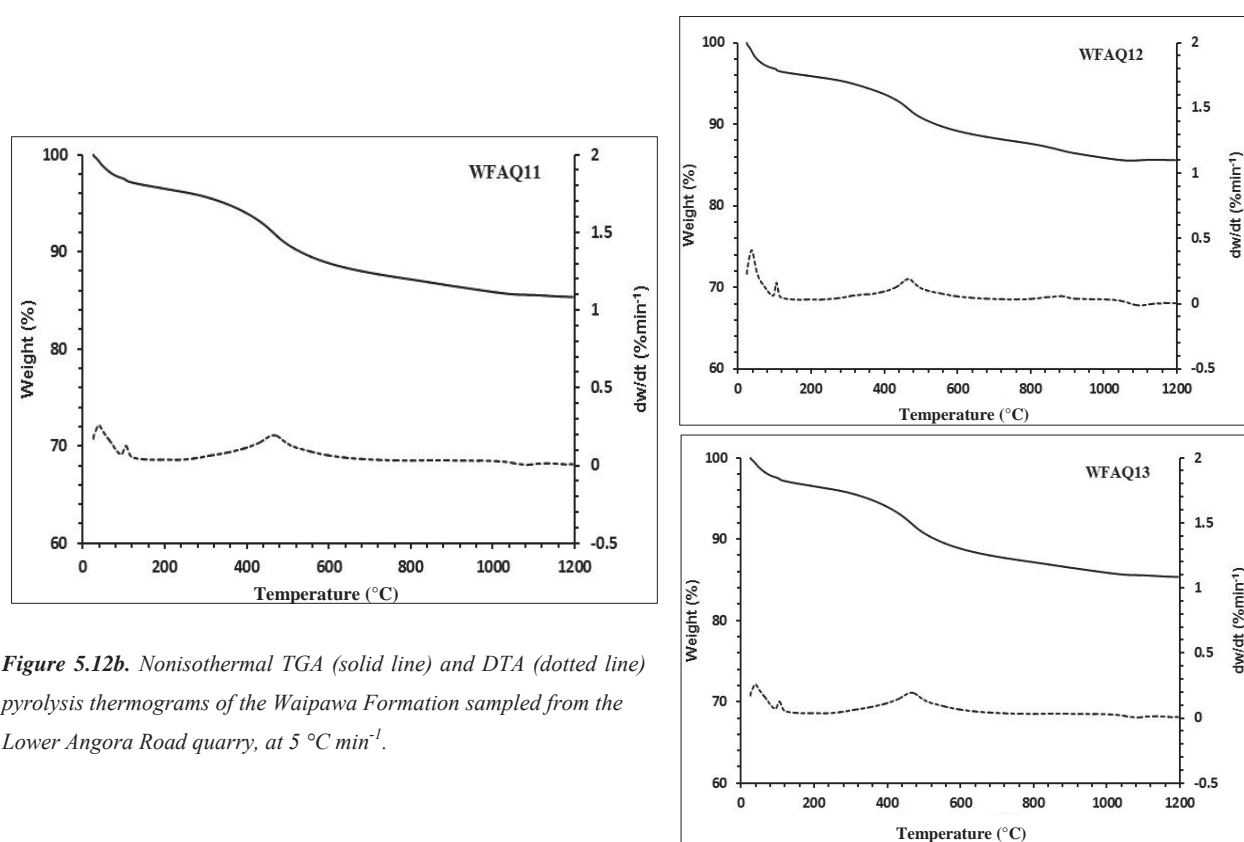
Figure 5.12b. Nonisothermal TGA (solid line) and DTA (dotted line) pyrolysis thermograms of the Waipawa Formation sampled from the Lower Angora Road quarry, at 5 °C min^{-1}.
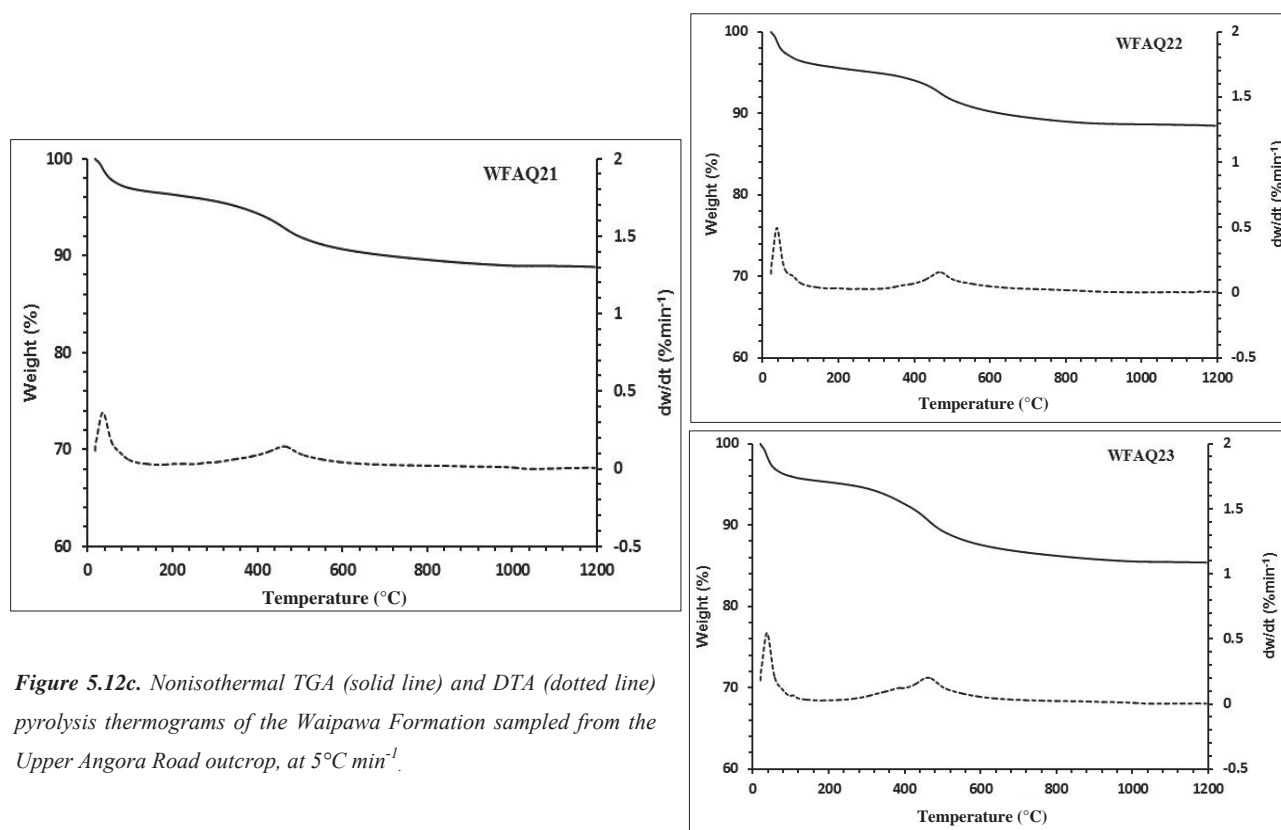
Figure 5.12c. *Nonisothermal TGA (solid line) and DTA (dotted line) pyrolysis thermograms of the Waipawa Formation sampled from the Upper Angora Road outcrop, at 5°C min⁻¹.*
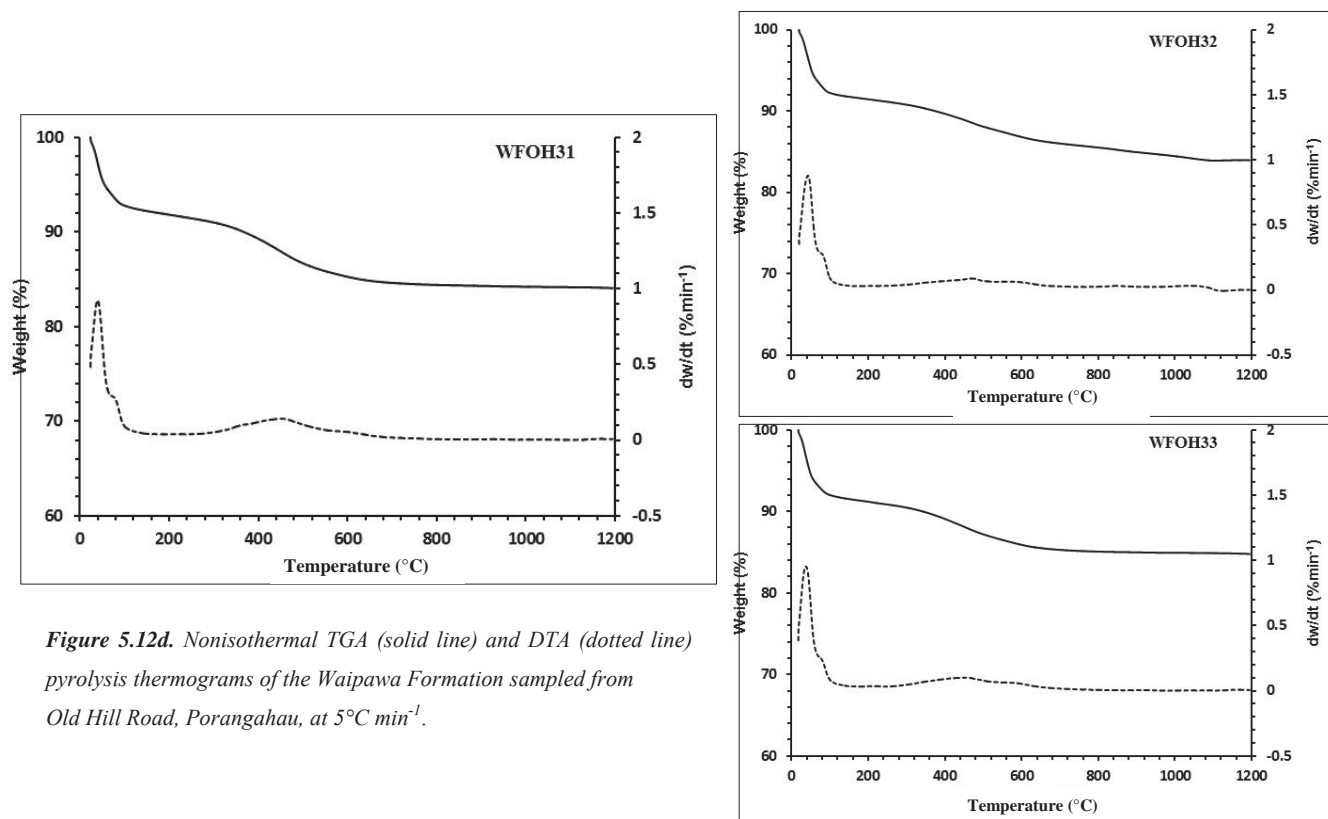
Figure 5.12d. Nonisothermal TGA (solid line) and DTA (dotted line) pyrolysis thermograms of the Waipawa Formation sampled from Old Hill Road, Porangahau, at 5°C min^{-1}.

5.5 Comparative discussion

The thermal data obtained through analysis of the rocks of this study by TGA allows for ranking of the samples based on Phase II weight loss (W_B), which can be mainly attributed to the loss of hydrocarbons, and decreases in the order:

Orepuki oil shale> Green River Formation> Waipawa type locality> Lower Angora Road quarry > Upper Angora Road> Porangahau, Old Hill Road> Mir Kalam Kala> Speena Banda> > argillite> Salt Range> sand

This ordering is in general terms for the purpose of this discussion. There are some data overlaps between some of the samples. The reason for these overlaps is that the weight loss in Pahse II which is mainly attributed to the loss of hydrocarbons can include some other weight losses due to mineral matter and carbonates as well. The Qianjiang Formation samples (QF1, QF2 and QF3) have similar thermal characteristics to graphite, therefore these are not considered in the ranking above. The weight losses during Phase II of the Qianjiang Formation samples are not consistent with their LOI and TOC results. The LOI and TOC values of the Qianjiang Formation samples are very high relative to their weight loss during Phase II of the TGA analysis.

Weight loss during Phase II (W_B) vs LOI

The TGA Phase II weight losses (W_B) of Waipawa Formation from Porangahau Old Hill Road, Mir Kalam Kala and Speena Banda samples do not follow the same pattern of decreasing as their LOI decreases. The LOI of Mir Kalam Kala and Speena Banda samples are very high relative to the weight loss during Phase II of the TGA analysis (Table 5.1, 5.3). The XRD analysis of MKK1, MKK2 and SB samples (Chapter 4) showed the presence of gypsum. The major weight losses in these samples occur during Phase I and Phase III and are attributed predominantly to the dehydration of gypsum (100-300°C) (Bhargava *et al.*, 2005; Deer & Howie, 1966) and decomposition of anhydrite (above 800°C) respectively (Ingo *et al.*, 1998). Thus gypsum dehydration (0-300°C) is contributing to the higher LOI values of MKK1, MKK2 and SB. As the

organic matter within the Qianjiang Formation samples is inert (section 5.4.4), combustion of these samples during LOI gives a higher weight loss as compared to the weight loss during Phase II in an inert atmosphere.

A correlation of R^2 = 0.72 is observed between the weight loss in Phase II (WB) and LOI (Figure 5.13a). The Speena Banda and Qianjiang Formation samples do not fit this correlation and the data points for these samples are anomalous to the data points for other samples in the study (Figure 5.13a)
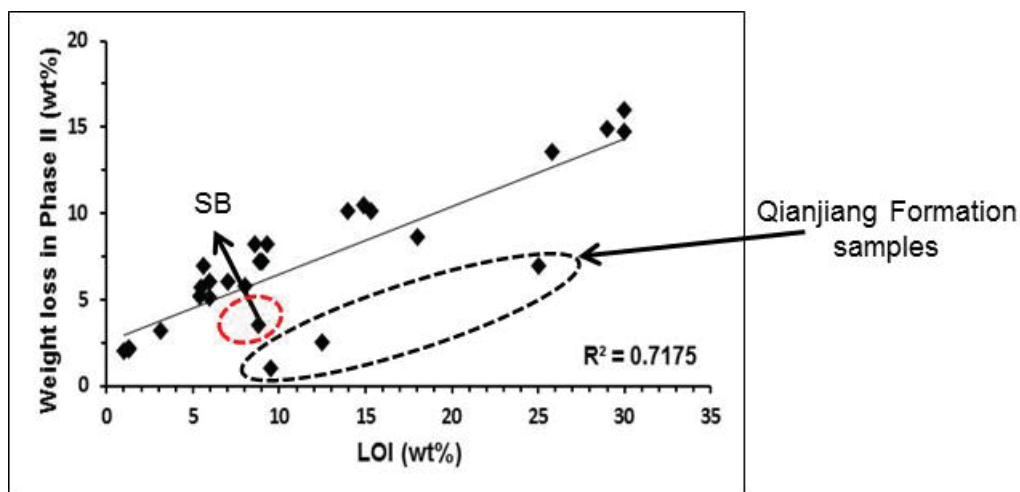
Figure 5.13a. *Correlation graph between the weight losses during Phase II from the TGA analysis and LOI of all samples of this study except sand.*

Due to the post mature nature of the Qianjiang Formation samples and the presence of gypsum on the SB sample, these samples appear very different on this bivariate plot (Figure 5.13). When the Speena Banda and Qianjiang Formation samples are removed from the plot and correlation of W_B and LOI is recalculated, (Figure 5.13b), the correlation is improved (R^2 = 0.94).
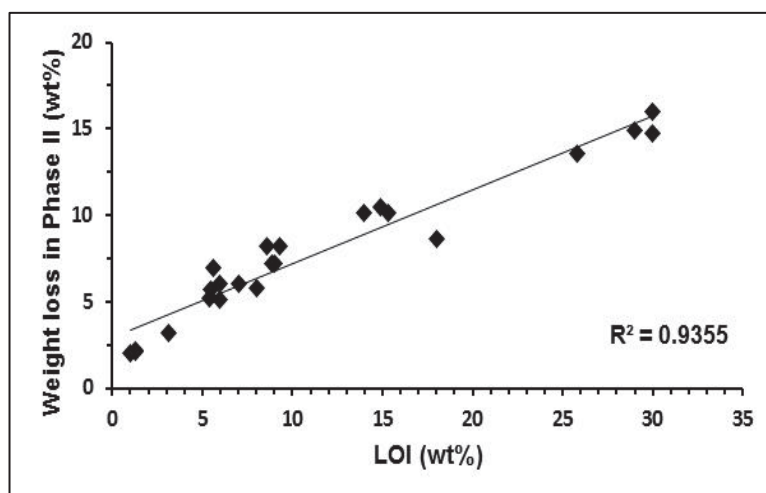
Figure 5.13b. Correlation graph between the weight losses during Phase II from the TGA analysis and LOI of samples of this study except the Qianjiang Formation, Speena Banda oil shale and sand.

Weight loss during Phase II (W_B) vs LECO analysed TOC

A very weak correlation (R^2 = 0.44) is observed between the weight loss in Phase II (W_B) and LECO analysed TOC (Figure 5.14a). The Qianjiang Formation samples do not fit this correlation and the data points for these samples are anomalous to the data points for the other samples in the study.
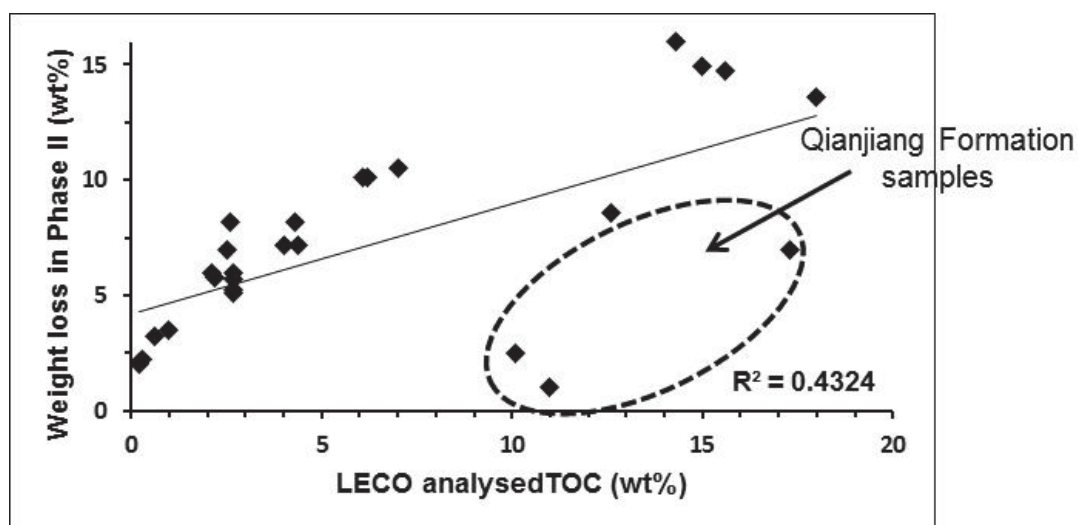
Figure 5.14a. Correlation graph between the weight losses during Phase II from the TGA analysis and LECO analysed TOC of all the samples of the study except sand.

Due to the post mature nature of the Qianjiang Formation samples, these samples appear very different on the bivariate plot (Figure 5.14a). When the Qianjiang Formation samples are neglected and the TOCs of the rest of the samples in the study are plotted against W_B (Figure 5.14b), the correlation is improved ($R^2 = 0.86$).
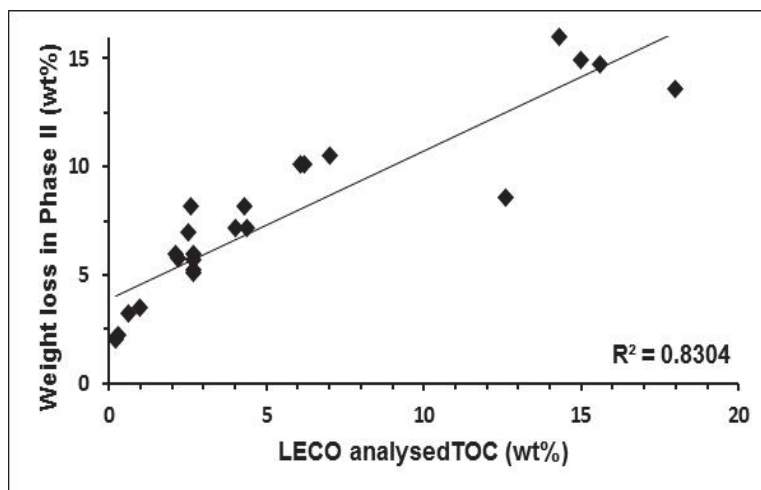
Figure 5.14b. *Correlation graph between the weight losses during Phase II from the TGA analysis and LECO analysed TOC of samples of the study except the Qianjiang Formation samples and sand.*

Weight loss in Phase II is not purely due to loss of organic matter and loss of hydrocarbons. Weight loss in this region can also be due to changes in the mineral component of a sample (Jiang *et al.*, 2007). For example, CBl, has a low weight loss during Phase II relative to the Orepuki oil shale samples (OOS1, OOS2, OOS3) (Table 5.3) but its TOC value is higher than the TOC values of the Orepuki samples (Table 5.2). Similarly the weight losses during Phase II of the WFAQ13 and WFAQ23 samples are almost similar to that for the brown rock of the Green River Formation (CBr) (Table 5.3). However, the TOC values of these samples are very low relative to CBr (Table 5.2). The reason for this anomaly might be the greater weight loss due to mineral matter (dehydration and dehydroxylation) in the Waipawa Formation samples (WFAQ13, WFAQ23) as compared to CBr.

The difference between weight loss in Phase II in CBr and MKK1 is 39.5% and that between CBr and MKK2 is 32.5%. However the difference between the TOCs of CBr and MKK1 is 71.6% and that between CBr and MKK2 is 76.8%. The reason for this discrepancy is the presence of gypsum in the Mir Kalam Kala samples as confirmed through XRD analysis (Chapter 4). Weight loss owing to gypsum dehydration (100-300°C) also contributes to weight loss during Phase II (200-600°C) and will therefore increase weight loss during Phase II that will appear to be due to organic matter decomposition (Bhargava *et al.*, 2005; Deer & Howie, 1966). Hence TGA should be performed in conjunction with TOC to estimate a reliable content of organic matter in source rock.

Weight loss during Phase III vs total inorganic carbon

The correlation between total inorganic carbon (which is calculated as the difference between total carbon (TC) and total organic carbon (TOC) from the LECO analysis) and weight loss during Phase III (the third stage of decomposition above 650°C) is very weak ($R^2 = 0.50$) (Figure 5.15). According to the LECO protocol used in the current study, total carbon is measured for raw samples and TOC is measured for acid washed samples. Therefore the difference between TC and TOC is the percentage of inorganic carbon due to carbonates. However Phase III weight loss is not solely due to the decomposition of carbonates. This weight loss is actually attributed to the continued pyrolysis of organic material within the oil shale and also to the decomposition of mineral matter (Jaber & Probert, 2000). This weight loss in Phase III can also be attributed to the possibility that CO_2 present (which is evolved as a result of carbonate decomposition) is reacting with the residual char and forming carbon monoxide (Jaber & Probert, 2000; Watanabe *et al.*, 2013). Therefore the weak correlation between the two data sets is logical.

Figure 5.15. Correlation graph between the weight loss during Phase II (TGA) and LECO- analysed total inorganic carbon[18] of all the samples in the study except sand.

The Pakistani rock samples have low contents of inorganic carbon (Table 5.2) which are inconsistent with the higher weight losses during Phase III for these samples (Table 5.3). High weight losses for the Mir Kalam Kala and Speena Banda samples are attributed to the decomposition of anhydrite (above 800°C) (Ingo *et al.*, 1998). Similarly the Green River Formation and Orepuki oil shale samples have higher weight losses in Phase III as opposed to the amount of inorganic carbon present in these samples. These higher weight losses may be due the continued pyrolysis within these samples after 650°C. Also in the CBl and CBr, analcime decomposition may occur between 550°C and 700°C making the Phase III weight losses (>650°C) in these samples very high relative to the amount of inorganic carbon (Table 5.2). The QF1, QF2 and QF3 samples have a very low content of total inorganic carbon (Table 5.2). But due to the presence of inert carbon in these samples, continued decomposition of the organic material occurs with an increase in temperature within the TGA.

---

[18] $(Total\ inorganic\ Carbon = TC - TOC)$

TGA (W_B) vs SRA (S1+S2)

When weight losses during Phase II (W_B) are compared with the S1+S2 data from SRA (Chapter 3, Table 3.1), there is a very weak correlation ($R^2 = 0.46$) (Figure 5.16). The Qianjiang Formation samples are losing weight continuously in the TGA but their S1+S2 values are very low due to minimal hydrocarbon content. The parameter W_B for CBr (8.6 wt%) is less than WFT1 (10.5 wt%), but its S1+S2 (65.2 mg HC/g rock) is very high relative to that for WFT1 (13.4 mg HC/g rock) (Table 3.1, Table 5.3). Similarly, the Orepuki oil shale sample (OOS1) has a W_B of 14.7 wt% which is only slightly higher than that of CBl (13.6 wt%), but its S1+S2 is very low (36.7 mg HC/g rock) relative to that of CBl (152.5 mg HC/g rock).
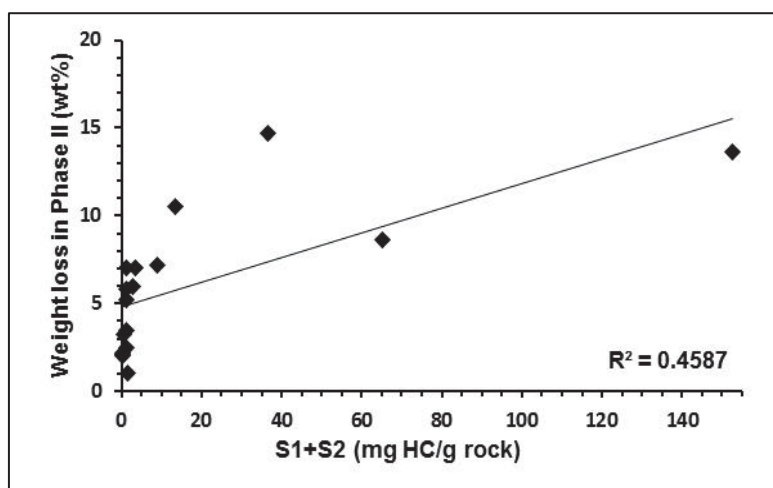
Figure 5.16. Correlation graph between the weight loss during Phase II (TGA) and S1+S2 from SRA, of all the samples in the study except sand.

The reason for this anomaly is that, W_B, which is mainly attributed to the loss of organic matter, can be associated with other weight losses due to mineral matter present. From the photo micrographs of the Orepuki oil shale, some higher-plant cork and wood tissues were apparent in this sample (Chapter 4, section 4.3.1.3). The higher weight loss in the organic matter decomposition region in this oil shale might be due to weight loss of these higher-plant cork and wood tissues. From XRD analysis no minerals were

identified that could have contributed to higher weight loss during TGA Phase II. Based on the data presented here, a conclusive explanation for the observed higher weight loss during Phase II of this oil shale cannot be given.

TGA (Tmax) vs SRA (Tmax)

The Tmax values quantified by TGA (Table 5.3) and SRA (Table 3.1) are different for each of the samples analysed in the current study. This is because the SRA S2 peak (from which Tmax is derived) is measuring a different analyte to that being measured by TGA. In TGA, Tmax is the temperature at which maximum devolatilisation occurs (weight loss due to dehydroxylation of minerals, decomposition of organic matter, loss of CO and CO_2 and other O- and S-containing compounds) in the Phase II (200-650°C) region of weight loss (Borrego *et al.*, 2000). However, in SRA, Tmax is the temperature at which the maximum rate of hydrocarbon generation occurs (section 3.2.1.2). The pyrolysis conditions (final temperature, heating rate, pyrolysis atmosphere and flow rate) vary between the two analytical techniques. Different pyrolysis conditions can cause a shift in the value for Tmax. For example Wang *et al.* (2013) observed a shift in Tmax from 453 to 519°C with an increase in heating rate from 2 to 50°C min^{-1}.

When the Tmax values determined from the TGA are compared with the Tmax values determined from the SRA (Chapter 3, Table 3.1), there is a moderate (R^2 = 0.68), inverse relationship between the two data sets (Figure 5.17). The heating rate was different between the two techniques (25°C min^{-1} and 5°Cmin^{-1} for SRA and TGA respectively). However, differences in the pyrolysis conditions were constant and do not explain the variability to the relationship described in Figure 5.17. Correlation of Tmax for SRA and TGA suggests that some factor other than pyrolysis conditions is the main cause of differences between the two sets of results. The inverse relationship and the underlying reason for the difference between the two parameters cannot be explained from the current data set and should be further investigated.
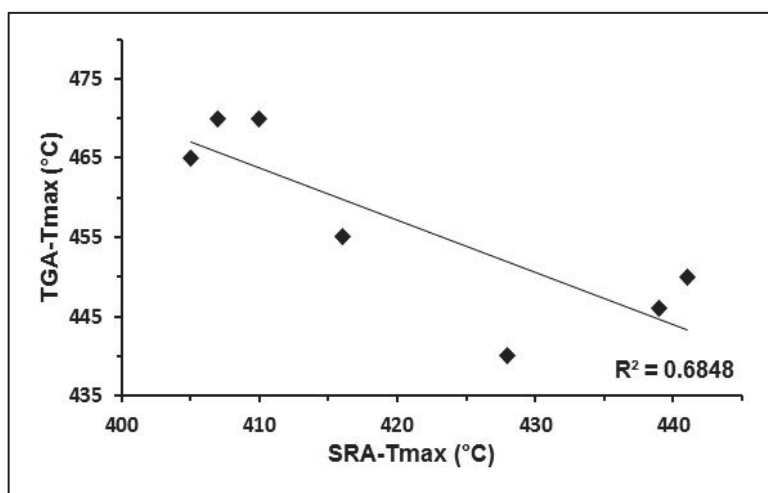
Figure 5.17. *Correlation graph between the Tmax from TGA and the Tmax from SRA, of the Colorado oil shale, Orepuki oil shale and Waipawa Formation samples in the study.*

Conclusion

The TGA data reported in this chapter, supported by the TOC values, establishes that the Green River Formation and Orepuki oil shales, with relatively high organic matter, have production potential. The Qianjiang Formation samples on the other hand have high TOC values but no distinct region of weight loss that can be attributed to organic matter decomposition. The results from LECO and TGA of graphite were found to be similar to those of the Qianjiang Formation samples. The Qianjiang Formation samples are therefore interpreted to be post-mature samples with no production potential. The Pakistani oil shales have high LOI values but low TOC and weight loss during Phase II of the TGA spectra. Thus the Pakistani shales are suggested to have no production potential. Sampling of the Waipawa Formation from multiple outcrops showed that the Waipawa Formation is a heterogeneous formation with the different facies having different production potentials. Shale rock collected from the Waipawa type locality shows a production potential similar to the Green River Formation considering the thermal data presented in this chapter.

Thermogravimetric Analysis (TGA) is used to accurately calculate the weight change in a sample as a function of increasing temperature at a certain heating rate, to determine the characteristics of devolatilisation and to investigate the different weight loss regions as the pyrolysis temperature increased. As the slope of the TGA curve (expressed as DTA) changes in different regions of weight loss, it provides a better estimation of the amount of organic matter present than LOI. However TGA analysis should be performed in conjunction with LECO combustion analysis to provide a better estimation of the organic content of a sample.

Chapter 6 – Chemical Analyses

6.1 Introduction

The quality of an oil shale can be evaluated through analysis of its constituent amount and types of kerogen and bitumen, and through quantification of the evolutionary stage of kerogen, otherwise known as its maturity (Tissot & Welte, 1978b). Bitumen is defined by Durand (1988) and Dyni (2003) as that part of the organic matter in oil shales which is soluble in organic solvents and contains "free" hydrocarbons, asphaltenes and resins that formed during geological processes. Hydrocarbons are the main constituents of bitumen and they are formed when organic matter within sedimentary rocks is altered under raised temperatures and raised pressures (Yang *et al.*, 1997). Kerogen, on the other hand, is insoluble in organic solvents but can be extracted by thermal cracking and pyrolysis (Al-Harasheh, 2011). The type and quantity of organic matter present in sedimentary rocks determine the source potential for hydrocarbons, while the extent of thermal evolution or the burial of sediment, both processes that lead to temperature increase, determine the generation potential for hydrocarbons (Tissot & Welte, 1978a). In this chapter an organic geochemical investigation of the various reference shales, reference samples and New Zealand shales is presented. This chapter discusses the extraction of the bitumen phase of organic matter using a solvent, Fourier Transform Infrared (FTIR) spectroscopy characterisation of the solvent extracts, and identification of various hydrocarbons in the extracts by gas chromatography mass spectrometry (GC-MS).

The bitumen phase of the organic matter was specifically selected for study in this research due to the existence of published methods to extract bitumen from rock using organic solvents. Processing produces a clean extracted bitumen sample that is suitable for geochemical investigation using FTIR and GC-MS. Specifically, the process of solvent extraction leaves behind mineral constituents that might produce complicating interferences during geochemical studies. Furthermore, the bitumen content of an oil

shale is useful because Peters and Cassa (1994) have used it, together with TOC, to estimate the thermal maturity and petroleum potential of source rocks (Table 6.1).

Table 6.1. Bitumen to TOC ratio describing the level of thermal maturation. After Peters and Cassa (1994).

Stage of thermal maturity for oil	Bitumen/TOC(LECO)
Immature	<0.05
Mature	
Early	0.05-0.10
Peak	0.15-0.25
Late	--
Post mature	--

6.2   Solvent extraction using the soxhlet apparatus

Organic solvent extraction using the soxhlet apparatus is a common and reliable procedure for the extraction of bitumen from oil shales and has been used in several previous studies (Altun, 2009; Razvigorova *et al.*, 2008; Wolfson *et al.*, 2011). The extraction yield (Y), depends on the solubility of the bitumen in the solvent. The physical and chemical properties of an organic solvent define its ability to dissolve or break bonds based on electron donor-acceptor interactions and hydrogen bonding. The polarity of the solvent is another factor which affects its ability to dissolve organic matter (He *et al.*, 2012; Wolfson *et al.*, 2011). The structure and composition of an oil shale (Bonder & Koel, 1998) and porosity of the shale are other parameters that affect extraction yields (Wolfson *et al.*, 2011). Different authors have used different solvents for extracting bitumen from oil shale. For example, Blanco *et al*. (1992) used carbon disulphide, pyridine, chloroform and dichloromethane and reported extraction yields from the Puertollano (Spain) oil shale. These authors showed that there was no significant difference between the yields obtained using different solvents under

conditions of soxhlet extraction. However, Wolfson *et al.* (2011) found that the extraction yields from two different Israeli oil shales decreased in the order:

Chloroform>ethanol>methanol>hexane

Al-Harasheh (2011) studied the effects of different types of solvent on the yield and fractional composition of bitumen in the Middle Eastern El-lajjun and Sultani oil shales. He found that extraction yields decrease in the order:

Chloroform> toluene> hexane> ethanol

Al-Harasheh's studies also showed that the percentages or fractional composition of different organic compounds in the solvent extract is affected by the polarity and structure of the solvent.

Dichloromethane (DCM) was selected for use in the present study due to the common use of chlorinated solvents reported in the literature, and the reported ability of this solvent to produce consistent results. Dichloromethane has very similar solvent properties to chloroform (Blanco *et al.*, 1992).

The soxhlet extraction yields of different oil shale samples, sand and argillite are shown in Figure 6.1 and tabulated in Table 6.2. The extraction yield, Y, is calculated by

$$Y = [(W - I)/W] * 100,$$

where W is weight of the oil shale, I is the weight of the insoluble material.
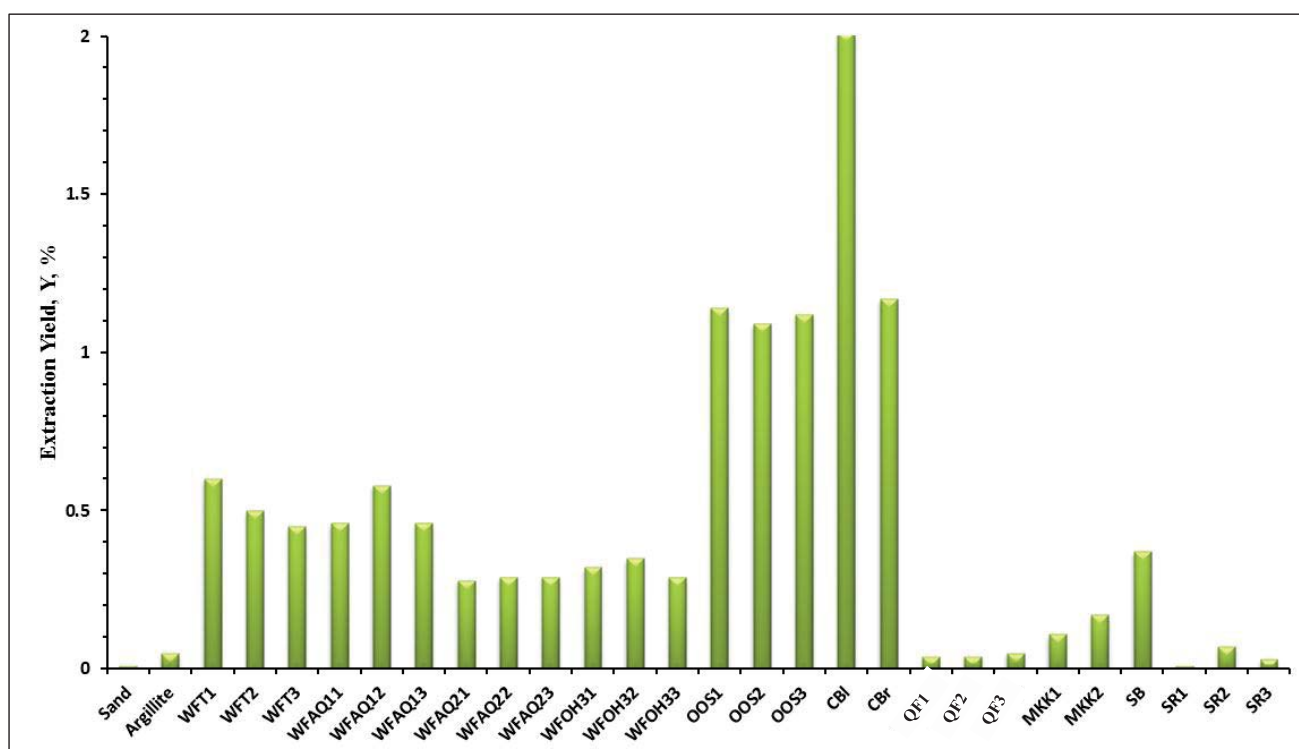
Figure 6.1. Solvent extraction yields from different oil shale samples, sand and argillite (samples are identified in Chapter 2, section 2.2, Table 2.1).

Table 6.2. Bitumen yield and yield to TOC ratios providing an index of thermal maturity for the rocks of the current study. The stage of thermal maturity is defined using the criteria of Peter and Cassa (1994) (Table 6.1).

Samples	Bitumen Yield, Y (wt%)	TOC (wt%) (LECO combustion)	Y/TOC	Stage of thermal maturity for oil
Sand	--	--	--	--
Argillite	0.05	0.6	0.08	Early-mature
OOS1	1.14	15.6	0.07	Early-mature
OOS2	1.09	15	0.07	
OOS3	1.12	14.3	0.08	
CBl	2.01	18.5	0.11	Early-mature
CBr	1.17	9.5	0.12	
QF1	0.04	11	0.00	--
QF2	0.04	10.1	0.00	
QF3	0.05	17.3	0.00	
MKK1	0.11	2.7	0.04	Immature
MKK2	0.17	2.2	0.08	Early-mature
SB	0.20	1	0.20	Peak-mature
SR1	0.01	0.2	0.05	Early-mature
SR2	0.07	0.3	0.23	Peak-mature
SR3	0.03	0.2	0.15	
WFT1	0.60	7	0.08	Early-mature
WFT2	0.50	6.2	0.08	
WFT3	0.45	6.1	0.07	
WFAQ11	0.46	4.4	0.10	Early-mature
WFAQ12	0.58	4	0.14	
WFAQ13	0.46	4.3	0.11	
WFAQ21	0.28	2.7	0.10	Early-mature
WFAQ22	0.29	2.7	0.11	
WFAQ23	0.29	2.6	0.11	
WFOH31	0.32	2.5	0.13	Early-mature
WFOH32	0.35	2.7	0.13	
WFOH33	0.29	2.1	0.14	

The results in Figure 6.1, Table 6.2 show that the Orepuki and Colorado oil shales samples have the highest bitumen extraction yields. The black rock from the Green River Formation has a greater bitumen yield than the brown rock. The Waipawa Formation samples have an average bitumen yield <0.60% which is very low compared to both the Orepuki oil shale and Colorado oil shale, but is greater than the Qianjiang Formation samples and Pakistani oil shale samples. Among the Waipawa oil shale samples, the samples collected from the Waipawa type locality have a greater average bitumen yield than samples from Lower Angora Road quarry, Upper Angora Road and Old Hill Road outcrops.

As bitumen in sedimentary rocks is formed from organic matter during geological processes when the organic matter is altered under increasing temperature and increasing pressure (Dyni, 2003; Yang *et al.*, 1997), the amount of bitumen can be related to maturity and depth of burial and also related to how organic matter is distributed through the rock (Tissot & Welte, 1978d). Peter and Cassa (1994) proposed a relationship between bitumen content and thermal maturity of source rocks (Table 6.1). An index of maturity is therefore inferred based on the Y/TOC using the TOC from the LECO analysis. The grade of maturity of sand, argillite and the Salt Range samples is unreliable because they have very low TOC and bitumen yield levels. The grade of maturity of the Qianjiang Formation samples is also unreliable, not due to their TOC values but because their bitumen yield is low.

According to Table 6.2 only the Speena Banda rock was identified to be at the peak of maturity (Table 6.1, 6.2). This sample is defined as being at the peak of oil maturation based in its yield parameter. However, this result is anomalous as the sample contains a very low TOC (1%). At such a low TOC, the Speena Banda sample cannot be a source rock. Hence it appears that an assessment of the stage of thermal maturity may not be reliable for rocks with a TOC less than approximately 2 wt%.

6.3 Fourier Transform Infrared spectroscopy, FTIR

Spectra obtained from FTIR allow for qualitative analysis of the elemental bonds that exist in a sample. With respect to the oil shale and rock samples examined in this chapter, absorption bands on the FTIR spectra of the solvent extracts identify the terminal functional groups in the hydrocarbons extracted by the solvent. For all the FTIR spectra obtained in the current study, a 'base line correction'[19] was performed using OMNIC software (Thermo Electron Corporation, 1992).

6.3.1 Various FTIR absorption bands and their proposed assignments

The absorption bands at 2920 cm^{-1} and 2850 cm^{-1} correspond to the aliphatic CH stretching vibrations of asymmetric and symmetric methylene compounds respectively (Borrego, 1996; Khraisha *et al.*, 2003; Pavia *et al.*, 2001; Sharma *et al.*, 2004; Silverstein *et al.*, 1963). The absorption band at 1700 cm^{-1} corresponds to C=O stretching vibrations from carboxyl and carbonyl groups (Ibarra *et al.*, 1996; Qing *et al.*, 2011). This band at 1700 cm^{-1} is more likely due to the carboxylic acid group if there is also an absorption band in the region 1280-1315 cm^{-1}, which is partly due to C−O stretching and O−H bending of carboxylic acid (Silverstein *et al.*, 1963). According to Silverstein *et al.* (1963), the band in the region 1280-1315 cm^{-1} is due to the C−O stretching band and usually appears as a doublet in the spectra of long chain fatty acids. Pradhan and Sandle (1999) has a similar correlation/interpretation for the bands at 1707 cm^{-1} and 1290 cm^{-1}. The band at 1630 cm^{-1} is due to C=C stretching vibrations of aromatic groups and C=O stretching vibrations of carbonyl groups (Altun, 2009). The band at 1470 cm^{-1} is due to the C−H bending vibrations of CH_3 and CH_2. The band at 1370 cm^{-1} belongs to the C−H bending vibrations of methyl groups (Petersen *et al.*, 2008; Silverstein *et al.*, 1963). C–H bands between 837-800 cm^{-1} and at 730 cm^{-1}

---

[19] A spectra manipulation technique used to flatten the base lines of spectra with sloped or varying baselines and make it equal to zero. This resets the Y-axis scale to 0-100%.

provide evidence for the degree of aromaticity in a bitumen sample (Radlinski *et al.*, 2004; Sharma *et al.*, 2004; Uden *et al.*, 1978).

6.3.2 FTIR spectra of sand and argillite

The FTIR spectrum of the sand extract shows no bands (Figure 6.2). This is consistent with no extraction of organic matter into the solvent. The FTIR spectrum of the argillite extract has absorption bands at around 2919 cm^{-1} and 2850 cm^{-1} as shown in Figure 6.2. These correspond to aliphatic asymmetric and symmetric C−H vibrations of methylene compounds respectively (see Table 6.3) (Borrego, 1996; Khraisha *et al.*, 2003; Sharma *et al.*, 2004; Silverstein *et al.*, 1963). The band at about 1470 cm^{-1} corresponds to the CH bending vibrations of CH$_3$ and CH$_2$ (Pavia *et al.*, 2001).
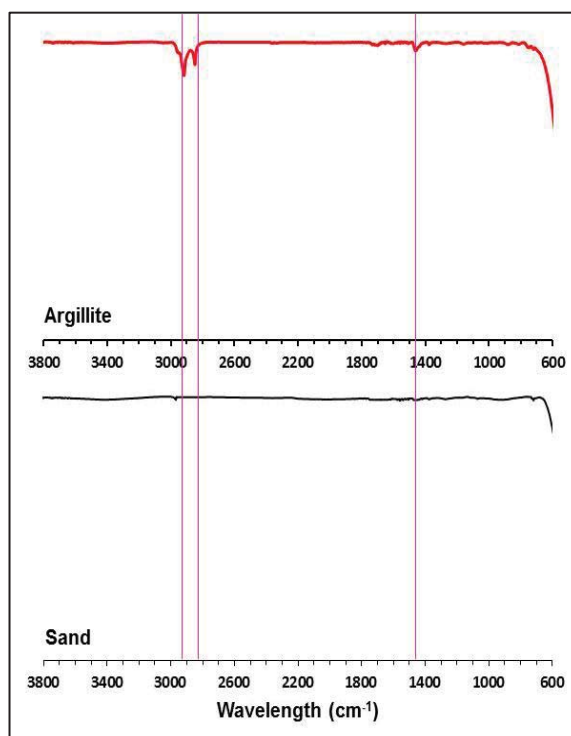
Figure 6.2. *FTIR spectra of the solvent extract from sand and argillite. The Y-axes of the sand and argillite Y-axis scale is 0-100%.*

Table 6.3. FTIR bands positions for sand, argillite, Orepuki oil shale, Green River Formation, Qianjiang Formation and Pakistani oil shale samples (√: identified and --: not identified).

Wavenumbers (cm^{-1})	Proposed assignment	1	2	3	4	5	6	7	8	9	10	11	12	13	14	15	16
3400	O—H stretch intermolecular bonding	--	--	--	--	--	--	--	--	--	--	--	--	--	--	--	--
2920 & 2850	CH asymmetric and symmetric CH$_2$ stretching	--	√	√	√	√	√	√	√	√	√	√	√	√	√	√	√
1750	C=O of unsaturated ester	--	--	√	√	√	--	--	--	--	--	--	--	--	--	--	--
1700	C=O stretch of aliphatic ketone, or carboxylic acid	--	--	√	√	√	√	√	√	√	√	√	√	√	√	√	√
1630	Aromatic C=C stretching and C=O stretching vibrations of carbonyl groups	--	--	√	√	√	√	√	--	--	--	--	--		--	--	--
1510	Aromatic C=C ring stretching; Naphthalene; Phenanthene; C=C in-plane thiophene	--	--	√	√	√	--	--	--	--	--	--	--	--	--	--	--
1470	CH bending vibrations of CH$_3$ and CH$_2$	--	√	√	√	√	√	√	√	√	√	√	√	√	√	√	√
1370	CH bending of CH$_3$	--	--	√	√	√	√	√	√	√	--	√	√	√	√	√	√
1260/weak	C−H bending vibrations of alkynes or monosubstituted alkynes	--	--	√	√	√	--	--	--	--	--	√	√	√-	--	√	--
1260/strong	C−O stretching vibration of esters of aromatic acids	--	--	--	--	--	--	--	--	--	--	--	--	--	--	--	--
1170	C−O stretching in phenols, aliphatic ether	--	--	√	√	√	√	√	--	--	--	--	--	--	--	--	--
1115	Aromatic C−H deformation	--	--	--	--	--	√	√	--	--	--	--	--	--	--	--	--
1030	C−OH stretching due to primary or secondary alcohol	--	--	√	√	√	√	--	--	--	--	√	--	--	--	√	√
1010	C=C stretch; CCO stretch	--	--	--	--	--	√	√	--	--	--	--	--	--	--	--	--
837-800	Out-of-plane aromatic CH bend with two hydrogen atoms	--	--	--	--	--	√	√	--	--	--	--	--	--	--	--	--
730	Out-of-plane aromatic CH bend with four hydrogen atoms	--	--	√	√	√	√	√	--	--	--	--	--	--	--	√	√

*1: Sand, **2** Argillite, **3**: OOS1, **4**: OOS2, **5**: OOS3,**6**: CBl, **7**: CBr, **8**: QF1, **9**: QF2, **10**: QF3, **11**: MKK1, **12**: MKK2, **13**: SB, **14**:SR1, **15**: SR2, **16**: SR3*

6.3.3 FTIR spectra of Orepuki oil shale, Green River Formation, Qianjiang Formation and Pakistani oil shale samples

The Orepuki oil shale samples (OOS1, OOS2 and OOS3) all display similar FTIR spectra to each other, as shown in Table 6.3. A strong band at about 1750 cm^{-1} is probably related to the the C=O stretching in esters (K. N. Alstadt *et al.*, 2012; Sharma *et al.*, 2004; Wang *et al.*, 2009). A band identified at 1510 cm^{-1} in the Orepuki oil shale samples is explained as being due to aromatic C=C stretching, and this band is absent from all other samples in the study. The Green River Formation samples (CBl and CBr) also have similar spectral band positions to each other. Bands related to aliphatic structures at 2920, 2850, 1700, 1470, 1370 and 1168 cm^{-1} are identified in this Formation. In the FTIR spectra of the Qianjiang Formation (QF1, QF2 and QF3) and Pakistani oil shale samples (MKK1, MKK2, SB, SR1, SR2 and SR3) only aliphatic CH bands at 2920, 2850, 1470 and C=O stretching bands of aliphatic ketone or carboxylic acid at about 1700 cm^{-1} are identified (Table 6.3, Figures 6.5-6.8) suggesting the non-aromaticity and very low organic matter content of these oil shales. Band associated with aliphatic CH bending of CH$_3$ at 1370 cm^{-1} has been identified for all the Pakistani samples except SB. The conclusion from FTIR reported here is in agreement with other experimental work (LOI, LECO, and TGA) in this study. The band at about 1700 cm^{-1} identified in all the Orepuki, Green River Formation, Qianjiang Formation and Pakistani oil shale samples reveals the humic character of the oil shales. These absorption bands are dominant in both the Colorado and Orepuki samples, but less so in the other samples. The SB sample shows a band at 1700 cm^{-1} along with an absorption band at 1290 cm^{-1} suggesting the presence of carboxylic acid. Also there is band at ~1410 cm^{-1} in the SB spectrum which is associated with alkenes (Figure 6.7). The Green River Formation samples have successive aromatic bands at 1630, 1115, 1030, 1010, 837-800 and 730 cm^{-1} indicative of high organic matter content or an indication of the intense aromaticity of the constituent bitumen (Mongenot *et al.*, 1999; Radlinski *et al.*, 2004; Sharma *et al.*, 2004; Uden *et al.*, 1978). Some of the aromatic bands at 1630, 1510, 1030 and 730 cm^{-1} are also identified in the Orepuki oil shale samples.

Figures 6.3-6.8 show certain trends in the FTIR spectra that are apparent in each of Orepuki, Green River Formation, Qianjiang Formation, and Pakistani oil shale samples.

The spectra of all oil shale samples are dominated by aliphatic bands (CH_3+CH_2) at about 2920 and 2850 cm^{-1} and the deformation bands of methyl (1370 cm^{-1}) except SB and methyelene groups (CH_3+CH_2, 1470 cm^{-1}). The aliphatic hydrogen content related to these bands (2920, 2850, 1470 and 1370 cm^{-1}) seems to decrease from those with highest soxhlet yield to those with very low or almost no yield in the order:

Green River Formation> Orepuki> Mir Kalam Kala> Speena Banda> Qianjiang Formation> Salt Range

The signature of C═O structures also tends to decrease in the same order as above. The bands related to aromatic structures in the zone 700-1100 cm^{-1} are more intense for the Orepuki oil shale samples as compared to the Colorado oil shale samples. No bands related to aromatic structures are observed in the Qianjiang Formation, Mir Kalam Kala and Speena Banda samples, except very weak aromatic band at ~730 cm^{-1} is observed in the SR1 and SR2 samples.

The ordering of the samples described here has been made according to apparent peak intensities. This is not a quantitative rank. However quantitative ranking of FTIR data is possible as suggested by Guillen & Cabo (1997) and Vlachos *et al.* (2006). For the purpose of the current study quantitative ranking was not performed; the purpose of using FTIR in this work is to identify the presence or absence of specific functional groups that are attributable to hydrocarbons. However, quantification of the FTIR bands could be a useful area for future development of the model.

Of the Qianjiang Formation samples, sample QF1 has more intense absorption bands relative to QF2 and QF3 (Figure 6.5). In the spectra for Speena Banda and Mir Kalam Kala, the bands for Speena Banda are more intense than Mir Kalam Kala. In the Salt Range oil shale samples, SR2 has very intense bands relative to SR1 and SR3. However, the intensity of these bands is very low relative to the Green River Formation and Orepuki oil shale. A weak and broad band in SR2, MKK1, MKK2 and Orepuki oil shale samples is identified at about 1260 cm^{-1} which is indicative of C−H bending vibrations of alkynes or monosubstituted alkynes (Figure 6.3, 6.6, 6.8).
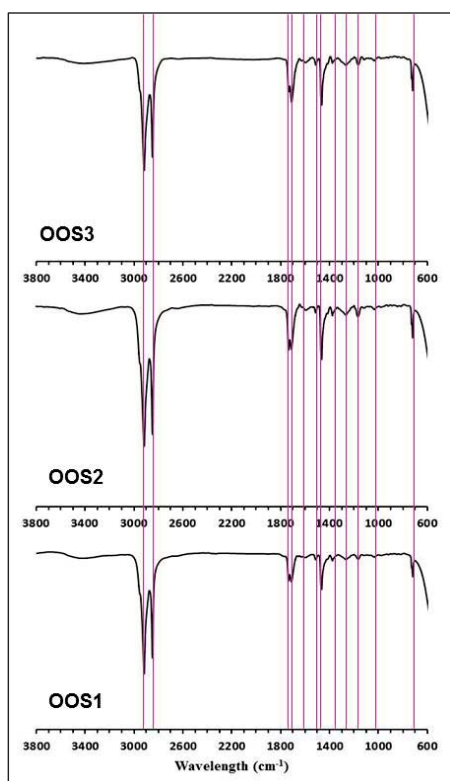
Figure 6.3. *FTIR spectra of the Orepuki oil shale*

Note: All Y-axes are 0-100%
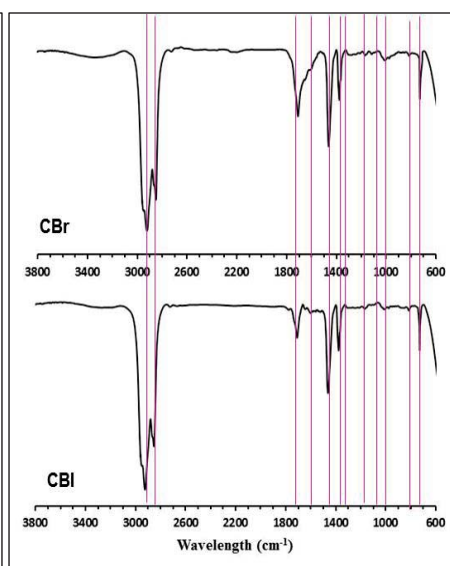
Figure 6.4. *FT-IR spectra of the Colorado oil shale*
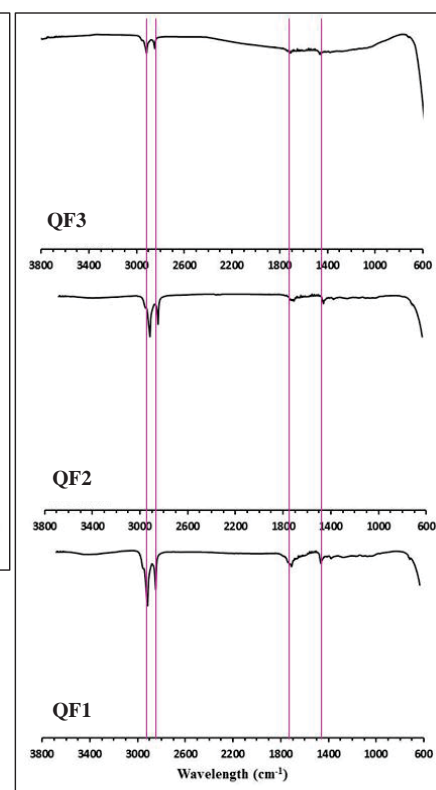
Figure 6.5. *FTIR spectra of the Qianjiang Formation*
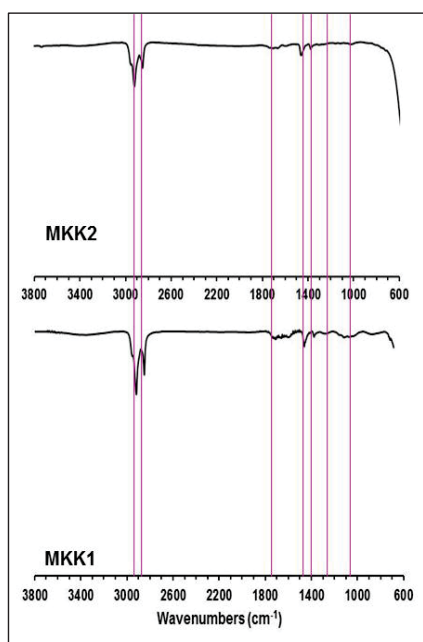
Figure 6.6. *FTIR spectra of the Mir Kalam Kala oil shale*
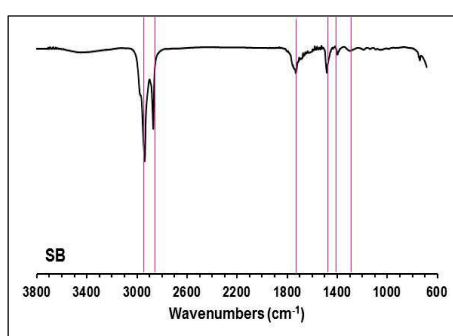
Figure 6.7. *FTIR spectra of the Speena Banda oil shale*
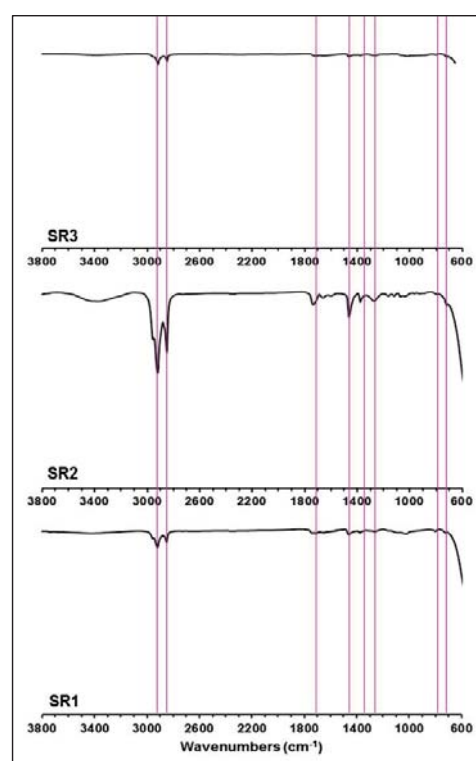
Figure 6.8. *FTIR spectra of the Salt Range oil shale*

Note: All Y-axes are 0-100%.

6.3.4 FTIR spectra of the Waipawa Formation samples

The FTIR spectra of the Waipawa Formation samples from the Waipawa type locality (WFT1, WFT2 and WFT3) (Figure. 6.9) display similarities to each other. However, differences are evident when the intensities of the bands are compared. Similarly, the FTIR spectra of Waipawa Formation samples from Lower Angora Road quarry (WFAQ11, WFAQ12 and WFAQ13) (Figure. 6.9) are also similar to each other but differ in band intensities. The various bands in WFAQ12 are very prominent relative to WFAQ11 and WFAQ13. Also in WFAQ12 the band at about 1260 cm^{-1} is strong and assigned to C−O stretching vibration of esters of aromatic acids. But in WFAQ11 and WFAQ13 this band at 1260 cm^{-1} is weak. Sample WFAQ12 also shows an extra band at 730 cm^{-1} attributed the aromatic CH bend. The spectra of the Waipawa Formation samples collected from Upper Angora Road (WFAQ21, WFAQ22, and WFAQ23) (Figure. 6.9) are similar when the bands positions and intensities are compared. Samples WFAQ21, WFAQ22 and WFAQ23 have two very prominent bands at 1265 and 730 cm^{-1} attributed to the C−O stretching vibration of esters of aromatic acids, and to aromatic C−H vibration respectively. The spectra of samples from the Old Hill Road, Porangahau (WFOH31, WFOH32 and WFOH33) are almost the same (Figure 6.9), having low intensity bands when compared to the spectra of the other Waipawa Formation samples.

Among the samples from the different outcrops of the Waipawa Formation, the aliphatic hydrogen content related to bands at 2920, 2850, 1470 and 1370 cm^{-1} seems to be variable suggesting variability in organic content of the Waipawa Formation. The relative intensities of the bands varies between samples collected from different outcrops, but there is also some variability in the intensities of the bands between samples collected from different points within the same outcrop. The band intensities related to aromatic structures (in the zone 700-1100 cm^{-1}) also varies between samples collected from different outcrops and from different points within the same outcrop (Table 6.4).
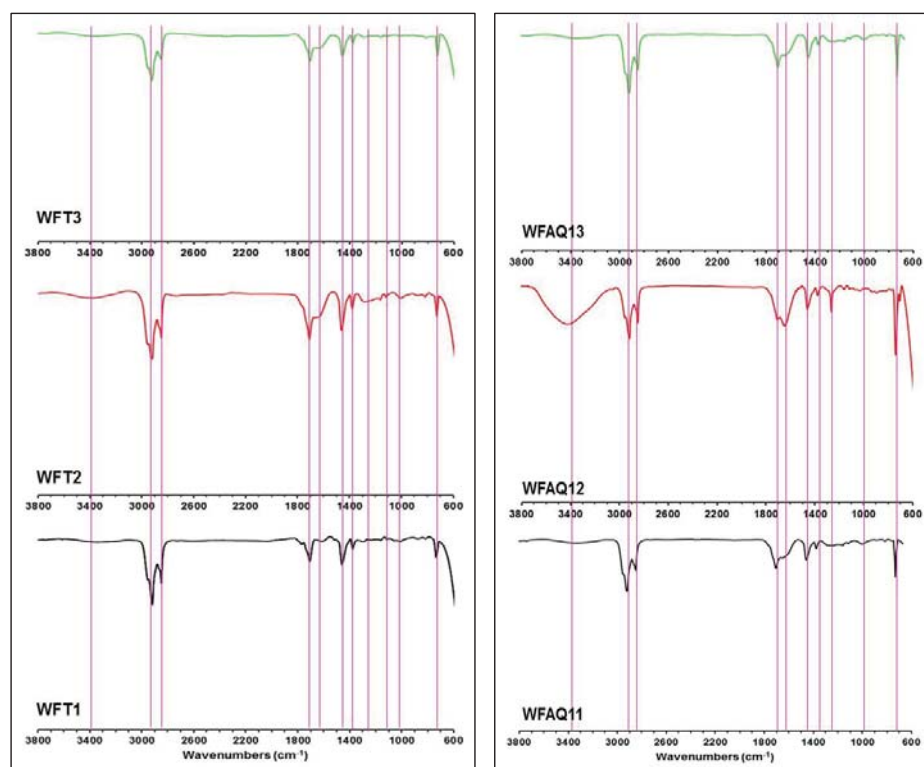
Figure 6.9. FTIR spectra of the Waipawa Formation from the Waipawa type locality and the Lower Angora Road quarry. All Y-axes are 0-100%.
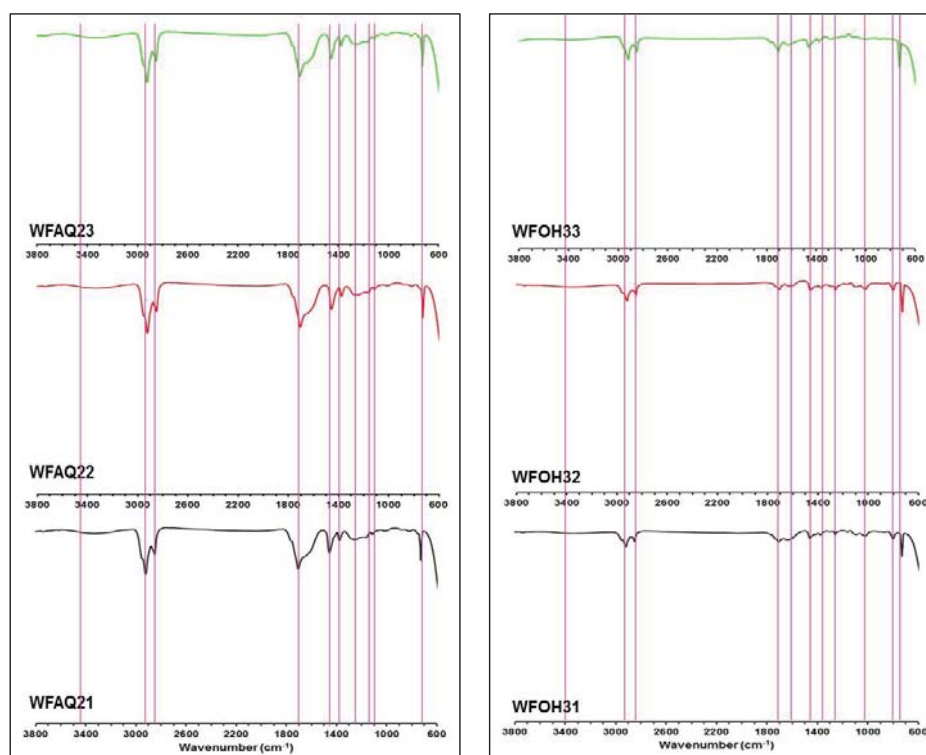
Figure 6.10. FTIR spectra of the Waipawa Formation from the Upper Angora Road and the Old Hill Road (Porangahau). All Y-axes are 0-100%.

Table 6.4. FTIR absorption bands positions of the Waipawa Formation samples (√: identified and --: not identified).

Wavenumbers (cm^{-1})	Proposed assignment	17	18	19	20	21	22	23	24	25	26	27	28
3400	O—H stretch intermolecular bonding	--	--	--	--	√	--	--	--	--	--	--	--
2920 & 2850	CH asymmetric and symmetric CH$_2$ stretching	√	√	√	√	√	√	√	√	√	√	√	√
1750	C=O of unsaturated ester	--	--	--	--	--	--	--	--	--	--	--	--
1700	C=O stretch vibrations of carboxyl and carbonyl groups	√	√	√	√	√	√	√	√	√	√	√	√
1630	Aromatic C=C stretching and C=O stretching vibrations of carbonyl groups	√	√	√	√	√	√	--	--	--	√	√	√
1510	Aromatic C=C ring stretching; Naphthalene; Phenanthene; C=C in-plane thiophene	--	--	--	--	--	--	--	--	--	--	--	--
1470	CH bending vibrations of CH$_3$ and CH$_2$	√	√	√	√	√	√	√	√	√	√	√	√
1370	CH bending of CH$_3$	√	√	√	√	√	√	√	√	√	√	√	√
1260/ weak	C−H bending vibrations of alkynes or monosubstituted alkynes	--	--	--	√	--	√	√	√	√	√	√	--
1260/ strong	C−O stretching vibration of esters of aromatic acids	--	--	--	--	√	--	--	--	--	--	--	--
1168	C−O stretching in phenols, aliphatic ether	√	√	√	--	--	--	√	√	√	--	--	--
1115	Aromatic C−H deformation	√	√	√	--	--	--	√	√	√	--	--	--
1030	C−OH stretching due to primary or secondary alcohol	√	√	--	--	--	--	--	--	--	√	√	--
1010	C=C stretch; CCO stretch	--	--	--	√	√	√	--	--	--	--	--	--
837-800	Out-of-plane aromatic CH bend with two hydrogen atoms	--	--	--	--	--	--	--	--	--	√	√	--
730	Out-of-plane aromatic CH bend with four hydrogen atoms	√	√	--	--	√	--	√	√	√	√	--	√

17: WFT1, 18: WFT2, 19: WFT3, 20:WFAQ11, 21: WFAQ12, 22: WFAQ13, 23: WFAQ21, 24: WFAQ22, 25: WFAQ23, 26: WFOH31, 27: WFOH32, 28: WFOH33.

Considering the FTIR spectra of each of the samples of the current study, the aliphatic hydrogen content, and the bands related to C═O structures, can be ordered according to apparent peak intensities:

Green River Formation> Orepuki> Waipawa Formation> Mir Kalam Kala> Speena Banda> Argillite> Qianjiang Formation > Salt Range

This trend of decreasing order of aliphaticity is almost consistent with the soxhlet bitumen yields (Figure 6.1), with the Green River Formation and Orepuki oil shales having the highest yields followed by the Waipawa Formation samples from the Waipawa type locality. The difference being that the Orepuki oil shale has a yield greater than the Green River Formation and also the Speena Banda shale has more yield than Mir Kalam Kala oil shale. The Waipawa Formation samples from Porangahau have an average yield of 0.13 greater than the Mir Kalam Kala and Qianjiang Formation samples.

The intensity of the bands related to aromatic structures for each of the samples for which aromatic components were identified using FTIR can be ordered according to the apparent peak intensities:

Waipawa Formation> Green River Formation> Orepuki

No aromatic bands were identified in the Qianjiang Formation and Pakistani oil shale samples.

The relatively high aliphaticity and aromaticity of the Green River Formation, Orepuki oil shale and the Waipawa Formation suggests that these oil shales may be potential source rocks. The variation in band intensities related to aliphatic and aromatic structures in samples from the different outcrops of the Waipawa Formation and also between samples collected from different points within the same outcrop suggests that the Waipawa Formation is a heterogeneous formation. However, the absence of aromatic structures in extracts from the Pakistani and Qianjiang Formation samples, and the relatively low aliphaticity of bitumen extracted from these rocks, suggests a low production potential of these rocks. This degree of aliphaticity and aromaticity gives a

qualitative index of the quality of oil that may derive from each of the rocks investigated in this study.

6.4 Gas Chromatography Mass Spectrometry, GC-MS

The analysis of organic material by GC-MS allows for the identification of constituent chemical compounds in a complex mixture of organic compounds such as bitumen (Macpherson *et al.*, 1998; Selby *et al.*, 2005; Wolfson *et al.*, 2011). These compounds include alkanes, aromatics, alicyclics, branched hydrocarbons, and non-hydrocarbon heteroatom compounds containing nitrogen, sulphur and oxygen (NSO). For example, Sporstol *et al*. (1983) used GC-MS to identify different aromatic hydrocarbons in sediments and Liang *et al*. (2009) used the technique to identify the constituents of crude oil. Identification of biomarkers, in particular, using GC-MS has become a valuable tool in determining the origin and maturity of organic matter (Frysinger & Gaines, 2001). Biomarkers are a suite of complex organic compounds composed of carbon, hydrogen and other elements such as oxygen, nitrogen and sulphur that are found in crude oils, bitumen and petroleum source rocks, and which are used by geologists and geochemists to unravel the origin and migration pathways of petroleum deposits (Peters *et al.*, 1993).

For the purpose of the current investigation, a qualitative comparative assessment was made of the organic chemicals present in the solvent extracted bitumen phase of a rock from each sampling location. Constituent organic chemicals were categorised as alkanes, cycloalkanes, aromatics and heteroatom compounds. These are the dominant organic compound classes present in crude oils (Demirel, 2012). The absolute peak areas of the constituent compounds identified by GC-MS from each of these four classes (given in Table 6.5), were divided by 100,000 for the purpose of the qualitative assessment and are summarised in Table 6.6. This parameter is hereafter defined as the GC-MS index. The most probable identity of the compounds present at high content in the extracts is summarised in Table 6.5.

No standards were run for GC-MS analysis in the current study. Peak areas were simply used to allow for qualitative comparison of the relative abundances of the different classes of chemical compounds present in the various samples. GC-MS analysis showed that there were more than 100 identifiable peaks in the bitumen extracts from the Green River Formation, Orepuki oil shale and Waipawa Formation, but relatively few peaks in extracts from argillite and the Qianjiang Formation and Pakistani oil shale samples.

Table 6.5. Absolute areas of the most probable and abundant organic compounds, alkanes, cycloalkanes, aromatics and heteroatom compounds from GC-MS analysis of argillite and different oil shales bitumen extracts. --: not identified.

Compounds	CBl	CBr	OOS3	WFT1	WFAQ11	WFAQ21	WFOH31	QF3	MKK2	SB	SR1	Argillite
Hexadecanes	1205242	--	939856	--	23228	202713	233764	22606	19997	17307	--	77503
2,6,10,14-tetramethyl hexadecane/phytane	1295982	1245102	--	79188	375195	72487	51534	--	--	--	--	--
Pentadecanes	770601	--	11727	222586	194955	6903	--	--	--	27655	--	55383
2,610,14-tetramethyl pentadecane/pristane	3225937	2709970	3354	59738	210148	49549	35232	--	--	--	--	20396
Tetracosanes	585662	--	1226233	45592	41951	27189	19635	--	--	19121	--	--
Octadecanes	254403	--	40976	2531858	2616290	12614	--	--	--	7254	--	--
Icosanes	288489	--	22365	17253	65875	6464	57417	4262	2937	128452	--	41898
Heptadecanes	34599	--	--	36772	--	--	--	--	18211	221436	11276	26334
Dodecanes	64587	--	10115	32139	10384	--	--	3213	--	21917	2379	8176
Tetratetracontanes	--	--	383458	--	--	--	23305	--	--	--	--	--
Octanes	80168	--	--	8185	--	16290	--	--	--	--	--	--
Octacosanes	125672	--	65869	--	--	--	--	--	--	26262	--	7233
Heptacosanes	--	--	315047	32103	--	36167	--	--	--	--	--	--
Stigmastanes	633688	--	--	--	--	--	--	--	--	--	--	524307
Cyclohexanes	272965	--	--	10660	16297	15423	--	--	--	--	--	--
Cyclopentanes	--	53309	1032296	--	--	12280	--	--	--	--	--	--

Table 6.5. Continued

Compounds	CBl	CBr	OOS3	WFT1	WFAQ11	WFAQ21	WFOH31	QF3	MKK2	SB	SR1	Argillite
Naphthalene	188179	--	--	121670	42341	15402	--	--	--	--	--	27322
Dodecanoic acids	52320	--	16671	46326	283434	20997	--	--	--	--	--	--
Heptadecanoic acids	56671	--	--	--	1302762	457708	--	--	--	--	--	--
Decanoic acids	101403	--	--	16751	34596	12509	--	--	--	--	--	--
Pentadecanoic acids	114154	--	17025	45104	1883106	45418	7197	3222	--	--	--	--
Tetradecanoic acids	--	--	23631	32856	159873	41560	10447	--	--	--	--	--
Hexadecanols	179484	--	110625	--	--	--	--	10896	--	8464	--	15578
Heptadecanones	--	--	--	61936	138943	--	--	--	--	--	--	--
Octadecanals	--	--	201784	15744	34623	--	--	--	--	--	--	--
2-Undecanone,6,10-dimethyl	114308	--	5406	52019	381309	68637	--	--	248001	--	--	--
Hexadecanals	6414	--	33505	8724	214554	10190	--	--	2866	--	--	--
Hexadecanoic acids	348498	--	117826	451437	1498905	367892	92151	121937	51173	55135	5191	44851
Sum of other alkanes	9658	1332652	543350	59586	--	358100	--	--	8857	90596	--	45077
Sum of other cycloalkanes	37667	831303	24704	4090	--	--	--	--	20041	--	--	8101
Sum of other aromatics	316821	485872	288841	576201	697005	175944	46033	25064	13145	98100	5004	--
Sum of other heteroatoms	4397246	2976043	834473	9453227	6180236	3933942	1493805	130945	--	345135	93841	185276

Note: Identity based on most probable compounds as determined by the computer software running the GC-MS analysis. Identity is not absolute.

Table 6.6. GC-MS index for organic compounds extracted from the samples of the current study identified as belonging to four chemical groups. Index parameters are unitless abundance.

Compounds	Alkanes	Cycloalkanes	Aromatic	Heteroatom compounds
CBl	79.41	9.44	5.05	53.70
CBr	52.88	8.85	4.86	29.76
OOS3	35.62	10.57	2.89	13.60
WFT1	31.25	0.15	6.98	101.84
WFAQ11	35.38	0.16	7.39	121.12
WFAQ21	7.88	0.28	1.91	49.59
WFOH31	4.21	--	0.46	16.04
QF3	0.30	--	0.25	2.67
MKK2	0.50	0.20	0.13	3.02
SB	5.60	--	0.98	4.09
SR1	0.14	--	0.05	0.99
Argillite	2.82	5.32	0.27	2.46
Sand	--	--	--	--

6.4.1 Main components of bitumen

6.4.1.1 Alkanes (paraffins)

Hydrocarbons falling under the chemical definition of alkanes are also known as paraffins [(C_nH_{2n+2})] and occur in most crude oils with an abundance generally in the range from 15-20% (Bjorlykke, 2010). This class of chemical compounds is the most abundant constituent of the solvent extracts of the Green River Formation, Orepuki oil shale, and Waipawa Formation from two localities (Waipawa type locality and Lower Angora Road quarry) (Table 6.5, 6.6). However abundance is relatively low for the Waipawa Formation samples from Upper Angora Road and Old Hill Road (Porangahau), Pakistani samples and Qianjiang Formation. No alkanes were detected in the sand.

Among the alkanes, the linear alkanes [hexadecanes ($C_{16}H_{34}$), pentadecanes ($C_{15}H_{32}$) and tetracosanes ($C_{24}H_{50}$)] are the most abundant hydrocarbons in the Green River Formation (Table 6.5). For the Orepuki oil shale the most abundant linear alkanes among the alkanes are tetracosanes, hexadecanes and tetratetracontanes ($C_{44}H_{90}$) (Table 6.5). However, in the Waipawa Formation the most abundant alkanes are hexadecanes, pentadecanes and octadecanes ($C_{18}H_{38}$) (Table 6.5). In the Speena Banda shale the most abundant alkanes are icosanes ($C_{20}H_{42}$), heptadecanes ($C_{17}H_{36}$) and pentadecanes (Table 6.5). In argillite the most abundant alkanes are hexadecanes, pentadecanes and icosanes (Table 6.5). In extracts from the Qianjiang Formation, Mir Kalam Kala, Salt Range rocks only a few alkanes out of the most probable alkanes are identified (Table 6.5).

According to Tissot and Vandenbrouck (1983), a dominance of linear and branched alkanes over aromatics, cycloalkanes and heteroatom compounds supports the presence of Type I kerogen in a source rock. Therefore, the higher distribution of alkanes in the Green River Formation and Orepuki oil shales suggests the presence of Type I kerogen in these rocks. However, in the Waipawa Formation, and in the rocks from China (Qianjiang Formation) and Pakistan, alkanes are not dominant over the other fractions within the bitumen. This is consistent with the relatively low aliphaticity of the extracts from these rocks as defined by FTIR analysis.

6.4.1.2   Cycloalkanes (alicyclics or naphthenes)

Cycloparaffins (naphthenes) $(CH_2)_n$, are a type of cyclic saturated hydrocarbon also present in all types of crude oils and constitutes 7-31% of a sample (Bjorlykke, 2010). Stigmastanes ($C_{29}H_{52}$), cyclohexanes (C_6H_{12}) and cyclopentanes (C_5H_{10}) (each a cycloalkane) are identified in samples of the Green River Formation, Orepuki oil shale, Waipawa Formation (except Old Hill Road, Porangahau) and argillite (Table 6.5). The content of cycloalkanes in an oil is proportional to the octane number (standard measure of the performance of fuel) and is generally associated with high performance (Daniels *et al.*, 2004). The relative abundance of cycloalkanes is high in the Orepuki oil shale and the Green River Formation suggesting that high performance oils may be derived from these bitumens. However, relative abundance is very low in the extracts of the

Waipawa Formation samples from the Waipawa type locality, Lower Angora Road quarry, Upper Angora Road and Mir Kalam Kala rocks (Table 6.6). No cycloalkanes were identified in the extracts of the Waipawa Formation from Old Hill Road (Porangahau) suggesting the very low to no performance of oil that may derive from bitumen in these rocks. No cycloalkanes were identified in the bitumen extracts of the Qianjiang Formation samples, the Speena Banda and Salt Range rocks, and sand (Table 6.6).

6.4.1.3   Aromatics

Aromatic hydrocarbons are unsaturated hydrocarbons which have one or more benzene rings with alternate single and double bonds according to the general formula of C_nH_{2n-6} (Demirel, 2012). Aromatics normally comprise from 10 to 39% of crude oil. The aromatic content of an oil is also proportional to octane number and so again can be associated with high performance (Bjorlykke, 2010; Oseev *et al.*, 2012). The relatively high abundance of aromatic compounds present in the bitumen extracts of the Green River Formation, Orepuki oil shale and Waipawa Formation suggests the bitumen in these rocks may produce good quality oil with high performance. Comparatively, the bitumen extracts of the Waipawa Formation from Waipawa type locality and Lower Angora Road quarry has the highest number of aromatic hydrocarbons present. This suggests that oil derived from the Waipawa Formation from these localities may have high performance. Relatively low abundance of aromatics present in the argillite, Pakistani and Qianjiang Formation extracts suggests a very low performance for oil that may be derived from bitumen in these rocks. No aromatic hydrocarbons were detected in the sand extract. The trend in relative aromaticity of the samples as qualified by GC-MS is consistent with the trend derived through FTIR.

6.4.1.4   Heteroatom compounds

Heteroatom compounds are those compounds which contain nitrogen, oxygen or sulphur (Deng *et al.*, 2011). Relatively high nitrogen and sulphur contents found in

shale oils can adversely affect the potential for use of these oils as a transport fuel. For example, high nitrogen content can create problems in an oil refinery through catalyst poisoning (Yen *et al.*, 1983). Combustion of oil with a high content of nitrogen and sulphur containing compounds leads to air pollution through emission of NO_x and SO_x (Yen *et al.*, 1983). Therefore, prior to any refining, the high nitrogen content of any crude oil must be reduced (Poulson, 1973).

Among the heteroatom compounds, a relatively high content of sulphur compounds is present in the Waipawa Formation from Upper Angora Road (Table 6.7). Pale yellow coating of jarosite was seen at the outcrop of these samples on the weathered surface and between laminae. The visual analysis and GC-MS data is consistent with the presence of high sulphur content of marine oil shale (Petersen *et al.*, 2010). In contrast, a very low content of sulphur compounds is present in the Waipawa Formation sample from the Waipawa type locality (WFT1) (Table 6.7). The Green River Formation samples CBl and CBr also contain fewer sulphur compounds among the heteroatom compounds when compared to the other oil shales (Table 6.7). Among the content of heteroatom compounds present in all samples, the highest content of nitrogen compounds is present in extracts from the Speena Banda oil shale (Table 6.7). All other samples have no to very limited content of nitrogen compounds present. But the number of nitrogen compounds present is very low when compared to the number of sulphur compounds present (Table 6.7).

The low content of nitrogen and sulphur compounds in the extracts of the Waipawa Formation type locality and Orepuki oil shale suggests that oil that may derive from bitumen in these rocks will present limited production threat to refineries and the environment. Samples of the Waipawa Formation from Lower Angora Road quarry, Upper Angora Road and Old Hill Road outcrops and Green River Formation however, have a greater abundance of sulphur compounds. Therefore, it can be suggested that oil derived from these rocks would have be comparatively more difficult to refine, and could cause air pollution if exploited.

Table 6.7. Absolute GC-MS index of nitrogen and sulfur compounds present in argillite and different oil shales bitumen extracts. n.d. = not determined (all areas have been divided by 100, 000).

Samples	Sulfur compounds	Absolute areas of sulfur compounds	Nitrogen compounds	Absolute areas of nitrogen compounds
CBl	Sulfurous acid, octadecyl 2-propyl ester Distearyl sulfide	1.96	Piperidine, 3,5-dimethyl 13-Docosenamide	0.13
CBr	Sulfurous acid, 2-propyl undecyl ester Sulfurous acid, octadecyl 2-propyl ester Distearyl sulfide	2.92	n.d	n.d
OOS3	n.d	n.d	2-piperidinone, N-[4-bromo-n-butyl] 9-octadecenamide	0.38
WFT1	Benzothiophene, 2,5-dimethyl	0.32	Alpha-(aminomethylene) glutaconic anhydride	0.11
WFAQ11	Cyclic octaatomic sulfur	1.74	Aspartic acid, n-acetyl 1-nitrooctanone dodecenamide	0.59
WFAQ21	Cyclic octaatomic sulfur Cyclic hexaatomic sulfur	8.02	Tetra decenamide	0.03
WFOH31	Cyclic octaatomic sulfur Cyclic hexaatomic sulfur	2.01	n.d	n.d
QF3	Benzothiophene Naphtho [2,3-b] thiophene Tetra decenamide 9-octadecenamide	0.26	n.d	n.d

Table 6.7. Continued

Samples	Sulfur compounds	Absolute areas of sulfur compounds	Nitrogen compounds	Absolute areas of nitrogen compounds
MKK2	Cyclic octaatomic sulfur	0.04	2-carbomethoxyaziridine Tetra decenamide	0.18
SB	Sulfurous acid, dodecyl 2-propyl ester Sulfurous acid, octadecyl 2-propyl ester	0.18	Pyrrolidine 3-methyl 3-hexadecyloxycarbonyl methylimidazolium ion Dimethyl pyrrolidine-2-dione Tetra decenamide and 9-octadecenamide	0.92
SR1	n.d	n.d	n.d	n.d
Argillite	Sulfurous acid, 2-propyl undecyl ester	0.04	n.d	n.d

6.4.2 Index Compounds and Ratios

6.4.2.1 Pristane-Phytane ratio (Pr/Ph)

The pristane (2,6,10,14-tetramethyl pentadecane) to phytane (2,6,10,14-tetramethyl hexadecane) ratio of an oil is widely used as a palaeoenvironmental indicator biomarker of the redox conditions that existed during sediment accumulation. According to Brooks *et al*. (1969) and Didyk *et al*. (1978) a pr/ph ratio greater than 1 indicates an oxic environment of deposition, with a value less than 1 an anoxic environment of deposition. Both pristane and phytane are derived from phytol, a constituent of chlorophyll (Grice *et al.*, 2005).

The Green River Formation samples (CBl, CBr) have high pr/ph ratios, of about 2.48 and 2.17 respectively (Table 6.8), which suggests an oxic (lacustrine) environment of deposition that is likely to be oil prone. Hughes *et al*. (1995) also classified the Green River Formation as having an oxic environment of deposition based on pr/ph ratios of 1.09 and 1.35. The Waipawa Formation samples have pr/ph ratios of less than 1 (Table 6.8) consistent with an anoxic (reducing) (marine) environment of deposition that is likely to generate both oil and gas. This agrees with the marine environment of deposition proposed for the Waipawa Formation by Killops *et al*. (1996).

Table 6.8. Absolute areas of pristane, phytane and octadecane and their ratios from the GC-MS analysis of different oil shales bitumen extracts. --: not identified.

Samples	Pristane	Phytane	Octadecane	Pristane/Phytane	Phytane/Octadecane
CBl	3225937	1295982	254403	2.48	5.09
CBr	2709970	1245102	--	2.17	--
OOS3	3354	--	40976	--	--
WFT1	59738	79188	2531858	0.75	0.03
WFAQ11	210148	375195	2616290	0.56	0.14
WFAQ21	49549	72487	12614	0.68	5.75
WFOH31	35232	51534	--	0.68	--
QF3	--	--	--	--	--
MKK2	--	--	--	--	--
SB	--	--	7254	--	--
SR1	--	--	--	--	--

In the Orepuki oil shale, pristane was identified but no phytane was detected (Table 6.5, 6.8). No pristane or phytane was identified in extracts from the Pakistani and Qianjiang Formation (Table 6.5, 6.8). Todd Ventura (Pers. comm., 2013), GNS Science, suggested that their absence is highly unlikely because these compounds are the degradation products of chlorophyll in the original organic matter present in the rocks. He suggested three possibilities for the absence of these compounds from the GC-MS chromatograms. The first is there was no primary productivity during the deposition of the organic matter (an unlikely scenario). Secondly, bitumen in the Orepuki shale may be heavily biodegraded to an extent that n-alkanes have been removed from the chemical signature of the oil shale, followed by the degradation of acyclic isoprenoids such as pristane and phytane. The third possible reason is that bitumen in the Orepuki shale are very immature; so immature that phytol has not yet cleaved its hydroxyl group to yield phytane. However, it is possible that, because no chromatographic separation was run before the GC-MS analysis of the bitumen extracts, peak resolution may be poor. Because the signal strength may have been low and there may have been coelution effects due to which the peaks of these compounds may not have been easily separated (Ventura, Pers. comm., 2013).

6.4.2.2 Phytane-n Octadecane ratio

Another index reported in the literature is the phytane/n-octadecane ratio which provides insight to the maturity of sediments. Haven *et al*. (1987) define oil and sediment extracts with a ratio less than 0.5 to be sourced from mature sediment. Immature oils and sediment extracts are characterised by a high phytane/n-octadecane ratios. As hydrocarbons are generated during maturation the phytane/n-octadecane ratios decrease and eventually become less than 1.

The phytane/n-octadecane ratio of the solvent extract from the Green River Formation (CBl) is 5.1 (Table 6.8), suggesting this oil shale as immature. The ratio from the Waipawa Formation from the type locality is 0.03 (WFT1) (Table 6.8) and from the Lower Angora Road quarry (WFAQ11) is 0.14 (Table 6.8) which are much lower than 1, indicating that the Waipawa is a very mature formation. The phytane/n-octadecane

ratio of the Waipawa Formation sample from Upper Angora Road (WFAQ21) is 5.75 (Table 6.8) suggesting immaturity of the formation.

In each of the other samples phytane and/or octadecane was not identified (Table 6.8), meaning that the phytane/n-octadecane ratio cannot be expressed for the other samples of the study.

6.5   Discussion

The trend in relative aliphaticity and aromaticity of the samples of the current study defined by FTIR analysis is consistent with the GC-MS analysis. Relative hydrocarbon chemical composition is concluded to be key scientific information provided by the chemical techniques used in this study. Maturity suggested for the Green River Formation (mature oil shale) and Waipawa Formation (very mature for WFT1, WFAQ11 and immature for WFAQ21) from the GC-MS determined from the phytane/n-octadecane ratio is not consistent with the bitumen yield to TOC ratios of these oil shales. Due to a lack of chromatographic separation for GC-MS analysis of the bitumen extracts, quantitative interpretation of the maturity ratios such as phytane/n-octadecane is not, however, advised. A more accurate measure of maturity is judged to be interpretation of the bitumen yield and TOC parameters.

Chapter 7-General discussion: a non-conventional model to assess the production potential of oil shales

7.1 Introduction

In the context of hydrocarbon studies, a potential source rock is one that contains sufficient organic matter of a suitable type to generate petroleum, oil and/or natural gas. Source rocks contain varying amounts of bitumen, kerogen and organic carbon, but these represent only a small proportion of the rock matrix (Jones, 1984). The organic phase of a source rock is often affected by an inorganic phase which constitutes the bulk of the rock (Tannenbaum & Kaplan, 1985). Source Rock Analysis (SRA) is the conventional technique used by the petroleum industry to evaluate the hydrocarbon potential of source rocks. Source Rock Analysis was developed for conventional oil and gas targets, but is today being applied to non-conventional source rocks. Source Rock Analysis is a thermal technique that provides quantitative information on total organic carbon (TOC), hydrocarbon yield and maturity through assessment of the parameter **Tmax**. However, the literature reviewed in this thesis has indicated the maturity of a source rock, which includes oil shales, and its potential to generate oil may not be optimally assessed using SRA. Source Rock Analysis gives limited understanding of source rock petroleum potential and provides little information about the origin of the source rock. Furthermore, availability of this technique is not widespread. Commercial and research SRA equipment and technical expertise to operate such equipment are limited to facilities that specialise in hydrocarbon studies.

Various formations from different outcrops in different countries were studied to generate the model derived in this chapter. International reference samples were obtained from the Green River Formation, and from oil shale deposits in Pakistan and China. New Zealand samples were collected from field outcrops of the Orepuki oil shale in Southland and from outcrops of the Waipawa Formation within the East Coast

Basin. The Green River Formation is a well-studied formation and is a known excellent source rock. The Pakistani and Chinese rocks are less well studied. The Orepuki oil shale was exploited for shale oil production in the late 1800s to early 1900s (1899-1903) and has been subsequently studied to some extent. The Waipawa Formation has been studied for its hydrocarbon generation potential using conventional SRA (Leckie *et al.*, 1992), and is considered a source rock. There is no commercial production from the Waipawa Formation, although it is believed to be the most likely source of the extensive oil and gas seeps in the East Coast Basin.

In this chapter the qualitative and quantitative data generated through physical, thermal and chemical analysis of control samples (sand and argillite), the Pakistani rocks (Salt Range oil shale, Mir Kalam Kala and Speena Banda oil shale), Chinese rocks (Qianjiang Formation samples), and samples of the Green River Formation in USA are integrated, in order to propose a novel descriptive production assessment model for non-conventional source rocks. The model defines a sequence of analytical techniques running from simple to more complex that assess the hydrocarbon potential of the source rocks. The model first determines LOI using a muffle furnace and subsequently determines TOC using a LECO furnace. Rocks that show promise at this point can be subjected to the progressively more involved techniques: TGA, XRD, organic petrography and soxhlet extraction (bitumen phase of organic matter) followed by FTIR and GC-MS analyses of the solvent extracts.

Conventional SRA was used to rank the 'source rock potential' of each of the international reference samples. The non-conventional model was constructed such that the final conclusions generated through application of the model agreed with the conclusions of SRA.

The physical, thermal and chemical data of the New Zealand Orepuki oil shale and Waipawa Formation samples were then applied to the model, in order to generate scientifically valid conclusions and understanding of the production assessment potential of these rocks. The conclusions of the non-conventional model were then compared to SRA analysis. The non-conventional model was shown to derive the same conclusions as SRA, but with a better level of scientific understanding. These new data can therefore be used to update earlier assessments of the petroleum potential of the

Waipawa Formation using SRA (Field *et al.*, 1997; Hollis & Manzano-Kareah, 2005; Leckie *et al.*, 1992).

7.2 Summary of analytical data for the international shale and reference samples

A summary of the key data for the international reference oil shales collected from Pakistan, China and USA, and the non-source rock control samples (sand and argillite) is presented in Table 7.1. The oil shales are ranked from low or non-producing rocks to excellent producing oil shales based on interpretation of the Source Rock Generative Potentials (SP)[20] results from SRA (Table 7.1).

Loss on Ignition (LOI) provides a quick assessment of the abundance of organic matter in sediments. But this weight loss, which is estimated as weight loss due to organic content, can include weight loss due to the decomposition of mineral matter present and carbonates and is therefore not a reliable estimate of the abundance of organic matter. Incorporating measurement of TOC using LECO also provides a rapid and better assessment of the organic richness of a sample. However, using only TOC for assessing petroleum potential can be misleading, especially in the case of post-mature sediments. For example, graphite which is 100% carbon (dominantly mineral carbon) has no production potential. Graphite was used to explore the behaviour of post-mature source rocks. The TOC value of graphite alone in this study would have inferred some petroleum potential for graphite.

The LOI and TOC values of the control samples (sand and argillite) and Salt Range oil shale samples (SR1, SR2 and SR3) were found to be very low (Table 7.1). However, for the Mir Kalam Kala (MKK1, MKK2) and Speena Banda (SB) samples, the LOI values were found to be relatively high when compared to their TOC values. The TGA results showed a low weight loss, W_B, in the organic matter decomposition region (200-650°C) for these samples, but higher weight losses were observed in the temperature regions

---

[20] Where SP = (S1 + S2) where S1 and S2 are parameters that account for the free oil content (S1) and hydrocarbon potential (S2) of a source rock measured by SRA.

25-200°C and 650-1200°C (Chapter 5, Table 5.3). Abundant gypsum was identified by XRD analysis of the untreated samples, and hence the high weight losses in these temperature regions were predominantly attributed to the dehydration of gypsum (100-300°C) (Bhargava *et al.*, 2005; Deer & Howie, 1966) and decomposition of anhydrite (above 800°C) respectively (Ingo *et al.*, 1998). Therefore, the reason that the Mir Kalam Kala and Speena Banda samples have higher LOI values relative to their TOCs is that weight loss due to gypsum dehydration was contributing to their LOI values.

Organic petrography identified dispersed and sparse terrestrial and marine organic macerals in the Mir Kalam Kala oil shale, inferring this sample to be a very low quality oil shale. This conclusion was validated by the low SP values from the SRA analysis of these samples (Table 7.1), which were below the cut-off values defined by Peters and Cassa (1994) for the definition of poor quality or non-producing oil shales. No organic petrographical assessment was made for the Speena Banda oil shale, but its low LOI, TOC and W_B values from the thermal analyses suggested this sample to be a low quality oil shale, a conclusion validated by SRA analysis. The bitumen yield from all the Pakistani rocks and control samples after soxhlet extraction was very low. When these extracts were analysed by FTIR, only aliphatic bands were identified. No aromatic bands that could be related to aromatic structures were identified suggesting its low performance because the aromatic content of oil is proportional to its octane number. GC-MS analysis of these same extracts showed only a few peaks that could be attributed to the constituent chemicals of bitumen. Peaks were qualitatively allocated to alkanes, aromatic compounds and heteroatom compounds, but no cycloalkanes were identified.

The Qianjiang Formation samples (QF1, QF2 and QF3) were found to be rich in organic matter as quantified by their high LOI (9-25 wt%) and TOC (10-17.3 wt%). However, when these rocks were analysed using a TGA no distinct region of weight loss or changes in slope of the weight curve were identified. Therefore, weight loss that could be attributed to organic matter content was not clear. From the SRA results, these samples were also found to have very high TOC, but very low SP values (Table 7.1). To explain this, graphite (sourced from a chemistry laboratory) was analysed using a TGA under the same operating conditions. It was found that the behaviour of weight loss in graphite was quite similar to the Qianjiang Formation samples (Chapter 5, Figure 5.8).

Hence, it was concluded that even though the LOI, TOC and total weight loss in the TGA organic weight loss region (W_B) of these rocks was very high, the organic matter was inert or post-mature for petroleum generation and therefore these rocks gave very low SP values. No organic petrography assessment was conducted for these samples. The bitumen yield of these samples after soxhlet extraction was found to be very low (0.04 wt%). FTIR analysis of these bitumen extracts showed no aromatic peaks in the FTIR spectra. GC-MS analysis showed only a few peaks that could be qualitatively attributed to alkanes, aromatic and heteroatom compounds, but no cycloalkanes were identified.

The Green River Formation samples (CBl, CBr) had very high LOI and TOC values relative to the Pakistani oil shales (Table 7.1). These samples also have a greater weight loss in the organic matter decomposition region as quantified by TGA analysis. The organic petrography photomicrographs of the Green River Formation showed abundant lacustrine algal macerals inferring the rocks of this formation to be high quality oil shale. High soxhlet yields (bitumen extract) were found for these samples quantifying a high content of bitumen in each sample. FTIR analysis of these extracts showed the presence of both aliphatic and aromatic bands and this was confirmed by GC-MS. All extracts from these two oil shales were found to contain alkanes, cycloalkanes, aromatics and heteroatom compounds (Table 7.1). The conclusion that shales from the Green River Formation represent an excellent source rock for petroleum generation was validated by the SRA results. The exceptionally high SP values infer that the analysed shales are excellent source rock for petroleum generation.

A general relationship between the content of illite and the petroleum potential of each of the international oil shale and reference samples was found through consideration of the data obtained by XRD analysis of clay separated from each sample. In the non-producing argillite, Mir Kalam Kala samples and Salt Range samples illite was the dominant[21] clay mineral. This clay mineral was common in the excellent source rock Green River Formation samples (Table 7.1).

---

[21] See Chapter 4 for definitions of dominant (d), common (c) and present (p).

Table 7.1. Summary of the results obtained through analysis of the rocks from Pakistan, Qianjiang Formation, the Green River Formation and the control samples (sand and argillite) using non-conventional techniques (dominant: d, common: c, present: p, trace: t, abundant: a, not identified: --, AL: aliphatic bands, AR: aromatic bands, Al: Alkanes, Ar: Aromatic hydrocarbons, Ha: heteroatom compounds, Ca: cycloalkanes, shaded areas represent samples which have not been analysed by a stated technique).

Samples	XRD (content of illite)	Organic petrography (content of macerals) [22]	LOI (wt%)	LECO TOC (wt%)	TGA W_B (wt %) (200-650°C)	Soxhlet extraction (bitumen yield (wt %)	FTIR (bands related to aliphatic & aromatic structures)	GC MS (constituent compounds in bitumen)	SRA (Generative potential) SP (mg HC/g rock)
Sand	--		0.1	--	--	--	--	--	--
SR2	d		1.3	0.3	2.2	0.07	AL	Al, Ar, Ha	0.3
SR3	d		1.3	0.2	2.1	0.03	AL	Al, Ar, Ha	0.3
SR1	d		1	0.2	2	0.01	AL	Al, Ar, Ha	0.3
Argillite	d		3.1	0.6	3.2	0.05	AL	Al, Ar, Ha, Ca	0.5
MKK1	d	t	5.4	2.7	5.2	0.11	AL	Al, Ar, Ha, Ca	1.1
QF3	p		25	17.3	7	0.05	AL	Al, Ar, Ha	1.2
QF2	p		12.5	10.1	2.5	0.04	AL	Al, Ar, Ha	1.2
SB	c		8.8	1	3.5	0.20	AL	Al, Ar, Ha	1.3
QF1	p		9.5	11	1	0.04	AL	Al, Ar, Ha	1.4
MKK2	c		8	2.2	5.8	0.17	AL	Al, Ar, Ha, Ca	1.3
CBr	c		18	12.6	8.6	1.17	AL, AR	Al, Ar, Ha, Ca	66
CBl	c	a	25.8	18	13.6	2.01	AL, AR	Al, Ar, Ha, Ca	151.7

---

[22] Polished section of CBl showed the presence of abundant, fluorescing lacustrine alginite (*Lamalginite*). However polished section of MKK2 showed the presence of sparse and dispersed macerals such as terrestrial *inertodetrinite* and *vitrodetrinite* and marine *liptodetrinite*.

7.3 Derivation of a non-conventional production potential assessment model for oil shales

Based on the conclusions on source rock potential that could be drawn through interpretation of the SRA data, cut off values were selected for each non-conventional physical, thermal and chemical analytical parameter to set assessment criteria for the production potential of an oil shale. Using these criteria, the control samples (sand and argillite), Pakistani (Salt Range, Mir Kalam Kala and Speena Banda) and Qianjiang Formation samples were each defined as having no to poor production potential. The Green River Formation samples are defined as oil shales with excellent production potential. Cut-off values for each of the non-conventional techniques were therefore defined at values between the Mir Kalam Kala and Green River Formation samples. However, specific values were chosen carefully because there were variations between the analytical techniques in the ordering of the different samples from low production potential to high production potential. For example, the Pakistani oil shales Mir Kalam Kala and Speena Banda had low TOC's but comparatively high LOI values. Also, discussion of the organic matter in the Qianjiang Formation samples highlighted the anomalous data (Figures 5.1a, 5.13a, 5.14a in Chapter 5) that can be returned where LOI, LECO and TGA are applied to post-mature carbon (i.e. graphite). The cut off values for the non-conventional production potential model are defined in Table 7.2.

Table 7.2. Cut off values from the analytical techniques (based on the suite of non-conventional analytical analyses) those have been used in the non-conventional production potential assessment model.

Analytical techniques	Poor quality oil shale	Good quality oil shale
LOI (wt%)	<5	>5
TOC (wt%)	<2.5	>2.5
W_B (wt%)	<7	>7
XRD	Dominant illite	Common/present illite
Organic petrography	Macerals absent or few	Macerals abundant
FTIR	Bands related to aliphatic and/or aromatic structures absent	Bands related to aliphatic and aromatic structures present
GC-MS	Absence of all or some constituent chemicals (Alkanes, aromatics, cycloalkanes and heteroatoms)	Presence of all constituent chemical compounds (Alkanes, aromatics, cycloalkanes and heteroatoms)

Considering the SRA data of the poor oil shales, the Mir Kalam Kala oil shale, despite having poor production potential, was found to have comparatively high SP (Table 7.1). Therefore, values determined through analysis of this shale were considered in the definition of cut-off values (Table 7.2). The cut off value for LOI, lower than the LOI values of Mir Kalam Kala samples, was chosen carefully because these samples were found to be rich in gypsum, and hence their LOI might include additional weight loss due to gypsum dehydration. Therefore, a lower LOI of 5% was selected as the cut off value for an oil shale. The average TOC value of the Mir Kalam Kala shale (2.5%) was chosen as the cut off value for this parameter. The cut off value for TGA W_B was also chosen after consideration of the possible contribution to weight loss that might be apparent due to gypsum dehydration in these samples. The cut off value for W_B was chosen to be an average value of W_B for the Mir Kalam Kala samples, defined as 7%.

Based on the results of qualitative analyses of each of the international reference shale and control samples using XRD, FTIR and GC-MS, the presence or absence of

particular minerals in the clay fraction of each rock, or bands or constituent chemicals in the solvent-extracted bitumen extract of each rock, was considered in the definition of cut-off values (Table 7.2). A trend in illite content was observed in the data set generated through XRD analysis of the clay fraction of the various potentially-producing and potentially- non-producing oil shales. Illite was found to be dominant in the non-producing oil shales, but was found to be common in the Green River Formation samples (Table 7.1). The relative presence of aliphatic and aromatic bands in the FTIR spectra of the solvent extract was considered in defining cut-off values for the non-conventional model; very few aliphatic bands were identified for the non-producing argillite, Pakistani and Qianjiang Formation samples, while both aliphatic and aromatic bands were identified in the Green River Formation samples. Interpretation of the GC-MS spectra of each sample showed the presence of each of the four chemical compound classes of bitumen (aliphatics, aromatics, heteroatom compounds and cycloalkanes) in the Green River Formation samples as well as the Mir Kalam Kala samples, but no cycloalkane signatures and only a few peaks due to chemical compounds (aliphatics, aromatics and heteroatoms) in the other low production potential shale samples. Therefore, the degree of aliphaticity, aromaticity, and the presence or absence of the chemical components of bitumen, qualified as a function of relative band intensity for FTIR and peak area for GC-MS, were defined as the cut-off criteria for an oil shale with production potential (Table 7.2).

Each of the described non-conventional analytical techniques, and the cut-off values defined by comparison of the qualitative and quantitative results obtained through application of these techniques with the conclusions of SRA of the same samples, were integrated to generate a non-conventional model to assess the production potential of oil shales (Figure 7.1). This model represents a step-wise sequence of analytical techniques that can be applied to assess the production potential of an oil shale. Each technique increases sequentially in its analytical complexity. Therefore, samples with poor production potential can be rapidly and cheaply discounted before the more complex, time consuming and expensive techniques are employed. After each step a conclusion can be made as to whether the sample being analysed has 'no potential as a source rock' or should be subjected to further study. The final conclusion that is reached by the model, for a sample that passes each and every analytical step, is that the oil shale being investigated has 'potential as a source rock'. The production potential as assessed by

this non-conventional model can generate the same conclusions as SRA analysis, but this non-conventional model has the advantage of providing detailed scientific understanding of the:

- Oil generation potential of the source rocks based on cross-checked thermal analyses
- Clay mineralogy of the rocks
- Degree of mineral decomposition
- Aliphaticity and aromaticity of the bitumen fraction of the rocks
- Constituent compounds present in the bitumen phase
- Maturity via the bitumen yield to TOC ratio

Due to a discrepancy between the inferred production potential of the Orepuki oil shale assessed through the applied set of thermal and chemical techniques, and that inferred through organic petrography (Chapter 4, section 4.3.2), organic petrography is not integrated as part of the model. For this study organic petrography was performed only on four samples. In the future, with further research, organic petrography may prove itself as a useful assessment parameter and could then be integrated into the model. This technique provides detailed scientific understanding of the:

- Identification of macerals present
- Origin of depositional environment
- Quality of oil shale
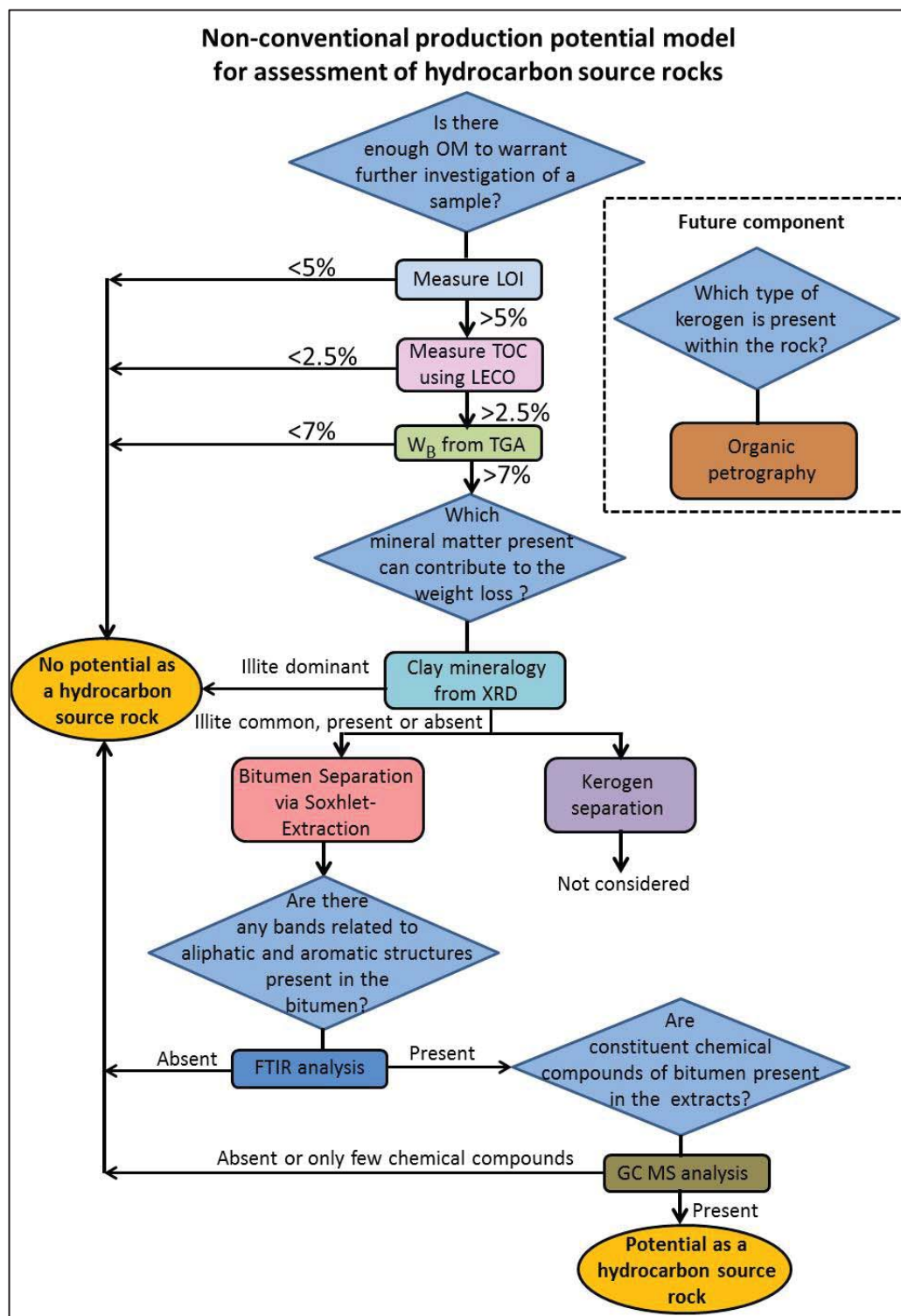
Figure 7.1. *A non-conventional production potential assessment model of hydrocarbon-bearing source rocks based on various non-conventional techniques. The model was derived through the analysis of samples from the Green River Formation, Mir Kalam Kala, Speena Banda and Salt Range oil shales and two control samples (sand and argillite) using both conventional (SRA) and non-conventional analytical techniques. W_B is weight loss due to kerogen cracking during TGA. Dichloromethane is used for the extraction of bitumen via soxhlet extraction from the various oil shales. (Note: Illite is considered dominant if the number of counts recorded for its main peak (at 10Å) are >500 and it is considered common if the number of counts are 150-500. Similarly if the number of counts are <150, then it is present).*

7.4 Waipawa and Orepuki oil shales: new insights obtained through analysis of these rocks using the non-conventional model

The non-conventional production potential assessment model presented in Figure 7.1 can now be applied to data obtained through analysis of samples from the historically producing Orepuki oil shale, and from four outcrops of oil shale belonging to the Waipawa Formation. The physical, thermal and chemical data obtained through analysis of these oil shales are summarised in Table 7.3. Interpretation of these data using the non-conventional production potential model allows for detailed and scientifically sound commentary on the hydrocarbon production potential of these two oil shales. For comparison, and to verify the validity of the assumptions of the non-conventional production potential assessment model, SRA data for each of the samples are also presented in Table 7.3.

Table 7.3. Summary of the results obtained through analysis of the rocks from the Waipawa Formation; from the Waipawa type locality, Lower Angora Road quarry, Upper Angora Road and Old Hill Road using non-conventional techniques (common: c, present: p, not identified: --, AL: aliphatic bands, AR: aromatic bands, Al: Alkanes, Ar: Aromatic hydrocarbons, Ha: heteroatom compounds, Ca: cycloalkanes, shaded areas represent samples which have not been analysed by a stated technique).

Samples	XRD (content of illite)	Organic petrography (content of macerals)	LOI wt%	LECO TOC (wt%)	TGA W_B (wt %) (200-650°C)	Soxhlet extraction (bitumen yield (wt%)	FTIR (bands related to aliphatic & aromatic structures)	GC-MS (constituent compounds in bitumen)	SRA (Generative potential) SP (mg HC/g rock)
OOS1	--	p	30	15.6	14.7	1.14	AL, AR	Al, Ar, Ha, Ca	36.7
OOS2	--		29	15.0	14.9	1.09	AL, AR	Al, Ar, Ha, Ca	
OOS3	--		30	14.3	16	1.12	AL, AR	Al, Ar, Ha, Ca	
WFAQ21	c		7.0	2.7	6	0.28	AL, AR	Al, Ar, Ha	2.9
WFAQ22	c		5.5	2.7	5.7	0.29	AL, AR	Al, Ar, Ha	
WFAQ23	c		8.6	2.6	8.2	0.29	AL, AR	Al, Ar, Ha	
WFOH31	c		5.6	2.5	7	0.32	AL, AR	Al, Ar, Ha	3.5
WFOH32	c		6.0	2.7	5.1	0.35	AL, AR	Al, Ar, Ha	
WFOH33	p		6.0	2.1	6	0.29	AL, AR	Al, Ar, Ha	
WFAQ11	p		9.0	4.4	7.2	0.46	AL, AR	Al, Ar, Ha, Ca	9
WFAQ12	p		8.9	4.0	7.2	0.58	AL, AR	Al, Ar, Ha, Ca	
WFAQ13	p		9.3	4.3	8.2	0.46	AL, AR	Al, Ar, Ha, Ca	
WFT1	c	p	14.9	7.0	10.5	0.60	AL, AR	Al, Ar, Ha, Ca	13.4
WFT2	c		14.0	6.2	10.1	0.50	AL, AR	Al, Ar, Ha, Ca	
WFT3	c		15.3	6.1	10.1	0.45	AL, AR	Al, Ar, Ha, Ca	

7.4.1 Assessment model applied to the Orepuki oil shale

Interpretation of the production potential assessment of the Orepuki oil shale using the non-conventional model is presented in Figure 7.2. Analysed samples of the shale had a high organic matter content as quantified by its high LOI (30 wt%) and TOC (15 wt%) (Table 7.3). The magnitude of these organic matter parameters were confirmed by TGA which quantified high weight loss (W_B = 15 wt%) in the region which is mainly attributed to the decomposition of kerogen (weight loss Phase II) (Table 7.3).

However, due to a low abundance of the macerals *vitrodetrinite*, *inertodetrinite* and *liptodetrinite*, and only a sparse distribution of *lamalginite*, the Orepuki oil shale was defined as a low quality, freshwater lacustrine oil shale with some terrestrial input (Hutton, 1987; Sykes, Pers. comm., 2012) (Table 7.3). This result is in disagreement with the conclusion of the non-conventional model.

The XRD spectra of the clay fraction separated from the Orepuki oil shale show an absence of illite (Table 7.3). The mineralogical index of oil-production potential defined in the current study is a low abundance or absence of illite. Hence, the Orepuki oil shale has relatively good production potential according to this relationship between illite abundance and shale oil potential observed in the current study.

An average bitumen yield of 1.12 wt% was quantified in the samples through solvent extraction using the soxhlet apparatus (Table 7.3). Aliphatic and aromatic bands were identified in the bitumen extracts, inferring a high degree of richness to the organic content of the oil shale. The quality of the organic matter was confirmed through GC-MS of the bitumen extract. Approximately 110 peaks indicative of each of the four constituent compounds of bitumen (alkanes, aromatics, cycloalkanes and heteroatom compounds or NSO fraction) were identified.
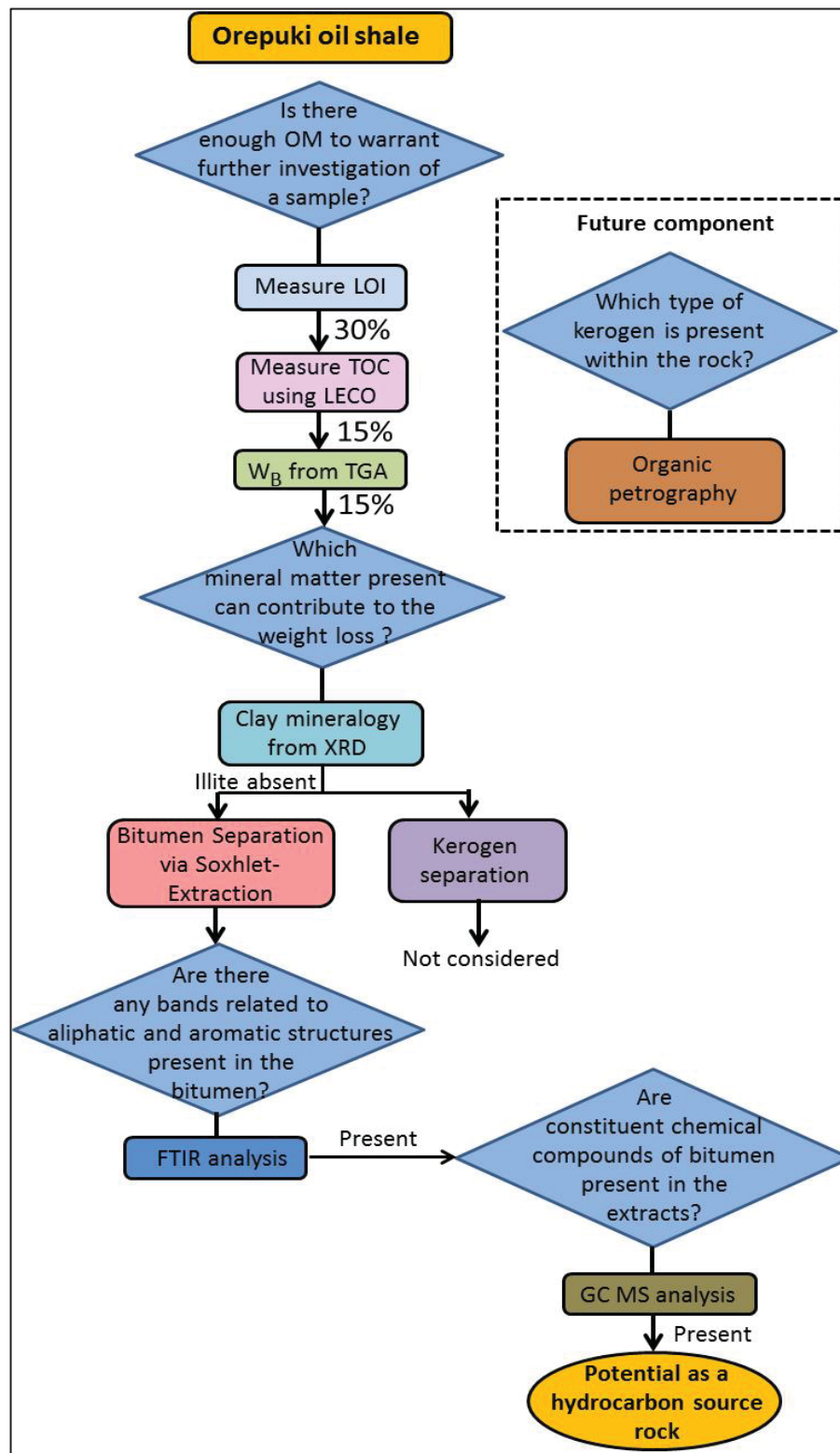
Figure 7.2. *Assessment of source rock hydrocarbon potential of the Orepuki oil shale using the non-conventional production assessment model.*

The conclusion from the non-conventional production potential model is that the Orepuki oil shale is an excellent production potential source rock (Figure 7.2). This conclusion is consistent with that which can be inferred through consideration of the SRA results (Chapter 3). But the model yields superior understanding regarding the production potential of the Orepuki oil shale compared to SRA. The non-conventional model defines an absence of illite in this oil shale, and quantifies with more certainty the richness of organic matter (content and quality). A detailed understanding of the composition of the bitumen fraction of an oil shale cannot be obtained using SRA. The non-conventional model also defines a mixed lacustrine and terrestrial origin of deposition for the kerogen present in the Orepuki oil shale. This is an understanding that could not be derived from SRA.

7.4.2 Assessment model applied to oil shales from the Waipawa Formation

The non-conventional production assessment model (Figure 7.1) can next be used to interpret the physical, thermal and chemical analytical data generated through analysis of samples collected from each of the four outcrops of the Waipawa Formation sampled during the current study (Waipawa type locality, Lower Angora Road quarry, Upper Angora Road and Old Hill Road, Porangahau) (Figure 7.3, 7.4).

Samples of the Waipawa Formation collected from the different outcrops in the East Coast Basin were found to have a wide range of organic matter content as demonstrated by a wide range of LOI and TOC values (Table 7.3). The Waipawa Formation from the Waipawa type locality had the highest LOI and TOC values followed by the Waipawa Formation from the Lower Angora Road quarry, Upper Angora Road and Old Hill Road, Porangahau. Samples from the Waipawa type locality were found to have highest weight loss due to organic matter (W_B) as quantified using TGA (Table 7.3).

Only the Waipawa type locality sample was subjected to organic petrography. This outcrop was chosen over the other outcrops due to the higher yield of organic matter as quantified by thermal analyses. Shale from the Waipawa type locality sample contained

a low content of vitrinite and liptinite macerals, which makes it a low quality oil shale with relatively low production potential relative to the Green River Formation (used as a high quality index sample in the current study). The XRD spectra of the clay separated fraction of each of the samples from the Waipawa Formation show a variable illite content. Illite was generally common (c) as opposed to present (p) in nine out of the twelve Waipawa Formation samples investigated.

The range in bitumen yield was quantified through solvent extraction of samples from the different outcrops (0.28-0.60 wt%) (Table 7.3). The FTIR spectra of each of these extracts displayed aliphatic and aromatic bands which are a function of the presence of aliphatic and aromatic structures. The highest degree of relative aliphaticity was found for samples from the Waipawa type locality and the lowest for samples from Porangahau. This trend in decreasing order of aliphaticity was consistent with the soxhlet bitumen yields. The Waipawa Formation was determined to be more aromatic than the Green River Formation and Orepuki oil shales, due to a relatively higher intensity of bands related to aromatic structures. This conclusion was confirmed by GC-MS analysis. The Waipawa Formation was found to have more peaks associated with aromatic hydrocarbons than the Green River and Orepuki oil shales. Due to the qualitative presence of a large number of aromatic compounds in bitumen extracts from the Waipawa Formation, shale oil from this formation is predicted to have a high octane number. Among the Waipawa Formation samples, the relative contents of the chemical compound classes that define bitumen (alkanes, cycloalkanes, aromatic and heteroatom compounds) were higher for samples from the Waipawa type locality. No cycloalkanes were found in the Waipawa Formation samples collected from the Upper Angora Road and Old Hill Road, Porangahau outcrops.
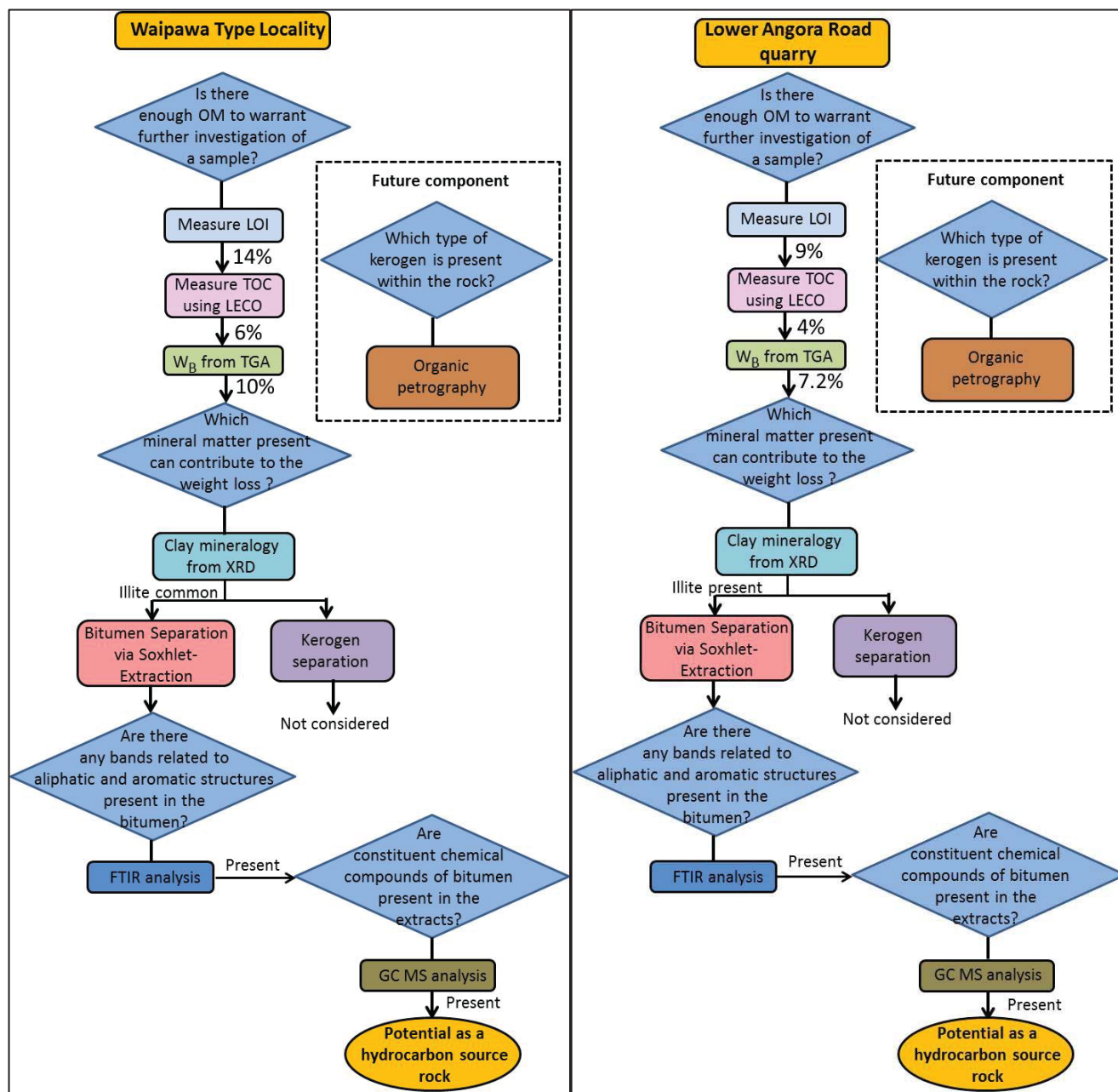
Figure 7.3. Assessment of the source rock hydrocarbon potential of the Waipawa Formation collected from the Waipawa type locality and the Lower Angora Road quarry, using the non-conventional production assessment model. (Note: Illite is considered common if the number of counts recorded for its main peak (at 10Å) are 150-500. Similarly if the number of counts are <150, then it is considered present).
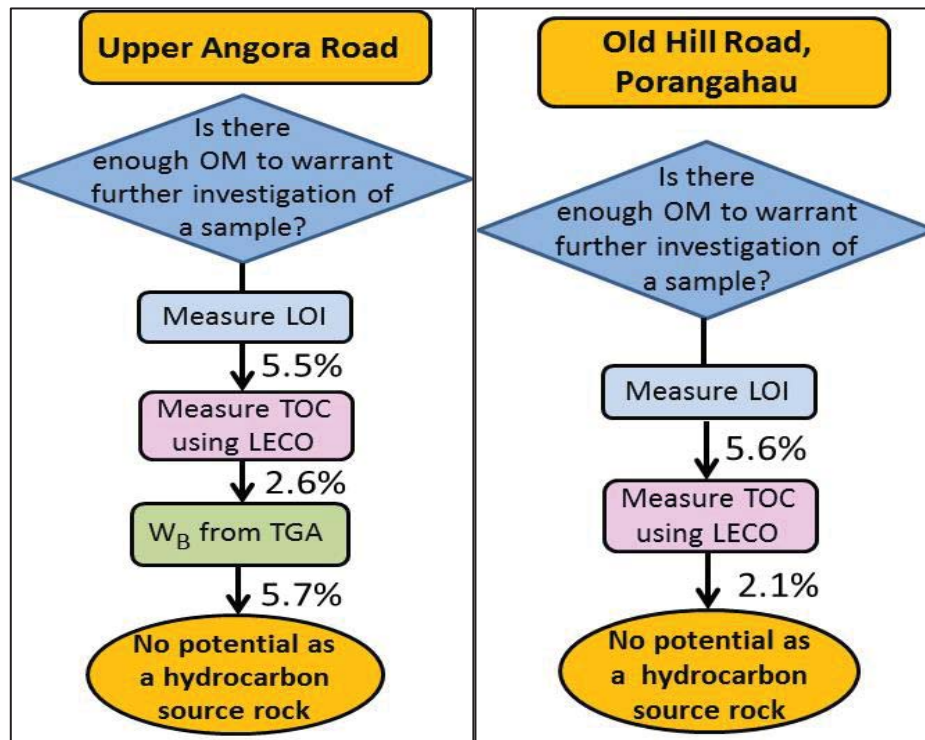
Figure 7.4. *Assessment of the source rock hydrocarbon potential of samples of the Waipawa Formation collected from the Upper Angora Road and Old Hill Road, Porangahau using the non-conventional assessment model.*

The conclusions from the non-conventional production potential model are that the rocks collected from the Waipawa Formation type locality and Lower Angora Road quarry are oil shales, contain organic matter, and have some production potential as source rocks for hydrocarbons (Figure 7.3). This production potential is lower than that exhibited for rocks from the Green River Formation and the Orepuki oil shale. However, samples of the Waipawa Formation collected from Upper Angora Road and Old Hill Road (Porangahau) outcrops have no production potential. Thus there is variation in production potential between the four outcrop locations: the production potential of the Waipawa oil shale is therefore variable in the Waipawa Formation across the East Coast Basin.

These conclusions suggest that the Waipawa type locality and the Lower Angora Road quarry sampling locations could be subjected to further petroleum company resource definition. But the Waipawa Formation exposed at Upper Angora Road and Old Hill

Road outcrops should not be further studied due the low TOC and W_B. The limited production potential of the Waipawa Formation from these two outcrops was defined using very simple thermal techniques: LOI and LECO supported by TGA. The model discounted the potential of these samples before more complex techniques needed to be employed.

The conclusions from the non-conventional production potential model are consistent with those which can be inferred through consideration of the SRA results (Chapter 3). But the model yields superior understanding regarding the production potential of the Waipawa Formation compared to SRA. The low content of illite (common), mixed marine and terrestrial origin of this formation, high degree of richness of the constituent organic content, and the inferred good quality of oil which may be derived from its bitumen are information and understanding that cannot be obtained from SRA.

7.5 General conclusions

Using a suite of physical, thermal and chemical analytical techniques, a novel non-conventional production potential model has been derived that can assess the production potential of the Orepuki oil shale of Southland, New Zealand and rocks from the Waipawa Formation of East Coast Basin. The conclusions drawn though application of this model to understand the physical, thermal and chemical characteristics of the shale rocks, have been validated against conventional SRA analysis, and when compared to this benchmark technique, are valid. However, the non-conventional model provides superior scientific data, and could be employed for source rock analysis in earth science laboratories around the world.

The conclusions drawn through using the model support the hypothesis that a non-conventional analytical tool is better suited to the assessment of the production potential of oil shales than conventional SRA. The suite of analytical techniques used in this study (LOI, LECO, TGA, organic petrography, XRD, FTIR and GC-MS) provided scientifically detailed information on the petroleum potential of source rocks. To understand the context and mechanism of hydrocarbon resource, detailed thermal, physical and chemical analyses should be performed rather than relying solely on

Source Rock Analysis (SRA) which is only a thermal decomposition process giving hydrocarbon yield, maturity and TOC.

As a final conclusion to this thesis, it is proposed that the non-conventional production potential model defined in the study should be used in future shale rock assessments. The model has been derived through consideration of a range of productive and non-productive oil shales, including the well-studied Green River Formation, and generated accurate conclusions when applied to the historically producing Orepuki oil shale and the Waipawa Formation. Oil shales within the Waipawa Formation continue to be the subject of conventional exploration efforts. The next stage of model development should be rigorous testing using a greater number of samples collected from different shale rocks, and from within specific formations. The sample number of the current study was appropriate to develop the underpinning analytical methodology and to integrate the various techniques into a model. However, an extensive phase of testing will give better confidence in the abality of the model to accurately describe the production potential of subject shale rocks.

There are some limitations to the defined model. 1) The relationship between an absence or low abundance of illite and shale oil potential is based only on the samples assessed in the current study and requires further verification before definite conclusions can be drawn. 2) Organic petrography is not part of the integrated model proposed in this study. Only four samples were assessed using this technique and so provided only limited confidence in the robustness of the obtained data. However, organic petrography shows good potential for future integration into the model. 3) Resolution of hydrocarbon signals may have been limited in the GC-MS spectra of the solvent-extracted bitumen due to a coelution effect and masking of low abundance hydrocarbon signatures by higher abundance compounds.

7.6 Opportunities for further development of the non-conventional production potential assessment model for oil shales

This thesis is a first attempt to propose a non-conventional production model to assess hydrocarbon source rocks. There are many areas for further research and development which could strengthen the model. As described, the next phase of work should be extensive testing of the conclusions of the model against benchmark conventional techniques (SRA as well as vitrinite reflectance) using an increased number of samples. I believe there are certain specific aspects that should be explored in subsequent work:

- The proposed model should be tested on other international oil shales in order to further verify the reliability of the model to derive valid conclusions. An increased number of samples from within individual formations and outcrops should be collected and analysed to further explore analytical variability that can be attributed to the techniques of the study rather than heterogeneity of the physio-chemical properties of the shale rocks.

- An increased number of samples of the Waipawa Formation from additional outcrops should be analysed to **a)** place the data of the techniques of the non-conventional model into better context with published literature on the Waipawa Formation, and **b)** to further test the ability of the non-conventional production potential model to provide superior scientific understanding of this potential source rock.

- The relationship between illite and shale oil production potential should be investigated through generating additional data on the mineralogy of shale deposits. This is a poorly studied and potentially very interesting area of earth science.

- Further study on the effect of different minerals, specifically illite and montmorillonite, on the production of shale oil per unit of organic carbon should be carried out to see if the mineral phase has a catalytic effect on oil expulsion and quality.

- Replicate samples should be prepared and analysed by organic petrography. Grains selected for study, especially from samples with dispersed organic matter, might not be representative of the whole sample. The organic petrography physical analysis technique should be integrated into the non-conventional production potential model.

- Vitrinite reflectance, an extensively used and accurate conventional technique to measure the maturity of source rocks, should be used in tandem with SRA to further validate the conclusions of the non-conventional model and to provide a stronger baseline against which the conclusions of the non-conventional model can be tested.

- Quantitative analytical data on the organic composition and maturity of hydrocarbon source rocks should be generated to expand and strengthen the non-conventional production potential model.

- There is good future potential for FTIR data to be quantified and to be used in tandem with GC-MS data to give quantitative chemical information about the production potential of oil shales. Quantification of the FTIR data was not performed in the current study (FTIR was used qualitatively to indicate the presence or absence of functional groups that could be attributed to hydrocarbons). However, there are methods available for the quantification of FTIR data and these could be used in the future, with the subsequent integration of quantitative trigger point into the non-conventional model.

- Specifically, calibrated Pyrolysis-GC-MS or Pyrolysis-GC analysis could be used to identify the different of hydrocarbons physically evolved from the cracking of kerogen in shale rocks.

References

Aboulkas, A., Makayssi, T., Bilali, L., El-harfi, K., & Nadifiyine, M. (2012). Co-pyrolysis of oil shale and high density polyethylene: structural characterisation of the oil. *Fuel Processing Technology, 96*, 203-208.

Afzal, S., Younas, M., & Hussain, K. (1999). Physical and chemical characterisation of the agriculture lands of the Soan−Sakesar Valley, Salt Range, Pakistan. *Australian Journal of Soil Research, 37*(6), 1035-1046.

Ahmad, K. A., Man, H. Q., & Zeb, Y. (2012). Seismic facies modelling of Potwar Basin using seismic and well log data. *Geosciences, 2*(6), 192-211.

Ahmad, S. (2003). A comparative study of structural styles in the Kohat Plateau, NW Himalayas, NWFP, Pakistan. *PhD thesis*, National Centre of Excellence in Geology, University of Peshawar.

Ahmad, W., & Alam, S. (2007). Organic geochemistry and source rock characteristics of Salt Range Formation, Potwar Basin, Pakistan. *Pakistan Journal of Hydrocarbon Research, 17*, 37-59.

Akande, S. O., Egenhoff, S. O., Obaje, N. G., Ojo, O. J., Adekeye, O. A., & Erdtmann, B. D. (2012). Hydrocarbon potential of Cretaceous sediments in the Lower and Middle Benue Trough, Nigeria: Insights from new source rock facies evaluation. *Journal of African Earth Sciences, 64*, 34-47.

Akinlua, A., Jochmann, M. A., Qian, Y., Sulkowski, M., & Schmidt, T. C. (2012). Factors controlling leaching of polycyclic aromatic hydrocarbons from petroleum source rock using non-ionic surfactant. *Chromatographia, 75*(5-6), 213-221.

Akinlua, A., Maende, A., Adekola, S. A., Swakamisa, O., Fadipe, O. A., & Akinyemi, S. A. (2011). Source rock potential of selected Cretaceous shales, Orange Basin, South Africa. *International Geology Review, 53*(13), 1508-1521.

Al-Harahsheh, A., Al-Harahsheh, M., Al-Otoom, A., & Allawzi, M. (2009). Effect of demineralisation of El-lajjun Jordanian oil shale on oil yield. *Fuel Processing Technology, 90*(6), 818-824.

Al-Harahsheh, M., Al-Ayed, O., Robinson, J., Kingman, S., Al-Harahsheh, A., Tarawneh, K., Saeid, A., & Barranco, R. (2011). Effect of demineralisation and

heating rate on the pyrolysis kinetics of Jordanian oil shales. *Fuel Processing Technology, 92*(9), 1805-1811.

Al-Harahsheh, M., Shawabkeh, R., Al-Harahsheh, A., Tarawneh, K., & Batiha, M. M. (2009). Surface modification and characterization of Jordanian kaolinite: Application for lead removal from aqueous solutions. *Applied Surface Science, 255*(18), 8098-8103.

Al-Harasheh, A. M. (2011). The effect of a solvent system on the yield and fractional composition of bitumen extracted from the El-lajjun and Sultani oil shale deposits. *Energy Sources, Part A: Recovery, Utilization, and Environmental Effects, 33*(7), 665-673.

Alderson, V. C. (2008). *Oil shale*. Colorado School of Mines.

Allix, P., Burnham, A., Fowler, T., Herron, M., Kleinberg, R., & Symington, B. (2010). Coaxing oil from oil shale. *Oilfield Review, 22*(4).

Allred, V. D. (1966). Kinetics of oil shale pyrolysis *Chemical Engineering Progress, 62*, 55-60.

Alpern, B. (1980). Petrography of kerogen. In B. Durand (Ed.), *Kerogen: insoluble organic matter from sedimentary rocks* (pp. 339-368). Paris: Editions Technip.

Alstadt, K. N., Katti, D. R., & Katti, K. S. (2012). An *in-situ* FTIR step-scan photoacoustic investigation of kerogen and minerals in oil shale. *Spectrochimica Acta Part A: Molecular and Biomolecular Spectroscopy, 89*, 105-113.

Alstadt, K. N., Katti, D. R., & Katti, K. S. (2012). An in situ FTIR step-scan photoacoustic investigation of kerogen and minerals in oil shale. *Spectrochimica Acta - Part A: Molecular and Biomolecular Spectroscopy, 89*, 105-113.

Altun, N. E. (2009). Incidental release of bitumen during oil shale grinding and impacts on oil shale beneficiation. *Oil Shale, 26*(3), 382-398.

American Geological Institute. (1962). *Dictionary of geological terms* (Dolphin reference books ed.). Garden city, New York: Dolphin Books Doubleday & company, Inc.

Andrews, A. (2006). *Oil Shale: History, Incentives, and Policy. Congressional Research Service* (No. RL33359).

Arro, H., Prikk, A., & Pihu, T. (2003). Calculation of qualitative and quantitative composition of Estonian oil shale and its combustion products, part 1, calculation on the basis of heating value. *Fuel, 82*(18), 2179-2195.

Asif, M., Fazeelat, T., & Grice, K. (2011). Petroleum geochemistry of the Potwar Basin, Pakistan: 1. Oil−oil correlation using biomarkers, δ^{13}C and δD. *Organic Geochemistry, 42*(10), 1226-1240.

Asif, M., & Muneer, T. (2007). Energy supply, its demand and security issues for developed and emerging economies. *Renewable and Sustainable Energy Reviews, 11*(7), 1388-1413.

Aunela-Tapola, L. A., Frandsen, F. J., & Hasanen, E. K. (1998). Trace metal emissions from the Estonian oil shale fired power plant. *Fuel Processing Technology, 57*(1), 1-24.

Avery, B. W., & Bullock, P. (1977). Mineralogy of clayey soils in relation to soil classification. *Technical Monograph No. 10*, 1-64.

Azevedo, D. A., Lacorte, S., Vinhas, T., Viana, P., & Barcelo, D. (2000). Monitoring of priority pesticides and other organic pollutants in river water from Portugal by gas chromatography-mass spectrometry and liquid chromatography-atmospheric pressure chemical ionization mass spectrometry. *Journal of Chromatography A, 879*(1), 13-26.

Barker, J. F., Dickhout, R. D., Russell, D. J., Johnson, M. D., & Gunther, P. R. (Eds.). (1983). *The organic geochemistry of the Ordovician Whitby Formation- a possible Ontario shale*. Washington: American Chemical Society.

Behar, F., Beaumont, V., & Penteado, H. L. D. B. (2001). Rock-Eval 6 technology: Performances and developments. *Oil & Gas Science and Technology, 56*(2), 111-134.

Behar, F., Vandenbroucke, M. D., Tang, Y., & Marquis, F. (1997). Thermal cracking of kerogen in open and closed systems: determination of kinetic parameters and stoichiometric coefficients for oil and gas generation. *Organic Geochemistry, 26*(5/6), 321-339.

Bell, J. S. (1990). Investigating stress regimes in sedimentary basins using information from oil industry wireline logs and drilling records. *Journal of Petroleum Technology, 48*(1), 305-325: Geological Society, London, Special Publication.

Berg, V. (2008). *Basin-wide evaluation of the uppermost Green River Formation's oil shale resource, Uinta Basin, Utah and Colorado*. Utah Geological Survey Special Survey, 128.

Bernard, S., Horsfield, B., Schulz, H.-M., Wirth, R., Schreiber, A., & Sherwood, N. (2012). Geochemical evolution of organic-rich shales with increasing maturity:

A STXM and TEM study of the Posidonia Shale (Lower Toarcian, northern Germany). *Marine and Petroleum Geology, 31*(1), 70-89.

Bertram, R. G., Eng, P., & Boyd, L. D. (2008). *Resources estimation and economic evaluation East Coast Basin, New Zealand*. Trans-Orient Petroleum LTD.

Bertrand, P., Bordenave, M. L., Brosse, E., Espitalie, J., & Houzay, J. P. (1993). Other methods and tools for source rock appraisal. In M. L. Bordenave (Ed.), *Applied petroleum geochemistry*. Paris: Editions Technip.

Bhargava, S., Awaja, F., & Subasinghe, N. D. (2005). Characterisation of some Australian oil shale using thermal, X-ray and IR techniques. *Fuel, 84*(6), 707-715.

Birdwell, J. E., Ruble, T. E., Laughrey, C. D., Roper, D. R., & Walker, G. (2011). Differentiating organic carbon residues in spent oil shale. *30th Oil Shale Symposium*, Colorado School of Mines, 1-22.

Bjorlykke, K. (2010). Source rocks and petroleum geochemistry. In K. Bjorlykke (Ed.), *Petroleum Geoscience: From sedimentary environments to rock physics* (pp. 339-348). Oslo: Springer-Verlag.

Blanco, C. G., Prado, J. G., Guillen, M. D., & Borrego, A. G. (1992). Preliminary results of extraction experiments in an oil shale. *Organic Geochemistry, 18*(3), 313-316.

Bonder, E., & Koel, M. (1998). Application of supercritical fluid extraction to organic geochemical studies of oil shales. *Fuel, 77*(3), 211-213.

Borrego, A. G. (1996). 1H NMR and FTIR spectroscopic studies of bitumen and shale oil from selected Spanish oil shales. *Energy and Fuels, 10*(1), 77-84.

Borrego, A. G., Prado, J. G., Fuente, E., Guillen, M. D., & Blanco, C. G. (2000). Pyrolytic behaviour of Spanish oil shales and their kerogens. *Journal of Analytical and Applied Pyrolysis, 56*(1), 1-21.

Bradley, W. H. (1931). Origin and microfossils of the oil shale of the Green River Formation of Colorado and Utah. *US Geological Survey Professional Paper, 168*, 58.

Braun, R. L., Burnham, A. K., Reynolds, J. G., & Clarkson, J. E. (1991). Pyrolysis kinetics for lacustrine and marine source rocks by programmed micropyrolysis. *Energy & Fuels, 5*(1), 192-204.

Brooks, J. D., Gould, K., & Smith, J. W. (1969). Isoprenoid hydrocarbons in coal and petroleum. *Nature, 222*(5190), 257-259.

Brown, R. L. (1990). Exploration and geology techniques. In B. A. Kennedy (Ed.), *Surface mining* (pp. 15-21). Baltimore, Maryland: Port City Press.

Brownfield, M. E., Johnson, R. C., & Dyni, J. R. (2010). Sodium carbonate resources of the Eocene Green River Formation, Uinta Basin, Utah and Colorado *oil shale resources of the Uinta Basin, Utah and Colorado* (pp. 1-12). Virginia: U.S. Geological Survey Digital Data Series DDS-69-BB, Chapter 2.

Bruce, C. H. (1984). Smectite dehydration-its relation to structural development and hydrocarbon accumulation in Northern Gulf of Mexico Basin. *Bulletin of the American Association of Petroleum Geologists, 68*(6), 673-683.

Budinova, T., Razvigorova, M., Tsyntsarski, B., Petrova, B., Ekinci, E., & Yardim, M. F. (2009). Characterization of Bulgarian oil shale kerogen revealed by oxidative degradation. *Chemie der Erde - Geochemistry, 69*(3), 235-245.

Burnham, A. K. (2008). 28th Oil Shale Symposium, Colorado School of Mines, Golden.

Burnham, A. K., Braun, R. L., & Coburn, T. T. (1996). An appropriate kinetic model for well-preserved algal kerogens. *Energy & Fuels, 10*(1), 49-59.

Burnham, A. K., Huss, B. E., & Singleton, M. F. (1983). Pyrolysis kinetics for Green River oil shale from the saline zone. *Fuel, 62*, 1199-1204.

Cahill, J. P. (1995). Evolution of Winton Basin, Southland. *New Zealand Journal of Geology and Geophysics, 38*(2), 245-258.

Cane, R. F. (1942). Studies in Orepuki oil shale. On *The N.Z. Journal of Science and Technology*.

Cane, R. F. (1967). The constitution and synthesis of oil Shale. *7th World Petroleum Congress*, April 2-9 (Mexico City), 681.

Carmona, V. B., Oliveira, R. M., Silva, W. T. L., Mattoso, L. H. C., & Marconcini, J. M. (2013). Nanosilica from rice husk: Extraction and characterisation. *Industrial Crops and Products, 43*, 291-296.

Carr, D. E. (1962). In-situ retorting of oil shale. *U.S. Patent office, 3,017,168*.

Cashion, W. B. (1967). *Geology and fuel resources of the Green River Formation south-eastern Uinta Basin, Utah and Colorado*: Geological survey professional paper 548.

Chengzao, J., Min, Z., & Yongfeng, Z. (2012). Unconventional hydrocarbon resources in China and the prospect of exploration and development. *Petroleum Exploration and Development, 39*(2), 139-146.

Cho, Y., Jin, J. M., Witt, M., Birdwell, J. E., Na, J. G., Roh, N. S., & Kim, S. (2013). Comparing laser desorption ionization and atmospheric pressure photoionization coupled to fourier transform ion cyclotron resonance mass spectrometry to characterize shale oils at the molecular level. *Energy & Fuels, 27*(4), 1830-1837.

Christian, B. (Pers. comm., 2013). Current oil shale production in the World. *International Energy Agency (IEA)*.

Churcher, P. L., & Dickhout, R. D. (1987). Analysis of ancient sediments for total organic carbon - some new ideas. *Journal of Geochemical Exploration, 29*, 235-246.

Clayton, J. L., & King, J. D. (1987). Effects of weathering on biological marker and aromatic hydrocarbon composition of organic matter in Phosphoria shale outcrop. *Geochimica et Cosmochimica Acta, 51*(8), 2153-2157.

Comstock, S. C. (1981). *Source rock potential of West Coast samples*. Ministry of Economic Development. Ministry of Economic Development.

Cumming, V. M., Selby, D., & Lillis, P. G. (2012). Re-Os geochronology of the lacustrine Green River Formation: insights into direct depositional dating of lacustrine successions, Re-Os systematics and paleocontinental weathering. *Earth and Planetary Science, 259-360*, 194-205.

D'Ath, M. W. (2002). *The clay mineralogy and erosion of the Waipaoa River catchment, Gisborne, New Zealand.* (Masters of Science), Massey University (Unpublished thesis). 133p.

Dahl, B., Bojesen-Koefoed, J., Holm, A., Justwan, H., Rasmussen, E., & Thomsen, E. (2004). A new approach to interpreting Rock-Eval S_2 and TOC data for kerogen quality assessment. *Organic Geochemistry, 35*(11-12), 1461-1477.

Daniels, A., Johnston, L., & Otter, C. (2004). *Revise as chemistry for salters (SAR)* (T. Jackson Ed.): Heinemann Educational Publishers (pp.27).

Daoudi, L., Rocha, F., Ouajhain, B., Dinis, J. L., Chafiki, D., & Callapez, P. (2008). Palaeoenvironmental significance of clay minerals in Upper Cenomanian-Turonian sediments of the Western High Atlas Basin (Morocco). *Clay Minerals, 43*, 615-630.

Davies, E. J., Frederick, J. B., Leask, W. L., & Williams, T. J. (1998). East Coast Basin exploration. *New Zealand Petroleum Conference proceedings 1998* (pp. 101-113). Wellington: New Zealand. Ministry of Economic Development.

Davies, E. J., Frederick, J. B., Leask, W. L., & Williams, T. J. (2000). East Coast drilling results. *New Zealand Petroleum Conference Proceedings 2000* (pp. 84–93): New Zealand. Ministry of Economic Development.

Dean, W. E. (1974). Determination of carbonate and organic matter in calcareous sediments and sedimentary rocks by loss on ignition: Comparison with other methods. *Journal of Sedimentary, 44*(1), 242-248.

Deer, W. A., & Howie, J. Z. (1966). *An Introduction to rock-forming minerals*. New York: Longmans, Green and Co Ltd, pp. 528.

Demirel, Y. (2012). Energy and energy types *Energy: production, conversion, storage, conservation and coupling* (pp. 27-68). London: Springer-Verlag London Ltd.

Deng, S., Wang, Z., Gu, Q., Meng, F., Li, J., & Wang, H. (2011). Extracting hydrocarbons from Huadian oil shale by sub-critical water. *Fuel Processing Technology, 92*(5), 1062-1067.

Derenne, S., Largeau, C., Brukner-Wein, A., Hetenyi, M., Bardoux, G., & Mariotti, A. (2000). Origin of variations in organic matter abundance and composition in a lithologically homogeneous maar-type oil shale deposit (Gerce, Pliocene, Hungary). *Organic Geochemistry, 31*, 787-798.

Didyk, B. M., Simoneit, B. R. T., Brassell, S. C., & Eglinton, G. (1978). Organic geochemical indicators of palaeoenvironmental conditions of sedimentation. *Nature, 272*(5650), 216-222.

Dogan, O. M., & Uysal, B. Z. (1996). Non-isothermal pyrolysis kinetics of three Turkish oil shales. *Fuel, 75*(12), 1424-1428.

Donnell, J. R. (1961). Oil shale resources of the Piceance Creek Basin between the Colorado and White Rivers, north-western Colorado. *Geological Survey Bulletin 1082 — L*, 835-885.

Duncan, D. C., Hail, W. J., O'Sullivan, R. B., & Pipiringos, G. N. (1974). *Four newly named tongues of Eocene Green River Formation, Northern Piceance Creek Basin, Colorado*. Geological Survey Bulletin 1394 - F.

Durand, B. (1988). Sedimentary organic matter and kerogen, definition and quantitative importance of kerogen. In E. A. Beaumont & N. H. F. Tulsa (Eds.), *Geochemistry* (pp. 81-102). Oklahoma: AAPG.

Durham, L. S. (2012, pp 6-8). Study cautions overenthusiasm on shale capacity, *AAPG Explorer*.

Dutton, S. P. (1980). Petroleum source rock potential and thermal maturity, Palo Duro Basin, Texas. *Geological Circular 80-10, Bureau of Economic Geology*, 17-22.

Dyni, J. R. (1981). *Geology of the Nahcolite deposits and associated oil shales of the Green River Formation in the Piceance Basin, Colorado.* (PhD), University of Colorado, Colorado.

Dyni, J. R. (2003). *Geology and resources of some world oil shale deposits* (H. Uibopuu & N. Kareva Eds. 3 ed. Vol. 20): Estonian Academy Publishers.

Dyni, J. R. (2006). Geology and resources of some world oil-shale deposits. *U.S. Geological Survey Scientific Investigations Report*

Elphick, J. O. (1954). The coal mines of New Zealand. *Coal Section, Dominion Laboratory, Wellington: unpublished report*.

Enefit. (2011). World Reserves. Retrieved 30th December, 2012, from https://www.enefit.com/en/oil-shale

Eslinger, E., & Pevear, D. (1926). Clay minerals for petroleum geologists and engineers. *SPEM short course No. 22*.

Espitalie, J., Deroo, G., & Marquis, F. (1985). *Rock-Eval Pyrolysis and its applications*. Institut Francais du Petrole.

Espitalie, J., Laporte, J. L., Madec, M., Marquis, F., Leplat, P., Paulet, J., & Boutefeu, A. (1977). Methode rapide de caracterisation des roches meres, de leur potential petrolier et de leur degre devolution. *Revue de Institut Francais de Petrole, 32*(1), 23-42.

Etheridge, R. D., Pesti, G. M., & Foster, E. H. (1998). A comparison of nitrogen values obtained utilising Kjeldahl nitrogen and Dunmas combustion methodologies (LECO CNS 2000) on samples typical of an animal nutrition analytical laboratory. *Animal Feed Science and Technology, 73*, 21-28.

Fazeelat, T., & Yousaf, M. S. (2004). Geochemical characterisation of outcrop sediments from Dharangi-Upper Indus Basin Pakistan. *Jour. Chem. Soc. Pak, 26*(4), 355-359.

Field, B., Funnell, R., Killops, S., Rogers, K., & Uruski, C. (1998). Petroleum systems of the East Coast region, New Zealand. In G. B. Arehart & J. R. Hulston (Eds.), *Water-rock interaction: Proceedings of the 9th International Symposium on Water-Rock Interaction* (pp. 317-319). (pp. 317-319). Rotterdam: A.A. Balkema.

Field, B. D., Uruski, C. I., & others. (1997). Cretaceous - Cenozoic geology and petroleum systems of the East Coast Region, New Zealand. *Geological and Nuclear Sciences (GNS), Monograph 1*.

Finlay, H. J. (1939). New Zealand foraminifera: the occurrence of Rzehakina, Hantkenina and Zeauvigerina. *Transactions of Royal Society of New Zealand, 68*(4), 534-543.

Fischer, A. G., & Arthur, M. A. (1977). Secular variations in the pelagic realm. *Society of Economic Palaeontologists and Mineralogists special publication 25*, 19-50.

Fowler, T., & Chronicle, H. (2012). Report says we have more oil than we thought, Business, *Chron*. Retrieved from http://www.chron.com/default/article/Report-says-we-have-more-oil-than-we-thought-2173154.php

Francu, J., Harvie, B., Laenen, B., Siirde, A., & Veiderma, M. (2007). A study on the EU oil shale industry-viewed in the light of the Estonian experience. A report by EASAC to the committee on industry, research and energy of the European parliament. *European Academies Science Advisory Council*.

Frost, R. L., Ruan, H., Kloprogge, J. T., & Gates, W. P. (2000). Dehydration and dehydoxylation of nontronites and ferruginous smectite. *Thermochimica Acta, 346*(1-2), 63-72.

Frysinger, G. S., & Gaines, R. B. (2001). Separation and identification of petroleum biomarkers by comprehensive two-dimensional gas chromatography. *Journal of Separation Science, 24*(2), 87-96.

Gang, L. (2007). The application of geochemical analysis to the study of sedimentary environment of Qianjiang Formation in Qianjiang Depression. *Acta Geoscientica Sinica, 28*(4), 335-340.

Gee, E. R. (1945). The age of saline series of the Punjab and Kohat. *Nat. Acad. Sci. India Proc., Section B, 14*(6), 269-310.

GeoSphere Consulting Ltd. (1999). Source rock character and maturation review, PEP 38213, Waiau Basin, Southland, New Zealand. *Ministry of Economic Development, PR 2448, pp 4-49*.

Ghazi, S., & Mountney, N. P. (2011). Petrography and provenance of the Early Permian Fluvial Warchha sandstone, Salt Range, Pakistan. *Sedimentary Geology, 233*(1−4), 88−110.

Gibbons, M. J. (1980). *A review of the maturity and source rock potential in the Gisborne region, East Coast Basin, North Island, New Zealand* (No. 835).

Gordon, D. (2012). Understanding unconventional oil- Carnegie endowment for international peace. *Energy and Climate*, 1-28.

Gosden, E. (2012). Saudis may run out of oil to export by 2030. *The Telegraph*. http://www.telegraph.co.uk/finance/newsbysector/energy/oilandgas/9523903/Saudis-may-run-out-of-oil-to-export-by-2030.html

Grice, K., Changqun, Love, G. D., Bottcher, M. E., Twitchett, R. J., Grosjean, E., Summons, R. E., Turgeon, S. C., Dunning, W., & Jin, Y. (2005). Photic Zone Euxinia during the Permian-Triassic superanoxic event. *Science, 307*(5710), 706-709.

Grice, K., Schouten, S., Peters, K. E., & Damste, J. S. S. (1998). Molecular isotopic characterisation of hydrocarbon biomarkers in Palaeocene-Eocene evaporitic, lacustrine source rocks from the Jianghan Basin, China. *Organic Geochemistry, 29*(5-7), 1745-1764.

Guillen, M. D., & Cabo, N. (1997). Characterisation of edible oils and lard by Fourier Transform Infrared Spectroscopy. Relationships between composition and frequency of concrete bands in the fingerprint region. *JAOCS, 74*(10), 1281-1286.

Haddadin, R. A., & Mizyed, F. A. (1974). Thermogravimetric Analysis Kinetics of Jordan Shale. *Industrial & Engineering Chemistry Process Design and Development, 13*(4), 332-336.

Hakimi, M. H., & Abdullah, W. H. (2013). Organic geochemical characteristics and oil generating potential of the Upper Jurassic Safer shale sediments in the Marib-Shabowah Basin, western Yemen. *Organic Geochemistry, 54*, 115-124.

Harris, W., & White, N. (2008). X-ray diffraction techniques for soil mineral identification. In A. L. Ulery & L. R. Drees (Eds.), *Methods of soil analysis: Part 5 — Mineralogical methods* (pp. 81-116). Madison: Soil Science Society of America.

Hartman-Stroup, C. (1987). The effect of organic matter type and organic carbon content on Rock-Eval hydrogen index in oil shales and source rocks. *Organic Geochemistry, 11*(5), 351-369.

Haven, H. L. t., Leeuw, J. W. d., Rullkotter, J., & Sinninghe, J. S. (1987). Restricted utility of the pristane/phytane ratio as a palaeoenvironmental indicator. *Nature, 330*(6149), 641-643.

He, L., Li, X., Du, Y., Wu, G., Li, H., & Sui, H. (2012). Parameters of solvent extraction for bitumen recovery from oil sands. *Advanced Materials Research, 347-353*, 3728-3731.

Hector, J. (1866). Coal deposits of New Zealand. *New Zealand Geological Survey, Reports of Geological Explorations 1*, 46 p.

Heinberg, R. (2003). The party's over: Oil, war and the fate of industrial societies (pp. 81-122). Gabriola Island: New Society Publishers.

Henley, R. W., & Berger, B. R. (1993). What is an exploration model anyway? An analysis of the cognitive development and use of models in mineral exploration. *Mineral deposit modelling, 40*.

Hetenyi, M. (1995). Simulated thermal maturation of type I and III kerogens in the presence, and absence, of calcite and montmorillonite. *Organic Geochemistry, 23*(2), 121-127.

Hillier, J. L., Fletcher, J. S., Isackson, C., Orgill, J., & Flemming, T. H. (2009). An improved method for determination of kinetic parameters from constant heating rate TGA oil shale pyrolysis data. *ACS National Meeting Book of Abstracts, 54*, 155-157.

Hillier, J. L., & Fletcher, T. H. (2011). Pyrolysis kinetics of a Green River oil shale using pressurized TGA. *Energy Fuels, 25*(1), 232-239.

Hollis, C. J., Field, B. D., Crouch, E. M., & Sykes, R. (2006). How good a source rock is the Waipawa (Black Shale) Formation beyond the East Coast Basin? An outcrop based case study from Northland.   Retrieved 10 August 2012, from http://www.nzpam.govt.nz/cms/petroleum/conferences/conference-proceedings-2006

Hollis, C. J., & Manzano-Kareah, K. (2005). Source rock potential of the East Coast Basin (central and northern regions). *Ministry of Economic Development petroleum report 3179*, 1-156.

Hornibrook, N. B. (1959). Waipawa Black Shale (siltstone). *Lexique stratigraphique international, 6*(4), 443-444.

Hornibrook, N. B., & Harrington, H. J. (1957). The status of the Wangoloan State. *New Zealand Journal of Science and Technology, 38B*(6), 655-670.

Hower, J., Eslinger, E. V., Hower, M. E., & Perry, E. A. (1976). Mechanism of burial metamorphism of argillaceous sediment: 1. mineralogical and chemical evidence. *Geological Society of America Bulletin, 87*(5), 725-737.

Hughes, W. B., Holba, A. G., & Dzou, L. I. P. (1995). The ratios of dibenzothiophene to phenanthrene and pristane to phytane as indicators of depositional environment and lithology of petroleum source rocks. *Geochem et Cosmochimica Acta, 59*(17), 3581-3598.

Hussain, K., Siddiqui, M. A., & Shams, F. A. (1985). Clay mineralogy of some thin cover soils of Punjab and their bearing on engineering properties. *The Geological Bulletin of Punjab University, 20*, 11-23.

Hutson, R. J., & Smith, G. O. (1987). Geological evaluation of PPL 38074, Southland Basin, New Zealand. *New Zealand unpublished petroleum report 1241*, Crown Minerals, Ministry of Economic Development, 1-190.

Hutton, A., Bharati, S., & Robl, T. (1994). Chemical and petrographic classification of kerogen/macerals. *Energy & Fuels, 8*(6), 1478-1488.

Hutton, A. C. (1987). Petrographic classification of oil shales. *International Journal of Coal Geology, 8*(3), 203-231.

Hutton, A. C. (1988). The lacustrine Condor oil shale sequence. *Geological Society, London, Special Publications, 40*(1), 329-340.

Hwang, R. J., Teerman, S. C., & Carlson, R. M. (1998). Geochemical comparison of reservoir solid bitumens with diverse origins. *Organic Geochemistry, 29*(1-3).

Ibarra, J. V., Munoz, E., & Moliner, R. (1996). FTIR study of evolution of coal structure during the coalification process. *Organic Geochemistry, 24*(6-7), 725-735.

Ingo, G. M., Chiozzni, G., Faccenda, V., Bemporad, E., & Riccucci, C. (1998). Thermal and microchemical characterisations of $CaSO_4-SiO_2$ investment materials for casting jewellery alloys. *Thermochimica Acta, 321*(1-2), 175-183.

Ingram, L. L., Ellis, J., Crisp, P. T., & Cook, A. C. (1983). Comparative study of oil shales and shale oils from the Mahogany Zone, Green River Formation (U.S.A) and Kerosene Creek Seam, Rundle Formation (Australia). *Chemical Geology, 38*(3-4), 185-212.

International Energy Agency. (2011). World Energy Outlook 2011. from www.iea.org/weo/docs/weo2011/executive_summary.pdf.

Jaber, J. O., Abu-Qudis, M., & Sawalha, S. (2005). Kinetics of pyrolysis of Attarat oil shale by thermogravimetry. *Oil Shale, 22*(1), 51-64.

Jaber, J. O., & Probert, S. D. (1999). Pyrolysis and gasification kinetics of Jordanian oil-shales. *Applied Energy, 63*(4), 269-286.

Jaber, J. O., & Probert, S. D. (2000). Non-isothermal thermogravimetry and decomposition kinetics of two Jordanian oil shales under different processing conditions. *Fuel Processing Technology, 63*(1), 57-70.

Jaber, J. O., Probert, S. D., & Williams, P. T. (1999). Evaluation of oil yield from Jordanian oil shales. *Energy, 24*, 761-781.

Jackson, M. L. (1956). *Soil chemical analysis – Advanced Course*.

Jamal, A. (2006). *Jordan oil shale, availability, distribution and investment opportunity*. Paper presented at the International conference on oil shale: "Recent trends in oil shale", Amman, Jordan.

Jamil, A., & Sheikh, R. A. (2012). An overview of Neoproterozoic reservoirs in Pakistan. *Geological Society, London, Special Publications, 366*(1), 111-121.

Jarvie, D. M. (1991). Factors affecting Rock-Eval derived kinetic parameters. *Chemical Geology, 93*(1-2), 79-99.

JCPDS. (1980). (1980 ed.): International Centre for Diffraction Data.

Jiang, X. M., Han, X. X., & Cui, Z. G. (2007). Progress and recent utilization trends in combustion of Chinese oil shale. *Progress in Energy and Combustion Science, 33*(6), 552-579.

JianPing, B., CuiShan, Z., & AnLai, M. (2009). The relationship between methylated chromans and maturity of organic matter in the source rocks from Jianghan hypersaline basin. *Science in China Series D: Earth Sciences, 52*(1), 34-41.

Jin, J. M., Kim, S., & Birdwell, J. E. (2012). Molecular characterisation and comparison of shale oils generated by different pyrolysis methods. *Energy & Fuels, 26*(2), 1054-1062. doi: 10.102/ef201517a

Johnson, R. C. (2012). The systematic geologic mapping program and a quadrangle -by-quadrangle analysis of time-stratigraphic relations within oil shale-bearing rocks of the Piceance Basin, western Colorado. *U. S. Geological Survey Scientific Investigation Report 2012-5041*, 1-22.

Johnson, R. C., Mercier, T. J., Brownfield, M. E., Pantea, M. P., & Self, J. G. (2009). Assessment of in-place oil shale resources of the Green River Formation, Piceance Basin, western Colorado. *U. S. Geological Survey Fact Sheet 209-3012*, 6 p.

Johnson, R. C., Mercier, T. J., Brownfield, M. E., Pantea, M. P., & Self, J. G. (2010). An assessment of in-place oil shale resources in the Green River Formation, Piceance Basin, Colorado *Oil shale and nahcolite resources of the Piceance*

Basin, Colorado (pp. 1-187). Reston, Virginia: U.S. Geological Survey Digital Data Series, DDS-69-Y, Chapter 1.

Johnston, J. H., Rogers, K. M., Collen, J. D., & Francis, D. A. (1991). A comparison of some crude oils and potential source rocks of the East Coast Basin, using geochemical biomarkers. *1991 New Zealand petroleum conference,*, Ministry of economic development, 299-309.

Jokuty, P. L., & Gray, M. R. (1991). Resistant nitrogen compounds in hydrotreated gas from Athabasca bitumen. *Energy & Fuels, 5*(6), 791-795.

Jones, R. W. (1984). Comparison of carbonate and shale source rocks. *AAPG Study in Geology, 18*, 163-180.

Kayacan, I., & Do Gan, Ö. M. (2008). Pyrolysis of low and high density polyethylene (part II): analysis of liquid products using FTIR and NMR spectroscopy. *Energy Sources, Part A: Recovery, Utilization, and Environmental Effects, 30*(5), 392-400.

Kennett, J. P. (1982). Marine geology. *Prentice-Hall, Eaglewood Cliffs, N. J.*, 813.

Kerimov, K. M. (2004). Flash Pyrolysis and Kinetic Parameters of Decomposition of Oil Shales. *Russian Journal of Applied Chemistry, 77*(1), 154-158.

Khan, A. A., & Zaman, M. N. (2003). Stratigraphic and tectonic architecture of the north western part of the Kohat Basin, NWFP, Pakistan. *ATC 2003 Conference and Oil Show*.

Khraisha, Y. H. (1998). Kinetics of isothermal pyrolysis of Jordan oil shales. *Energy Conversion and Management, 39*(3), 157-165.

Khraisha, Y. H. (2000). Retorting of oil shale followed by solvent extraction of spent Shale: Experiment and kinetic analysis. *Energy Sources, Part A: Recovery, Utilization, and Environmental Effects, 22*(4), 347-355.

Khraisha, Y. H., Irqsousi, N. A., & Shabib, I. M. (2003). Spectroscopic and chromatographic analysis of oil from an oil shale flash pyrolysis unit. *Energy Conversion and Management, 44*(1), 125-134.

Killops, S., Hollis, C., Morgans, H., Sutherland, R., Field, B., & Leckie, D. (2000). Paleoceanographic significance of late Paleocene dysaerobia at the shelf/slope break around New Zealand. *Paleogeography, Paleoclimatology, Paleoecology, 156*(1), 51-70.

Killops, S., Morgans, H., & Leckie, D. (1996). The Waipawa Black Shale- a ubiquitous super source rock? *Proceedings of the 1996 New Zealand Petroleum Conference*, Ministry of Commerce, 12-21.

Killops, S. D., Cook, R. A., Sykes, R., & Boudou, J. P. (1997). Petroleum potential and oil source correlation in the Great South and Canterbury Basins. *New Zealand Journal of Geology and Geophysics, 40*(4), 405-423.

Kingma, J. T. (1971). *Geology of the Te Aute subdivision* (New Zealand Geological Survey Bulletin, No. 70).

Kleinberg, R., Allison, E. C., Holditch, S. A., Collett, T. S., Howard, J. J., Hardage, R. A., & Sloan, E. D. (2007). Oil shales (Topic Paper No. 27, National Petroleum Council). Retrieved 20th July 2009, from http://www.npc.org/Study_Topic_Papers/27-TTG-Oil-Shales.pdf

Kloss, W. S. (1974). *Differential thermal analysis: applications and results in mineralogy*. Berlin Heidelberg: Springer-Verlag.

Kok, M. V. (2001). Thermal investigation of Seyitomer oil shale. *Thermochimica Acta, 369*(1-2), 149-155.

Kok, M. V., & Pamir, M. R. (2000). Comparative pyrolysis and combustion kinetics of oil shales. *Journal of Analytical and Applied Pyrolysis, 55*(2), 185-194.

Kolonic, S., Damste, J. S. S., Bottcher, M. E., Kuypers, M. M. M., Kuhnt, W., Beckmann, B., Scheeder, G., & Wagner, T. (2002). Geochemical characterisation of Cenomanian/Turonian black shales from the Tarfaya Basin (SW Morocco). Relationships between palaeoenvironmental conditions and early sulphurization of sedimentary organic matter. *Journal of Petroleum Geology, 25*(3), 325-350.

Korte, C., Jones, P. J., Brand, U., Mertmann, D., & Veizer, J. (2008). Oxygen isotope values from high-latitude: clues for Permian sea-surface temperature gradients and Late-Palaeozoic deglaciation. *Paleogeography, Paleoclimatology, Paleoecology, 269*(1-2), 1-16.

Kunze, G. W. (1965). Pretreatment of mineralogical analysis. In C. A. Black (Ed.), *Methods of soil analysis – Part 1* (pp. 568-577). Madison, Winconsin: American Society of Agronomy.

Kunze, G. W., & Dixon, J. B. (1986). Pretreatment for mineralogical analysis. In A. Klute (Ed.), *Methods of soil analysis, part 1−physical and mineralogical methods* (2nd ed., pp. 91-99): Madison, Winconsin USA.

Laird, D. H., & Scharff, M. F. (1983). *Intercomparison and correlation of steady state operating data from the paraho semiworks retort*. California: U. S. Department of Energy.

Leckie, D. A., Morgans, H. E. G., Wilson, G. J., & Uruski, C. I. (1992). *Stratigraphic framework and source-rock potential of Maastrichtian to Paleocene marine shale: East Coast, North Island, New Zealand* (Institute of Geological and Nuclear Sciences Science Report No. 92/5). Lower Hutt.

Lee, J. M., & Begg, J. G. (2002). Geology of the Wairarapa area. *Institute of Geological and Nuclear Sciences 1:250 000 geological map 11*, Institute of Geological and Nuclear Sciences (GNS) Limited, Lower Hutt, New Zealand.

Lee, J. M., Bland, K. J., Townsend, D. B., & Kamp, P. J. J. (2011). Geology of the Hawke's Bay area. *Institute of Geological and Nuclear Sciences 1:250 000 geological map 8*, Institute of Geological and Nuclear Sciences (GNS) Limited, Lower Hutt, New Zealand.

Lewan, M. D. (1997). Experiments on the role of water in petroleum formation. *Geochem et Cosmochimica Acta, 61*(17), 3691-3723.

Lewan, M. D., & Roy, S. (2011). Role of water in hydrocarbon generation from Type-I kerogen in Mahogany oil shale of the Green River Formation. *Organic Geochemistry, 42*(1), 31-41.

Lewan, M. D., Spiro, B., Illich, H., Raiswell, R., Mackenzie, A. S., Durand, B., Manning, D. A. C., Comet, P. A., Berner, R. A., & Leeuw, J. W. D. (1985). Evaluation of petroleum generation by hydrous pyrolysis experimentation [and discussion]. *Philosophical Transactions of the Royal Society of London. Series A, Mathematical and Physical Sciences, 315*(1531), 123-134.

Lewan, M. D., Winters, J. C., & McDonald, J. H. (1979). Generation of oil like pyrolyzates from organic-rich shales. *Science (New York, NY), 203*(4383), 897-899.

Li, S., & Yue, C. (2003). Study of pyrolysis kinetics of oil shale. *Fuel, 82*(3), 337-342.

Liang, Y., Zhang, X., Dai, D., & Li, G. (2009). Porous biocarrier-enhanced biodegradation of crude oil contaminated soil. *International Biodeterioration and Biodegradation, 63*(1), 80-87.

Likhacheva, A. Y., Veniaminov, S. A., & Paukshtis, E. A. (2004). Thermal decomposition of NH_4 -analcime. *Physics and Chemistry of Minerals, 31*(5), 306-312.

Lindstrom, C. B. R. (2012). America's water future and deep energy. *Army War Coll Carlisle Barracks PA*.

Lomborg, B. (2001, 16th August). Running on empty? , *The Guardian (UK)*. Retrieved from

http://www.guardian.co.uk/education/2001/aug/16/highereducation.climatechange

Macpherson, T., Greer, C. W., Zhou, E., Jones, A. M., Wisse, G., Lau, P. C. K., & Sankey, B. (1998). Application of SPME/GC-MS to characterise metabolites in the biodesulfurization of organosulfur model compounds in bitumen. *Environmental Science and Technology, 32*(3), 421-426.

Maloney, K. O., & Yoxtheimer, D. A. (2012). Production and disposal of waste materials from gas and oil extraction from the marcellus shale play in Pennsylvania. *Environmental Practice, 14*(4), 278-287.

McKee, R. H., & Goodwin, R. T. (1923). The organic matter in oil shales. *Industrial & Engineering Chemistry, 15*(4), 343-349.

McKellar, J. M., Charpentier, A. D., Bergerson, J. A., & MacLean, H. L. (2009). A life cycle greenhouse gas emissions perspective on liquid fuels from unconventional Canadian and US fossil sources. *International Journal of Global Warming, 1*(1), 160-178.

Meissner, C. R., Master, J. M., Rashid, M. A., & Hussain, M. (1974). Stratigraphy of the Kohat Quadrangle, Pakistan. *Geological Survey Professional Paper 716 — D, United States Government Printing Office, Washington*.

Meunier, A., & Velde, B. (2004). Dynamics of smectite-to-illite transformation *Illite: origins, evolution and metamorphism* (pp. 145-182). New York: Springer-Verlag.

Milliken, K. L. (Ed.). (2005). *Late diagenesis and mass transfer in sandstone-shale sequences* (Vol. 1). Oxford, UK: Elsevier Ltd.

Ministry of Economic Development. (2009, 28th May 2009). East Coast Basin exploration potential.   Retrieved   14th   July,   2009,   from http://www.crownminerals.govt.nz/cms/petroleum/petroleum-basins/east-coast-basin

Ministry of Economic Development. (2012). Government welcomes report on fracking in   New   Zealand.   Retrieved   27th   November,   2012,   from

http://www.nzpam.govt.nz/cms/news_media/2012/government-welcomes-report-on-fracking

Mirza, K., Sameeni, S. J., Munir, M. H., & Yasin, A. (2005). Biostratigraphy of the middle Eocene Kohat Formation, Shekhan Nala Kohat Basin, Northern Pakistan. *Geog. Bull. Punjab Univ, 40-41*(6), 57-67.

Mittal, A. K. (2012). Unconventional oil and gas production: oppertunities and challenges of oil shale development.   Retrieved 12 December, 2012, from http://ehis.ebscohost.com/eds/detail?vid=3&hid=117&sid=db039158-9c50-45b7-8fba-e238f42179ac%40sessionmgr104&bdata=JnNpdGU9ZWRzLWxpdmU%3d#db=bth&AN=75289580

Mongenot, T., Derenne, S., Largeau, C., Tribovillard, N.-P., Lallier-Verges, E., Dessort, D., & Connan, J. (1999). Spectroscopic, kinetic and pyrolytic studies of kerogen from the dark parallel laminae facies of the sulphur-rich Orbagnoux deposit (Upper Kimmeridgian, Jura). *Organic Geochemistry, 30*(1), 39-56.

Moody, R. (2007). Oil and gas shales, definitions and Distribution in Time and Space *HOGC The history of onshore hydrocarbon use in the UK*: PESGB.

Moore, P. R. (1986). A revised Cretaceous - Early tertiary stratigraphic nomenclature for Eastern North Island, New Zealand 1-31.

Moore, P. R. (1987). Maturation and petroleum source rock potential of the Whangai and Waipawa Formations (Late Cretaceous-Paleocene), eastern North Island. *New Zealand geol. survey record* 17-23.

Moore, P. R. (1988). Stratigraphy, composition, and environment of deposition of the Whangai Formation and associated Late Cretaceous-Paleocene rocks, eastern North Island, New Zealand. 1-82.

Moore, P. R. (1989). Stratigraphy of the Waipawa black shale (Paleocene), eastern North Island, New Zealand. 1-19.

Mrigadat, M. (2008). The perspective of NOC on global energy supply and demand for petroleum. *2008 New Zealand petroleum conference,*, Ministry of Economic Development, 11-18.

Munsell Soil Colour Charts. (1954). Maryland: Munsell Colour Company.

Murphy, D. J. (2012). Fossil fuels: peak oil is affecting the economy already. *Nature, 483*(7391), 541-541.

Myers, T. (2012). Potential contaminant pathways from hydraulically fractured shale to aquifers. *Ground Water, 50*(6), 872-882.

Nakicenovic, N., Grubler, A., & McDonald, A. (1998). *Global energy perspectives*. Cambridge: Cambridge University Press

National Oil Shale Association. (2013). Current oil shale project.   Retrieved 1st October, 2013, from http://www.oilshaleassoc.org/oil_shale_project.html.

National Petroleum Council. (2011, pp 1-13). Prudent development- realizing the potential of North America's abundant natural gas and oil resources, *National Petroleum Council*.

Nedd, M. (2011). Notice of intent to prepare a programmatic environmental impact statement (EIS) and possible land use plan amendments for allocation of oil shale and tar sands resources on lands administered by the Bureau of land management in Colorado, Utah and Wyoming. *Bureau of Land Management, Federal Register, 76*(72), 21003-21005.

Neef, G. (1992). Geology of the Akitio area (1:50,000 metric sheet U25BD, east), north-eastern Wairarapa, New Zealand. *New Zealand Journal of Geology and Geophysics, 35*(4), 533-548.

Nelson, D. W., & Sommers, L. E. (1996). Total Carbon, organic Carbon and organic matter. In J. M. Bigham (Ed.), *Methods of soil analysis - Part 3 Chemical Methods*. Madison, Wisconsin: Soil Science Society of America, Inc.

North, F. K. (1985). *Petroleum geology*. Boston: Unwin Hyman.

O'brien, T. B., & Blaine, W. (2009). Method and system for extraction of hydrocarbons from oil shale and limestone formations. (Patent Application 12/278,509).

Oseev, A., Zubtsov, M., & Lucklum, R. (2012). Octane number determination of gasoline with a phononic crystal sensor. *Procedia Engineering, 47*, 1382-1385.

Ots, A. (2007). Estonian oil shale properties and utilization in power plants. *Energetika 53*(2), 8-18.

Oudin, J. L., & Vandenbrouck, M. (1993). Screening techniques for source rock evaluation. *Applied Petroleum Geochemistry*, 217.

Owen, N. A., Inderwildi, O. R., & King, D. A. (2010). Energy Policy. *Energy Policy, 38*(8), 4743-4749.

Oyal, N., Yurtsever, T. S., & Demirel, I. H. (2010). Hydrocarbon source rock assessments of the Late Jurassic black shales (Tokmar Formation) in the central

Taurus region of Turkey. *Petroleum Science and Technology, 28*(17), 1719-1727.

PADEP. (2011). Marcellus Shale.   Retrieved 14th December, 2012, from http://www.portal.state.pa.us/portal/server.pt/community/marcellus_shale/20296

Palmer, J. (Pers. comm., 2013). Bitumen content and its relation to maturity of source rocks.

Patterson, J. (2012). Exploitation of unconventional fossil fuels: enhanced greenhouse gas emissions. 148-169.

Pavia, D. L., Lampman, G. M., & Kriz, G. S. (2001). Infrared Spectroscopy. In J. Vondeling (Ed.), *Introduction to spectroscopy* (3rd ed.). Colonia polanco: Thomson Learning.

Pavia, D. L., Lampman, G. M., Kriz, G. S., & Vyvyan, J. R. (2009). *Introduction to spectroscopy* (4th ed.): Brooks/Cole Cengage Learning.

Pearson, M. J., & Small, J. S. (1988). Illite-smectite diagenesis and palaeotemperatures in northern north sea Quaternary to Mesozoic shale sequences. *Clay Minerals, 23*(2), 109-132.

Peng, S., Shan, H., Li, Y., Yang, Z., & Zhong, Z. (2013). Feasibility of CO_2 geological storage in the Xingou oil field, Jianghan Basin, China. *Earth and Planetary Science, 7*(669-672).

Peters, K. E. (1986). Guidelines for evaluating petroleum source rock using programmed pyrolysis. *The American Association of Petroleum Geologists Bulletin, 70*(3), 318-329.

Peters, K. E., & Cassa, M. R. (1994). Applied source rock geochemistry. In L. B. Magoon & W. G. Dow (Eds.), *The petroleum system — from source to trap* (pp. 93-120). Taxas, USA: American Association of Petroleum Geologists, Chapter 5.

Peters, K. E., Cunningham, A. E., Walters, C. C., Jiang, J., & Fan, Z. (1996). Petroleum systems in the Jiangling-Dangyang area, Jianghan Basin, China. *Organic Geochemistry, 24*(10-11), 1035-1060.

Peters, K. E., Walters, C. C., & Moldowan, J. M. (1993). Origin and preservation of organic matter *The biomarker guide: biomarkers and isotopes in the environment and human history* (Vol. 1, pp. 3-16). New Jersey: Prentice Hall, Inc.

Petersen, H. I., Bojesen-Koefoed, J. A., & Mathiesen, A. (2010). Variations in composition, petroleum potential and kinetics of Ordovician-Miocene Type I and Type II source rocks (oil shales): implications for hydrocarbon generation characteristics. *Journal of Petroleum Geology, 33*(1), 19-41.

Petersen, H. I., Rosenberg, P., & Nytoft, H. P. (2008). Oxygen groups in coals and alginite-rich kerogen revisited. *Coal Geology, 74*(2), 93-113.

Pevear, D. R. (1999). Illite and hydrocarbon exploration. *Proceedings of the National Academy of Sciences, 96*(7), 3440-3446.

Philp, R. P., & Zhaoan, F. (1987). Geochemical investigation of oils and source rocks from Qianjiang depression of Jianghan basin, a terrigenous saline basin, China. *Organic Geochemistry, 11*(6), 549-562.

Polettini, A., Groppi, A., Vignali, C., & Montagna, M. (1998). Fully-automated systematic toxicological analysis of drugs, poisons and metabolites in whole blood, urine and plasma by gas chromatography-full scan mass spectrometry. *Journal of Chromatography B: Biomedical Sciences and Applications, 713*(1), 266-279.

Pollastro, R. M. (1993). Considerations and applications of the illite/smectite geothermometer in hydrocarbon-bearing rocks of Miocene to Mississippian age. *Clays and Clay Minerals, 41*(2), 119-133.

Pollastro, R. M., & Scholle, P. A. (1984). Hydrocarbons exploration, development from low permeability chaltks - Upper Cretaceous Niobrara Formation, rocky mountains region. *Oil and Gas Journal, 82*, 140-145.

Poole, D. T. (2012). Hydraulic fracturing of unconventional gas shales: potential pollutants, treatments and remediation. 1-36.

Potter, P. E., Maynard, J. B., & Depetris, P. J. (2005). Mud and mudstones: Introduction and overview. Springer, New York.

Poulson, R. E. (1973). Nitrogen and Sulphur in raw and refined shale oils. *American Chemical Society, 20*(2), 183-197.

Pradhan, B. K., & Sandle, N. K. (1999). Effect of different oxidizing agent treatments on the surface properties of activated carbons. *Carbon, 37*(8), 1323-1332.

Pytte, A. M., & Reynolds, R. C. (1989). The thermal transformation of smectite to illite. *Thermal history of sedimentary basins*, Springer New York, 133-140.

Qian, J., & Wang, J. (2006). *World oil shale retorting technologies*. Paper presented at the Recent trends in oil shale research and applications conference, Amman.

Qing, W., Biazhong, S., Aijuan, H., Jingru, B., & Shaohua, L. (2007). Pyrolysis characteristics of Huadian oil shales. *Oil Shale, 24*(2), 147-157.

Qing, W., Jingru, B., Baizhong, S., & Jian, S. (2005). Strategy of Huadian oil shale comprehensive utilization. *Oil Shale, 22*(3), 305-315.

Qing, W., Liang, Z., Jingru, B., Hongpeng, L., & Shaohua, L. (2011). The influence of microwave drying on physicochemical properties of Liushuhe oil shale. *Oil Shale, 28*(1), 29-41.

Radlinski, A. P., Mastalerz, M., Hinde, A. L., Hainbuchner, M., Rauch, H., Baron, M., Lin, J. S., Fan, L., & Thiyagarajan, P. (2004). Application of SAXS and SANS in evaluation of porosity, pore size distribution and surface area of coal. *Coal Geology, 59*(3-4), 245-271.

Rajeshwar, K. (1981). The Kinetics of thermal decomposition of green river oil shale kerogen by non-isothermal thermogravimetry. *Thermochimica Acta, 45*(3), 253-263.

Rajeshwar, K. (1983). Thermal analysis of coal, oil shales and oil sands. *Thermochimica Acta, 63*(1), 97-112.

Rajnauth, J. (2012). *Is the time to focus on unconventional resources?* Paper presented at the SPETT Energy Conference and Exhibition (11-13 June) 2012, Port of Spain, Trinidad. http://www.onepetro.org/mslib/servlet/onepetropreview?id=SPE-158654-MS

Raza, H. A., Alam, S., Khan, A., & Iqbal, M. (1993). Source rock potential of oil shale deposits in Kohat Basin, Pakistan. *Pakistan Journal of Hydrocarbon Research, 5*(1&2), 1-14.

Razvigorova, M., Budinova, T., Tsyntsarski, B., Petrova, B., Ekinci, E., & Atakul, H. (2008). The composition of acids in bitumen and in products from saponification of kerogen: investigation of their role as connecting kerogen and mineral matrix. *International Journal of Coal Geology, 76*(3), 243-249.

Reeves, G. M., Sims, I., & Cripps, J. C. (2006). *Clay materials used in construction*: The Geological Society Publishing House (Bath, UK).

Regtop, R. A., Ellis, J., Crisp, P. T., Ekstrom, A., & Fookers, C. J. R. (1985). Pyrolysis of model compounds on spent oil shales, minerals and charcoal: implications for shale oil composition. *Fuel, 64*(12), 1640-1646.

Robertson, E. P., McKellar, M. G., & Nelson, L. O. (2012). Integration of high temperature gas reactors with in-situ oil shale retorting. *Fusion Science and Technology, 61*(1).

Robinson, W. E., & Cumins, J. J. (1959). Composition of low-temperature thermal extracts obtained from Colorado oil shale kerogen. *Journal of Chemical and Engineering Data, 5*(1), 74-80.

Robson, S. G., & Saulnier, G. J. (1981). *Hydrogeochemistry and simulated solute transport, Piceance Basin, north-western Colorado*. Washington: Geological Survey Professional Paper 1196.

Roehler, H. W. (1992). Correlation, composition, areal distribution and thickness of Eocene stratigraphic units, greater Green River Basin, Wyoming, Utah and Colorado. *U.S. Geological Survey Professional Paper, 1506-E*, 49 p.

Rogers, K. M., Collen, J. D., Johnston, J. H., & Elgar, N. E. (1994). Biomarker geochemistry of seep oils and potential hydrocarbon source rocks from the northern East Coast Basin, New Zealand. *New Zealand petroleum conference*, Ministry of Economic Development, 352-360.

Rogner, H.-H. (1997). An assessment of world hydrocarbon resources. *Annual Review of energy and the environment, 22*(1), 217-262.

Rouxhet, P. G., Robin, P. L., & Nicaise, G. (1980). Characterisation of kerogens and study of their evolution by infrared spectroscopy. In B. Durand (Ed.), *Kerogen: insoluble organic matter from sedimentary rocks* (pp. 163-188). Paris: Editions Technip.

Ruble, T. E., Bakel, A. J., & Philp, R. P. (1994). Compound specific isotopic variability in Uinta Basin native bitumen: palaeoenvironmental implications. *Organic Geochemistry, 21*(6-7).

Santana, G. S., Dick, D. P., Tomazi, M., Bayer, C., & Jacques, V. A. (2013). Chemical composition and stocks of soil organic matter in a south Brazilian oxisol under pasture. *Journal of Brazilian Chemical Society, 24*(5), 821-829.

Schiøler, P., Rogers, K., Sykes, R., Hollis, C. J., Illg, B., Meadows, D., Roncaglia, L., & Uruski, C. I. (2010). Palynofacies, organic geochemistry and depositional environment of the Tartan Formation (Late Paleocene), a potential source rock in the Great South Basin, New Zealand. *Marine and Petroleum Geology, 27*(2), 351-369.

Selby, D., Creser, R. A., Dewing, K., & Fowler, M. (2005). Evaluation of bitumen as a [187]Re- 187 Os geochronometer for hydrocarbon maturation and migration: a test case from the Polaris MVT deposit, Canada. *Earth and Planetary Science Letters, 235*(1-2), 1-15.

Self, J. G., Johnson, R. C., Mercier, T. J., Brownfield, M. E., & Mercier, T. J. (2010). Stratigraphic cross sections of the Eocene Green River Formation in the Piceance Basin, north-western Colorado *Oil shale and nahcolite resources of the Piceance Basin, Colorado* (pp. 1-7). Reston, Virginia: U.S. Geological Survey Digital Data Series, DDS-69-BB, Chapter 5.

Seljom, P., & Rosenberg, E. (2011). A study of oil and natural gas resources and production. *International Journal of Energy Sector Management, 5*(1), 101-124.

Sen, S. (2011). Petroleum Source Rock Assessment of the south-western Thrace Basin, NW Turkey. *Energy Sources, Part A: recovery, utilization and environmental effects, 33*(11), 1005-1017.

Serra, O. (1984). Review of basic concepts *Fundamentals of well-log interpretation: the acquisition of logging data* (Vol. 1, pp. 1-24): Elsevier Science Limited.

Sert, M., Ballice, L., Yuksel, M., & Saglam, M. (2009). Effect of mineral matter on product yield and composition at isothermal pyrolysis of Turkish oil shales. *Oil Shale, 26*(4), 463-474.

Shah, S. M. I. (2009). Stratigraphy of Pakistan. *Memoirs of the Geological Survey of Pakistan, 22*, 1-170.

Sharma, R. K., Wooten, J. B., Baliga, V. L., Lin, X., Chan, W. G., & Hajaligol, M. R. (2004). Characterization of chars from pyrolysis of lignin. *Fuel, 83*, 1469-1482.

Silverstein, R. M., Webster, F. X., & Kiemle, D. J. (1963). Infrared spectrometry. In J. Yee (Ed.), *Spectrometric identification of organic compounds* (7th ed.): John Wiley & Sons, Inc.

Smith, M. E., Carroll, A. R., & Singer, B. S. (2008). Synoptic reconstruction of a major ancient lake system: Eocene Green River Formation, western United States. *Geological Society of America Bulletin, 120*(1-2), 54-84.

Snyder, R. W., Painter, P. C., & Cronauer, D. C. (1983). Development of FTIR procedures for the characterisation of oil shale. *Fuel, 62*(10), 1205-1214.

Solomon, P. R., & Miknis, F. P. (1980). Use of Fourier transform infrared spectroscopy for determining oil shale properties. *Fuel, 59*(12), 893-896.

Song, W., Dong, Y., Xue, L., Ding, H., Li, Z., & Zhou, G. (2012). Hydrofluoric acid-based ultrasonic upgrading of oil shale and its structure characterisation. *Oil Shale, 29*(4), 334-343.

Sonibare, O. O., Jacob, D. E., Ward, C. R., & Foley, S. F. (2011). Mineral and trace element composition of the Lokpanta oil shales in the Lower Benue Trough, Nigeria. *Fuel, 90*(9), 2843-2849.

Speight, J. G. (2006). The chemistry and technology of petroleum (4th ed., pp. 1-28): CRC Press.

Speight, J. G. (2012). Origin and properties of oil shale. *Shale oil production process*. Kidlington, Oxford: Gulf Professional Publishing.

Sperling, L. H. (2006). Chain structure and configuration *Introduction to physical polymer science* (4th ed., pp. 30-67): John Wiley and Sons.

Sporstol, S., Gjos, N., Lichtenthaler, R. G., Gustavsen, K. O., Urdal, K., & Oreld, F. (1983). Source identification of aromatic hydrocarbons in sediments using GC-MS. *Environmental Science and Technology, 17*(5), 282-286.

Stein, R. (2007). Upper Cretaceous/lower Tertiary black shales near the north pole: organic-carbon origin and source-rock potential. *Marine and Petroleum Geology, 24*(2), 67-73.

Stein, S. E. (1999). An integrated method for spectrum extraction and compound identification from gas chromatography/mass spectrometry. *Journal of the American Society for Mass Spectrometry, 10*(8), 770-781.

Sun, M., Ma, X.-X., Yao, Q.-X., Wang, R.-C., Ma, Y.-X., Feng, G., Shang, J.-X., Xu, L., & Yang, Y.-H. (2011). GC-MS and TG-FTIR study of petroleum ether extract and residue from low temperature coal tar. *Energy & Fuels, 25*(3), 1140-1145.

Sun, X., & Wang, P. (2005). How old is the Asian monsoon system? - paleobotanical records from China. *Paleogeography, Paleoclimatology, Paleoecology, 222*(3-4), 181-222.

Sutherland, R., & King, P. (2008). Leaving Gondwana behind. In I. J. Graham (Ed.), *A continent on the Move: New Zealand geoscience into the 21st century* (pp. 128-129): GSNZ Miscellaneous Publication 124.

Sykes, R. (1996). New Zealand oil shale deposits: prospects for exploration. *Institute of Geological and Nuclear Sciences client report 52656A.*

Sykes, R. (Pers. comm., 2012). [Type of kerogen in Orepuki oil shale].

Sykes, R. (Pers. comm., 2013). [Link between petroleum potential (S1+S2) and maturity].

Sykes, R., & Johansen, P. E. (2007). Maturation characteristics of the New Zealand coal band: part 1 - evolution of oil and gas products. *The 23rd International Meeting on Organic Geochemistry, Torquay, England, 9th-14th September: book of abstracts*, 571-572 (abstract P222-WE).

Sykes, R., & Snowdon, L. R. (2002). Guidelines for assessing the petroleum potential of coaly source rocks using Rock-Eval pyrolysis. *Organic Geochemistry, 33*(12), 1441-1455.

TAG Oil. (2012). Retrieved 8th October, 2012 from http://www.tagoil.com/east-coast-basin.asp

Tana, J., Horsfielda, B., Mahlstedta, N., Zhangb, J., Primioa, R., Vua, T. A. T., Borehamc, C. J., Graasd, G. v., & Tocherd, B. A. (2013). Physical properties of petroleum formed during maturation of Lower Cambrian shale in the upper Yangtze Platform, South China, as inferred from PhaseKinetics modelling. *Marine and Petroleum Geology, 48*, 47-56.

Tanavsuu-Milkeviciene, K., & Sarg, J. F. (2012). Evolution of an organic-rich lake basin - stratigraphy, climate and tectonics: Piceance Creek Basin, Eocene Green River Formation. *Sedimentology, 59*, 1735-1768.

Tannenbaum, E., & Kaplan, I. R. (1985). Role of minerals in the thermal alteration of organic matter-I: generation of gases and condensates under dry condition. *Geochem et Cosmochimica Acta, 49*(12), 2589-2604.

Tao, S., Wang, Y., Tang, D., Wu, D., Xu, H., & He, W. (2012). Organic petrology of Fukang Permian Lucaogou Formation oil shales at the northern foot of Bogda Mountain, Junggar Basin, China. *International Journal of Coal Geology, 99*, 27-34.

Te Ara The Encyclopedia of New Zealand. (2006). Story: Southland places. Retrieved 12 February, 2012, from http://www.teara.govt.nz/

Thakur, D. S., & Nuttall Jr, H. E. (1987). Kinetics of pyrolysis of Moroccan oil shale by thermogravimetry. *Industrial & Engineering Chemistry Research, 26*(7), 1351-1356.

The Japan Times Online. (2012). Shale oil extracted from Japan's Akita field. Retrieved   13th   December,   2012,   from http://www.japantimes.co.jp/text/nn20121004a1.html

Thermo Electron Corporation. (1992). OMNIC software package. *Version 7.0*.

Tissot, B. P., & Vandenbrouck, M. (1983). Geochemistry and pyrolysis of oil shales. In F. P. Minknis & J. F. McKay (Eds.), *Geochemistry and chemistry of oil shales* (pp. 1-11). Washington: American Chemical Society.

Tissot, B. P., & Welte, D. H. (1978a). From kerogen to petroleum *Petroleum formation and occurrence: A new approach to oil and gas exploration* (pp. 148-184). Berlin: Springer-Verlag

Tissot, B. P., & Welte, D. H. (1978b). Identification of source rocks *Petroleum formation and occurrence: A new approach to oil and gas exploration* (pp. 464-465). Berlin: Springer-Verlag

Tissot, B. P., & Welte, D. H. (1978c). Kerogen: Composition and classification *Petroleum formation and occurrence: A new approach to oil and gas exploration* (pp. 123-147). Berlin: Springer-Verlag.

Tissot, B. P., & Welte, D. H. (1978d). *Petroleum formation and occurrence*. Berlin: Springer, 538 pp.

Tiwari, P., & Deo, M. (2012). Compositional and kinetic analysis of oil shale pyrolysis using TGA-MS. *Fuel, 94*, 333-341.

Tiwari, P., & Deo, M. (2012). Detailed kinetic analysis of oil shale pyrolysis TGA data. *AIChE Journal, 58*(2), 505-515.

Tixier, M. P., & Alger, R. P. (1970). Log evaluation of nonmetalic mineral deposits. *Geophysics, 35*(1), 124-142.

Toby, B. H. (2005). Classification and use of powder diffraction data. In S. Hall (Ed.), *International tables for crystallography, definition and exchange of crystallographic data*. Netherland: Springer.

Tucker, M. E. (1988). *Techniques in sedimentology*: Blackwell Scientific Publications.

Tucker, M. E. (1991). *Sedimentary petrology: An introduction to the origin of sedimentary rocks* (2nd ed.). Oxford: Blackwell Scientific.

Turnbull, I. M., & Allibone, A. H. (2003). Geology of the Murihiku area. *Institute of Geological and Nuclear Sciences (GNS) 1:250 000 geological map 20*, Lower Hutt, Institute of Geological and Nuclear Sciences. p 55.

Turnbull, I. M., Uruski, C. I., & others. (1993). *Cretaceous and Cenozoic sedimentary basins of western Southland, South Island, New Zealand*. Institute of Geological and Nuclear Sciences Ltd, Monograph 1.

Tuttle, M. L. (1973). Geochemical, Biogeochemical and Sedimentological studies of the Green River Formation, Utah and Colorado. *US Geological Survey Bulletin 1973-A-G*, A1-A11.

Tyson, R. V. (1987). The genesis and palynofacies characteristics of marine petroleum source rocks. In J. D. Brooks & A. J. Fleet (Eds.), *Marine petroleum source rocks* (Vol. 26, pp. 47-67): Geological Society Special Publication (Vol. 26, pp. 47-67).

Uden, P. C., Siggia, S., & Jensen, H. B. (1978). *Analytical chemistry of liquid fuel sources: tar sands, oil shale, coal and petroleum*: American Chemical Society.

Uruski, C. I. (2010). New Zealand's deep water frontier. *Marine and Petroleum Geology, 27*(9), 2005-2026.

Uruski, C. I., Field, B. D., Funnell, R., Hollis, C. J., Nicol, A., & Maslen, G. (2006). Developments in the central and north-eastern East Coast Basin, North Island, New Zealand. *AAPEA, 46*(2).

Uruski, C. I., Field, B. D., Funnell, R., Sykes, R., & Darby, D. (2003). Tawatawa prospect review, offshore Wairarapa, East Coast Basin, North Island, New Zealand. *New Zealand Petroleum Report 2785*, New Zealand Petroleum and Minerals, Wellington.

Vanderbroucke, M., Albrecht, P., & Durand, B. (1976). Geochemical studies on the organic matter from the Douala Basin (Cameroon)-III. Comparison with the Early Toarcian shales, Paris Basin, France. *Geochem. Cosmochim. Acta, 40*(10), 1241-1249.

Vassileva, C. G., & Vassilev, S. V. (2006). Behaviour of inorganic matter during heating of Bulgarian coals: 2. Subbituminous and bituminous coals. *Fuel Processing Technology, 87*(12), 1096-1116.

Velde, B., & Barre, P. (2010). *Soils, plants and clay minerals: minerals and biologic interactions*. Berlin: Springer-Verlag, 1-37.

Ventura, T. (Pers. comm., 2013). Reasons for the absence of pristane and phytane from the bitumen extracts of various oil shales.

Veres, D. S. (2002). A comparative study between Loss on Ignition and total carbon analysis on mineralogenic sediments. *Studia Universitatis Babes-Bolyia, Geologia, XLVII*(1), 171-182.

Vlachos, N., Skopelitis, Y., Psaroudaki, M., Konstantinidou, V., Chatzilazarou, A., & Tegou, E. (2006). Applications of Fourier transform-infrared spectroscopy to edible oils. *Analytica Chimica Acta, 573*, 459-465.

Wandrey, C. J., Law, B. E., & Shah, H. A. (2004). *Patala-Nammal composite total petroleum system, Kohat-Potwar geologic province, Pakistan*. (U. S. Department of Interior, USGS) U.S. Geological Survey Bulletin, 2208-B.

Wang, S., Wang, K., Liu, Q., Gu, Y., Luo, Z., Cen, K., & Fransson, T. (2009). Comparison of the pyrolysis behaviour of lignins from different tree species. *Biotechnology Advances, 27*(5), 562-567.

Wang, Z., Deng, S., Gu, Q., Zhang, Y., Cui, X., & Wang, H. (2013). Pyrolysis kinetic study of Huadian oil shale, spent oil shale and their mixtures by thermogravimetric analysis. *Fuel Processing Technology, 110*, 103-108.

Watanabe, H., Shimomura, K., & Okazaki, K. (2013). Effect of high CO_2 concentration on char formation through mineral reaction during biomass pyrolysis. *Proceedings of the Combustion Institute, 34*(2), 2339-2345.

Watson, G. H., McWhorter, D. B., & Brown, A. (1985). 4,529,497. Standard Oil Company (Indiana), Gulf Oil Corporation.

Weatherford Laboratories Operators Manual. (2010). Source Rock Analyser (SRA TPH/TOC[TM]).

Weaver, C. E. (1960). Possible uses of clay minerals in search for oil. *AAPG Bulletin, 44*(9), 1505-1518.

Weitkamp, A. W., & Gutberlet, L. C. (1970). Application of a micro retort to problems in shale pyrolysis. *Industrial & Engineering Chemistry Process Design and Development, 9*(3), 386-395.

West, I. (2009). Kimmeridge field guide - blackstone, oil shale: geology of the Wessex Coast. Retrieved 20th July, 2009, from http://www.soton.ac.uk/~imw/kimblack.htm

Whitton, J. S., & Churchman, G. J. (1987). *Standard methods for mineral analysis of soil survey samples for characterisation and classification in NZ Soil Bureau* (No. 79). Lower Hutt, Wellington: Department of Scientific and Industrial Research.

Willett, R. W. (1946). Orepuki coalfield, Southland. *New Zealand Journal of Science and Technology, 27*(6B), 439-445.

Willett, R. W., & Wellman, H. W. (1940). The oil shale deposit of Orepuki, Southland. *The New Zealand Journal of Science and Technology, 22*(2B), 84B-99B.

Williams, P. F. V. (1985). Thermogravimetry and decomposition kinetics of British Kimmeridge clay oil shale. *Fuel, 64*(4), 540-545.

Williams, P. T., & Ahmad, N. (1998). Influence of particle grain size on the yield and composition of products from the pyrolysis of oil shales *Journal of Analytical and Applied Pyrolysis, 46*, 31-49.

Williams, P. T., & Ahmad, N. (1999). Influence of process conditions on the pyrolysis of Pakistani oil shales. *Fuel, 78*(6), 653-662.

Williams, P. T., & Ahmad, N. (2000). Investigation of oil-shale pyrolysis processing conditions using thermogravimetric analysis. *Applied Energy, 66*(2), 113-133.

Wolfson, A., Elmugrabi, Y., Levi, R., Tavor, D., & Wisniak, J. (2011). Green process for simultaneous extraction of oil shale and enrichment of ethanol. *Oil Shale, 28*(4), 516-527.

Wood, B. L. (1969). Geology of Tuatapere Subdivision, western Southland (Sheets S167, S175). *Geological Survey No. 79-80*.

World Energy Council. (2007). *2007 Survey of energy resources*. London: World Energy Council.

Yang, M. Y., Jeon, C. W., Yang, M. K., Lee, S. H., & Wakita, H. (1997). Analysis of the organic matter in oil shales distributed in Korea *Analytical Sciences, 13*(SUPPLEMENT), 433-436.

Yen, T. F., & Chilingar, G. V. (1976). *Oil shale*. New York: Elsevier

Yen, T. F., Shue, F. F., Wu, E. H., & Tzeng, D. (1983). Ferric Chloride-clay complexation method: removal of nitrogen-containing components from shale oil and related fossil fuels. In F. P. Miknis & J. F. Mckay (Eds.), *Geochemistry and chemistry of oil shales* (pp. 457-466). Washington: American Chemical Society.

Yen, Y. F. (1976). Structural investigations on Green River oil shale. In Y. F. Yen (Ed.), *Science and Technology of oil shale*: Ann Arbor Science Publishers.

Youheng, Z. (2010). Exploration direction and strategy for lithologic accumulations in Qianjiang Formation of the Qianjiang Sag, Jianghan Basin. *Petroleum Geology and Exploration, 32*(4).

Zheng, H., Jia, D., Chen, J., & Wang, P. (2011). Did incision of the Three Gorges begin in the Eocene? *Geology, 39*(9), 244.
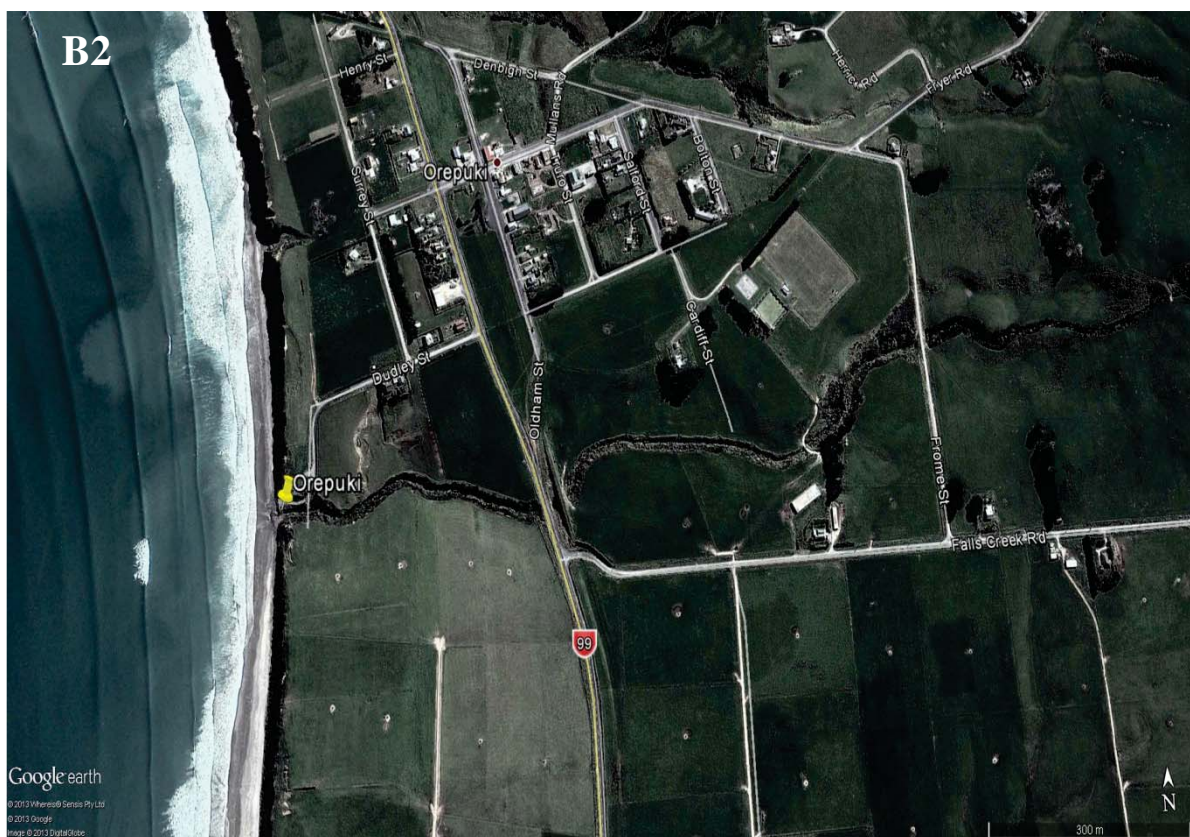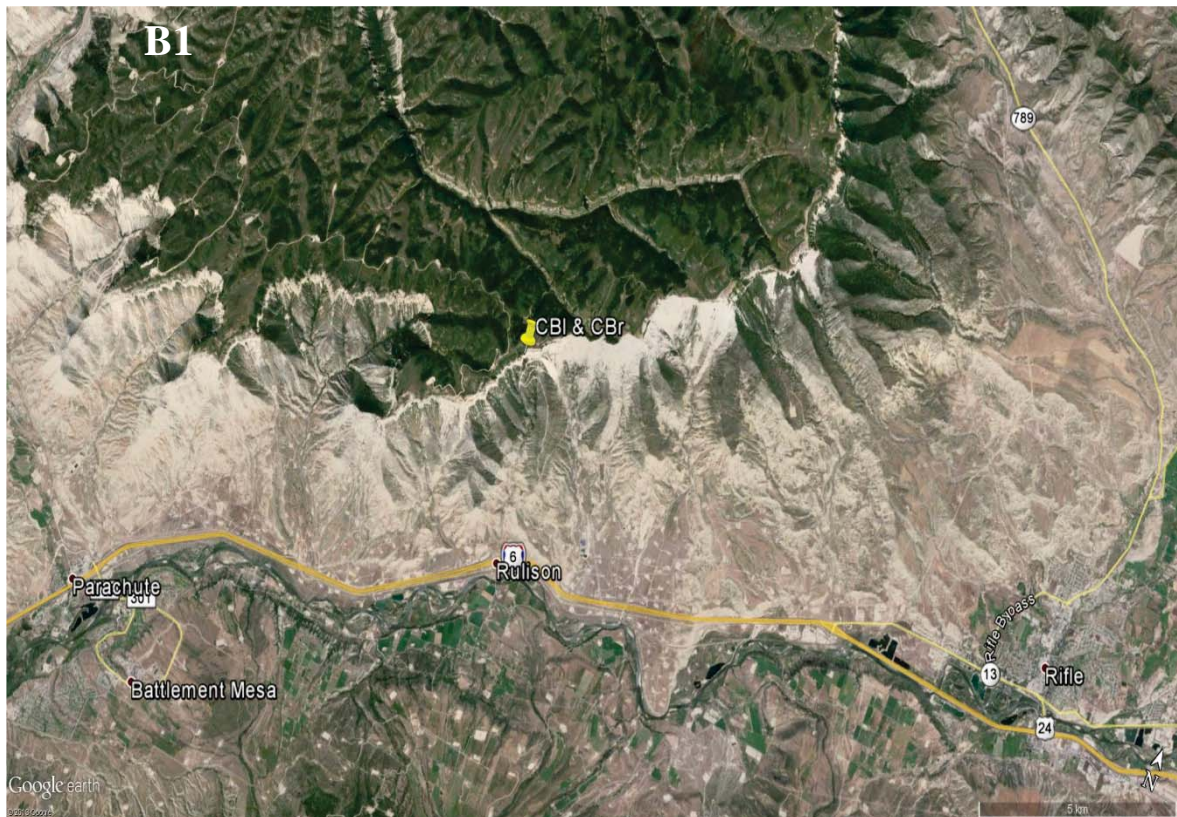
Appendix A

Gray King assay method

In this method ~20 g of crushed oil shale is placed in a retort which is connected to a condenser and a gas chamber. The gas chamber consists of activated carbon or sulphuric acid and in which constant pressure is maintained. Temperature of the retort is increased gradually until it reaches 600°C, held for a short time, then the current is cut off, the gas holder is disconnected, and the volume of the gas and yield calculation made (Cane, 1942).
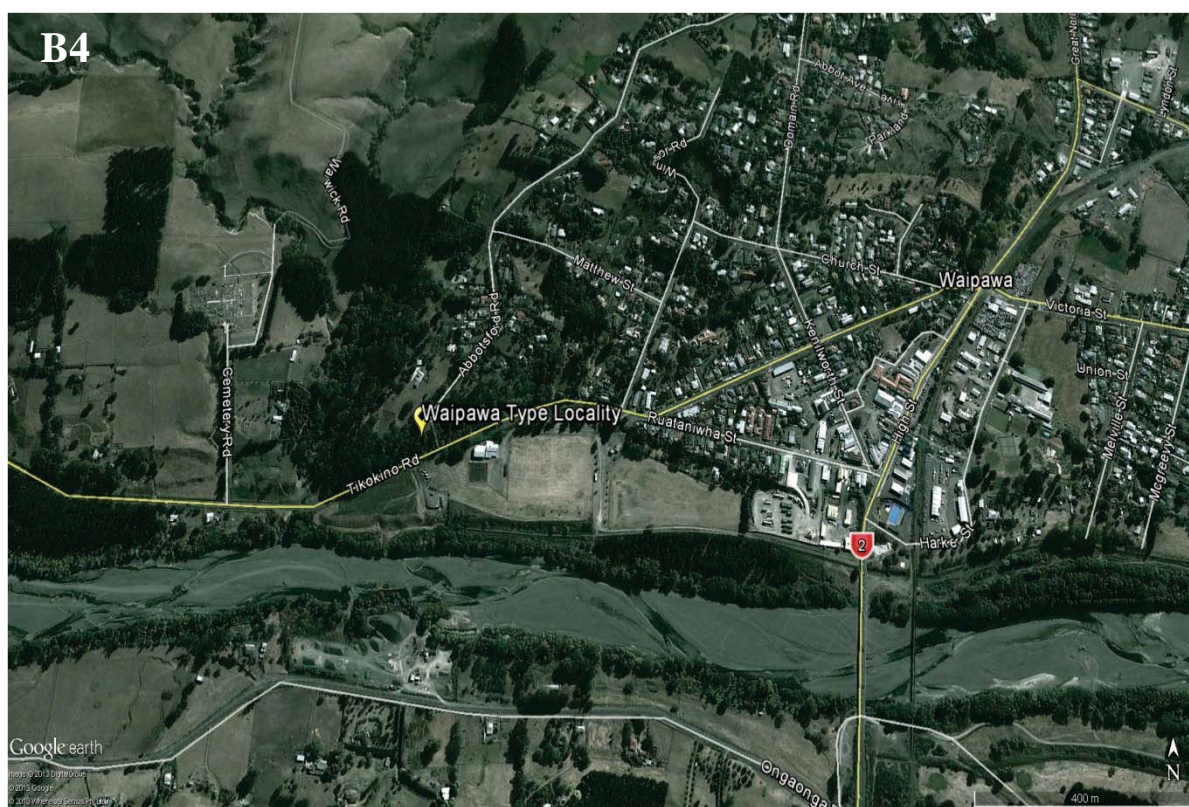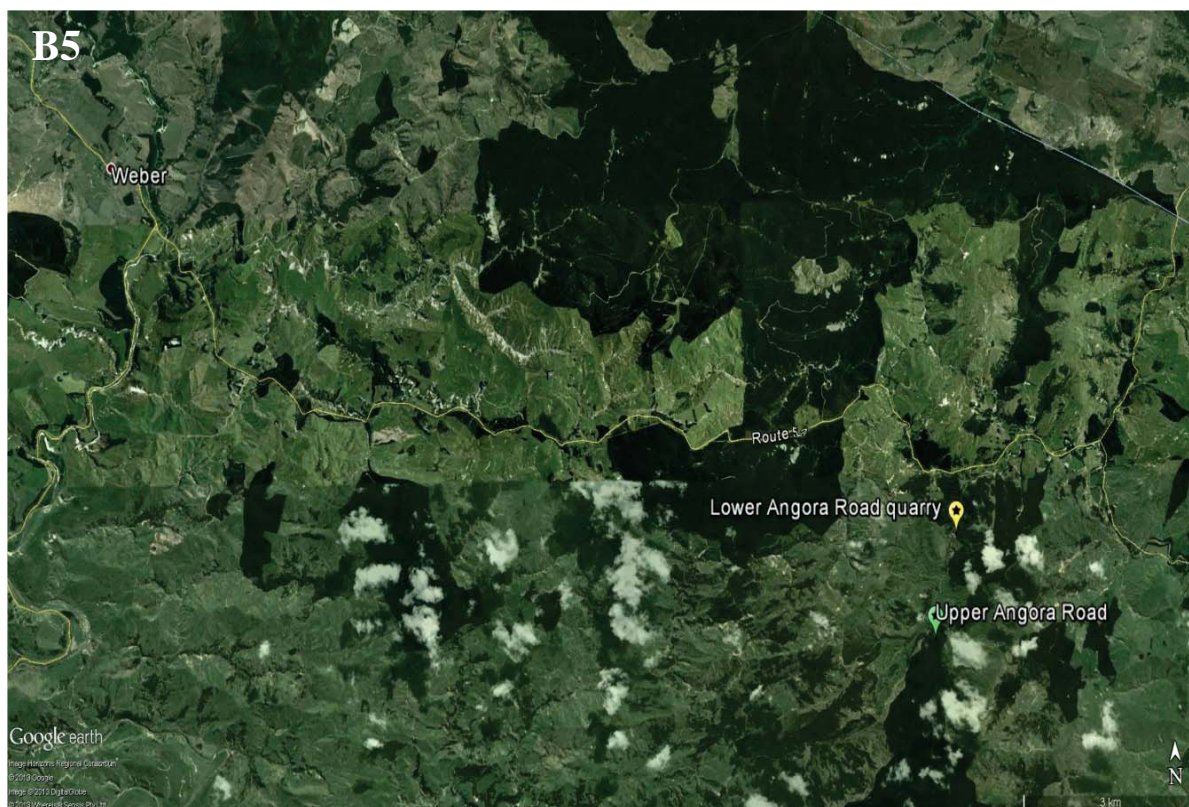
Appendix B
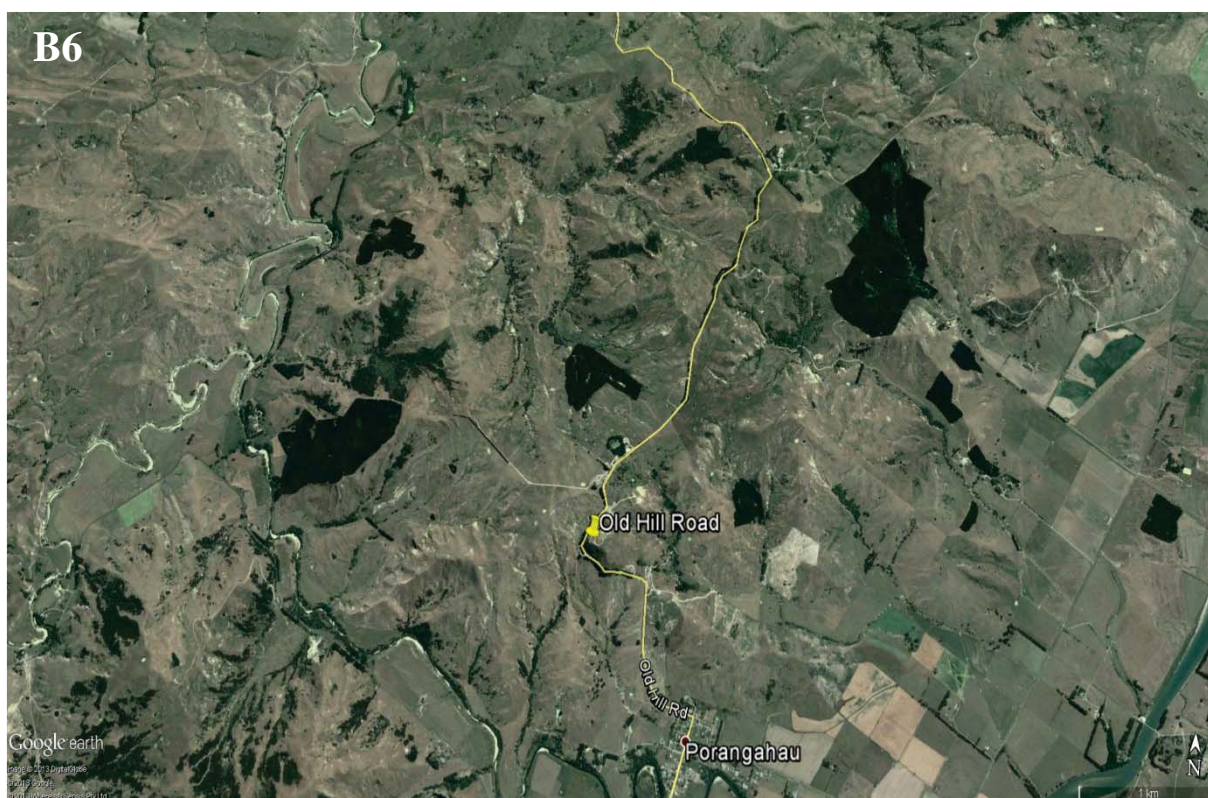
Google images showing samples locations

B3

B4

Note: *The Lower Angora Road quarry outcrop is 1.2 km south on Angora Road from the intersection of Angora Road and Route 52. The Upper Angora Road locality is 2.7 km south on Angora Road from the intersection of Angora Road and Route 52.*

Appendix C

Commentary on the reliability of analytical data

Every effort was made to obtain accurate and reliable data for the current study. Samples were ground in a ring grinder for 20 seconds in order to avoid any volatilization of the hydrocarbons. LECO combustion analysis was performed on three replicate samples for each sample in this study and then the mean of the results was presented in the thesis. The LECO raw data for all samples is presented in Table C1. From the LECO analysis there is a maximum standard deviation of 0.6 which is 4% of the mean.

Table C1. TOC data of three replicate samples. Sample preparation was performed exactly the same way for all samples in this study. (Rep = Replicate)

Samples	LECO analysed TOC (wt%)			Mean	Standard deviation
	Rep 1	Rep 2	Rep 3		
Sand	0.060	0.060	0.060	0.06	0.00
Argillite	0.565	0.610	0.601	0.59	0.02
OOS1	15.631	15.592	15.610	15.61	0.02
OOS2	15.236	15.621	14.143	15.00	0.63
OOS3	14.450	14.521	13.929	14.30	0.26
CBl	18.050	17.787	18.193	18.01	0.17
CBr	12.804	12.418	12.587	12.60	0.16
QF1	11.012	11.002	10.986	11.00	0.01
QF2	9.994	9.864	10.381	10.08	0.22
QF3	17.321	17.320	17.259	17.30	0.03
MKK1	2.695	2.740	2.785	2.74	0.04
MKK2	2.230	2.210	2.250	2.23	0.02
SB	0.990	0.987	0.993	0.99	0.00
SR1	0.234	0.221	0.235	0.23	0.01
SR2	0.318	0.321	0.321	0.32	0.00
SR3	0.179	0.185	0.176	0.18	0.00
WFT1	6.986	6.882	7.102	6.99	0.09
WFT2	6.184	6.231	6.184	6.20	0.02
WFT3	5.999	6.211	5.969	6.06	0.11
WFAQ11	4.399	4.462	4.369	4.41	0.04
WFAQ12	4.012	4.011	4.097	4.04	0.04
WFAQ13	4.281	4.280	4.279	4.28	0.00
WFAQ21	2.698	2.699	2.762	2.72	0.03
WFAQ22	2.690	2.692	2.688	2.69	0.00
WFAQ23	2.557	2.561	2.562	2.56	0.00
WFOH31	2.481	2.480	2.479	2.48	0.00
WFOH32	2.732	2.733	2.725	2.73	0.00
WFOH33	2.000	2.101	2.199	2.10	0.08
Graphite	9.601	9.612	9.587	9.60	0.01

Similarly in order to obtain reliable TGA results, six replicate samples (being ground exactly the same way, for 20 seconds in a ring grinder), were analysed according to standard and established TGA methods available in the literature, as described by Carmona *et al.* (2013), Santana *et al.* (2013), Jaber *et al.* (1999), Williams and Ahmad (1998, 1999, 2000). The weight losses in the different temperature regions (0-200°C, 200-650°C and 650-1200°C) were recorded for each replicate sample. The mean and

standard deviation of all the weight losses [(Phase I (0-200°C), Phase II (200-650°C, Phase III (650-1200°C)] were then calculated (Table C2). In the TGA a maximum standard deviation of 0.1 for Phase II was calculated (Table C2a) which is 2.1% of the mean.

Table C2a. Phase I weight loss data during the thermal gravimetric analysis of six replicate samples. Sample preparation was performed exactly the same way for all samples in this study. (Rep = Replicate)

Samples	Phase I weight loss in TGA (wt%) [0-200°C]						Mean	Standard deviation
	Rep 1	Rep 2	Rep 3	Rep 4	Rep 5	Rep 6		
Sand	--	--	--	--	--	--	--	--
Argillite	0.921	0.865	0.792	0.862	0.865	0.855	0.86	0.04
OOS1	6.190	6.182	6.158	6.128	6.210	6.272	6.19	0.04
OOS2	4.718	4.762	4.770	4.738	4.835	4.797	4.77	0.04
OOS3	6.322	6.290	6.285	6.274	6.288	6.281	6.29	0.01
CBl	0.389	0.383	0.379	0.380	0.395	0.414	0.39	0.01
CBr	0.122	0.120	0.104	0.120	0.130	0.124	0.12	0.01
QF1	0.823	0.825	0.826	0.822	0.819	0.805	0.82	0.01
QF2	1.571	1.578	1.565	1.568	1.582	1.556	1.57	0.01
QF3	6.532	6.555	6.521	6.524	6.533	6.395	6.51	0.05
MKK1	12.121	12.310	12.165	12.354	12.120	12.190	12.21	0.1
MKK2	12.531	12.653	12.775	12.751	12.658	12.652	12.67	0.1
SB	16.021	16.031	16.000	16.015	16.011	16.102	16.03	0.03
SR1	0.785	0.786	0.754	0.699	0.697	1.019	0.79	0.10
SR2	0.942	0.934	0.934	0.942	0.945	0.883	0.93	0.02
SR3	0.935	0.941	0.942	0.936	0.935	0.951	0.94	0.01
WFT1	4.944	4.931	4.933	4.945	4.942	4.945	4.94	0.01
WFT2	4.812	4.816	4.727	4.842	4.852	4.811	4.81	0.04
WFT3	4.810	4.799	4.812	4.815	4.820	4.804	4.81	0.01
WFAQ11	3.508	3.518	3.512	3.538	3.535	3.449	3.51	0.03
WFAQ12	4.100	4.054	4.094	4.123	4.120	4.109	4.10	0.02
WFAQ13	3.495	3.481	3.489	3.491	3.498	3.486	3.49	0.01
WFAQ21	3.714	3.722	3.697	3.715	3.720	3.694	3.71	0.01
WFAQ22	4.454	4.435	4.465	4.410	4.431	4.431	4.44	0.02
WFAQ23	4.732	4.698	4.760	4.725	4.734	4.725	4.73	0.02
WFOH31	8.189	8.184	8.156	8.180	8.187	8.197	8.19	0.01
WFOH32	8.562	8.519	8.465	8.489	8.652	8.569	8.55	0.06
WFOH33	8.879	8.821	8.856	8.824	8.823	8.759	8.82	0.04
Graphite	0.935	0.934	0.939	0.934	0.935	0.921	0.93	0.01

Table C2b. Phase II weight loss data during the thermal gravimetric analyses of six replicate samples. Sample preparation was performed exactly the same way for all samples in this study. (Rep = Replicate)

Samples	Phase II weight loss in TGA (wt%) [200-650°C]						Mean	Standard deviation
	Rep 1	Rep 2	Rep 3	Rep 4	Rep 5	Rep 6		
Sand	--	--	--	--	--	--	--	--
Argillite	3.163	3.152	3.345	3.224	3.129	3.307	3.22	0.10
OOS1	14.789	14.712	14.719	14.738	14.742	14.740	14.74	0.02
OOS2	14.898	14.912	15.010	14.946	14.923	14.951	14.94	0.03
OOS3	16.001	15.972	15.967	15.983	15.981	15.976	15.98	0.01
CBl	13.581	13.564	13.595	13.464	13.469	13.807	13.58	0.11
CBr	8.600	8.651	8.705	8.645	8.600	8.699	8.65	0.04
QF1	0.984	0.984	0.972	1.019	0.976	0.945	0.98	0.02
QF2	2.456	2.462	2.462	2.444	2.435	2.501	2.46	0.02
QF3	6.988	6.999	6.983	6.963	6.867	7.140	6.99	0.10
MKK1	5.234	5.211	5.162	5.211	5.166	5.216	5.20	0.03
MKK2	5.697	5.764	5.849	5.77	5.764	5.814	5.732	0.05
SB	3.492	3.546	3.612	3.551	3.492	3.607	3.55	0.05
SR1	2.000	2.012	2.018	1.999	2.122	1.909	2.01	0.10
SR2	2.145	2.142	2.193	2.154	2.166	2.160	2.16	0.02
SR3	2.135	2.121	2.134	2.131	2.122	2.137	2.13	0.01
WFT1	10.494	10.512	10.51	10.497	10.515	10.472	10.5	0.01
WFT2	10.121	10.13	10.121	10.100	10.211	10.037	10.12	0.05
WFT3	10.143	10.122	10.111	10.130	10.145	10.129	10.13	0.01
WFAQ11	7.235	7.496	6.990	7.234	7.236	7.189	7.23	0.15
WFAQ12	7.215	7.256	7.245	7.231	7.245	7.068	7.21	0.01
WFAQ13	8.216	8.240	8.201	8.215	8.300	8.148	8.22	0.04
WFAQ21	6.124	6.105	5.889	5.978	5.845	5.999	5.99	0.10
WFAQ22	5.756	5.689	5.725	5.624	5.890	5.816	5.75	0.10
WFAQ23	8.130	8.156	8.165	8.170	8.175	8.164	8.16	0.01
WFOH31	6.975	7.035	6.950	6.988	6.947	6.985	6.98	0.03
WFOH32	5.121	5.135	5.138	5.110	5.134	5.142	5.13	0.01
WFOH33	5.674	5.689	5.732	5.666	5.632	5.687	5.68	0.03
Graphite	1.450	1.460	1.444	1.399	1.426	1.461	1.44	0.02

Table C2c. Phase III weight loss data during the thermal gravimetric analyses of six replicate samples. Sample preparation was performed exactly the same way for all samples in this study. (Rep = Replicate)

Samples	TGA Phase III weight loss (wt%) [650-1200°C]						Mean	Standard deviation
	Rep 1	Rep 2	Rep 3	Rep 4	Rep 5	Rep 6		
Sand	--	--	--	--	--	--	--	--
Argillite	0.230	0.233	0.224	0.215	0.231	0.247	0.23	0.01
OOS1	9.985	9.996	10.120	10.024	10.026	9.969	10.02	0.05
OOS2	7.589	7.612	7.621	7.630	7.632	7.636	7.62	0.02
OOS3	9.198	9.147	9.222	9.198	9.223	9.212	9.20	0.03
CBl	21.073	21.071	21.068	21.069	21.023	21.116	21.07	0.03
CBr	21.731	21.731	21.735	21.717	21.712	21.754	21.73	0.01
QF1	2.466	2.459	2.467	2.478	2.477	2.473	2.47	0.01
QF2	7.473	7.436	7.482	7.471	7.469	7.489	7.47	0.02
QF3	9.500	9.478	9.479	9.465	9.482	9.476	9.48	0.01
MKK1	17.454	17.444	17.471	17.468	17.462	17.461	17.46	0.01
MKK2	16.712	16.710	16.658	16.688	16.729	16.763	16.71	0.03
SB	10.179	10.169	10.196	10.185	10.190	10.221	10.19	0.02
SR1	3.889	4.185	3.956	3.892	3.983	3.975	3.98	0.10
SR2	2.772	2.765	2.768	2.774	2.749	2.792	2.77	0.01
SR3	1.010	1.000	1.125	1.016	1.068	1.021	1.04	0.04
WFT1	5.699	5.592	5.685	5.632	5.590	5.822	5.67	0.08
WFT2	4.635	4.638	4.658	4.589	4.568	4.692	4.63	0.04
WFT3	4.654	4.645	4.615	4.586	4.591	4.569	4.61	0.03
WFAQ11	3.956	3.912	3.879	3.888	3.905	3.920	3.91	0.02
WFAQ12	3.086	3.059	3.103	3.099	3.094	3.099	3.09	0.01
WFAQ13	2.765	2.821	2.845	2.816	2.785	2.888	2.82	0.04
WFAQ21	1.562	1.479	1.482	1.485	1.444	1.428	1.48	0.04
WFAQ22	1.338	1.334	1.346	1.345	1.378	1.239	1.33	0.04
WFAQ23	1.759	1.558	1.745	1.721	1.785	1.752	1.72	0.10
WFOH31	0.810	0.682	0.779	0.772	0.801	0.776	0.77	0.04
WFOH32	2.369	2.419	2.410	2.345	2.366	2.311	2.37	0.04
WFOH33	0.714	0.772	0.685	0.658	0.712	0.719	0.71	0.03
Graphite	4.068	4.085	4.069	4.122	4.001	4.015	4.06	0.04

Soxhlet extraction was performed to extract bitumen from the rocks ground for 20 seconds in a ring grinder. All the samples were treated the same way and same amount of dichloromethane (DCM) was used to extract the bitumen fraction of all samples. All extractions were carried out for the same period of 48 hours.
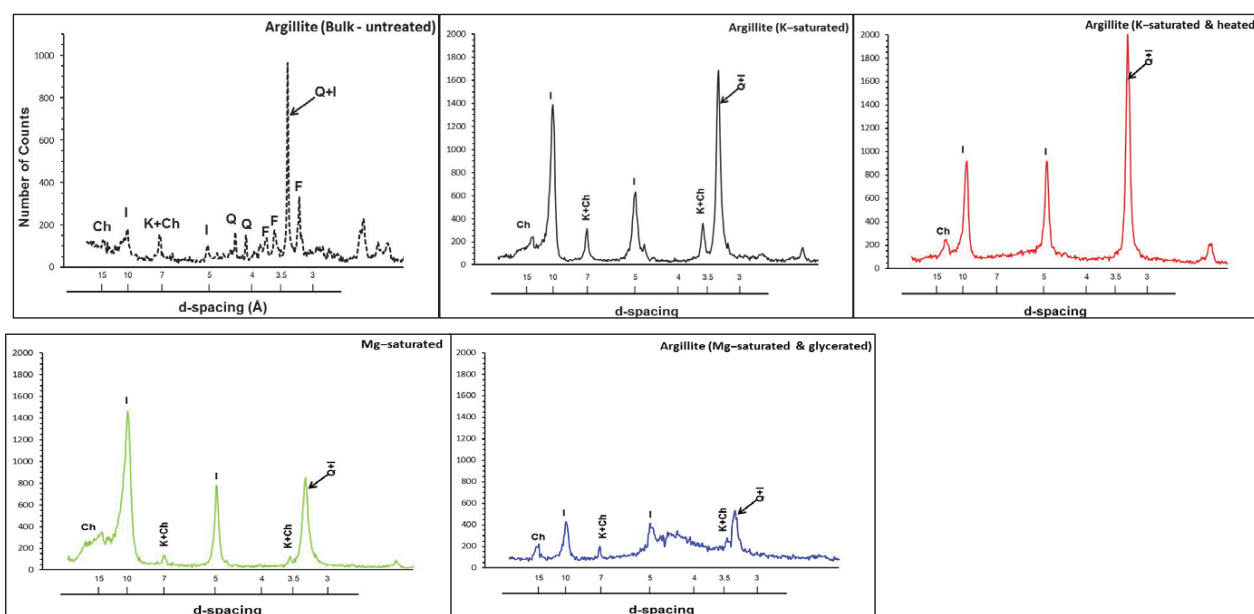
The extracted bitumen was then analysed by GC-MS and FTIR. Developing a new methodology for the FTIR took almost six months. Efforts were made to develop a method which gives more reliable and accurate results than those of the methods available already available in the literature. Methods available in the literature mainly involve FTIR on a raw powdered sample or KBr pellet prepared by mixing KBr powder and an oil shale sample in a certain ratio (Rouxhet *et al.*, 1980; Snyder *et al.*, 1983; Solomon & Miknis, 1980). At the outset of the FTIR studies, the raw, powdered samples were analysed using an FTIR, but the spectra were not good. To improve the quality of the spectra a second analysis was made using the potassium bromide (KBr) pressed disc technique (Rouxhet *et al.*, 1980). The KBr pellets prepared were oven dried under vacuum for 18 hours at 200°C, in order to remove any peaks appearing due to hydroxyl ions, but raw powdered samples analysed using an FTIR can give resultant spectra having interferences from the mineral part of the samples as well. Therefore it was decided to run FTIR on the solvent extracted bitumen fraction of each rock in order to get more reliable results. The samples were analysed on a Nicolet 5700 FT-IR spectrometer at the Institute of Fundamental Sciences, Massey University collecting 32 scans at 4 cm^{-1} resolution between 4000 and 400 cm^{-1} for each sample spectrum. No replicates of the samples in the study were run as the extracted bitumen in DCM was considered representative of the whole sample.

A single disc was prepared for the extract of each homogenised sample. The sample was then analysed by the FTIR. During analysis the machine automatically scanned each disc 32 times to generate an average spectrum. The number of scans at 4 cm^{-1} resolution was selected as shown in the work of Alstadt *et al.* (2012), (Sun *et al.*, 2011) and (Jokuty & Gray, 1991). To test the precision of the FTIR analysis, each sample was manually analysed 12 times on the FTIR. However no variability over the 12 repeats was observed and the spectra recorded were found identical. Therefore one spectrum out of those 12 spectra was randomly selected and used in the thesis to represent each sample.
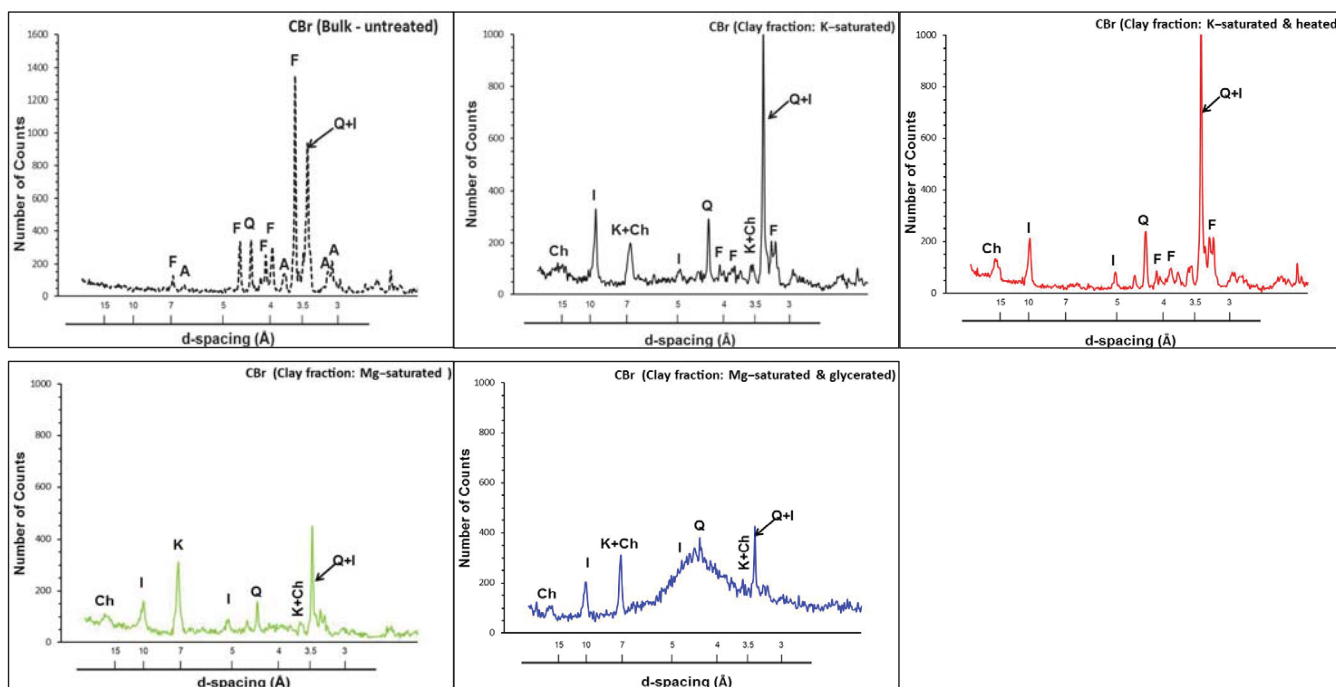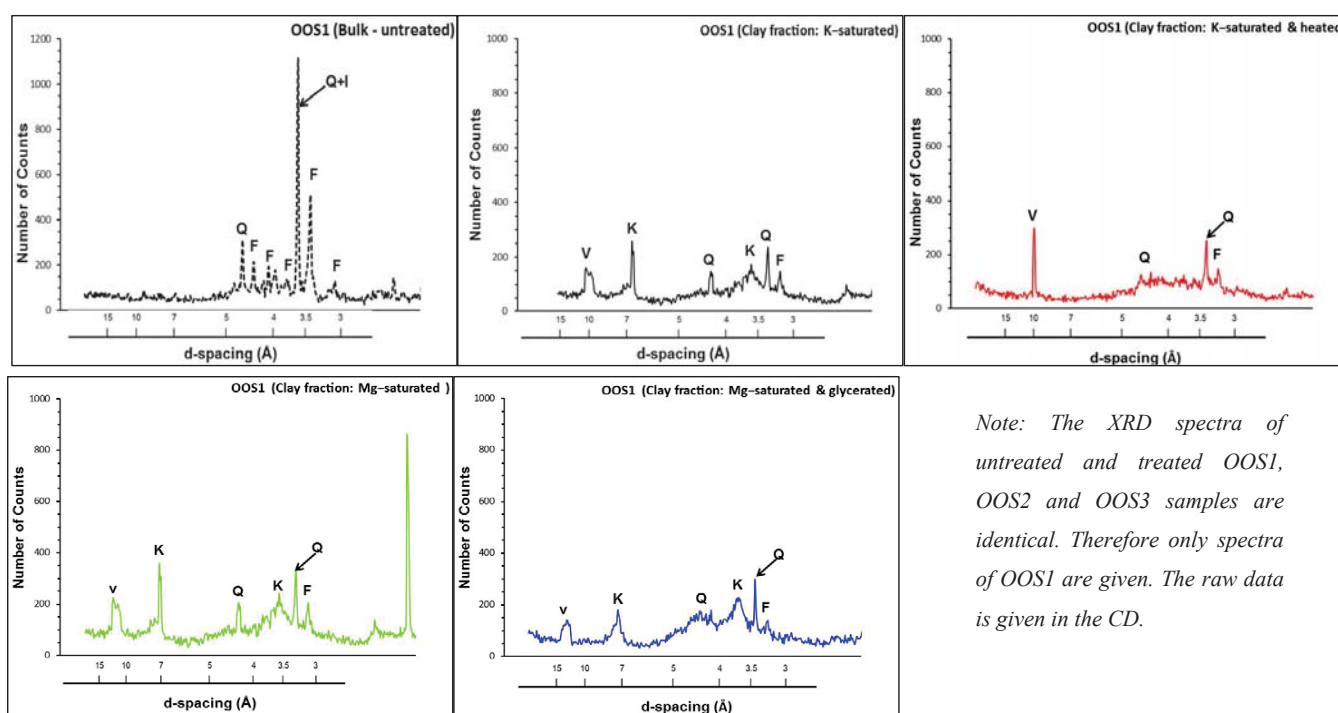
Appendix D

XRD spectra of samples investigated in this study

XRD spectra of the argillite, Green River Formation, Qianjiang Formation, Orepuki oil shale, Waipawa Formation, Mir Kalam Kala, Speena Banda and Salt Range rocks are given.
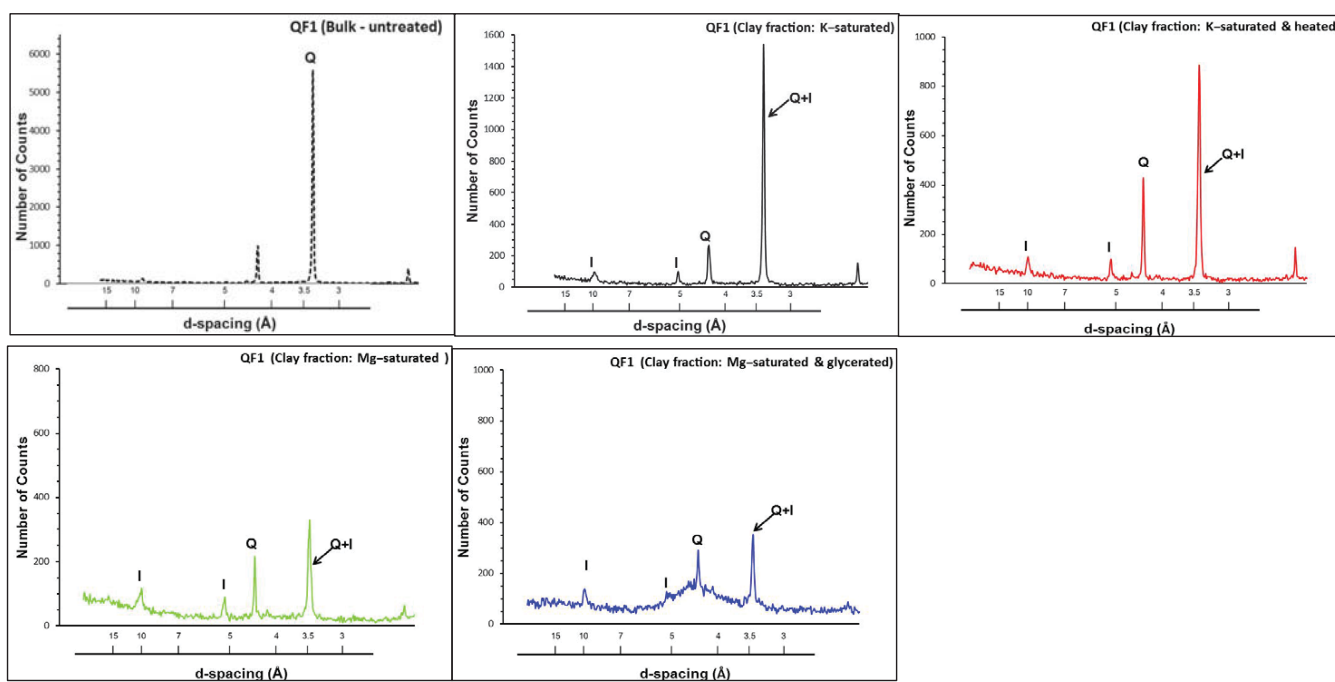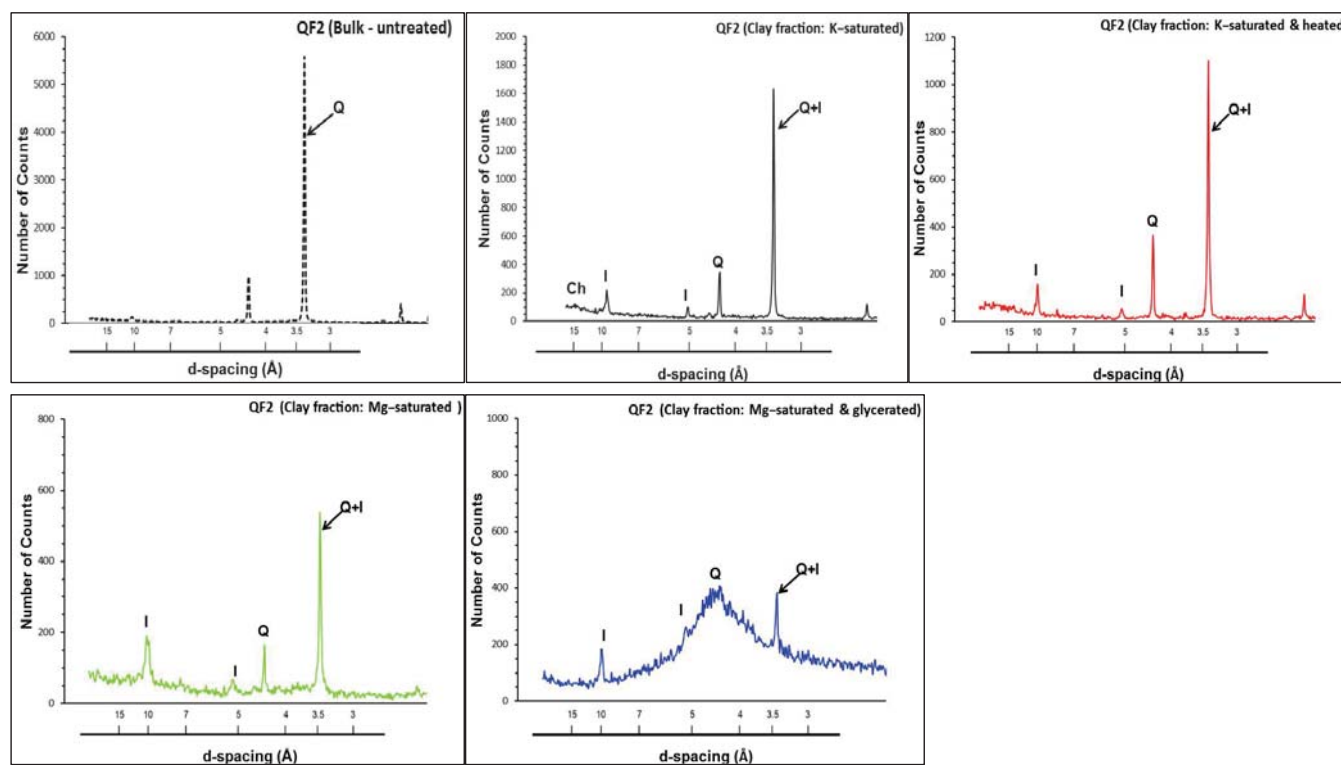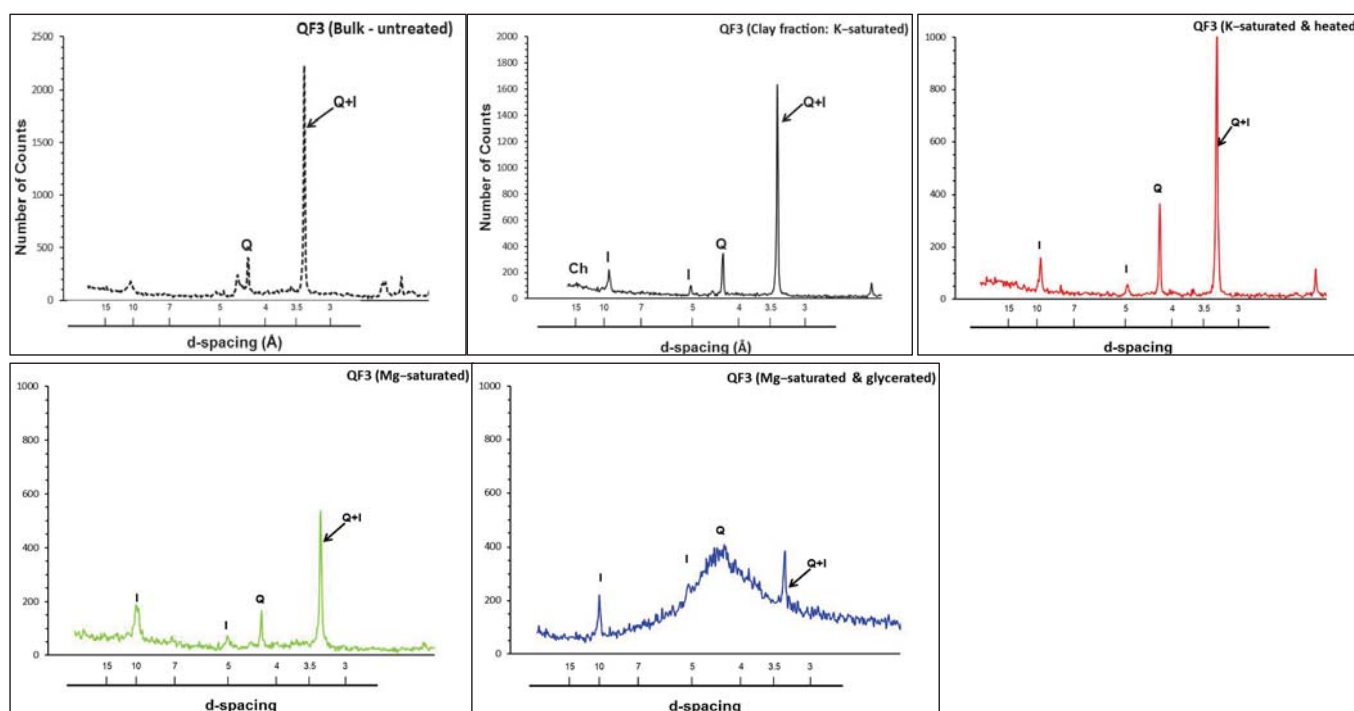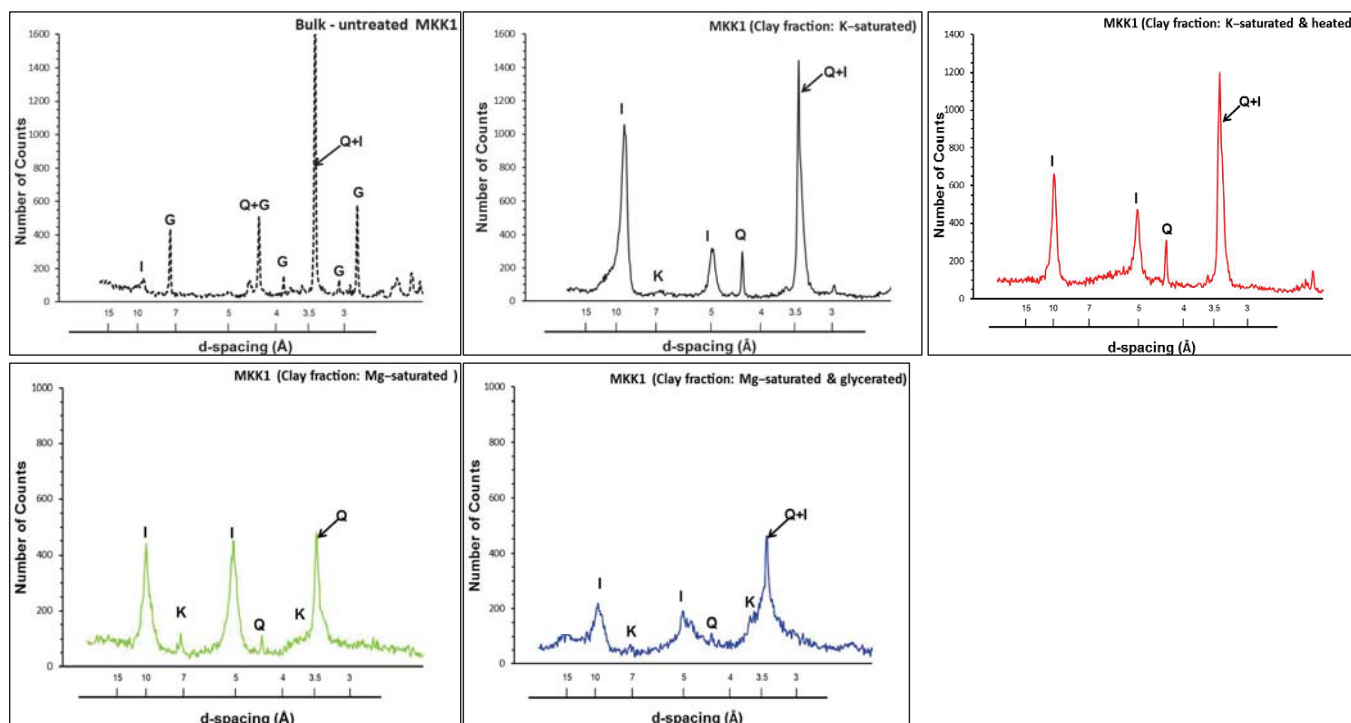
OOS1 (Bulk - untreated)

OOS1 (Clay fraction: K–saturated)

OOS1 (Clay fraction: K–saturated & heated)

OOS1 (Clay fraction: Mg–saturated)

OOS1 (Clay fraction: Mg–saturated & glycerated)
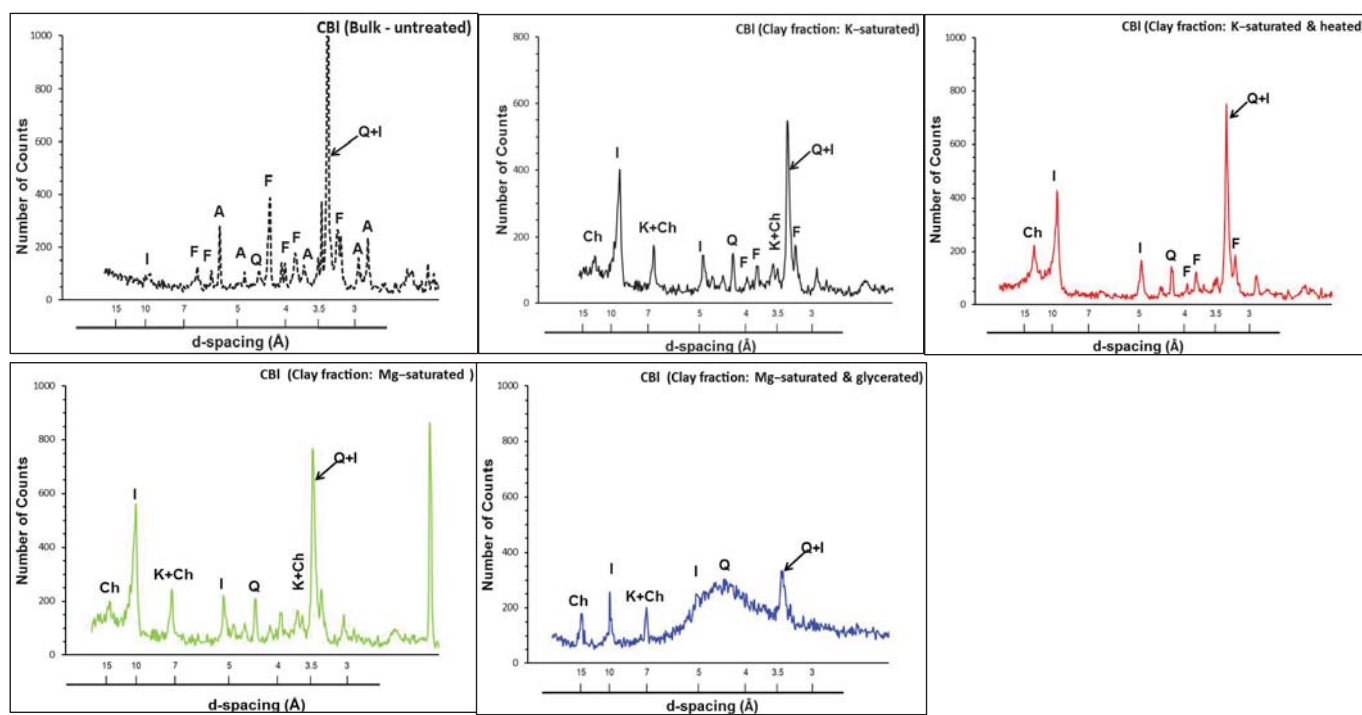
Note: The XRD spectra of untreated and treated OOS1, OOS2 and OOS3 samples are identical. Therefore only spectra of OOS1 are given. The raw data is given in the CD.
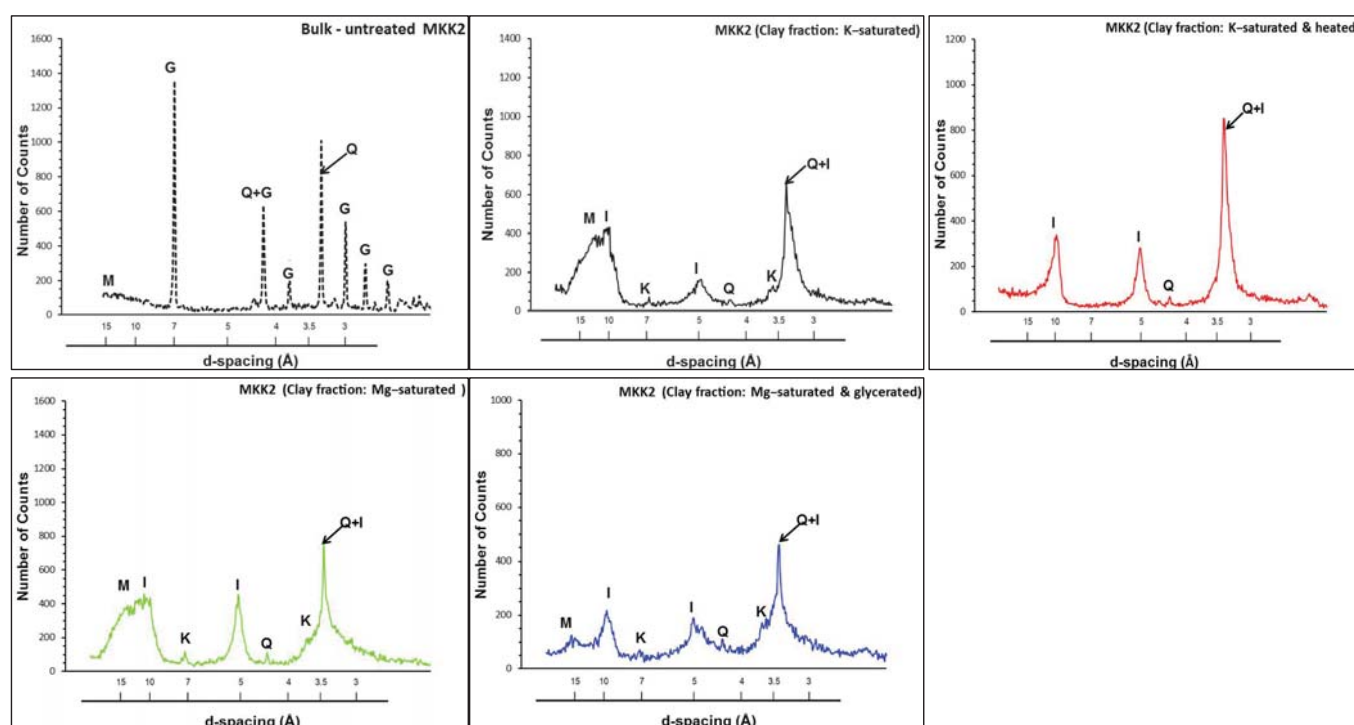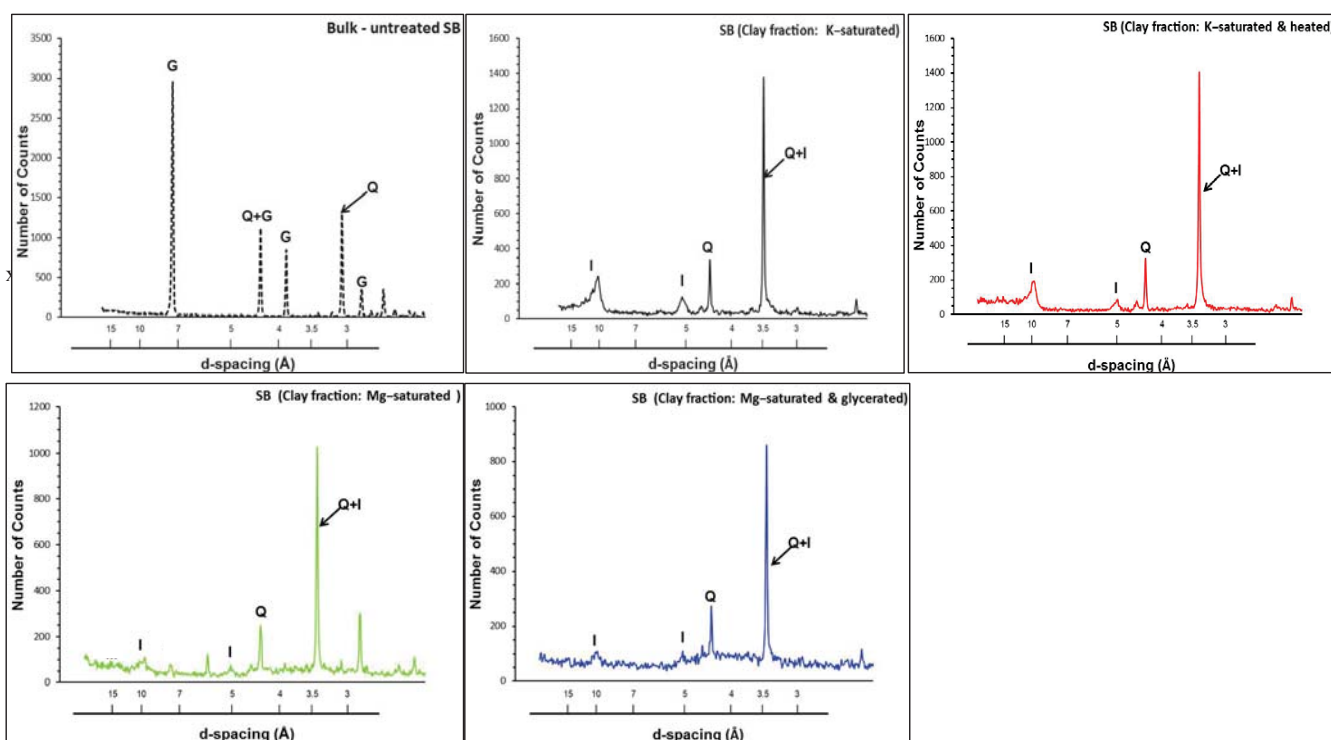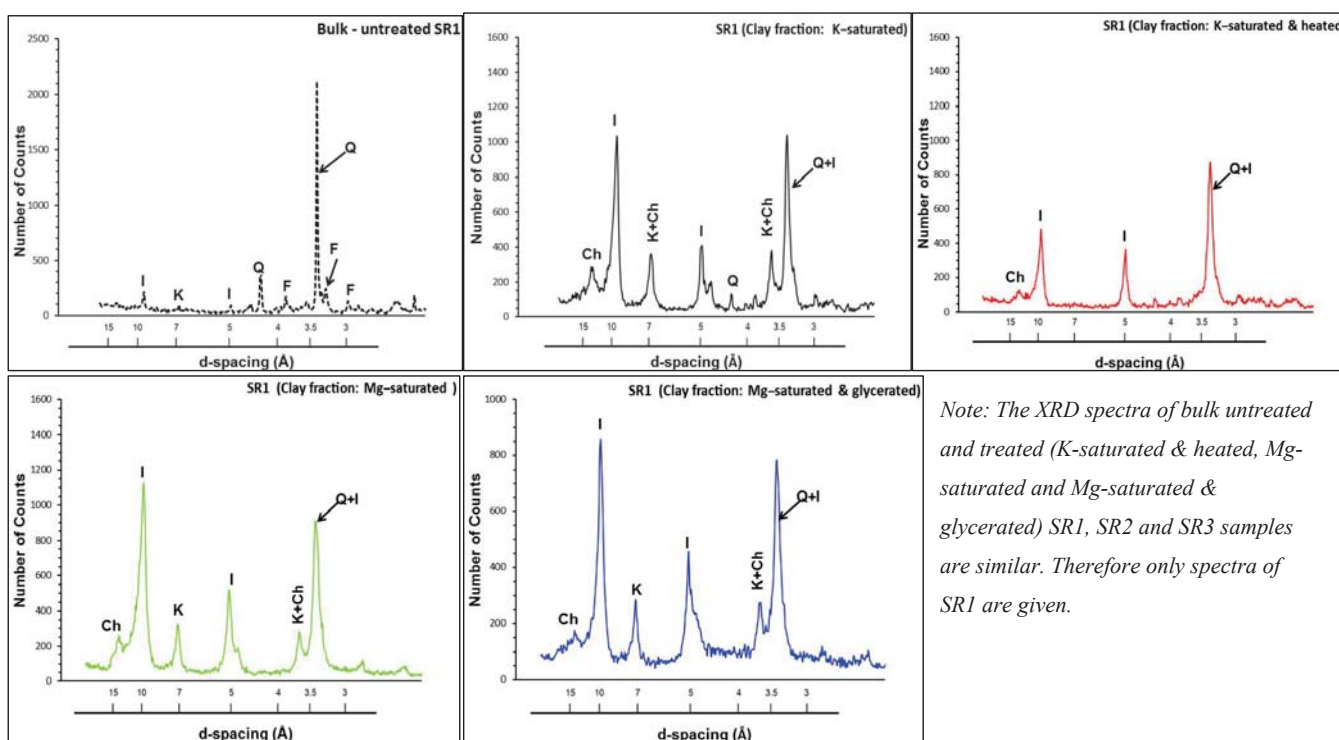
QF1 (Bulk - untreated)

QF1 (Clay fraction: K–saturated)

QF1 (Clay fraction: K–saturated & heated)

QF1 (Clay fraction: Mg–saturated)

QF1 (Clay fraction: Mg–saturated & glycerated)

Note: The XRD spectra of bulk untreated and treated (K-saturated & heated, Mg-saturated and Mg-saturated & glycerated) SR1, SR2 and SR3 samples are similar. Therefore only spectra of SR1 are given.
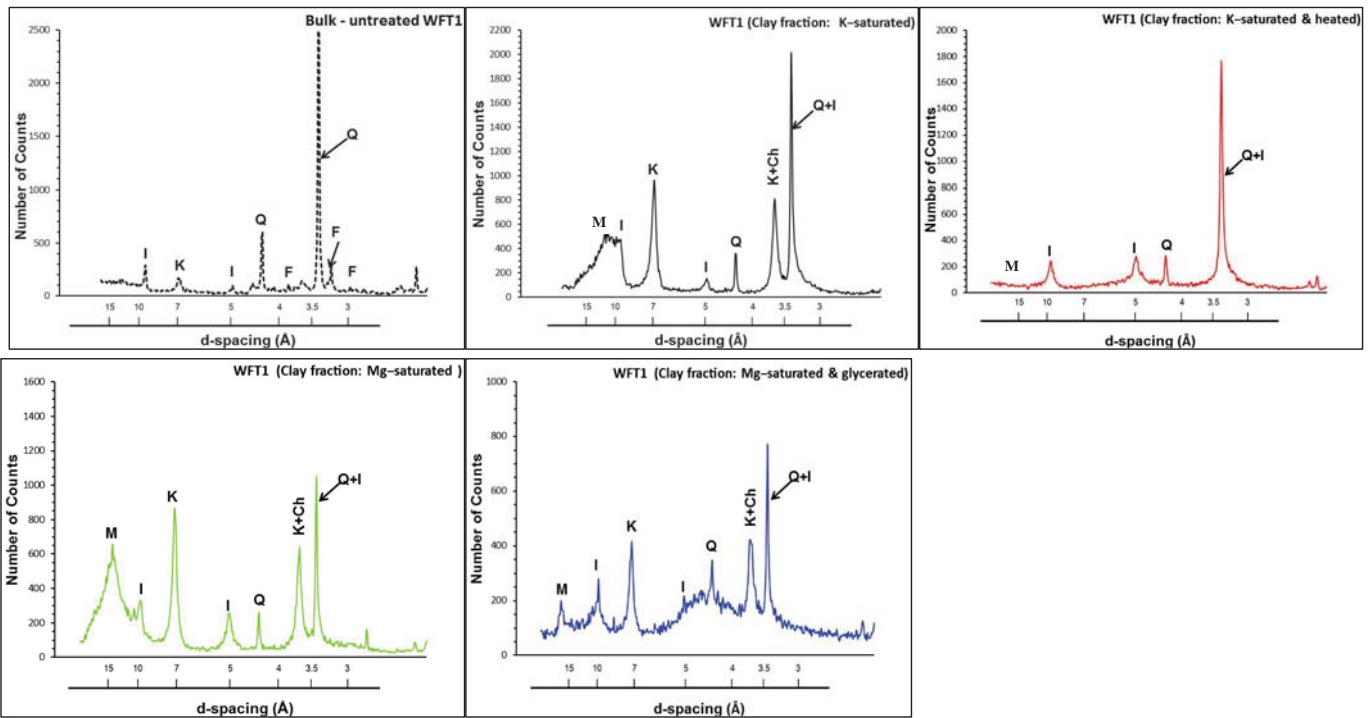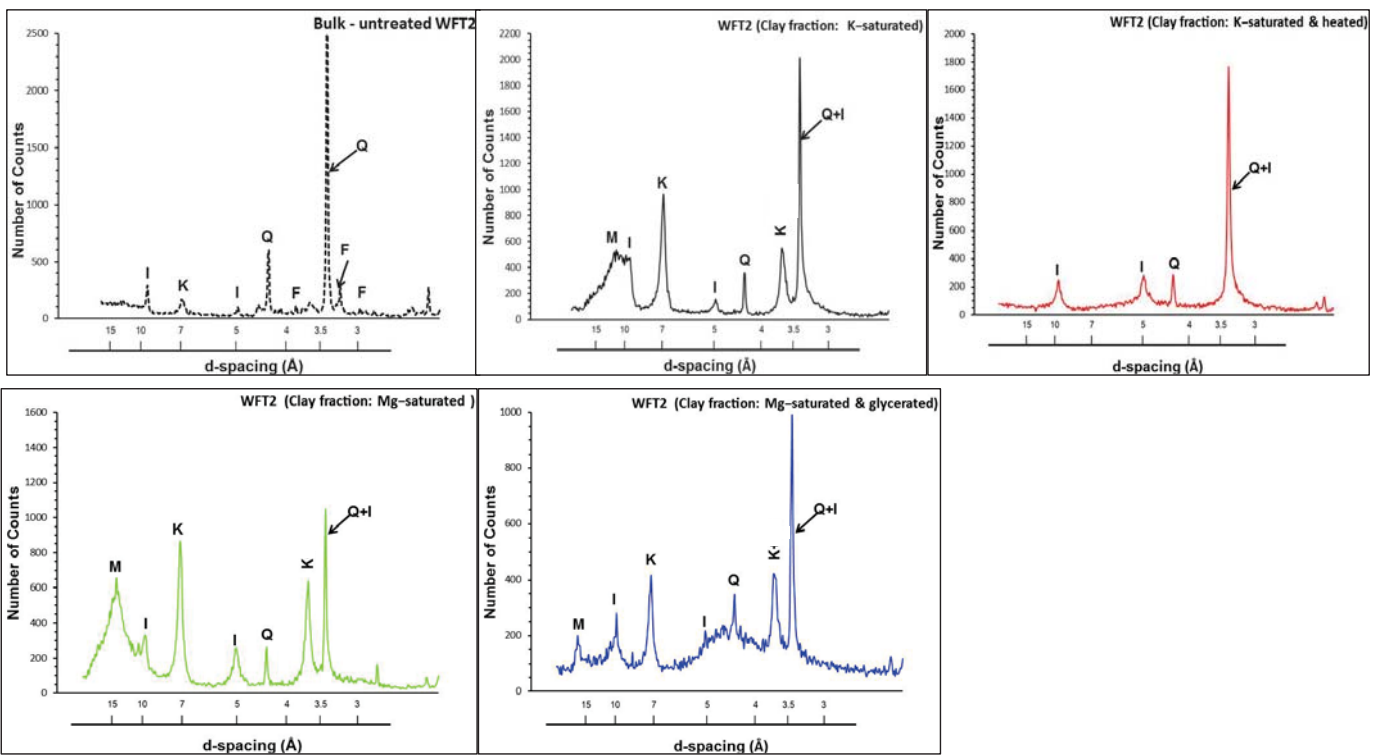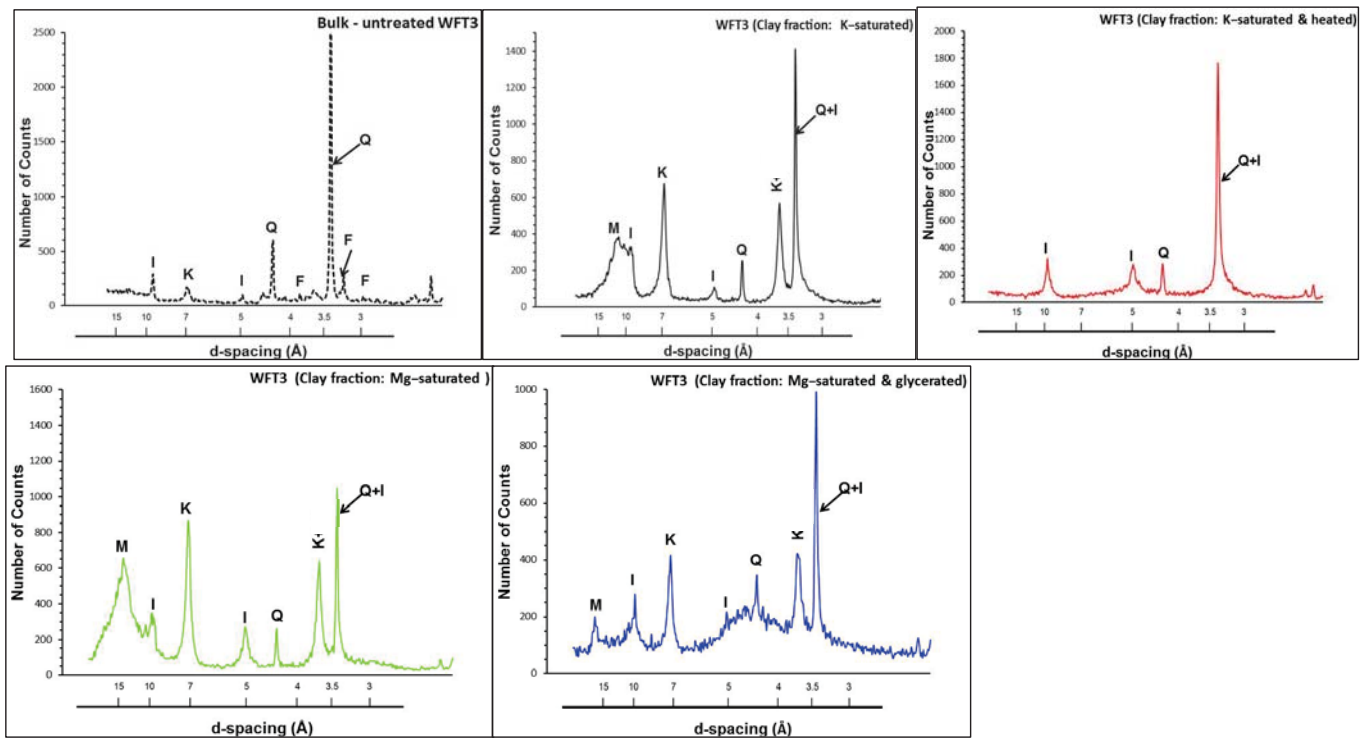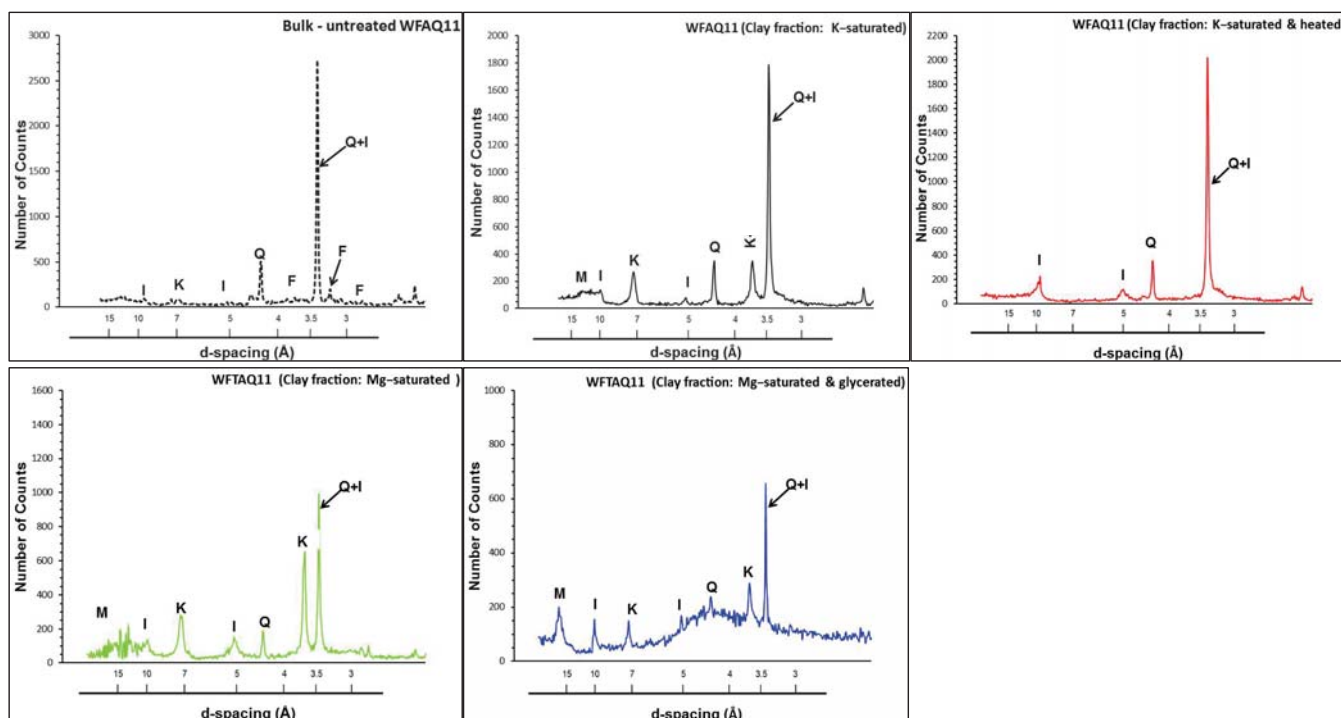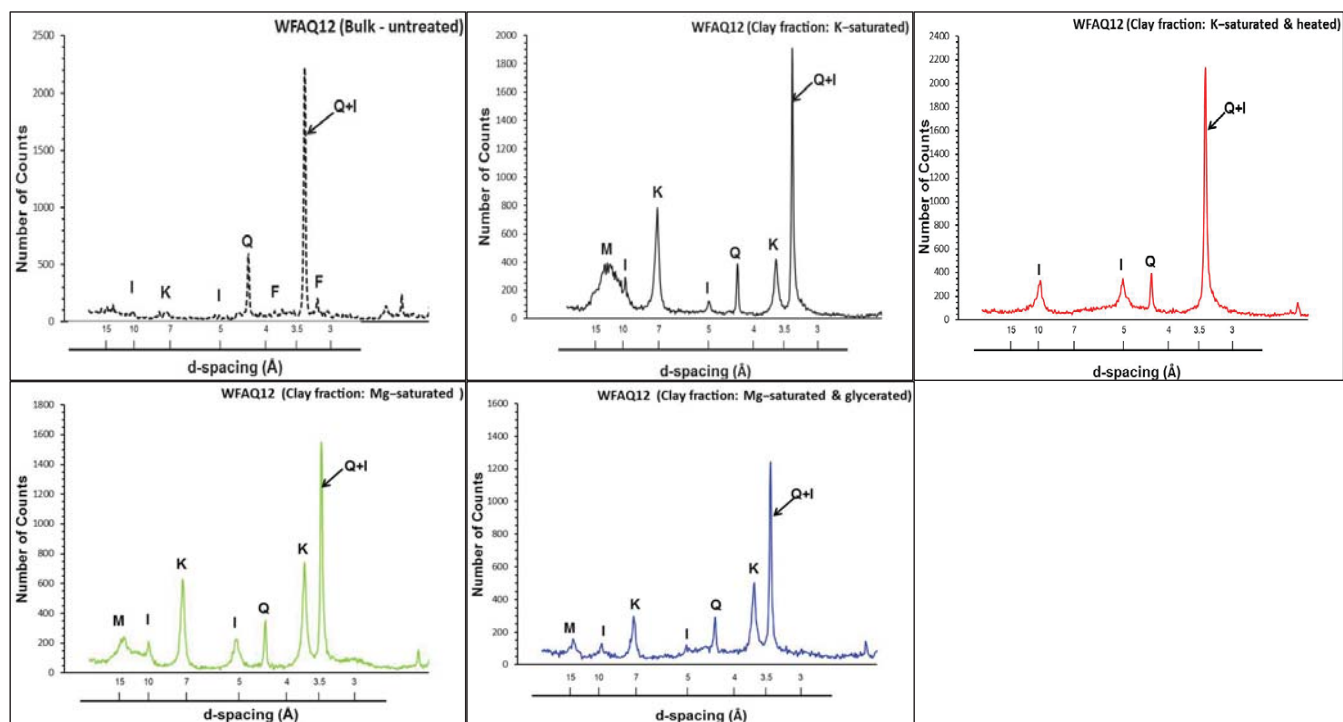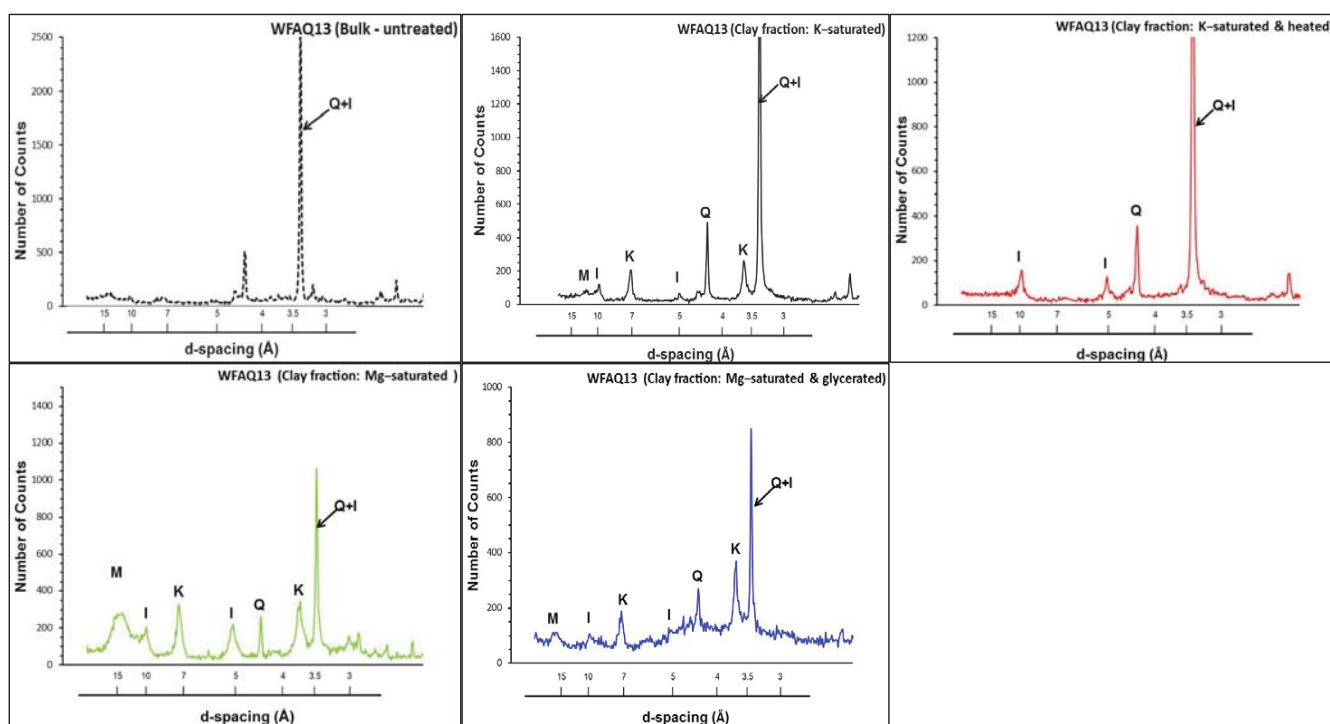
WFAQ12 (Bulk - untreated)

WFAQ12 (Clay fraction: K–saturated)

WFAQ12 (Clay fraction: K–saturated & heated)

WFAQ12 (Clay fraction: Mg–saturated)
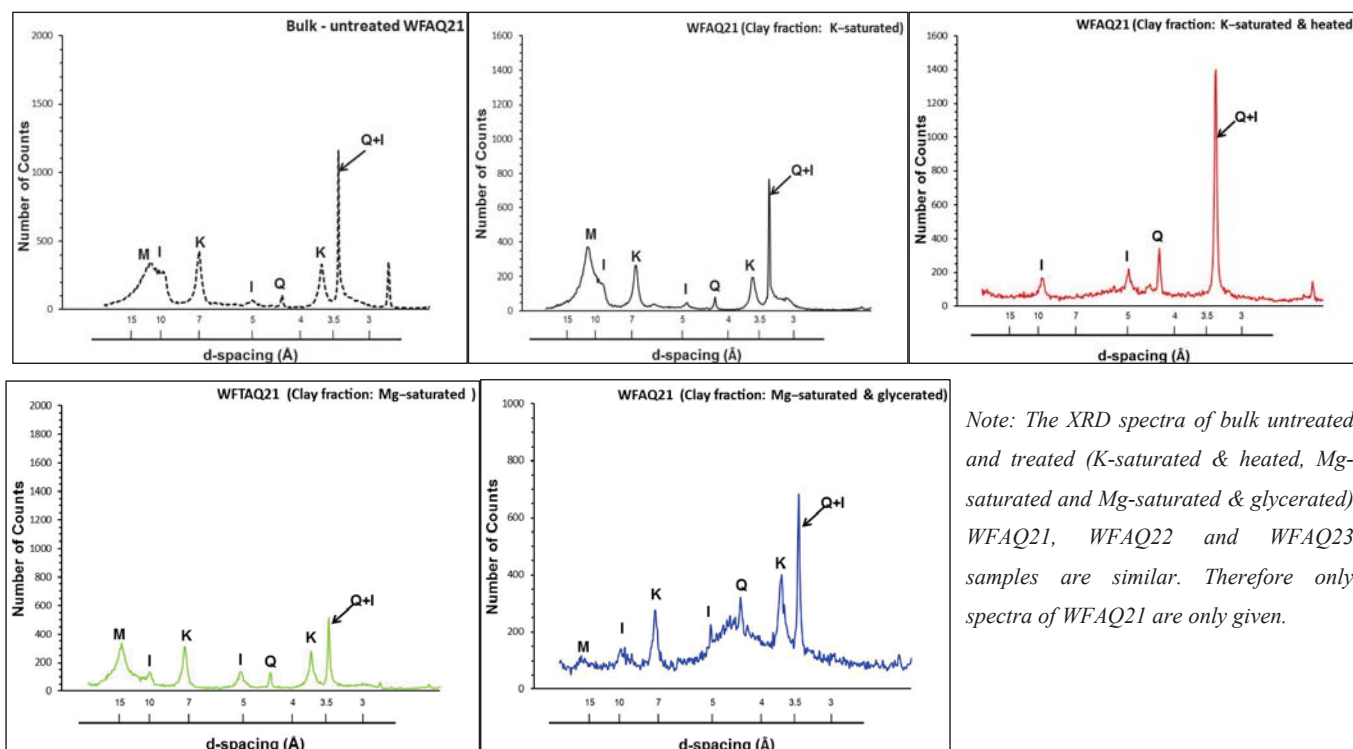
WFAQ12 (Clay fraction: Mg–saturated & glycerated)

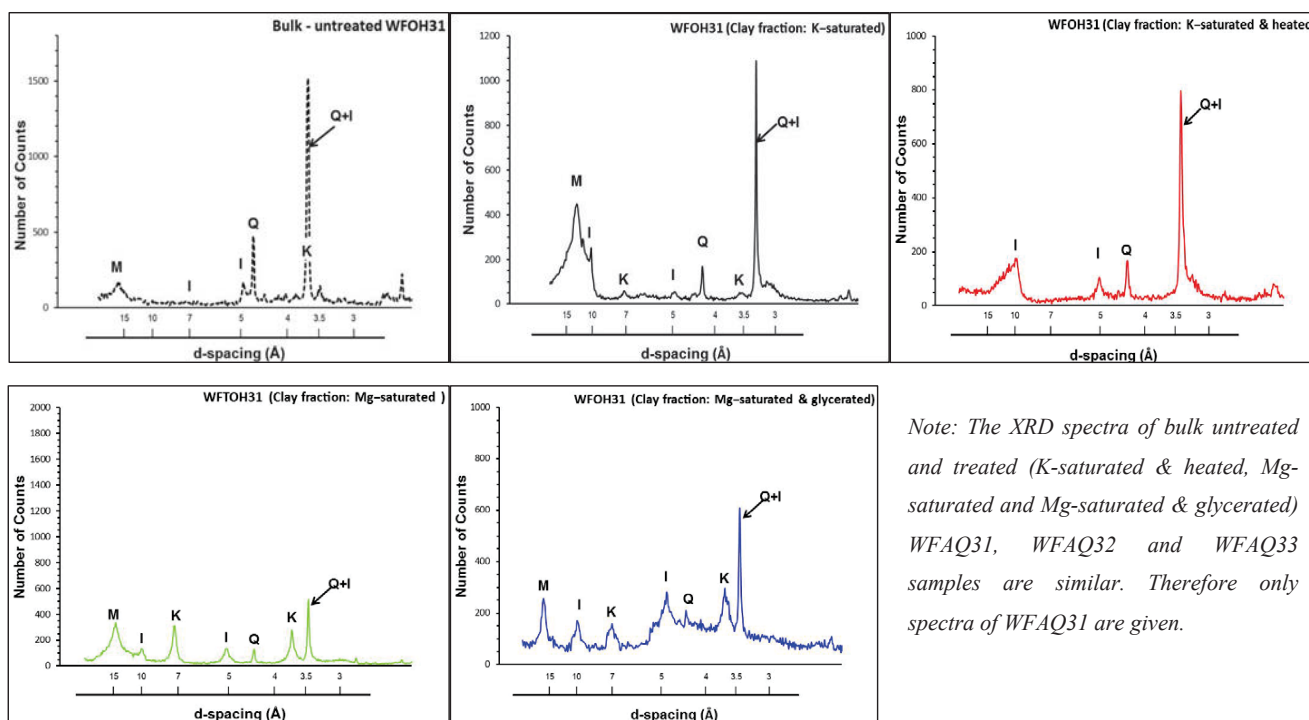Note: The XRD spectra of bulk untreated and treated (K-saturated & heated, Mg-saturated and Mg-saturated & glycerated) WFAQ21, WFAQ22 and WFAQ23 samples are similar. Therefore only spectra of WFAQ21 are only given.

Note: The XRD spectra of bulk untreated and treated (K-saturated & heated, Mg-saturated and Mg-saturated & glycerated) WFAQ31, WFAQ32 and WFAQ33 samples are similar. Therefore only spectra of WFAQ31 are given.